



University
of Glasgow

Cull, Benjamin (2012) Autophagy and organelle turnover in Leishmania major. PhD thesis

<http://theses.gla.ac.uk/4396/>

Copyright and moral rights for this thesis are retained by the author

A copy can be downloaded for personal non-commercial research or study, without prior permission or charge

This thesis cannot be reproduced or quoted extensively from without first obtaining permission in writing from the Author

The content must not be changed in any way or sold commercially in any format or medium without the formal permission of the Author

When referring to this work, full bibliographic details including the author, title, awarding institution and date of the thesis must be given.

**Autophagy and Organelle Turnover
in *Leishmania major***

Benjamin Cull
BSc (Hons)

Submitted in fulfilment of the requirements for the
Degree of PhD

Institute of Infection, Immunity and Inflammation
College of Medical, Veterinary and Life Sciences
University of Glasgow

September 2012

Abstract

Leishmania are parasitic protozoa of medical and veterinary importance. They exist in various developmental forms that are morphologically and metabolically adapted to the different environmental conditions encountered as they are transferred between the insect vector and the mammalian host. Differentiation between developmental forms requires considerable cellular remodelling, which is associated with increased protein turnover. Autophagy is known to be important for this protein turnover, and thus for the successful differentiation and virulence of *Leishmania*. Autophagy is a eukaryotic intracellular degradation mechanism that targets long lived proteins and organelles to the lysosome. As well as non-selective bulk degradation of cytoplasm and its contents, autophagy can be a selective process in which specific organelles or protein aggregates are targeted. The major autophagy pathway is macroautophagy, which is characterised by the formation of double-membrane vesicles called autophagosomes that sequester cargo and traffic it to the lysosome to be degraded. Autophagosome biogenesis is regulated by ATG proteins, including the ubiquitin-like protein ATG8, which is thought to control the expansion of the autophagic vesicle.

Leishmania appear to be unique in that they possess four classes of ATG8-like proteins: ATG8, ATG8A, ATG8B and ATG8C. Although ATG8 is known to be present on autophagosomes, the functions of the other ATG8-like proteins are not well understood. The aims of this project were to study the cargoes that might be degraded in *L. major* autophagosomes, as well as the further characterisation of ATG8A, ATG8B and ATG8C. Using fluorescently labelled ATG8 as an autophagosome marker no co-localisation was observed with fluorescent proteins labelling acidocalcisomes, the flagellum, or the mitochondrion in promastigotes, indicating that these organelles are not autophagic cargo during normal growth or under starvation conditions. In contrast, glycosomes, which are peroxisome-like organelles that compartmentalise metabolic enzymes, were found to be cargo in ~19 % of autophagosomes in procyclic promastigotes. These were trafficked to the lysosome for degradation. Autophagy increases during differentiation or starvation, yet the percentage of autophagosomes containing glycosomes remained constant, indicating that increased turnover of glycosomes

is due to a global increase in autophagy, rather than an up-regulation of selective cargo engulfment. Glycosome turnover was impaired in *L. major* $\Delta atg5$ macroautophagy-deficient mutants, resulting in increased glycosome numbers following both metacyclogenesis and promastigote - amastigote differentiation, and reduced appearance of the glycosomal marker within lysosomal structures. These data suggest that *Leishmania* utilise autophagy as a mechanism for glycosome turnover, which may be important for its adaptation to the host environment. This work also led to the characterisation of the relative sizes of autophagosomes and lysosomal compartments in promastigotes, which have mean diameters of $\sim 0.35 \mu\text{m}$ and $\sim 0.60 \mu\text{m}$, respectively. Although the mitochondrion did not appear to be degraded by autophagy, the majority of autophagosomes associated closely with this organelle, perhaps suggesting that it acts as a membrane source for the biogenesis of autophagic vesicles.

The ATG8-like proteins contain a conserved glycine residue that is expected to be the site of cleavage by one of the cysteine peptidases ATG4.1 and ATG4.2. This processing is thought to be required for conjugation of ATG8-like proteins to their substrate; in the case of ATG8, phosphatidylethanolamine in the autophagosome membrane. Using site-directed mutagenesis to introduce a glycine - alanine mutation into both GFP-ATG8 and GFP-ATG8A, it was determined that glycine 120 of ATG8 is indeed required for its localisation to autophagosomes, whereas mutation of ATG8A's glycine 109 did not affect its localisation to puncta, but appeared to alter its processing. Expression of GFP-tagged ATG8-like proteins in *L. major* $\Delta atg5$ parasites showed that ATG5 is required for formation of GFP-ATG8 autophagosomes, but its loss did not affect formation of puncta labelled by GFP-ATG8A, GFP-ATG8B or GFP-ATG8C, suggesting that these structures form independently of the canonical autophagy pathway. Further investigation of GFP-ATG8A and GFP-ATG8B puncta showed that they localise to distinct regions of the cell close to the flagellar pocket, although they did not overlap with markers of the endosomal system. These data suggest that these proteins may label novel compartments, but their functions remain unknown. They are probably not involved in the canonical autophagy pathway, as they do not appear to be trafficked to the lysosome. Although ATG8A puncta are increased during starvation, they are not induced by differentiation. ATG8B and ATG8C puncta appear to be static and their

occurrence is not altered during starvation or differentiation. The ATG8-like proteins belong to the ubiquitin-like protein family, which carry out diverse functions through the post-translational modification of other cellular proteins. Their ubiquitin-like structure indicates that the ATG8-like proteins could play roles in vesicular cargo sorting or the packaging of proteins into secretory vesicles; however, expression of GFP-tagged ATG8-like proteins in mutants displaying secretion defects did not support a function in secretory pathways.

Table of Contents

1	INTRODUCTION	1
1.1	<i>Leishmania</i>	1
1.1.1	The leishmaniasis and their treatment	1
1.1.2	The <i>Leishmania</i> life cycle: sand fly	5
1.1.3	The <i>Leishmania</i> life cycle: mammalian host	7
1.2	The <i>Leishmania</i> cell and differentiation.....	9
1.2.1	<i>Leishmania</i> gene expression	11
1.2.2	Changes in the expression of surface molecules.....	12
1.2.3	The mitochondrion	13
1.2.4	Glycosomes	14
1.2.5	Acidocalcisomes	15
1.2.6	The flagellum	16
1.2.7	The endo-lysosomal system	17
1.3	Autophagy.....	18
1.3.1	The molecular machinery of autophagy.....	20
1.3.2	The origin of autophagic membranes.....	25
1.3.3	Autophagic cell death.....	27
1.3.4	Autophagy-mediated unconventional secretion.....	28
1.3.5	Autophagy in trypanosomatid parasites	28
1.4	Project aims	35
2	MATERIALS AND METHODS.....	36
2.1	Bacterial strains and culture	36
2.1.1	<i>E. coli</i> strains used	36
2.1.2	Generation of competent <i>E. coli</i> cell lines	36
2.1.3	Transformations.....	37
2.1.4	Bacterial culture and storage	37
2.2	<i>Leishmania</i> culture methods.....	37
2.2.1	Culture of <i>Leishmania</i> promastigotes.....	37
2.2.2	Determination of cell density	38
2.2.3	Creating <i>Leishmania</i> stabilates	38
2.2.4	Transfection and selection of clones	38
2.2.5	Extraction of genomic DNA.....	39
2.2.6	Verification of <i>Leishmania</i> species by PCR.....	39
2.2.7	Preparation of protein extracts	39
2.2.8	Purification of <i>Leishmania major</i> metacyclic promastigotes	39
2.2.9	Extraction of murine peritoneal macrophages	39
2.2.10	Macrophage infection.....	40
2.2.11	Induction and analysis of autophagy	40
2.3	Molecular biology techniques	41
2.3.1	Polymerase Chain Reaction	41
2.3.2	Oligonucleotides used in this project.....	42
2.3.3	DNA gel electrophoresis and gel extraction	43

2.3.4	Restriction digests.....	44
2.3.5	Ligations	44
2.3.6	DNA sequencing	45
2.3.7	Vectors used in this project.....	45
2.3.7.1	Expression vectors for <i>Leishmania</i>	46
2.3.7.2	Construction of Multisite Gateway knockout constructs	47
2.3.8	Bioinformatic analysis.....	49
2.3.9	Purification of plasmids.....	49
2.3.10	Preparation of DNA for transfection	49
2.3.11	Southern blotting	49
2.3.12	Site-directed mutagenesis.....	50
2.4	Fluorescent microscopy.....	50
2.4.1	DeltaVision systems	50
2.4.2	Live cell imaging.....	51
2.4.3	Immobilisation of live parasites for imaging in CyGel.....	51
2.4.4	DAPI staining	51
2.4.5	FM4-64 staining	51
2.4.6	MitoTracker staining	52
2.4.7	Concanavalin A labelling.....	52
2.4.8	Immunofluorescence analysis	52
2.5	Analysis of microscopy images.....	53
2.5.1	Co-localisation analysis	53
2.5.2	Analysis of vesicle size	53
2.6	Statistical analyses	53
2.7	Biochemical methods	54
2.7.1	SDS-PAGE.....	54
2.7.2	Coomassie staining	54
2.7.3	Western blotting.....	54
3	THE ROLE OF AUTOPHAGY IN ORGANELLE TURNOVER IN <i>L. MAJOR</i>.....	56
3.1	Introduction	56
3.1.1	Autophagic organelle turnover	56
3.1.2	Mechanisms of selective autophagy.....	56
3.1.3	Pexophagy	58
3.1.4	Mitophagy.....	59
3.1.5	Reticulophagy	61
3.1.6	Nucleophagy.....	62
3.1.7	Cytoplasm to vacuole targeting (Cvt) pathway	62
3.1.8	Aggrephagy	63
3.1.9	Ribophagy.....	64
3.1.10	Xenophagy.....	64
3.1.11	Evidence of selective autophagy in trypanosomatids.....	65
3.2	Identification of autophagic cargo in <i>L. major</i>	67
3.3	The mitochondrion as a possible source of autophagic membrane.....	70
3.3.1	Interactions of autophagosomes with the mitochondrion	70
3.3.2	Interactions of early autophagosomes with the mitochondrion	72

3.3.3	Autophagy during H ₂ O ₂ -induced fragmentation of the mitochondrion..	74
3.4	A role for autophagy in glycosome turnover	79
3.4.1	Analysis of glycosome turnover by autophagy.....	79
3.4.2	Trafficking of autophagosomes and glycosomes to the lysosomal compartment.....	83
3.4.3	Characterisation of autophagosomes and lysosomes based on size of vesicles.....	86
3.4.4	Comparison of autophagosome size based on cargo.....	89
3.4.5	Glycosome numbers throughout <i>Leishmania major</i> life cycle	90
3.4.6	Comparison of glycosome turnover in autophagy-deficient mutants ...	92
3.5	Discussion	95
4	FURTHER CHARACTERISATION OF <i>L. MAJOR</i> ATG8-LIKE PROTEINS	105
4.1	Introduction	105
4.1.1	Multiple ATG8 homologues in eukaryotes.....	105
4.1.1.1	Atg8 homologues in mammals.....	105
4.1.1.2	Atg8 homologues in plants.....	108
4.1.1.3	Atg8 homologues in trypanosomes.....	109
4.1.2	The multiple ATG8 families of <i>Leishmania</i>	111
4.1.3	Additional functions of ubiquitin-like proteins.....	116
4.2	Analysis of ATG8, ATG8A, ATG8B and ATG8C.....	118
4.2.1	Generation and analysis of ATG8 and ATG8A C-terminal Gly mutants.118	
4.2.1.1	Comparison of GFP-ATG8 and GFP-ATG8 ^{G120A}	118
4.2.1.2	Comparison of GFP-ATG8A and GFP-ATG8A ^{G109A}	121
4.2.2	Expression of ATG8-like proteins in $\Delta atg5$ mutants	124
4.2.3	Further analysis of ATG8A and ATG8B localisation	127
4.2.4	Analysis of ATG8-like proteins in secretion mutants	129
4.3	Analysis of an ATG12-like protein.....	132
4.4	Discussion	137
5	GENERAL DISCUSSION.....	145
	APPENDIX.....	154
	REFERENCES	156

List of Tables

1 Introduction

Table 1-1 Leishmania species that are pathogenic to humans, and their clinical manifestations, geographical distribution and vector species.....	4
Table 1-2 The core Atg and Atg-related proteins involved in autophagosome formation in the yeast <i>S. cerevisiae</i> and their homologues from humans and trypanosomatid parasites.	29

2 Materials & Methods

Table 2-1 Details of oligonucleotides used in this project.	42
Table 2-2 Details of oligonucleotides used in this project (continued)	43
Table 2-3 Details of plasmids used or generated in this project.	45
Table 2-4 Details of plasmids used or generated in this project (continued).	46

3 The Role of Autophagy in Organelle Turnover in *L. major*

Table 3-1 Summary of autophagosome - acidocalcisome co-localisation experiments ..	69
Table 3-2 Summary of autophagosome - flagellum co-localisation experiments.	70
Table 3-3 Summary of autophagosome - mitochondrion experiments.....	72
Table 3-4 Association of mCherry-ATG5-labelled autophagosomes with the mitochondrion	73
Table 3-5 Summary of autophagosome - glycosome co-localisation experiments	82

4 Further Characterisation of *L. major* ATG8-like Proteins

Table 4-1 Comparison of sequence identity between <i>L. major</i> ATG12s and those of other organisms.....	134
Table 4-2 Analysis of GFP-ATG12L and mCherry-ATG5 co-localisation on puncta	136
Table 4-3 Summary of current knowledge on <i>Leishmania major</i> ATG8-like proteins ...	144

Appendix

Table A-1 Raw data from glycosome turnover experiments	154
Table A-2 Percentage of glycosomes co-localised with autophagosomes in different life cycle stages.....	155

List of Figures

1 Introduction

Figure 1-1 Geographical distribution of the different clinical forms of leishmaniasis	2
Figure 1-2 The life cycle of <i>Leishmania</i> within the sand fly insect vector.....	6
Figure 1-3 The <i>Leishmania</i> life cycle showing mammalian immune cells that are infected	8
Figure 1-4 Schematic representation of <i>Leishmania</i> promastigote and amastigote forms including the main organelles	10
Figure 1-5 Schematic showing the three major types of autophagy	19
Figure 1-6 The macroautophagy pathway and the ATG8 and ATG12 conjugation systems	23

2 Materials & Methods

Figure 2-1 Schematic showing Multisite Gateway construction of ATG8 knockout constructs	48
---	----

3 The Role of Autophagy in Organelle Turnover in *L. major*

Figure 3-1 Mechanisms of selective autophagy and architecture of proteins involved ..	57
Figure 3-2 Identification of autophagic cargo in <i>L. major</i> promastigotes.....	69
Figure 3-3 Analysis of RFP-ATG8 interactions with the <i>Leishmania</i> mitochondrion	71
Figure 3-4 Analysis of mCherry-ATG5 interactions with the mitochondrion	73
Figure 3-5 Analysis of autophagy in H ₂ O ₂ -treated cells	75
Figure 3-6 Analysis of large ATG8-labelled structures induced by treatment with 1 mM H ₂ O ₂	76
Figure 3-7 Detection of membrane potential in a fragmented mitochondrion.....	78
Figure 3-8 Example of co-localisation analysis in glycosome turnover experiments	81
Figure 3-9 Graphical representation of data in Table 3-5.....	82
Figure 3-10 Autophagosome - glycosome co-localisation in differentiating amastigotes	83
Figure 3-11 Visualisation of GFP-ATG8 labelling nascent autophagosomal structures ...	84
Figure 3-12 Trafficking of GFP-ATG8 to the lysosomal compartment	85
Figure 3-13 Visualisation of autophagosome fusion with the lysosome.....	86
Figure 3-14 Characterisation of vesicle size in stationary phase <i>L. major</i> parasites	88
Figure 3-15 Comparison of sizes of GFP-ATG8 puncta during glycosome turnover	89

Figure 3-16 Analysis of glycosome numbers per parasite in different stages of the life cycle	91
Figure 3-17 Comparison of glycosome turnover in WT, $\Delta atg5$ and $\Delta atg5::ATG5$ parasites	92
Figure 3-18 Comparison of glycosome turnover in WT and $\Delta atg5$ parasites during promastigote - amastigote differentiation	94

4 Further Characterisation of *L. major* ATG8-like Proteins

Figure 4-1 Alignment of <i>L. major</i> ATG8-like proteins with those of other eukaryotes..	112
Figure 4-2 Phylogenetic analysis of ATG8 and ATG12 proteins in trypanosomatids, yeast and higher eukaryotes	116
Figure 4-3 Comparison of <i>L. major</i> promastigotes expressing GFP-ATG8 or GFP-ATG8 ^{G120A}	120
Figure 4-4 Comparison of GFP-ATG8A and GFP-ATG8A ^{G109A} localisation during starvation	121
Figure 4-5 Comparison of GFP-ATG8A and GFP-ATG8A ^{G109A} processing by Western blot	123
Figure 4-6 Localisation of <i>L. major</i> ATG8-like proteins in WT and $\Delta atg5$ parasites	125
Figure 4-7 Localisation of GFP-ATG8A in relation to markers of the endosomal system	128
Figure 4-8 Localisation of GFP-ATG8B puncta in relation to endosomal markers.....	129
Figure 4-9 Comparison of GFP-ATG8 localisation in WT and $\Delta isp1/2/3$ parasites	131
Figure 4-10 Localisation of GFP-ATG8A and GFP-ATG8B in WT and $\Delta isp1/2/3$ parasites	132
Figure 4-11 Alignment of ATG12-like proteins of <i>L. major</i> and other eukaryotic organisms.....	133
Figure 4-12 Occurrence of GFP-ATG12L puncta formation in WT and $\Delta atg5$ parasites .	135
Figure 4-13 Co-localisation of GFP-ATG12L with mCherry-ATG5 on punctate structures	136
Figure 4-14 Localisation of ATG8-like punctate structures in <i>L. major</i> promastigotes .	140

5 General Discussion

Figure 5-1 Schematic showing the structures labelled by the ATG8 families of <i>L. major</i>	153
--	-----

Acknowledgements

I would like to thank my supervisor Jeremy Mottram for allowing me to work on this project, giving me opportunities to attend interesting conferences and training courses, and helping to develop my scientific thinking. My assessors Tansy Hammarton and Liam Morrison have provided useful feedback and discussion on my work throughout the project. I would also like to acknowledge the Medical Research Council who have funded my PhD studies.

Many thanks to Kerry Woods and Esther Castanys-Muñoz who helped me get started on my project, and to Elaine Brown and Jim Scott who have given me a lot of advice on lab techniques throughout my work (and told me where to find everything). Thank you to the autophagy meeting regulars Graham Coombs, Rod Williams, Sylke Müller, Andy Tomlins and Will Proto, who have given useful comments on my project and helped to guide its direction.

I would also like to thank the past and present members of level 6, who have always been ready to help and offer advice, and made this a great place to work. Thanks to Amy, Catarina, Elizabeth, Ellie, Larissa, Manuel, Nath, Sam, and Saskia, it has been fun working and going on trips/nights out with you!

Thank you to my family who are always very supportive, even though they are not completely sure what I have been doing for the past 3 years. Finally many thanks to Susan (Zhihua) Song who has been a great friend and supported me with everything, listened to me practising presentations, and fed me with some excellent cooking!

Author's Declaration

The research reported in this thesis is the result of my own original work, except where stated below, and has not been submitted for any other degree.

Benjamin Cull, September 2012

Dr. S Besteiro produced plasmids for the expression of GFP-ATG8 and proCPB-RFP. The *L. major* $\Delta isp1/2/3$ mutants described in 4.2.4 were produced by Dr L Morrison. Plasmids for the fluorescent labelling of acidocalcisomes, the flagellum and the mitochondrion were generated by Dr. D Tonn. Dr. R Williams produced plasmids for labelling ATG8, ATG5, glycosomes and the mitochondrion, generated the *L. major* $\Delta atg5$ parasites, and performed the experiment described in Figure 4-5 B. Dr K Woods designed primers for site-directed mutagenesis of *L. major* ATG8-like proteins and generated plasmids for expression of GFP-labelled ATG8, ATG8A, ATG8B and ATG8C.

Some of the results presented in Chapter 3 have been published in PLoS Pathogens:

Williams RA, Smith TK, Cull B, Mottram JC, Coombs GH. (2012). ATG5 is essential for ATG8-dependent autophagy and mitochondrial homeostasis in *Leishmania major*. *PLoS Pathogens* 8 (5): e1002695.

List of Abbreviations

3-MA	3-methyladenine
AIM	Atg8-interacting motif
ALFY	autophagy-linked FYVE protein
AmsI	α -mannosidase I
ANOVA	analysis of variance
Apel	aminopeptidase I
ATG	autophagy-related
ATP	adenosine triphosphate
bp	base pair
BSA	bovine serum albumin
cAMP	cyclic adenosine monophosphate
CL	cutaneous leishmaniasis
CMA	chaperone-mediated autophagy
CPA/CPB	cysteine peptidase A / cysteine peptidase B
CUPS	compartment for unconventional protein secretion
Cvt	cytoplasm-to-vacuole pathway
DAPI	4,6-diamidino-2-phenylindole
DC	dendritic cell
DCL	dermal cutaneous leishmaniasis
DHFR	dihydrofolate reductase
DIC	differential interference contrast
DMSO	dimethyl sulfoxide
DNA	deoxyribonucleic acid
EDTA	ethylenediamine tetra acetic acid
ER	endoplasmic reticulum
ERAD	ER-associated degradation
ESCRT	endosomal sorting complex required for transport
FIP200	FAK family-interacting protein of 200 kDa
FM4-64	<i>N</i> -(3-Triethylammoniumpropyl)-4-(6-(4-(Diethylamino)phenyl)hexatrienyl) Pyridinium Dibromide
fPPG	filamentous proteophosphoglycan
GABARAP	γ -aminobutyric acid type A (GABA _A)-receptor associated protein
GATE-16	Golgi-associated ATPase enhancer of 16 kDa
GFP	green fluorescent protein
GIPL	glycoinositolphospholipid
GPI	glycosylphosphatidylinositol
GRASP	Golgi reassembly and stacking protein
h	hour/s
HASPB	hydrophilic acylated surface protein B
HDAC6	histone deacetylase 6
HIFCS	heat-inactivated foetal calf serum
HRP	horseradish peroxidase
IFT	intraflagellar transport
IL	interleukin
IPTG	isopropyl- β -D-thiogalactopyranoside
kb	kilobase
kDa	kilo Dalton
KO	knockout
LB	Luria-Bertani
LC3	microtubule-associated protein 1 light chain 3
LIR	LC3-interacting region
LPG	lipophosphoglycan
μ	micro
m	milli / metre

M	molar
MAD	mitochondria-associated degradation
MCA	metacaspase
MCL	mucocutaneous leishmaniasis
MDV	mitochondrial-derived vesicle
MHC	major histocompatibility complex
min	minute
MIPA	micropexophagy-specific membrane apparatus
mRNA	messenger RNA
MVB	multivesicular body
MVT	multivesicular tubule
NBR1	neighbour of Brca1 gene
NDP52	nuclear dot protein 52 kDa
NSF	<i>N</i> -ethylmaleimide-sensitive factor
NVJ	nuclear-vacuolar junction
OD	optical density
OPTN	optineurin
PAS	phagophore assembly site / pre-autophagosomal structure
PCD	programmed cell death
PBS	phosphate-buffered saline
PCC	Pearson's correlation coefficient
PCR	polymerase chain reaction
PE	phosphatidylethanolamine
PI3K	phosphoinositide 3-kinase
PI3P	phosphatidylinositol 3-phosphate
PKDL	post-kala azar dermal leishmaniasis
PMN	piecemeal microautophagy of the nucleus
PMP	peroxisomal membrane protein
PS	phosphatidylserine
PSG	promastigote secretory gel
PTS	peroxisomal targeting sequence
RFP	red fluorescent protein
RNA	ribonucleic acid
RNAi	RNA interference
ROM	rhomboid serine peptidase
SAT	streptothricin acetyltransferase
SDS-PAGE	sodium dodecylsulphate polyacrylamide gel electrophoresis
SILAC	stable isotope labelling of amino acids in cell culture
SHERP	small hydrophilic endoplasmic reticulum-associated protein
SNARE	soluble NSF-attachment protein receptor
TMRM	tetramethylrhodamine, methyl ester
TOR	target of rapamycin (kinase)
Ub	ubiquitin
Ubl	ubiquitin-like protein
ULK	Unc51-like kinase
UPR	unfolded protein response
UPS	ubiquitin-proteasome system
UTR	untranslated region
V-H ⁺ -PPase	vacuolar proton pyrophosphatase
VL	visceral leishmaniasis
WHO	World Health Organisation
WT	wild-type
X-Gal	5-bromo-4-chloro-3-indolyl-β-[D]-galactopyranoside

1 Introduction

1.1 Leishmania

Leishmania are protozoan parasites responsible for the leishmaniasis, a spectrum of diseases of both medical and veterinary importance. Leishmania, which belong to the Order Kinetoplastida and Family Trypanosomatidae, are transmitted between their mammalian hosts by phlebotomine sand flies.

1.1.1 The leishmaniasis and their treatment

The leishmaniasis occur in tropical, subtropical and temperate regions of the world, and are endemic in 88 countries worldwide (Figure 1-1). The majority of these are developing countries; leishmaniasis is associated with poverty, malnutrition, poor housing, displacement and lack of resources, and is also linked to environmental changes such as deforestation, dam building, agricultural development and urbanisation (Alvar et al., 2006). The spread of Leishmania between its mammalian hosts depends on sand flies of the genus *Phlebotomus* in the Old World and *Lutzomyia* in the New World (Table 1-1). Today, an estimated 12 million cases of leishmaniasis exist worldwide, with an estimated 1.5 - 2 million new cases occurring annually (<http://www.who.int/leishmaniasis/en/>). Over 20 species of *Leishmania* cause disease; it is thought that, for the majority of these, mammals such as rodents are the primary host and that humans become infected when moving into the natural host range (Bañuls et al., 2007). Infection of humans results in diseases of varying morbidity and mortality, depending on the Leishmania species involved and the host immune response, which can be classified into three major clinical forms (Bañuls et al., 2007).

The most severe form of the disease, visceral leishmaniasis (VL; also known as kala azar) is almost always fatal if untreated. It is characterised by fever, weight loss, hepatomegaly, splenomegaly and anaemia, and can cause large-scale epidemics with high fatality rates, especially in difficult to access areas (Bañuls et al., 2007). VL is also an important opportunistic infection in HIV patients; HIV infection is associated with a significantly elevated risk of developing VL, and this emerging problem is a major threat to efforts to control VL (Bañuls et al.,

2007). The vast majority (90 %) of VL cases occur in India, Nepal, Bangladesh, Sudan and Brazil (Figure 1-1 A). After treatment and recovery, a number of VL patients may develop a cutaneous form called post-kala azar dermal leishmaniasis (PKDL). This usually develops within 2 years after apparent clinical cure of VL, and requires long and expensive treatment to clear up (Bañuls et al., 2007).

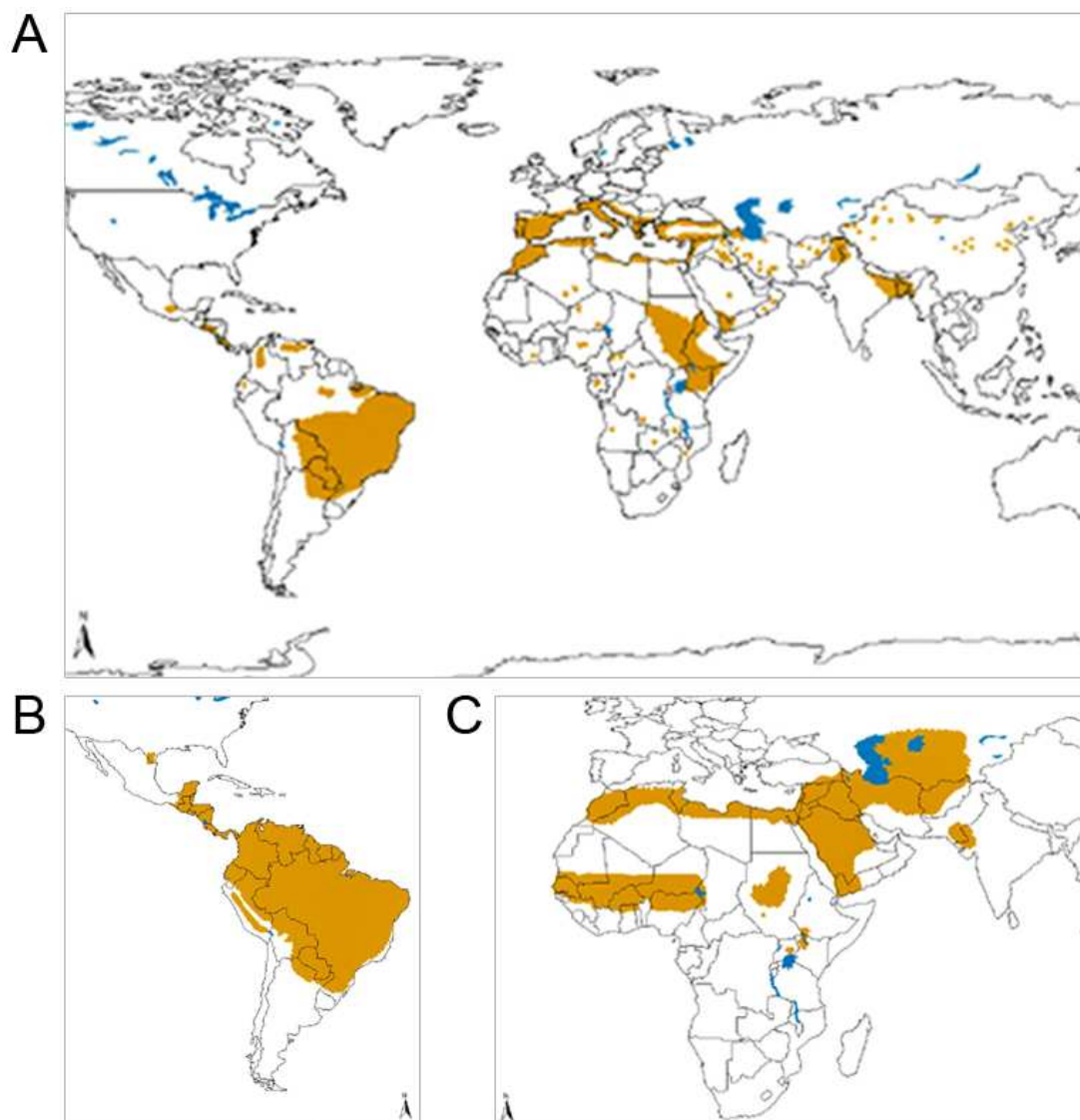


Figure 1-1 Geographical distribution of the different clinical forms of leishmaniasis. A. Distribution of visceral leishmaniasis. B. Distribution of cutaneous and mucocutaneous leishmaniasis in the New World. C. Distribution of cutaneous leishmaniasis caused by *L. major* in the Old World. Source: World Health Organisation (WHO) Essential Leishmaniasis maps (http://www.who.int/leishmaniasis/leishmaniasis_maps/en/index.html).

Mucocutaneous leishmaniasis (MCL) leads to extensive destruction of the mucous membranes of the oro-nasal and pharyngeal cavities, and damage to surrounding tissues, resulting in disfiguring facial injuries (Bañuls et al., 2007). These cause life-long distress for MCL patients and can cause them to be rejected by their

communities. Bolivia, Brazil and Peru together contain 90 % of MCL cases (Figure 1-1 B).

Cutaneous leishmaniasis (CL) is the most common form of the disease, and results in ulcers on exposed parts of the body, such as the face, arms and legs (Bañuls et al., 2007). Although these lesions usually self-heal within months, they often leave disfiguring scars which can be a source of social stigma. In cases where large numbers of ulcers appear, serious disability may result. 90 % of CL cases occur in Afghanistan, Brazil, Iran, Peru, Syria and Saudi Arabia (Figure 1-1 B, C). Diffuse cutaneous leishmaniasis (DCL) affects patients with a defective cell-mediated immune response. It results in disseminated lesions resembling leprosy, which never heal spontaneously, and often relapses after drug treatment (Bañuls et al., 2007).

Appropriate treatment depends on identification of the causative *Leishmania* species (Croft and Olliaro, 2011). The first line drugs for the treatment of cutaneous and visceral leishmaniasis are pentavalent antimonials, such as sodium stibogluconate (Pentostam[®]) and meglumine antimoniate (Glucantime[®]). These drugs have been the mainstay of leishmaniasis treatment for over 60 years, and as such parasites have developed resistance to them, although drug resistance is so far limited to a few endemic areas, notably Bihar state in India. The release of generic sodium stibogluconate has resulted in reduced costs for leishmaniasis treatment. Amphotericin B and its liposomal formulation AmBisome[®], which exhibits reduced side effects, have become standard treatments for VL, and are useful for treating complex forms of leishmaniasis such as MCL and PKDL. However, a full course of AmBisome is expensive, and both Amphotericin B and AmBisome must be administered intravenously and cause adverse side effects (Croft and Olliaro, 2011). Miltefosine (Impavido[™]) is the first oral treatment for VL, and is also effective against some species responsible for CL, although it has been shown to be teratogenic so should not be taken by women of child-bearing age. The aminoglycoside Paromomycin shows promise for the treatment of leishmaniasis and has been used in clinical trials to treat VL (administered intramuscularly) and CL (applied topically). Pentamidine is a second line drug for leishmaniasis treatment, although has been withdrawn from use in India due to low efficacy, and is only effective against certain CL-causing *Leishmania* species in South America (Croft and Olliaro,

2011). Trials of various co-administrations of available leishmaniasis drugs show that drug combinations can improve treatment effectiveness and safety, as well as reducing treatment time (Sundar et al., 2005). With the limitations of current leishmaniasis drugs and no human vaccines available, there is an urgent need for new drug targets and vaccine candidates to be identified in *Leishmania*.

Table 1-1 Leishmania species that are pathogenic to humans, and their clinical manifestations, geographical distribution and vector species. CL, cutaneous leishmaniasis; DCL, diffuse cutaneous leishmaniasis; VL, visceral leishmaniasis; PKDL, post-kala azar dermal leishmaniasis; MCL, mucocutaneous leishmaniasis. Note: other New World species exist that are not included in this table.

Species	Disease	Distribution	Sand fly vectors
Old World Species			
<i>L. major</i>	CL	North Africa, West & Central Africa, West & Central Asia	<i>P. papatasi</i> , <i>P. duboscqi</i> , <i>P. salehi</i>
<i>L. tropica</i>	CL	Western India, West & Central Asia, North Africa	<i>P. sergenti</i>
<i>L. aethiopica</i>	CL, DCL	Ethiopia & Kenya	<i>P. longipes</i> , <i>P. pedifer</i>
<i>L. donovani</i>	VL, PKDL	India, Nepal, Bangladesh & East Africa	<i>P. argentipes</i> , <i>P. orientalis</i> , <i>P. martini</i>
<i>L. infantum</i>	VL	Mediterranean basin, West & Central Asia	<i>P. ariasi</i> , <i>P. perniciosus</i>
New World Species			
<i>L. braziliensis</i>	CL, MCL	South & Central America	<i>Lu. whitmani</i> , <i>Lu. ovallesci</i> , <i>Lu. trapidoi</i> & others
<i>L. mexicana</i>	CL, DCL	South & Central America, some regions of USA	<i>Lu. olmeca olmeca</i>
<i>L. amazonensis</i>	CL, DCL	South America	<i>Lu. flaviscutellata</i>
<i>L. guyanensis</i>	CL, MCL	South America	<i>Lu. umbralis</i> , <i>Lu. ovallesci</i>
<i>L. panamensis</i>	CL, MCL	Central America & Colombia	<i>Lu. trapidoi</i> , <i>Lu. hartmanni</i> , <i>Lu. panamensis</i> , <i>Lu. gomezi</i>
<i>L. peruviana</i>	CL	Peru	<i>Lu. peruensis</i> , <i>Lu. verrucarum</i>
<i>L. colombiensis</i>	CL, VL	Colombia & Venezuela	<i>Lu. hartmanni</i>
<i>L. infantum</i> (syn. <i>chagasi</i>)	VL	South & Central America	<i>Lu. longipalpis</i> , <i>Lu. evansi</i> , <i>Lu. olmeca olmeca</i>

1.1.2 The *Leishmania* life cycle: sand fly

Leishmania parasites have a complex life cycle which involves development within the sand fly insect vector before transmission to a mammalian host. Female sand flies ingest *Leishmania* parasites in the bloodmeal when they feed on an infected mammal (Bates, 2007). Due to the changes in environmental conditions as the parasites enter the fly midgut (decreased temperature and increased pH), parasites differentiate from immotile amastigote forms into procyclic promastigotes, elongated cells that move with the aid of a flagellum (Figure 1-2). At this stage, the bloodmeal and parasites are confined within the peritrophic matrix, a mesh composed of chitin and proteins secreted by the insect's midgut epithelium (Bates, 2007). Within the bloodmeal, procyclic promastigotes replicate, before undergoing differentiation into slender, strongly motile nectomonad forms after 2 - 3 days (Kamhawi, 2006). Degeneration of the peritrophic matrix, aided by chitinases secreted by *Leishmania*, allows nectomonads to migrate to the anterior midgut which they colonise by attachment to midgut epithelial cells (Kamhawi, 2006). *Leishmania* surface molecules, especially the abundant lipophosphoglycan (Späth et al., 2003), are important for binding to the sand fly midgut. LPG binds to sand fly epithelial galectins, and LPG structural polymorphisms amongst *Leishmania* species define the species of sand fly that each parasite species can colonise (Kamhawi, 2006).

Once nectomonad forms reach the stomodeal valve, separating the fly midgut and foregut, they transform into leptomonad promastigotes which resume replication (Figure 1-2). The leptomonads are also responsible for the production of promastigote secretory gel (PSG) which forms a plug that fills and blocks the thoracic midgut. By day 5 - 7, specialised leaf-shaped forms called haptomonads appear, although it is unknown whether these arise from nectomonads or leptomonads (Kamhawi, 2006). Haptomonads attach to the surface of the stomodeal valve through expansion of their anterior end to form hemidesmosome-like structures, and form a parasite plug; it is thought that they secrete chitinases that lead to degeneration of the valve, which aids parasite transmission (Bates, 2007). At the same time, leptomonads embedded in the PSG plug differentiate into mammalian-infective, non-replicative metacyclic promastigotes which move to the anterior end of the PSG plug (Rogers et al., 2002).

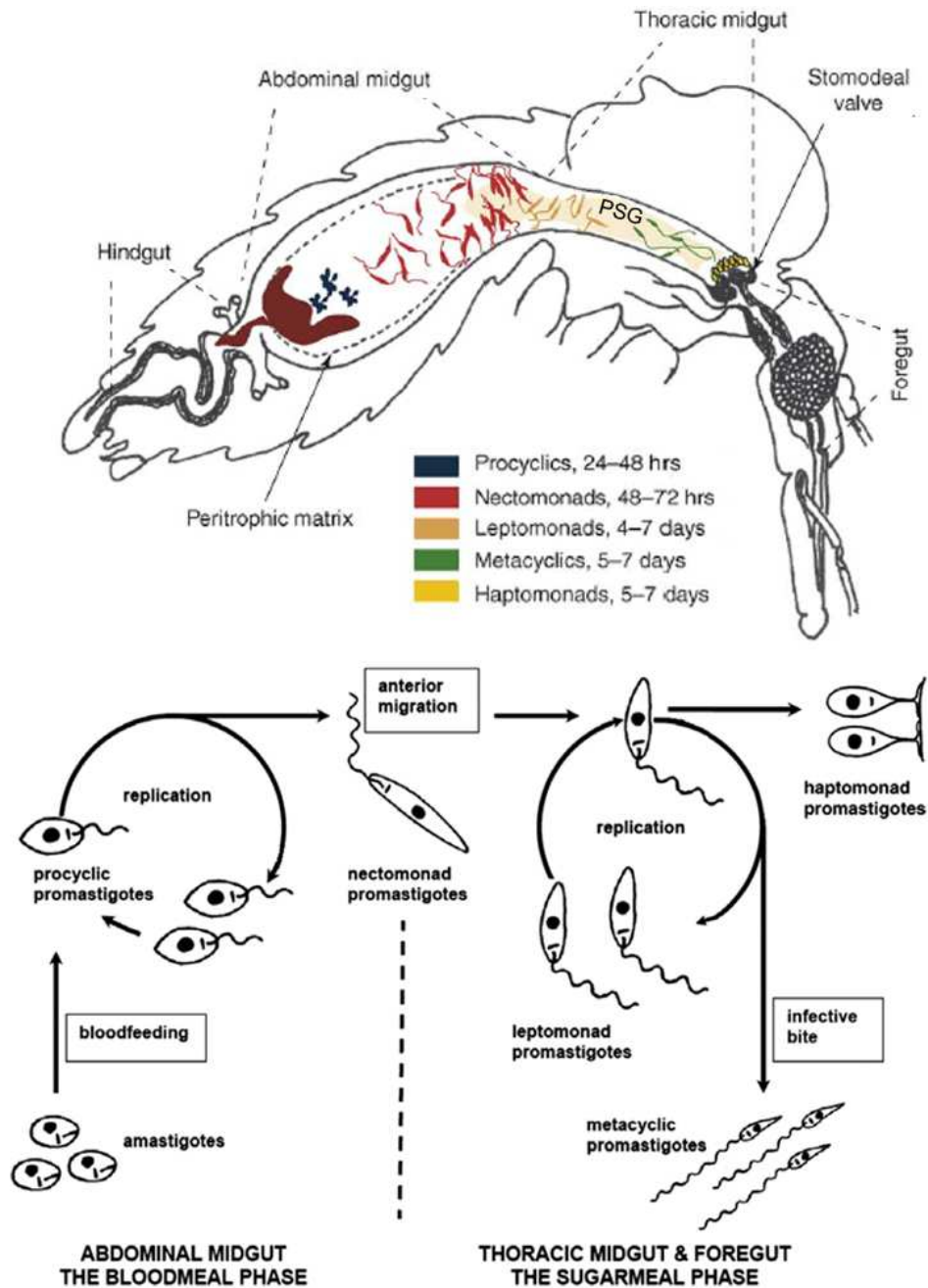


Figure 1-2 The life cycle of *Leishmania* within the sand fly insect vector. The parasite transits between various developmental forms as it migrates from the abdominal midgut up to the stomodeal valve and foregut, from whence infective forms are transmitted to the mammalian host when the sand fly feeds. Adapted from Kamhawi (2006) and Bates (2007).

The PSG, which is composed primarily of high molecular weight filamentous proteophosphoglycan (Rogers et al., 2004), obstructs the foregut and forces open the stomodeal valve so that the fly has difficulty feeding and is unable to ingest a full bloodmeal (Rogers et al., 2002). This results in infected sand flies feeding for longer and biting at greater frequency in order to drink their fill, which enhances transmission of *Leishmania* by increasing the number of

parasites injected into the host and enhancing the spread of the parasites as the fly feeds on multiple hosts (Rogers and Bates, 2007). Regurgitation of fPPG along with metacyclic promastigotes as the fly takes a bloodmeal has been shown to exacerbate disease (Rogers et al., 2004), suggesting that this component of PSG is important for transmission. Sand fly saliva is also known to aid in *Leishmania* transmission, as it contains molecules with vasodilatory, anti-coagulative and immuno-modulatory activities (Kamhawi, 2000). Damage to the stomodeal valve also contributes to *Leishmania* transmission by impairing sand fly feeding (Volf et al., 2004), which leads to longer and more frequent feeding periods.

1.1.3 The *Leishmania* life cycle: mammalian host

Upon entering the skin of a mammalian host through the bite of an infected sand fly, metacyclic promastigotes are taken up by a variety of host immune cells (Figure 1-3). Insertion of the insect's proboscis into the host tissue causes a strong localised inflammatory response, resulting in the rapid recruitment of neutrophils to the bite site. *L. major* parasites remain relatively immotile following their injection into the host skin, and are phagocytosed by neutrophils within 2 hours of infection (Peters et al., 2008). After 18 hours post infection, the majority of parasites remain within neutrophils, although some appear within macrophages and dendritic cells (DCs). By 6 - 7 days after infection most of the parasites are observed in the macrophage population, with only low numbers in neutrophils and DCs (Peters et al., 2008). Neutrophils are short-lived cells that usually have a half-life of 6 - 10 hours; however, *L. major*-infected neutrophils show a delay in apoptosis of 2 - 3 days (Aga et al., 2002). This is thought to suspend apoptosis of infected neutrophils until macrophages arrive at the site of infection. Apoptotic neutrophils containing viable *Leishmania* have been suggested to act as 'Trojan horses' which are phagocytosed by macrophages, passing the parasites silently to their final host cell without triggering anti-microbial immune responses (Laskay et al., 2003). The macrophage appears to be the major host cell of *Leishmania* because although the parasites can survive within neutrophils, they do not replicate or differentiate; these processes only occur within macrophages. *Leishmania* may also escape from dying neutrophils and be directly taken up by macrophages along with the apoptotic immune cells in a process termed the 'Trojan rabbit' (Ritter et al., 2009). In addition, promastigotes are able to directly enter

macrophages, as shown by recent *in vitro* work in which *L. donovani* (Forestier et al., 2011) and *L. major* (Wenzel et al., 2012) attached to macrophages with their flagellar tip, triggering engulfment of the parasite into a parasitophorous vacuole within the macrophage. This is also supported by data showing that in mice depleted of neutrophils, macrophages contained the same numbers of parasites as in non-depleted animals (Peters et al., 2008). Within the parasitophorous vacuole, metacyclic promastigotes differentiate into intracellular amastigotes (Figure 1-3), which replicate and are able to evade detection by the host's immune response. Amastigotes eventually escape from macrophages and re-infect new host cells (Figure 1-3), giving rise to the tissue destruction characteristic of the disease. *L. major* amastigotes readily infect macrophages, which they enter silently through an endocytic uptake mechanism that does not trigger release of pro-inflammatory cytokines (Wenzel et al., 2012), therefore protecting the parasite from immune destruction. The parasite life cycle continues when infected macrophages are taken up in the bloodmeal of a sand fly feeding on the host.

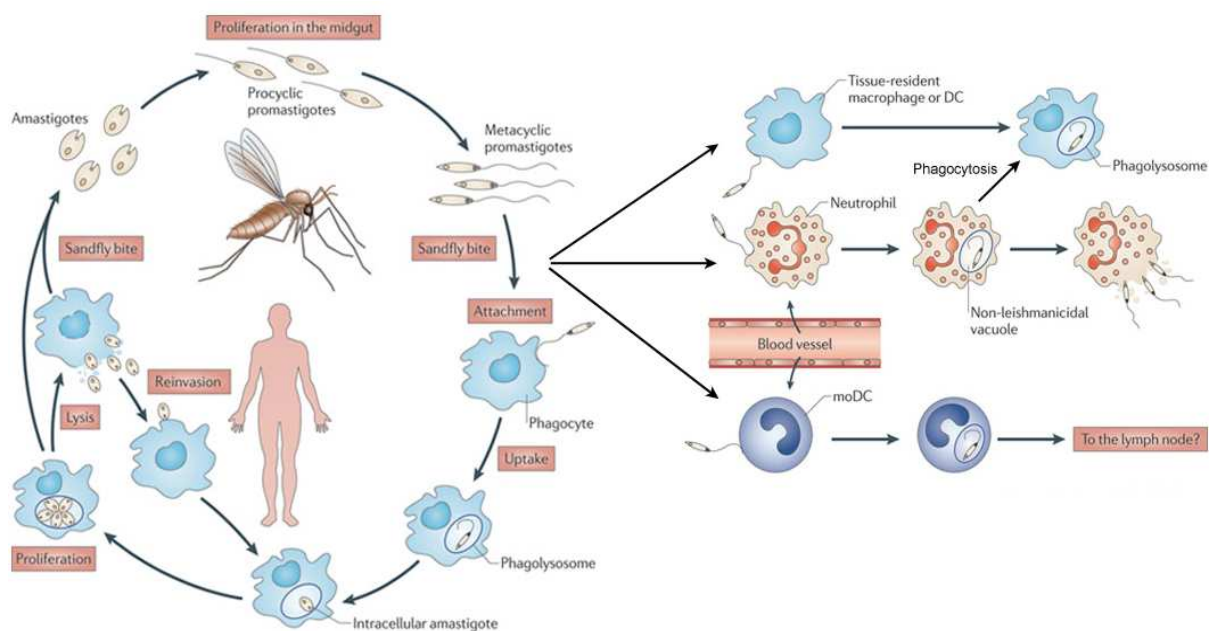


Figure 1-3 The Leishmania life cycle showing mammalian immune cells that are infected. Following their development into infective forms in the sand fly, *Leishmania* are transmitted to the vertebrate host in which they can infect various cells of the host immune system. Parasites eventually make their way to macrophages in which they differentiate and replicate, giving rise to clinical manifestations of leishmaniasis. The life cycle is completed when infected amastigotes are ingested by a sand fly feeding on the host. DC, dendritic cell; moDC, monocyte-derived dendritic cell. Adapted from (Kaye and Scott, 2011).

Dermal dendritic cells have been shown to phagocytose *Leishmania* parasites (Ng et al., 2008) and apoptotic neutrophils containing *Leishmania* (Ribeiro-Gomes et al., 2012) in the early stages of infection (Figure 1-3). Parasite uptake was selective and dependent on formation of pseudopodia (Ng et al., 2008). DCs containing parasites are expected to migrate to draining lymph nodes in order to present *Leishmania* antigens to T cells, generating an immune response against the pathogen, although no experimental evidence for this has been shown. Recently it has been suggested that the clearance of apoptotic neutrophils by DCs results in suppression of the T cell-mediated immune response and that this is exploited by *Leishmania* in order to establish infection (Ribeiro-Gomes et al., 2012).

To facilitate their survival within macrophages, *Leishmania* secrete a range of virulence factors, such as elongation factor 1 α , secreted acid phosphatase, fructose-1,6-bisphosphate aldolase, and the zinc metalloprotease GP63, that interfere with anti-microbial immune signalling pathways (Kaye and Scott, 2011; Lambertz et al., 2012). This results in down-regulation of the T helper 1 CD4⁺ cell (Th1)-mediated immune response, which is associated with macrophage activation, secretion of interferon- γ and interleukin (IL)-2, and elimination of intracellular pathogens. The parasites shift signalling to a Th2 immune response, which is associated with clearance of extracellular pathogens, allowing *Leishmania* to persist (Alexander and Brombacher, 2012). Exosomes, small extracellular vesicles that bud from the plasma membrane, are involved in the secretion and delivery of *Leishmania* virulence factors to host cells and appear to have roles in suppressing anti-leishmanial immune responses (Silverman et al., 2010a; Silverman et al., 2010b).

1.2 The *Leishmania* cell and differentiation

During their complex life cycle *Leishmania* parasites traverse various intra- and extracellular environments, each with different conditions such as changes in pH, temperature, and nutrient availability. To overcome these challenges, *Leishmania* possess different developmental forms, each structurally and functionally adapted to their environment. The promastigote forms found in the insect vector are motile, spindle-shaped cells with a cell body length of 6 - 12 μm and a flagellum 5 - 13 μm in length (Wheeler et al., 2011). The flagellum,

which extends from the anterior end of the cell, increases in length as promastigotes differentiate into highly motile metacyclic promastigotes that are adapted for effective transmission to the host (Figure 1-2). In contrast, intracellular amastigotes are immotile, rounded cells with a diameter of approximately 5 μm and a much reduced flagellum of $\sim 1.5 \mu\text{m}$ that does not protrude from the flagellar pocket (Figure 1-4). They are adapted to life within the acidic conditions of the parasitophorous vacuole and their metabolism is altered to take advantage of nutrients available in the host macrophage. Differentiation between life cycle stages is associated with developmentally regulated changes in gene expression, structural and functional modifications to organelles, and alterations in the expression of surface molecules. Some of these are discussed further below.

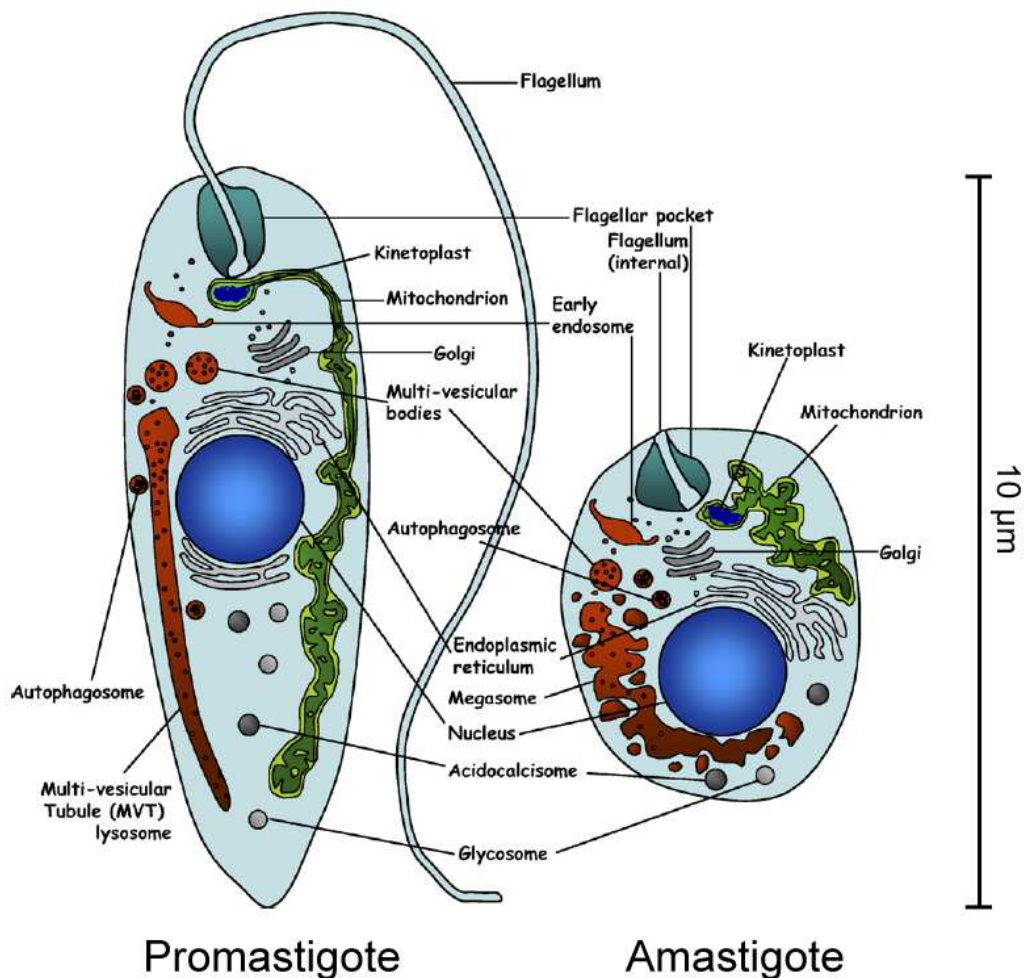


Figure 1-4 Schematic representation of *Leishmania* promastigote and amastigote forms including the main organelles. Adapted from (Besteiro et al., 2007).

1.2.1 *Leishmania* gene expression

The genomes of human-infective *Leishmania* species have been sequenced relatively recently; firstly *L. major* in 2005 (Ivens et al., 2005), followed by *L. infantum* and *L. braziliensis* (Peacock et al., 2007), and most recently *L. mexicana* (Rogers et al., 2011) and *L. donovani* (Downing et al., 2011). The genes of *L. major*, *L. donovani* and *L. infantum* are arranged over 36 chromosomes, whereas *L. mexicana* and *L. braziliensis* possess 34 and 35 chromosomes respectively, due to unique chromosome fusion events. Gene content and synteny appear highly conserved between species and there are only very few species-specific genes (Rogers et al., 2011). However, variations in gene copy number, due to the expansion of a single gene to create a multi-copy array or replication of whole chromosomes, are common in *Leishmania* (Rogers et al., 2011). Aneuploidy appears to be normal in these parasites; for example, chromosome 31 has undergone replication in all species, and other chromosomes are trisomic, tetrasomic or even pentasomic depending on the species. Changes in gene copy number can arise due to experimental conditions such as attempting to knock out genes or inducing drug resistance (Mannaert et al., 2012). It is possible that this mechanism also contributes to altered gene expression in response to different environmental conditions in the host, which may provide a genetic basis for disease tropism (Rogers et al., 2011).

Leishmania and other kinetoplastids are unusual in that their gene expression is not under transcriptional control. Instead, protein coding genes are organised into long tandem arrays and transcribed together as polycistrons of 10 - 100 genes that are often functionally unrelated. Polycistrons are then processed into mature mRNAs by trans-splicing at the 5' end and polyadenylation at the 3' end (Kramer, 2012). As all polycistronic RNAs are believed to be transcribed at a similar rate, control of gene expression must occur post-transcriptionally. This is achieved through trans-splicing, controlled changes in mRNA stability, translational control, protein degradation, and post-translational modifications, such as phosphorylation or ubiquitination, which result in changes to protein localisation, activity and/or binding (Kramer, 2012). It is likely that gene expression is developmentally regulated in order to quickly adapt parasites to their changing life cycle requirements, and that this control is triggered by environmental changes. Proteomic studies have revealed developmental changes

in protein expression in *Leishmania*; for example, in promastigotes flagellar proteins and glycolytic enzymes are up-regulated, whereas enzymes involved in gluconeogenesis and fatty acid β -oxidation are more abundant in amastigotes (Rosenzweig et al., 2008b; Brotherton et al., 2010). During *L. donovani* promastigote - amastigote differentiation, changes in gene expression are primarily regulated by changes in mRNA levels in the early stages whereas translational and post-translational control are more important in later stages of differentiation (Lahav et al., 2011). Differentiation is also associated with a transient global increase in protein synthesis, presumably as cells are producing proteins important for survival in their new environment. Changes in levels of post-translational modifications such as phosphorylation, methylation and glycosylation have also been recorded during promastigote - amastigote differentiation of *L. donovani* (Rosenzweig et al., 2008a). Comparison of phosphoproteins from different *L. donovani* life cycle stages found that phosphorylation of heat shock proteins and chaperones was increased in amastigotes (Morales et al., 2010). This suggests that phosphorylation is involved in the activation of these proteins, which are important for adaptation to the increased temperature within the mammalian host.

1.2.2 Changes in the expression of surface molecules

The surface of *Leishmania* promastigotes is coated with a dense glycocalyx comprised of LPG, glycosylphosphatidylinositol (GPI)-anchored glycoproteins, proteophosphoglycans and glycoinositolphospholipids (GIPLs). Of these, only LPG is important for the establishment of infection in the host; *L. major* mutants lacking LPG show attenuated virulence due to increased susceptibility to human complement and oxidant-mediated killing (Späth et al., 2003). LPG is also important for the attachment of promastigotes to the midgut epithelium whilst in the sand fly (Kamhawi, 2006). Upon differentiation to amastigotes, the expression of LPG and other surface macromolecules is down-regulated and the parasite surface is primarily covered by GIPLs and host-derived glycosphingolipids (Naderer and McConville, 2008). The latter are thought to shield *Leishmania* from detection by the host immune system. The amastigote plasma membrane contains high levels of exposed phosphatidylserine (PS) that mimics the exposure of PS by apoptotic cells, allowing their uptake into

macrophages without triggering an anti-microbial response (Wanderley et al., 2006).

The stage-regulated proteins HASPB and SHERP, encoded by the *cDNA16* locus, are expressed only in infective stage parasites, i.e. metacyclic promastigotes and amastigotes (McKean et al., 2001). Although found to be unimportant for host invasion (McKean et al., 2001), expression of these proteins is essential for development of metacyclic promastigotes in the sand fly vector (Sádlová et al., 2010). Further study of HASPB showed that it localised to the surface of metacyclic promastigotes and was shed as parasites infected macrophages so that HASPB was absent from the amastigote cell surface (MacLean et al., 2012).

1.2.3 The mitochondrion

Leishmania possess a single, reticulate mitochondrion that extends the length of the cell (Figure 1-4). This is in contrast to multicellular eukaryotes, which contain hundreds of mitochondria per cell. The primary role of the mitochondrion is the generation of ATP through oxidative phosphorylation, although it also has roles in the biosynthesis of fatty acids and sterols, and is linked to the regulation of apoptosis (de Souza et al., 2009). Trypanosomatid mitochondria also contain a kinetoplast, consisting of tightly packed circular DNA molecules that together represent approximately 30 % of total cellular DNA. The DNA rings of the kinetoplast can be divided into maxicircles and minicircles. Maxicircles encode ribosomal RNAs and subunits of mitochondrial respiratory complexes, whilst minicircles encode guide RNAs that are involved in RNA editing of maxicircle transcripts (de Souza et al., 2009).

During promastigote - amastigote differentiation, the size of the cell decreases, and the relative cell volume occupied by the mitochondrion is slightly but significantly reduced (Brun and Krassner, 1976), indicating a reduction in mitochondrial size. However, it is unclear how this reduction in size occurs, as no evidence exists for fragmentation or degradation of the *Leishmania* mitochondrion during differentiation or normal growth. A recent comparison of the mitochondrion in *L. donovani* suggests that, unlike that of promastigotes, the mitochondrion of amastigotes does not perform oxidative phosphorylation; instead, alternative mechanisms are used to generate energy within the hypoxic

environment of the parasitophorous vacuole (Chakraborty et al., 2010). This may provide an explanation for the reduced size of this organelle in amastigotes.

The mitochondrion can be labelled with various dyes that localise to this organelle depending on its membrane potential; these include MitoTracker Red and TMRM (Invitrogen Molecular Probes®). In addition, MitoTracker Green labels mitochondria irrespective of their membrane potential. Fluorescently tagged mitochondrial proteins can also be used; for example, in *Leishmania* both a mitochondrial serine peptidase (ROM-GFP) and a ubiquitin-like protein peptidase (MUP-GFP) localise to the mitochondrion (Williams et al., 2012b).

1.2.4 Glycosomes

Glycosomes are peroxisome-like organelles that compartmentalise enzymes of several metabolic pathways, including glycolysis, the pentose-phosphate pathway, β -oxidation of fatty acids, purine salvage, and biosynthetic pathways for pyrimidines, ether lipids and squalenes (Michels et al., 2006). The kinetoplastida are unique in the sequestration of glycolysis within organelles, as in other organisms this pathway is primarily cytosolic. Compartmentalisation of metabolic pathways in this manner is thought to benefit the parasitic lifestyle of kinetoplastids by allowing them to quickly and efficiently adapt to changes in available metabolites as they transition between insect and mammalian environments (Gualdrón-López et al., 2012).

The metabolism of *Leishmania* developmental forms is adapted to the conditions encountered at each stage; promastigotes exhibit up-regulation of glycolytic enzymes, whilst in amastigotes the expression of enzymes involved in gluconeogenesis, amino acid metabolism and β -oxidation of fatty acids is increased, and expression of pentose-phosphate pathway enzymes decreases (Rosenzweig et al., 2008b; Brotherton et al., 2010). These metabolic changes reflect the primary nutrient sources that are utilised by the parasites in the sand fly (glucose) and mammalian macrophage (fatty acids and amino acids). The number of glycosomes per cell also decreases upon promastigote - amastigote differentiation, from an estimated 50 - 100 in promastigotes (Opperdoes, 1987) to around 10 in amastigotes (Coombs et al., 1986), although these numbers were determined in different *Leishmania* species. The decrease in glycosome numbers

may be a consequence of the reduced reliance of amastigotes on glycolysis and/or the reduction in cell volume.

Glycosomal proteins contain a C-terminal tripeptide sequence that allows them to be packaged into glycosomes, and this peroxisomal targeting sequence (PTS) fused to a fluorescent protein has been shown to label these organelles (Sommer et al., 1992; Plewes et al., 2003). Immunofluorescence analysis using antibodies against known glycosomal proteins can also be used (Plewes et al., 2003).

1.2.5 Acidocalcisomes

Acidocalcisomes are acidic organelles for the storage of calcium and phosphorus (in the form of inorganic pyrophosphate and poly P chains) that have been identified in a number of eukaryotic and prokaryotic organisms. The acidocalcisome membrane differs from the composition of other organellar membranes and contains several pumps and exchangers, which are responsible for the concentration of protons and cations within the acidocalcisome (Docampo et al., 2010). As well as their functions in cation and phosphorus storage, acidocalcisomes play important roles in pH homeostasis and osmoregulation, which are thought to be required for dealing with the extreme environmental changes encountered by parasites during their life cycles (Moreno and Docampo, 2009).

In *L. major*, acidocalcisomes are present at a low level in replicating promastigotes but increased in infective stationary phase parasites and amastigotes (Zhang et al., 2005), suggesting important roles in transmission. In support of this, a *L. major* TOR3 kinase null mutant, which showed defects in acidocalcisome formation, was unable to survive within macrophages or establish infections in mice (Madeira da Silva and Beverley, 2010). This attenuated virulence was associated with defects in poly P accumulation within acidocalcisomes, leading to an inability to survive osmotic stress.

As they are acidic organelles, acidocalcisomes can be labelled with acidotropic dyes such as LysoTracker or Acridine Orange, although these also localise to the lysosome so are non-specific (Besteiro et al., 2008). The membrane proton pump

V-H⁺-PPase fused with GFP has been shown to be a specific marker for acidocalcisomes in *Leishmania* (Besteiro et al., 2008).

1.2.6 The flagellum

The flagellum plays important roles in both promastigotes and amastigotes of *Leishmania*. In promastigotes, it generates motility and mediates attachment to the sand fly midgut epithelium, processes that are critical for survival within the insect vector and transmission to the vertebrate host. During promastigote - amastigote differentiation there is considerable shortening and remodelling of the flagellum. The regulation of flagellar length in *Leishmania* is thought to be mediated by intraflagellar transport (IFT), a process in which cargoes can be transported bi-directionally along the flagellum by opposing molecular motors, kinesin and dynein, responsible for anterograde and retrograde transport, respectively (Gluenz et al., 2010a). It is also possible that IFT-independent mechanisms are involved in maintenance of flagellar length.

The flagellum of the immotile, intracellular amastigotes, rather than being just a shortened version of the promastigote flagellum, is in fact structurally different. Whereas the promastigote flagellum contains axoneme microtubules arranged in a canonical 9 + 2 pattern, that of the amastigote has a 9 + 0 (or 9v) structure, reminiscent of sensory cilia from other organisms (Gluenz et al., 2010b). Interestingly, *L. mexicana* amastigotes within the parasitophorous vacuole were observed to orientate themselves such that the flagellum tip, which just emerges from the flagellar pocket, closely associated with the vacuole membrane (Gluenz et al., 2010b), suggesting that the amastigote flagellum has roles in parasite - host interactions. These could include sensing of the environment, cell - cell signalling processes, or orientation of the parasite in order to direct secreted factors from the flagellar pocket toward the host cell.

The flagellum has primarily been studied by electron microscopy, although antibodies against proteins present in the flagellum, such as paraflagellar rod protein (Annoura et al., 2012), tubulin (Katta et al., 2009) or aquaglyceroporin (Figarella et al., 2007), have been used for immunofluorescence analysis.

1.2.7 The endo-lysosomal system

The flagellar pocket, an invagination at the anterior end of the parasite from which the flagellum emerges, is a highly specialised region of the cell membrane responsible for endocytosis, secretion of proteins, and the transfer of integral membrane proteins to the cell surface (Landfear and Ignatushchenko, 2001). As the only site of endocytosis, the flagellar pocket is the entry point to the endo-lysosomal system, a network of interconnected vesicles and tubules that is concentrated in the region between the nucleus and flagellar pocket. This network functions to sort endocytosed material, newly synthesised proteins from the *trans*-Golgi network, and internalised membrane proteins into the correct compartments for their degradation, secretion, recycling or trafficking to the cell surface. Endocytosed material is taken up into a vesicle, formed from the flagellar pocket membrane, which then fuses with early endosomes. Through a series of vesicle fusion and fission events involving protein sorting, early endosomes undergo maturation into acidic late endosomes, which may acquire intra-luminal vesicles and become multi-vesicular bodies (MVBs). Late endosomes deliver their contents to lysosomes, in which they are degraded; sugars, amino acids and lipids resulting from degradation can be transported back across the lysosomal membrane into the cytosol where they can be utilised by the cell. In addition to its roles in nutrient acquisition from the extracellular environment, the *Leishmania* endo-lysosomal system plays important roles in immune evasion through the internalisation and destruction of MHC class II molecules and associated proteins (Antoine et al., 1999).

Using various endocytic tracers such as fluorescent dextrans (Ghedini et al., 2001) and FM4-64 (Mullin et al., 2001), which are taken up and trafficked through the endosomal system to the lysosome, various compartments of this vesicular network have been characterised in *Leishmania*. Early and recycling endosomes are labelled by the proteins Rab5 and Rab11, respectively (Singh et al., 2003; Ambit et al., 2011), whereas Rab7 co-localises on late endosomal compartments with the lectin concanavalin A (Denny et al., 2002).

Due to the extensive cellular remodelling that occurs during *Leishmania* differentiation, protein turnover is greatly increased, as evidenced by the evolution of lysosome morphology and associated increases in expression of

peptidases throughout the life cycle. Using the lysosomal markers proCPB-RFP (the prodomain of lysosomal cysteine peptidase B) and GFP-syntaxin (a lysosomal SNARE protein), it has been shown that in procyclic promastigotes the lysosomal compartment appears as a single large vesicular compartment at the anterior end of the cell (Huete-Pérez et al., 1999; Besteiro et al., 2006b). After differentiation to the metacyclic promastigote a tubular lysosomal compartment, termed the multivesicular tubule (MVT) or MVT-lysosome, is observed (Mullin et al., 2001; Besteiro et al., 2006b). The intracellular amastigotes possess characteristic large lysosomal compartments known as megasomes which vary in size and number depending on the *Leishmania* species (Coombs et al., 1986; Ueda-Nakamura et al., 2001). The change in lysosome morphology to the megasomes of amastigotes is associated with the increased expression of lysosomal cysteine peptidases (Brooks et al., 2001; Ueda-Nakamura et al., 2002) and similarly, an increase in overall proteolytic activity is observed during procyclic - metacyclic differentiation which correlates with formation of the MVT-lysosome (Mullin et al., 2001). As the final compartment of the endo-lysosomal system, the lysosome mediates the degradation of numerous proteins, making it critical for the maintenance of cellular homeostasis. Another pathway involved in the trafficking of proteins to the lysosomal compartment is autophagy, an important protein turnover mechanism which is required for cellular homeostasis, survival during stress conditions, and *Leishmania* differentiation.

1.3 Autophagy

Autophagy (from the Greek “self-eating”) is an intracellular degradative pathway in which the cell targets its own proteins and organelles to the lysosome for degradation. This process is conserved amongst eukaryotes, highlighting the importance it plays in cellular homeostasis, surviving various stresses, and cellular remodelling during adaptation or developmental differentiation. During the last 10 - 15 years, there has been an explosion in autophagy research due to the discovery that deregulation of this pathway is involved in cancer, ageing, microbial infection, neurodegenerative disorders including Alzheimer’s, Parkinson’s and Huntington’s diseases, and inflammatory disorders such as Crohn’s disease and cystic fibrosis (Mizushima et al., 2008; Wong et al., 2011). This has led to great advances in our understanding of the

mechanisms underlying autophagy and the molecular machinery involved in its regulation.

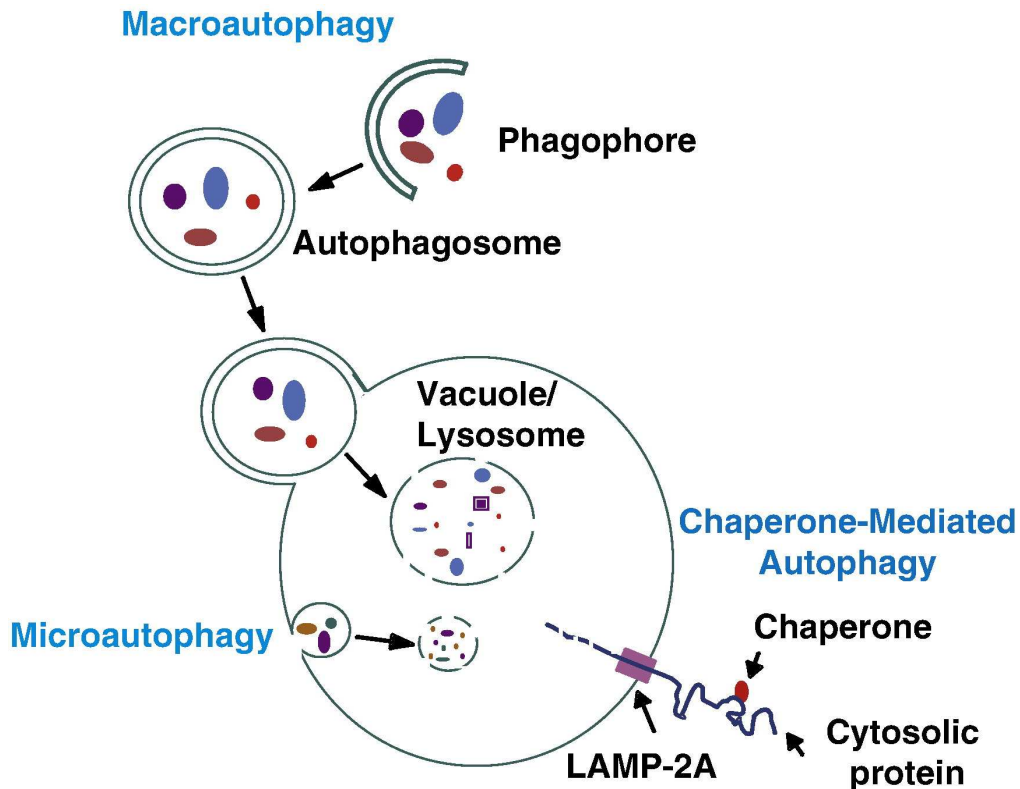


Figure 1-5 Schematic showing the three major types of autophagy. Macroautophagy results in formation of a double-membrane autophagosome that engulfs bulk cytoplasm, organelles or protein aggregates and trafficks its cargo to the lysosome. In microautophagy cargoes are directly sequestered by invaginations in the lysosomal membrane. Chaperone-mediated autophagy, which has only been described in higher eukaryotes, targets specific cytosolic proteins which are unfolded and translocated across the lysosomal membrane by a chaperone (hsc70) and LAMP-2A. Following degradation of autophagic cargoes, their constituents are transported out of the lysosome and can be re-used by the cell. From (Dargemont and Ossareh-Nazari, 2012); permission to re-use this figure granted by Elsevier Ltd. (License number: 3063570184638).

Three types of autophagy have been described (Figure 1-5); macroautophagy, microautophagy and chaperone-mediated autophagy (CMA). Macroautophagy is the best studied of these, and therefore is often referred to simply as ‘autophagy’. It is characterised by the formation of a double-membrane vesicle called the autophagosome, which sequesters cargo for transportation to the lysosome. Microautophagy involves the direct uptake of cargo into the lysosome through invaginations of the lysosomal membrane (Li et al., 2012b), whereas CMA mediates the selective degradation of KFERQ motif-containing proteins through the combined actions of the cytosolic chaperone hsc70 and the lysosomal membrane protein LAMP-2A (Arias and Cuervo, 2011). Both macro- and

microautophagy can occur selectively, in which a specific cargo is targeted for degradation (discussed in detail in Chapter 3), or non-selectively, in which bulk cytoplasm and its contents are degraded. Autophagy mediates the removal of damaged or superfluous proteins and organelles, and is therefore critical for maintaining cellular homeostasis. As macroautophagy is the most common and best characterised form of autophagy, it will be discussed further in the following sections.

1.3.1 The molecular machinery of autophagy

From genetic screens in the model yeast *Saccharomyces cerevisiae*, over 30 genes involved in the regulation of macroautophagy and related processes have been identified. These are known as *ATG* (AuTophagy-related) genes and encode proteins that act at various stages of the autophagy process or are required for certain selective forms of autophagy. The core *ATG* genes that are required for autophagosome formation are conserved across eukaryotes, but those required for selective forms of autophagy are not (Meijer et al., 2007; Duzenko et al., 2011), suggesting that different organisms use different mechanisms for autophagic degradation of specific cargoes. Autophagosome formation can be divided into successive steps (Figure 1-6 A), which are described below with details of the yeast molecular machinery involved at each stage.

1. Sensing & Autophagy Induction: A low level of basal autophagy occurs in cells under normal growth conditions, which is crucial for maintaining homeostasis. Upon encountering stress conditions, cells utilise efficient signalling mechanisms for the rapid induction of autophagy. Nutrient starvation is known to induce autophagy in all organisms tested. Nutrient sensing pathways involve target of rapamycin (TOR), a serine/threonine protein kinase that forms two distinct complexes, TOR complex 1 (TORC1) and TOR complex 2 (TORC2). TORC1 negatively regulates autophagy (Noda and Ohsumi, 1998), and TOR kinase inhibitors such as rapamycin have been widely used to induce autophagy in experimental systems (Mizushima et al., 2011). Under nutrient-rich conditions TORC1 hyperphosphorylates Atg13, reducing its binding affinity for the Atg1 protein kinase (Kamada et al., 2010) and preventing formation of the Atg1 kinase complex. During starvation- or rapamycin-induced inhibition of TORC1, Atg13 is able to bind to Atg1, leading to association of Atg1-Atg13 with the

Atg17-Atg31-Atg29 complex (Kawamata et al., 2008). Formation of this Atg1 kinase complex results in recruitment of downstream Atg proteins to the site of autophagosome formation, known as the phagophore assembly site or pre-autophagosomal structure (PAS).

In addition to TORC1 signalling, the Atg1 kinase complex is independently regulated by the cAMP-dependent protein kinase A (PKA) pathway (Stephan et al., 2009), which is important for glucose-sensing. Elevated PKA activation inhibits autophagy, and this control is mediated by phosphorylation of Atg13, but at different residues to those phosphorylated by TORC1.

2. Cargo Selection & Vesicle Nucleation: In the case of selective autophagy, specific proteins are involved at this stage of autophagosome formation for the selective recruitment of various cargoes to the PAS. For example, Atg30 or Atg36 recruit peroxisomes for autophagic degradation, and Atg32 is involved in selective autophagy of mitochondria. An adaptor protein, Atg11, links these cargo-specific proteins to the core autophagy machinery at the PAS. Non-selective autophagy results in formation of the autophagosome around a portion of cytoplasm and so no cargo recruitment machinery is required.

Vesicle nucleation refers to the initiation of the autophagosomal membrane structure. This requires formation of the class III phosphatidylinositol 3-kinase (PI3K) complex, which is made up of the PI3K Vps34, a serine/threonine kinase Vps15, Atg6 and Atg14. This complex is essential for autophagy and functions to enrich PAS membranes in phosphatidylinositol 3-phosphate (Filimonenko et al., 2010) which in turn leads to the recruitment of various PI3P-binding Atg proteins (Obara et al., 2008a; Obara et al., 2008b). One of these is Atg18, which forms a complex with Atg2, and facilitates the recruitment of Atg8-PE to the PAS as well as protecting it from premature deconjugation by the cysteine peptidase Atg4 (Nair et al., 2010). The precise role of the Atg18-Atg2 complex in autophagy is unknown, but it is also involved in the retrograde movement of Atg9 away from the PAS.

Atg9 is an integral membrane protein that is required for autophagosome formation (Noda et al., 2000). It forms a complex with Atg23 and Atg27 that localises to the PAS and peripheral punctate structures (Legakis et al., 2007),

and is thought to cycle between these sites in order to deliver membrane lipids to the forming autophagosome. Atg9 is recruited to the PAS downstream of Atg1 kinase complex formation and is recruited through interactions with Atg17 (Sekito et al., 2009). The ability of Atg9 to self-multimerise also appears essential to its function in phagophore expansion (He et al., 2008). The identity of the peripheral Atg9-labelled puncta is unknown but they have been suggested to be a novel compartment of tubules and vesicles adjacent to mitochondria (Mari et al., 2010). However, recent work employing high-sensitivity live microscopy shows that Atg9 is located on highly mobile cytoplasmic vesicles that are generated *de novo* from the Golgi apparatus upon autophagy induction in a process requiring Atg23 and Atg27 (Yamamoto et al., 2012). During starvation a small number of Atg9 vesicles assemble at the PAS and Atg9 ultimately becomes embedded in the outer autophagosomal membrane. Following autophagosome completion Atg9 is recycled back to the cytoplasm in vesicles formed during autophagosome-vacuole fusion (Yamamoto et al., 2012).

3. Vesicle Expansion & Completion: The expansion and completion of the autophagosome requires two ubiquitin-like conjugation systems (Figure 1-6 B). The first of these results in the conjugation of the C-terminal glycine residue of Atg12 to an internal lysine residue of Atg5 (Mizushima et al., 1998). This attachment is mediated by the subsequent actions of the E1-like Atg7 and the E2-like Atg10. The Atg12-Atg5 conjugate interacts with a coiled-coil protein Atg16, which is essential for recruitment of Atg12-Atg5 to the PAS (Suzuki et al., 2007). The self-oligomerisation of Atg16 results in formation of an Atg12-Atg5:Atg16 multimeric complex (Kuma et al., 2002).

The second system is responsible for the attachment of the ubiquitin-like protein Atg8 to phosphatidylethanolamine (PE). Firstly, the C-terminal arginine residue of Atg8 is cleaved by the cysteine peptidase Atg4, exposing a glycine residue (Kirisako et al., 2000). This processing allows Atg8 to be activated by Atg7 and then transferred to the E2-like enzyme Atg3 (Ichimura et al., 2000). Finally, an amide bond is formed between Atg8 and PE, facilitated by the E3 activity of Atg12-Atg5:Atg16 (Hanada et al., 2007); localisation of Atg8 to the PAS requires Atg12-Atg5:Atg16 (Suzuki et al., 2007). Lipidated Atg8 functions in the expansion of the autophagosomal vesicle (Xie et al., 2008); this function has been attributed to its ability to mediate the tethering and hemifusion of membranes

in vitro (Nakatogawa et al., 2007). Due to the molecular geometry of PE, its incorporation into lipid bilayers exerts a curvature stress on membranes (van Meer et al., 2008), which may explain the significance of this phospholipid in autophagosome formation. Following completion of the autophagosome, Atg8 on the outside of the vesicle is deconjugated from PE by Atg4 (Figure 1-6 C); this is necessary for optimal autophagosome formation as it allows Atg8 to be recycled back to the PAS to participate in further rounds of phagophore expansion, and is also a prerequisite for the retrieval of other Atg proteins from the completed autophagosome (Nair et al., 2012). Atg4-mediated deconjugation is also critical for the removal of Atg8 from various organelles, such as the vacuole, ER and endosomes, on which it accumulates through conjugation to PE in organelle membranes (Nakatogawa et al., 2012; Yu et al., 2012). This maintains a reservoir of unlipidated Atg8 that can be recruited to the PAS for autophagosome biogenesis.

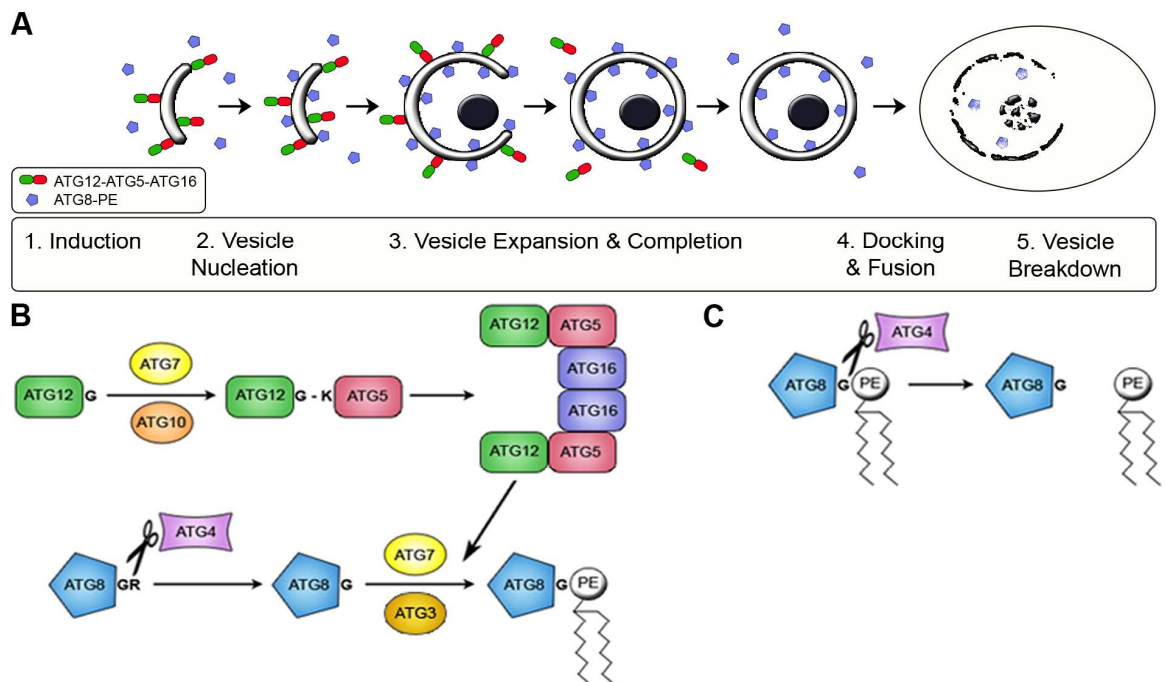


Figure 1-6 The macroautophagy pathway and the ATG8 and ATG12 conjugation systems. A. The participation of the Atg8 and Atg12 conjugation systems in autophagosome formation, which has been separated into various stages. B. The Atg proteins involved in the Atg8 and Atg12 systems. C. Deconjugation of Atg8 from PE is mediated by the cysteine peptidase Atg4.

Atg12-Atg5-Atg16 localises to the outer surface of early autophagosomal structures, and dissociates upon autophagosome completion. Atg8-PE is anchored on both inner and outer membranes from whence it controls

phagophore expansion. Although Atg8 on the surface of the vesicle is removed upon autophagosome closure, Atg8-PE remains associated with the inner membrane until the vesicle and its contents are degraded in the vacuole/lysosome (Figure 1-6 A). The ability of researchers to utilise Atg12/Atg5 and Atg8 as autophagosomal markers to follow the formation and trafficking of these structures has been fundamental to autophagy research.

Contrary to previous studies (Nakatogawa et al., 2007), recent work suggests that phagophore expansion by Atg8-PE through membrane hemifusion is unlikely to occur at physiological levels of PE (Nair et al., 2011). Instead, these authors suggest that autophagosome expansion and closure proceeds via a SNARE-dependent mechanism. Exocytic Q/t-SNAREs are implicated in this process, and appear to be involved in the organisation of Atg9 into tubulovesicular clusters that may form the early PAS, although further studies are required to gain direct evidence for this (Nair et al., 2011).

There is some evidence that autophagosome formation is regulated post-translationally: the acetylation of Atg5, Atg7, Atg8 and Atg12 by the p300 acetyltransferase negatively regulates their activity (Lee and Finkel, 2009), and phosphorylation of LC3 (the mammalian homologue of Atg8) reduces its recruitment to autophagosomes (Cherra et al., 2010).

4. Docking & Fusion: The cleavage of Atg8 from PE in the outer membrane of the autophagosomal membrane by Atg4 appears to be crucial for the maturation of autophagosomes into structures capable of fusing with the vacuole (Yu et al., 2012). Fusion of autophagosomes with the yeast vacuole requires the machinery necessary for homotypic vacuole membrane fusion events: the Rab GTPase Ypt7, the NSF homologue Sec18, the SNARE family proteins Vam3, Vam7, Vti1 and Ykt6, the class C Vps/HOPS complex, and two additional proteins Ccz1 and Mon1 (He and Klionsky, 2009). Autophagosome - vacuole fusion results in the release of the inner autophagic vesicle into the vacuole lumen, whereas the outer autophagosomal membrane becomes continuous with that of the vacuole.

5. Vesicle Breakdown: Within the vacuole, the inner autophagic vesicle and its contents are degraded by vacuolar hydrolases, such as peptidase A (PEP4) and B (PRB1), and the lipase Atg15. The small molecules resulting from this

degradation are recycled back into the cytoplasm by vacuolar permeases, such as Atg22, Avt3 and Avt4, which mediate the efflux of amino acids (He and Klionsky, 2009).

Other components required for autophagy: As well as the core Atg proteins, other cellular components are known to play important roles in autophagy. These include components of the secretory pathway, such as Sec12, Sec16, Sec23 and Sec24, which are required for autophagosome formation, and components of the NSF/SNARE membrane fusion machinery, which are required for autophagosome fusion with the vacuole (Ishihara et al., 2001). Trs85, a component of the TRAPP (transport protein particle) complexes, which regulate ER - Golgi and intra-Golgi trafficking, is also known to be essential for autophagy in yeast (Nazarko et al., 2005). These suggest that the secretory pathway may be important for sorting Atg proteins or be involved in membrane trafficking during autophagy. In mammalian cells autophagosomes are known to fuse with endosomes (Köchler et al., 2006), and mutants with defects in ESCRT (endosomal sorting complex required for transport) subunits display defects in autophagosome delivery to the lysosome (Filimonenko et al., 2007), suggesting important links between the endosomal system and autophagosome trafficking.

The movement of intracellular vesicles depends on cytoskeletal networks. In yeast, the actin cytoskeleton is required for selective but not non-selective forms of autophagy, being important for the recruitment of cargo to the PAS and for correct cycling of Atg9 (Reggiori et al., 2005). In mammals, microtubules are important for the movement of autophagosomes from the cell periphery to the microtubule organising centre where they fuse with endosomes and lysosomes (Köchler et al., 2006; Jahreiss et al., 2008). Movement of autophagosomes along microtubule tracks is driven by dynein motors.

1.3.2 The origin of autophagic membranes

The source of lipids for the biogenesis of autophagosomal membranes is not well understood, and various organelles have been suggested to be involved. In yeast, autophagosome formation occurs at a distinct region, the PAS, so membrane lipids must be trafficked to this site. Components of the secretory pathway and ER - Golgi trafficking are important for autophagosome formation (Ishihara et

al., 2001; Nazarko et al., 2005), and loss of proteins involved in the exit of vesicles from the Golgi disrupt localisation of Atg8 and Atg9 to the PAS and inhibit phagophore expansion (Yen et al., 2010; Geng et al., 2010; van der Vaart et al., 2010), providing evidence that membrane is delivered to the PAS from the Golgi. This delivery process appears to be mediated by Atg9 vesicles (Yamamoto et al., 2012). Atg9-labelled compartments localised close to mitochondria have also been implicated in this process, although this study also concluded that these structures originated from the secretory pathway (Mari et al., 2010).

Within mammalian cells, in contrast to yeast, autophagosomes appear to be formed throughout the cell with no defined location. As such, multiple sites for autophagosome biogenesis have been reported, including the ER, mitochondria, and plasma membrane. The majority of evidence supports the ER as the site of autophagosome biogenesis. Upon autophagy induction, a region of the ER membrane becomes enriched in PI3P, leading to the recruitment of machinery involved in autophagosome formation (Axe et al., 2008). This specialised membrane, termed the omegasome, appears to act as a platform from which autophagosomes are generated. Electron tomography has revealed that forming autophagosomes are connected to the ER by narrow membrane extensions (Hayashi-Nishino et al., 2009; Yla-Anttila et al., 2009), suggesting that autophagosomal membrane is derived from the ER.

Autophagosomes have also been observed to form from the mitochondrial outer membrane, but only during starvation-induced autophagy (Hailey et al., 2010). These authors found that both Atg5 and LC3 transiently localised to puncta on mitochondria, and observed the transfer of fluorescently-labelled lipid from the mitochondria to autophagosomes. Evidence suggests that mitochondrial lipids, but not proteins, can be transferred to autophagosomes. Interestingly, autophagosome biogenesis from mitochondria was dependent on connections between the ER and mitochondria, suggesting that PE taken from the mitochondria during autophagosome expansion is replenished by lipids from the ER.

Another study found that vesicles labelled with Atg16L1 were generated close to the plasma membrane, and suggests that these structures contribute to the formation of autophagosomes (Ravikumar et al., 2010). This is dependent on the

interaction of Atg16L1 with the heavy chain of clathrin during clathrin-mediated endocytosis at the plasma membrane, which results in formation of Atg16L1 vesicles which deliver membrane lipids for autophagosome biogenesis. Mammalian Atg9 associates with the Golgi and endosomes (Young et al., 2006) and cycles from these organelles to expanding autophagosomes during autophagy induction (Orsi et al., 2012), suggesting that, similarly to in yeast, Atg9 is responsible for the delivery of lipids from these structures to early autophagosomes.

The ability of mammalian cells to utilise a variety of membrane sources for autophagosome formation may be important for responding quickly to autophagy induction, as autophagic structures can be formed rapidly using the most convenient membrane source, or different membrane sources may be important during different stimuli. It also ensures that no one membrane source will be depleted of PE during periods of extensive autophagy induction.

1.3.3 Autophagic cell death

Cell death is often accompanied by autophagy, which has therefore been implicated as a cell death mechanism. However, this is controversial, as stress conditions leading to cell death also induce autophagy as a survival response, so the presence of autophagy in dying cells does not mean autophagy is responsible. Although evidence exists for genuine autophagic cell death (also known as type II programmed cell death (PCD)), this process remains poorly defined. Recent guidelines suggest that autophagic cell death can only be proven when (i) cell death occurs independently of apoptosis, (ii) autophagic flux is increased, rather than just the presence of autophagic markers, and (iii) suppression of autophagy by both pharmacological and genetic approaches can prevent cell death (Shen and Codogno, 2011).

The majority of PCD occurs by caspase-dependent apoptotic mechanisms, which are highly conserved in eukaryotic organisms. Autophagic cell death appears to be relatively uncommon, but studies to date suggest that it plays important roles in development. For example, autophagic cell death is involved in the differentiation of tracheary elements in the plant vascular system (Kwon et al., 2010), formation of spores during *Dictyostelium* starvation (Luciani et al., 2011),

and removal of the salivary glands and midgut during larvae - adult development in *Drosophila* (Denton et al., 2012). Complex crosstalk mechanisms seem to exist between the autophagic and apoptotic pathways, although these are not well understood. Autophagy primarily acts as a cell survival mechanism, but in certain contexts can directly induce cell death or can cooperate with apoptotic pathways to promote cell death (Denton et al., 2012).

1.3.4 Autophagy-mediated unconventional secretion

Although primarily a degradative pathway, recent studies have shown that autophagy also takes part in unconventional secretory pathways. Both in *Saccharomyces cerevisiae* and *Pichia pastoris*, the starvation-induced secretion of Acb1, a protein lacking a classical ER-targeting sequence, requires autophagy genes as well as SNAREs involved in the fusion of vesicles with the plasma membrane (Duran et al., 2010; Manjithaya et al., 2010). This unconventional secretion is dependent on GRASP (Golgi reassembly and stacking protein), and results in packaging of Acb1 into autophagosomes that bypass fusion with the vacuole and instead fuse with the plasma membrane to release their contents extracellularly. Further work showed that GRASP localises to novel membrane structures close to ER exit sites, termed compartments for unconventional protein secretion or CUPS (Bruns et al., 2011), which appear to be sorting stations for the packaging of Acb1 into autophagosomes (Bruns et al., 2011). CUPS are enriched in PI3P and contain both Atg8 and Atg9, suggesting that they act as a scaffold for the formation of Acb1-containing autophagosomes. A similar unconventional secretory pathway has been identified in mammals, where it mediates the secretion of the pro-inflammatory cytokine IL-1 β (Dupont et al., 2011). As in yeasts, this process requires autophagy genes and the mammalian GRASP55. The existence of autophagy-mediated secretory pathways in both yeasts and mammals suggests that autophagy may play roles in protein secretion in other eukaryotic organisms.

1.3.5 Autophagy in trypanosomatid parasites

The core molecular machinery required for autophagosome formation is widely conserved in eukaryotic organisms, whereas some ATG genes identified in yeast, including those required for selective autophagy, appear to be fungi-specific

(Meijer et al., 2007; Duszenko et al., 2011). Genetic screens in *Caenorhabditis elegans* have shown that multicellular eukaryotes possess essential autophagy genes that are not found in fungi (Tian et al., 2010), and although mammals do not encode Atg17 (Table 1-2), its role in the Atg1/ULK1 complex is performed by a mammalian counterpart, FIP200 (Hara et al., 2008). Mammalian cells also possess proteins involved in selective autophagy pathways, for example p62 (Lamark et al., 2009), which recruits ubiquitinated protein aggregates or organelles for autophagic degradation. This suggests that where higher eukaryotes lack orthologues of yeast *ATGs*, they may encode different proteins that fulfil similar functions.

Leishmania and the related trypanosomatid parasites *Trypanosoma brucei* and *Trypanosoma cruzi* possess orthologues of the majority of *ATG* genes required for autophagosome formation in *S. cerevisiae* (Table 1-2). Notably, *ATG8* has undergone expansion in *Leishmania*, which possesses four families of *ATG8*-like genes known as *ATG8*, *ATG8A*, *ATG8B* and *ATG8C* (Williams et al., 2006); these are present in various *Leishmania* species albeit with different copy numbers (TriTrypDB). *T. brucei* also possesses multiple *ATG8* isoforms (Duszenko et al., 2011). These trypanosomatids encode four TOR kinases. In *T. brucei* TOR1 forms the TORC1 complex and its knockdown by RNAi results in increased formation of autophagic structures, suggesting that TOR1 is important for the regulation of autophagy, although unlike yeast and mammalian TORs it is rapamycin insensitive (Barquilla and Navarro, 2009a). Instead rapamycin affects *T. brucei* TOR2 function, which is important for actin cytoskeleton remodelling during endocytosis and cytokinesis (Barquilla and Navarro, 2009b). The TOR3 of both *T. brucei* and *L. major* plays vital roles in acidocalcisome formation (Madeira da Silva and Beverley, 2010; de Jesus et al., 2010), whereas TOR4 is involved in the regulation of *T. brucei* differentiation between the slender and stumpy bloodstream forms (Barquilla et al., 2012).

Table 1-2 The core Atg and Atg-related proteins involved in autophagosome formation in the yeast *S. cerevisiae* and their homologues from humans and trypanosomatid parasites. Data compiled from (Williams et al., 2006; Herman et al., 2006; Rigden et al., 2009; Brennand et al., 2011; Duszenko et al., 2011). Trypanosomatid gene IDs are from TriTrypDB. Underlining indicates presence of predicted homologues for which gene IDs have not been published. *In the case of Atg1, trypanosomatids possess multiple serine/threonine kinases that may perform similar functions and as such there has been no clear candidate identified. **Multiple *ATG8*-like proteins are encoded; a representative of each family is shown. [?] Unknown whether these genes encode proteins with *ATG12*-like function. Note: Although on the same rows in the table, the *ATG4.1* and

ATG4.2 of trypanosomatids are not necessarily equivalent to human ATG4A and ATG4C. Similarly, *L. major* ATG8-like proteins are not equivalent to GABARAP, etc.

<i>S. cerevisiae</i>	<i>H. sapiens</i>	<i>L. major</i>	<i>T. brucei</i>	<i>T. cruzi</i>
1. Induction				
Atg1	ULK1 ULK2	No clear candidate*	No clear candidate*	No clear candidate*
Atg13	Atg13	<u>ATG13</u>	<u>ATG13</u>	<u>ATG13</u>
Atg17	-	-	-	-
TOR1 TOR2	mTOR	LmjF36.6320 (TOR1) LmjF34.4530 (TOR2) LmjF34.3940 (TOR3) LmjF20.1120 (TOR4)	Tb927.10.8420 Tb927.4.420 Tb927.4.800 Tb927.1.1930	TcCLB.508549.30 TcCLB.510689.40 TcCLB.508257.230 TcCLB.508997.20
Atg29	-	-	-	-
Atg31	-	-	-	-
2. Vesicle Nucleation				
Atg6	Beclin1	LmjF08.0400	Tb927.5.3270	TcCLB.507809.119
Atg14	Atg14 (Barkor)	<u>ATG14</u>	<u>ATG14</u>	-
Vps15	Vps15	LmjF28.1760	Tb11.01.0930	TcCLB.510901.120
Vps34	Vps34	LmjF24.2010	Tb927.8.6210	TcCLB.511067.4 TcCLB.511065.50
Atg2	Atg2A Atg2B	<u>ATG2</u>	<u>ATG2</u>	-
Atg18	WIPI1, 2, 3, 4	LmjF29.1575	Tb927.3.4150	TcCLB.509669.100
Atg9	Atg9L1 Atg9L2	LmjF27.0390	Tb11.03.0130	TcCLB.506925.450
3. Vesicle Expansion & Completion				
Atg3	Atg3	LmjF33.0295	Tb927.2.1890	TcCLB.510257.90
Atg4	Atg4A Atg4B Atg4C Atg4D	LmjF32.3890 (ATG4.1) LmjF30.0270 (ATG4.2)	Tb11.01.7970 (ATG4.1) Tb927.6.1690 (ATG4.2)	TcCLB.509443.30 (ATG4.1) TcCLB.511527.50 (ATG4.2)
Atg7	Atg7	LmjF07.0010	Tb10.26.0840	TcCLB.507711.150
Atg8	LC3A, B, C GABARAP GABARAPL1, 2, 3	LmjF19.1630 (ATG8) LmjF19.0840 (ATG8A)** LmjF19.0850 (ATG8B)** LmjF09.0150 (ATG8C)**	Tb927.7.5900 (ATG8.1) Tb927.7.5910 (ATG8.2)	TcCLB.508173.47 (ATG8.1)
Atg5	Atg5	LmjF30.0980	Tb927.6.2430	TcCLB.509965.280
Atg10	Atg10	LmjF31.3105	Tb927.8.7000	TcCLB.507389.50
Atg12	Atg12	LmjF22.1300	Tb927.7.3320 [?] (ATG8.3)	TcCLB.510533.180 [?] (ATG8.2)
Atg16	Atg16L1 Atg16L2	LmjF33.1410	Tb11.02.4790	TcCLB.506775.160

Protein turnover has long been known to be important during *Leishmania* differentiation, due to the changes in lysosomal morphology and associated alterations in peptidase activity that occur during transformation (Besteiro et al., 2007). Differentiation, both to metacyclic promastigotes and to amastigotes, is also associated with increased autophagosome formation as shown by the appearance of GFP-ATG8 labelled puncta, increased lipidation of ATG8 detected by Western blot, and trafficking of GFP-ATG8 to the lysosomal compartment (Williams et al., 2006; Besteiro et al., 2006a). *L. mexicana* parasites lacking the lysosomal peptidases CPA and CPB, or treated with a cysteine peptidase inhibitor, showed accumulation of autophagosomes in the cell as their degradation in the lysosome was blocked (Williams et al., 2006). This disruption of autophagy prevented the successful differentiation of parasites, and reduced their ability to survive starvation. Furthermore, *L. major* expressing dominant-negative Vps4, a protein involved in the formation of endosomal MVBs, also failed to differentiate into infective metacyclic forms and survived nutrient starvation poorly (Besteiro et al., 2006a). These parasites showed defects in the trafficking of autophagosomes to the lysosome, suggesting that autophagosome fusion with endosomal compartments is required for autophagosome maturation, as in mammalian cells. In addition, autophagy in *Leishmania* can be blocked by the classical autophagy inhibitors wortmannin and 3-methyladenine (Besteiro et al., 2006a), and autophagosomes appear to be delivered to lysosomes along microtubules (Williams et al., 2006). These studies have shown that autophagy in *Leishmania* is similar to that described in yeast and mammals, perhaps more alike to the mammalian process due to the involvement of the endosomal compartments and microtubules. They have also revealed the importance of autophagy in parasite differentiation and starvation.

Whereas *Leishmania* ATG8 has been characterised as a marker of autophagosomes (Besteiro et al., 2006a), the functions of the ATG8-like families remain unknown (Williams et al., 2009). Although able to complement an ATG8-deficient strain of *S. cerevisiae* and form punctate structures when expressed as GFP fusions in *L. major*, these proteins do not appear to play roles in autophagy (Williams et al., 2009). GFP-ATG8A forms puncta only in response to starvation, so conceivably could be involved in starvation-induced autophagy, although the distribution of puncta does not match that of ATG8 autophagosomes and

trafficking of ATG8A to the lysosome has not been reported. Both GFP-ATG8B and GFP-ATG8C label single puncta close to the flagellar pocket that are present only in very few cells in the population. *L. major* has two *ATG4* genes that encode the cysteine peptidases ATG4.1 and ATG4.2. These have been shown to selectively cleave the ATG8-like proteins, with ATG4.1 preferentially processing ATG8, ATG8B and ATG8C, and ATG4.2 showing activity only on ATG8A (Williams et al., 2009). Corresponding to these results, GFP-ATG8A puncta were unable to form in $\Delta atg4.2$ parasites. Interestingly, the $\Delta atg4.2$ mutant accumulated GFP-ATG8-labelled autophagosomes, exhibited a reduced ability to withstand starvation, and was impaired in its ability to differentiate, suggesting that ATG4.2 may play a role in delipidation of ATG8 which is important for autophagosome maturation (Besteiro et al., 2006a). This is supported by a recent study comparing *L. major* $\Delta atg4.1$ and $\Delta atg4.2$ (Williams et al., 2012a), which showed that loss of ATG4.1 affected early autophagosome formation, whereas ATG4.2 knockout caused defects in autophagosome maturation. In addition, knockout of ATG4.1 or ATG4.2 severely affected the ability of *L. major* to infect macrophages *in vitro* or mice, and an ATG4.1/ATG4.2 double knockout mutant could not be generated, implying that at least one of these peptidases is required for functional autophagy (Williams et al., 2012a).

Leishmania encodes components of the Atg12-Atg5 conjugation system, although these show low similarity to their orthologues in other organisms (Williams et al., 2006). Unlike canonical ATG12s, that of *L. major* more closely resembles ATG8s, with a C-terminal extension that requires cleavage before ATG12 can be conjugated to ATG5 (Williams et al., 2009); ATG12-ATG5 conjugation has been biochemically proven using an *in vitro* system (Williams et al., 2012b). ATG12 has been shown to co-localise with ATG5 on puncta, and localise to some ATG8-labelled puncta, consistent with a role for ATG12 in the early stages of autophagosome biogenesis (Williams et al., 2009; Williams et al., 2012b). Genes encoding components of the SNARE machinery that is involved in the fusion of autophagosomes with endosomes and lysosomes are also present in the *L. major* genome (Williams et al., 2006).

Bioinformatic analyses identified three isoforms of ATG8 in *T. brucei*. However, one of these, ATG8.3, is possibly syntenic with *L. major* ATG12 (Duszenko et al., 2011), suggesting that ATG8.3 may function as an ATG12 in *T. brucei*, although

this remains to be functionally proven. Whereas ATG8.1 ends in a glycine residue, and is therefore expected to function without processing, ATG8.2 has a C-terminal extension suggesting that it requires processing. *T. brucei* possesses two ATG4 homologues, and the crystal structure of ATG8.2 was shown to form interactions with a homology model of ATG4.1 resembling those between mammalian LC3 and ATG4B (Koopmann et al., 2009), suggesting that processing of ATG8.2 by ATG4.1 is likely. YFP-ATG8.2 has been used as a marker of autophagosomes in *T. brucei*, whose formation can be induced by starvation (Proto, PhD thesis 2010; Li et al., 2012a). Formation of YFP-ATG8.2 puncta was inhibited by wortmannin treatment or ATG3 knockdown, and depends on the lipidation of ATG8.2 at glycine 119 (Li et al., 2012a). ATG8.1 and ATG8.2 co-localise on the same structures, suggesting that they are both involved in autophagosome formation. These proteins have been suggested to be involved in autophagic cell death, as double knockdown of ATG8.1 and ATG8.2 resulted in increased cell survival during prolonged starvation (Li et al., 2012a). Autophagic cell death has also been reported in trypanosomes treated with neuropeptides, which led to increased formation of vacuoles that could be labelled by anti-LC3 (Delgado et al., 2008), but whether inhibition of autophagy prevented cell death was not examined. Autophagy also appears to be involved in the turnover of glycosomes during life cycle differentiation of *T. brucei*; increased association of glycosomes with the lysosome was observed during transformation from slender to stumpy bloodstream forms and from stumpy forms to procyclic forms (Herman et al., 2008). This association occurs to a much greater extent during stumpy to procyclic differentiation, and is associated with a dramatic enlargement of the lysosome. This is consistent with the more pronounced metabolic changes that occur during differentiation into procyclic forms, which adapt the metabolism of parasites to life within the insect vector. Autophagosomes were not observed by electron microscopy, but glycosomes were seen in contact with lysosomes, suggesting that glycosome degradation in *T. brucei* occurs by microautophagy rather than macroautophagy (Herman et al., 2008).

T. cruzi contains two ATG8 homologues and two ATG4 homologues. As in *T. brucei*, one of these ATG8s, ATG8.2, is likely to function as an ATG12 as it shows similarity to *L. major* ATG12 (Duszenko et al., 2011). ATG4.1 could efficiently cleave both ATG8.1 and ATG8.2 at conserved glycine residues within these

proteins, but ATG4.2 only showed minimal activity, although cleavage occurred at the same glycine residues within the ATG8s (Alvarez et al., 2008). In corresponding autophagy-deficient yeast strains, ATG4.1, ATG4.2 and ATG8.1 were able to restore autophagy, and ATG8.1 localised to puncta in response to starvation, a process that was dependent on glycine 121, whereas ATG8.2 was distributed in the cytosol. These data show that *T. cruzi* ATG8.1 is the functional homologue of yeast Atg8. Differentiation of *T. cruzi* between its developmental forms was associated with the localisation of ATG8.1 to puncta (Alvarez et al., 2008), suggesting that, as in *Leishmania*, autophagy is important for cellular remodelling during life cycle differentiation. In addition, the morphology of the lysosome-like reservosome of *T. cruzi* alters throughout the parasite's life cycle (Sant'Anna et al., 2008), suggesting that its degradative capacity may change in order to accommodate increased protein turnover during differentiation.

Because of autophagy's important role in the differentiation of these medically important parasites into their infective forms, inhibitors of autophagy have been proposed as attractive treatments for the diseases caused by trypanosomatids. Early studies describe the anti-parasitic effects of peptidase inhibitors, which prevented the differentiation of *Leishmania* and *T. cruzi* (Brennand et al., 2011). Recent studies have also shown promising results from the treatment of *T. cruzi*-infected animals with cysteine peptidase inhibitors (Barr et al., 2005; Doyle et al., 2007). As successful differentiation depends on autophagic degradation for cellular remodelling and parasite adaptation to the host environment, lysosomal cysteine peptidase inhibitors or compounds that target other components of the parasite autophagy machinery may represent feasible targets for anti-parasitic drug development.

1.4 Project aims

Autophagy is important for successful differentiation between *Leishmania* developmental forms, playing significant roles in protein turnover during the cellular remodelling that accompanies this process. However, the cargoes that are targeted for autophagic degradation in this parasite have not been identified, although structural and metabolic changes that occur during differentiation, and studies in other organisms, suggest that autophagy may be involved in organelle turnover.

Leishmania species appear unique in encoding three multi-copy families of ATG8-like proteins, which display some similarities to canonical ATG8s (Williams et al., 2009), although whether they play roles in autophagy or perform novel parasite-specific functions is currently unknown.

This projects aims to:

1. Identify organelles that are targeted by autophagy in *Leishmania* and determine how remodelling of these structures during differentiation may adapt the parasite to life in the mammalian host.
2. Further characterise the ATG8-like proteins of *L. major* to investigate potential roles in autophagy and intracellular trafficking.

2 Materials and Methods

2.1 Bacterial strains and culture

2.1.1 *E. coli strains used*

For routine transformations of plasmid DNA or ligation reactions, DH5 α competent cells (Invitrogen) were used. This strain contains the genetic markers *recA1*, to improve insert stability and prevent unwanted recombination, and *endA1*, to improve yield and quality of plasmid DNA from minipreps. It also contains *lacZ* Δ M15 for blue/white colour screening of colonies. MAX efficiency DH5 α competent cells (Invitrogen), a strain with improved transformation efficiency, were used for transformation of difficult plasmids such as those prepared using the Invitrogen Multisite Gateway technology. For transformation of difficult ligation reactions, XL10-Gold Ultracompetent cells (Stratagene) were used. In addition to *endA*, *recA* and *lacZ* Δ M15, these bacteria exhibit the Hte phenotype, which increases the transformation efficiency of ligated or large supercoiled DNA.

2.1.2 *Generation of competent E. coli cell lines*

Competent *E. coli* cells were prepared with rubidium chloride treatment. A single colony of the required bacterial strain was inoculated into 5 ml Luria Bertani (LB) broth and grown overnight at 37°C. The next day the culture was diluted 1:1000 into 50 ml LB broth and grown at 37°C until the culture's optical density reached 0.6 at 600 nm. After cooling on ice for 10 min, the culture was centrifuged at 2000 g for 15 min at 4°C. The cell pellet was carefully resuspended in 16 ml chilled RF1 buffer (100 mM rubidium chloride, 50 mM MnCl₂·4H₂O, 30 mM potassium acetate, 10 mM CaCl₂ and 15 % glycerol, adjusted to pH 5.8 with acetic acid) then incubated on ice for 15 min. Cells were centrifuged again as above and then resuspended in 4 ml ice cold RF2 buffer (10 mM MOPS pH 6.8, 10 mM rubidium chloride, 75 mM CaCl₂ and 15 % glycerol, adjusted to pH 6.8 with NaOH) and incubated on ice for 1 hour, before snap-freezing aliquots in an ethanol-dry ice bath. Aliquots of competent cells were stored at -80°C.

2.1.3 Transformations

Aliquots of 50 μl competent cells were thawed on ice before adding 1 - 5 μl (1 - 10 ng) DNA and incubating on ice for 30 min. Cells were subjected to heat shock for 45 sec in a 42°C water bath then incubated on ice for 2 min. 950 μl of pre-warmed medium were added to each tube, which were then incubated for 1 hour at 37°C with shaking at 225 rpm. ≤ 200 μl each transformation were plated out onto selective LB agar plates and incubated overnight at 37°C. For blue/white colour screening of ligation reaction transformations, cells were plated out on selective LB agar plates containing IPTG/XGal before overnight incubation at 37°C.

2.1.4 Bacterial culture and storage

Individual colonies of transformed bacteria were inoculated into LB broth with suitable antibiotic (Ampicillin 100 $\mu\text{g}/\text{ml}$; Kanamycin 50 $\mu\text{g}/\text{ml}$ (Sigma)) and cultured overnight, to select for bacteria expressing plasmid DNA of interest, at 37°C with shaking at 225 rpm. For long term storage of bacteria, 0.5 ml of culture was mixed with an equal volume of 2 % (w/v) peptone and 40 % (v/v) glycerol and stored at -80°C.

2.2 Leishmania culture methods

2.2.1 Culture of Leishmania promastigotes

Leishmania major (MHOM/JL/80/Friedlin) were grown in modified Eagle's medium (designated HOMEM) supplemented with 10 % (v/v) heat-inactivated foetal calf serum (HIFCS) and 1 % (v/v) penicillin streptomycin solution (Sigma) at 25°C. When referring to the stage of growth of cultures, mid-log phase corresponds to $\sim 5 \times 10^6$ parasites/ml and stationary phase to $\sim 2 \times 10^7$ parasites/ml. Transgenic parasites were maintained in appropriate antibiotics: G418 (Neomycin) at 50 $\mu\text{g}/\text{ml}$; Hygromycin at 50 $\mu\text{g}/\text{ml}$; Blastidicin S at 10 $\mu\text{g}/\text{ml}$; Phleomycin at 10 $\mu\text{g}/\text{ml}$ (InvivoGen).

2.2.2 Determination of cell density

20 μl parasites were mixed with 20 μl 2 % formaldehyde. 10 μl fixed cells were placed in a Neubauer haemocytometer (Weber Scientific) and cells counted under a light microscope. To set up a growth curve, a culture was started with 1×10^5 cells/ml and cells counted every day for up to 12 days.

2.2.3 Creating *Leishmania stabilates*

For long term storage of *Leishmania* cell lines, stabilates were prepared by mixing 500 μl cells with 500 μl HOMEM + 20 % HIFCS + 10 % DMSO in a 1.5 ml cryotube. These were stored overnight at -80°C before transferring to liquid nitrogen.

2.2.4 Transfection and selection of clones

Transfections of *Leishmania* were performed using an Amaxa human T cell nucleofector kit (Lonza) following the manufacturer's instructions. For each transfection, 5×10^7 cells in mid-log phase of growth were harvested by centrifugation at 1000 g for 10 min at 4°C , and then resuspended in 100 μl T cell nucleofector solution and transferred to a cuvette. Approximately 10 μg DNA in 10 μl sterile dH_2O were added to the cells and tapped gently to mix. Cells were electroporated using the U-033 program before being transferred to 10 ml fresh HOMEM + 20 % HIFCS. The culture was split between two flasks to select for independent transfection events and incubated overnight at 25°C to allow recovery. For each transfection a negative control was performed where 10 μl nucleofector solution was added instead of DNA. The following day appropriate antibiotics were added to select for transfectants. For transfections with non-integrative vectors, flasks were made up to 10 ml with HOMEM + 20 % HIFCS before adding the correct concentration of antibiotics. Cells transfected with integrative DNA were prepared in serial dilutions of 1 in 5, 1 in 50 and 1 in 500 in HOMEM + 20 % HIFCS + antibiotics and plated out onto 96 well microplates. Plates and flasks were maintained at 25°C for 2 - 6 weeks until transfectants appeared.

2.2.5 Extraction of genomic DNA

Genomic DNA was prepared from a cell pellet from 10 ml *Leishmania* culture using a QIAgen DNeasy Blood & Tissue kit, following the manufacturer's protocol for "cultured cells".

2.2.6 Verification of *Leishmania* species by PCR

Determination of *Leishmania* species was achieved by restriction fragment length polymorphism (RFLP) analysis of the internal transcribed spacer locus (ITS1) based on the method of Schonian *et al.* (Schonian *et al.*, 2003). Following PCR amplification of ITS1 with OL1853 and OL1854, restriction digest with *Hae*III allows differentiation between *Leishmania* species.

2.2.7 Preparation of protein extracts

A 10 ml culture of *L. major* in the desired life cycle stage was pelleted by centrifugation at 1000 g for 10 min, washed in PBS and then lysed by resuspending in 1 x SDS-PAGE loading buffer to a cell density of 1×10^7 parasites/10 μ l, with 25 x peptidase inhibitor cocktail. Samples were then boiled for 5 min at 100°C on a heat block before loading directly into SDS-PAGE gels or storing at -20°C.

2.2.8 Purification of *Leishmania major* metacyclic promastigotes

Metacyclic promastigotes were isolated from late stationary phase cultures using peanut lectin agglutination (Sacks *et al.*, 1985). Parasites were centrifuged at 1000 g for 10 min, washed and resuspended in PBS to a density of 1×10^8 /ml. Peanut lectin (Sigma) was added to a final concentration of 50 μ g/ml and incubated for 10 min at room temperature. Metacyclic promastigotes were recovered from the supernatant after separation of agglutinated procyclic promastigotes by centrifugation at 100 g for 5 min.

2.2.9 Extraction of murine peritoneal macrophages

CD1 mice were killed by CO₂ asphyxiation. The mouse was laid on its back and sprayed with 70 % ethanol. Its skin was incised at the abdomen and pulled away, then sterilised again with 70 % ethanol. The membrane at the sternum was

pulled taught and the cavity was filled with 10 ml RPMI 1640 + 1 % (v/v) gentamicin + 1 % (v/v) penicillin/streptomycin, using a syringe with a 21 G needle fitted. After shaking the mouse for ~30 seconds, a 26 G needle attached to an empty 10 ml syringe was inserted into the mouse's side in order to remove the fluid and macrophages. Macrophages were harvested by centrifuging at 1500 g for 10 min at 4°C, then resuspended in RPMI 1640 supplemented with 10 % (v/v) HIFCS + 1 % (v/v) gentamicin before determination of cell density using a Neubauer haemocytometer (Weber Scientific) under a light microscope. The macrophages were adjusted to a cell density of 5×10^5 /ml in RPMI 1640 + 10 % (v/v) HIFCS, and then 200 μ l were added to each well of an 8 chamber LAB-TEK tissue culture slide and maintained at 37°C in 5 % CO₂ for up to a week.

2.2.10 Macrophage infection

Peritoneal macrophages were extracted from CD1 mice and adhered overnight in RPMI 1640 medium (PAA) with 10 % HIFCS onto 8-chamber tissue culture slides (LAB-TEK) at 37°C in 5 % CO₂. Macrophages were then infected with peanut lectin-purified metacyclic promastigotes at a ratio of 10 parasites per macrophage and imaged 18 or 48 hours after infection in the DeltaVision Core environmental chamber at 37°C and 5 % CO₂, after DAPI staining and 3 washes in PBS.

2.2.11 Induction and analysis of autophagy

Autophagy was induced by starvation or differentiation as previously reported (Williams et al., 2006; Besteiro et al., 2006a). Promastigotes were starved by washing 3 times in PBS, followed by resuspension in PBS at 1×10^8 parasites/ml for up to 5 hours. To assess autophagy during procyclic - metacyclic promastigote differentiation, cells were observed in stationary phase of growth (Besteiro et al., 2006a); for metacyclic promastigote - amastigote differentiation, parasites were observed 18 hours after infection of macrophages (Williams et al., 2006). Live parasites expressing GFP-ATG8 or RFP-ATG8 were observed by fluorescence microscopy (see below) and the presence and number of GFP-/RFP-ATG8-labelled vesicles within these cells were recorded. The level of autophagy is expressed as the percentage of cells in a population containing

at least one GFP-/RFP-ATG8-labelled vesicle; these measurements were typically made from counting 200 cells from at least three independent experiments.

2.3 Molecular biology techniques

2.3.1 Polymerase Chain Reaction

Polymerase chain reactions (PCR) were performed in a PCR Sprint thermal cycler (Thermo Electron Corporation). Analytical PCRs were performed using *Taq* DNA polymerase (New England Biolabs) and the high-fidelity proof-reading Phusion DNA polymerase (Finnzymes) was used for DNA amplification for cloning work.

Analytical PCRs were typically prepared in 20 μ l volumes, made up of the following: template DNA (100 ng genomic DNA or 100 pg plasmid DNA), 10 x PCR mix (1.13 mg/ml BSA, 450 mM Tris pH 8.8, 110 mM ammonium sulphate, 45 mM $MgCl_2$, 68.3 mM β -mercaptoethanol, 44 μ M EDTA pH 8.0, 10 mM dCTP, 10 mM dATP, 10 mM dGTP, 10 mM dTTP), 10 pmol each primer, 0.5 units of *Taq* DNA polymerase, and distilled water. A typical PCR cycle would consist of an initial DNA denaturation for 5 min at 95°C, followed by 30 cycles of denaturation (95°C, 1 min), annealing (55°C, 1 min) and extension (72°C, time determined by size of amplicon), then a final extension step at 72°C for 10 min.

High fidelity PCR reactions using Phusion DNA polymerase to amplify genomic DNA were prepared in 50 μ l volumes, typically containing 100 ng template DNA, 10 pmol each primer, 10 mM dNTPs, 5x Phusion HF buffer, 0.02 units/ μ l Phusion polymerase, and, in the case of GC-rich amplicons, 3 % DMSO. Cycling reactions were performed according to the manufacturer's protocol, using 98°C denaturation temperature. As Phusion DNA polymerase produces blunt-ended PCR products, where amplified DNA was to be ligated into the cloning vector pGEMT-Easy, 3' A-overhangs were introduced by adding 1 unit *Taq* DNA polymerase directly to the PCR tube and incubating at 72°C for a further 20 min.

PCR conditions were optimised for each reaction, adjusting primer annealing temperature and extension time as required.

2.3.2 Oligonucleotides used in this project

Oligonucleotide primers were designed using CLC Genomics Workbench 4 (CLC Bio) and synthesised by Eurofins MWG Operon (Germany).

Table 2-1 Details of oligonucleotides used in this project. Description of targeted genes including TriTrypDB gene identifiers for *Leishmania* genes, with nucleotide sequence. Restriction endonuclease sites are indicated in bold. Residues in mutagenic primers for conversion of glycine to alanine are underlined and bold.

Gene & Description	Oligo number	Sequence	Restriction sites
Primers for site-directed mutagenesis of ATG8-like proteins' C-terminal glycine (designed by K. Woods)			
LmjF19.1630 Site-directed mutagenesis GFP-ATG8 G120A	OL2741	GGCGAGAACACGTACG <u>CC</u> GGGCAGGGGCTG	
	OL2742	CAGCCCCTGCCCG <u>G</u> CGTACGTGTTCTCGCC	
LmjF19.0840 Site-directed mutagenesis GFP-ATG8A G109A	OL2743	GCGCGAGTCGTCGATGG <u>C</u> CGCCAAGGACCTTTGC	
	OL2744	GCAAAGGTCCTTGCGG <u>G</u> CCATCGACGACTCGCGC	
LmjF19.0850 Site-directed mutagenesis GFP-ATG8B G111A	OL2745	CGAGCAGCCATGG <u>C</u> CGCTTTGCGAGTCCGTG	
	OL2746	CACGGACTCGCAAAGGCG <u>G</u> CCATGGCCTGCTCG	
LmjF09.0156 Site-directed mutagenesis GFP-ATG8C G111A	OL2747	GGAGCGCTGCATGG <u>C</u> CGCTGCGGTGTGCATGTCTG	
	OL2748	CGACATGCACACCGCAGCG <u>G</u> CCATGCAGCGCTCC	
LmjF22.1300 Site-directed mutagenesis GFP-ATG12 G185A	OL2749	GGAAAACACCTTCG <u>C</u> CGGAGACGTGCGCTCTGCC	
	OL2750	GGCAGAGCGCACGTCTCCG <u>G</u> CGAAGGTGTTTTCC	
Primers for fluorescent tagging of proteins			
LmjF28.2720 (ATG12-like)	OL3807	CGAGATCTATGAACACTACAACGGAG	<i>Bgl</i> II
	OL3808	GCCTCGAGTCACCCGCTGAAGACTTC	<i>Xho</i> I
Kaede-SQL (photoactivatable protein with glycosomal PTS1)	OL3949	GCCATATGGTGAGTCTGATTAACC	<i>Nde</i> I
	OL3950	GCTCGAGCAGCTGAGACTTGACGTTGTCCGGCA	<i>Xho</i> I
Cerulean fluorescent protein (CFP)	OL3970	GCCATATGGTGAGCAAGGGCGAGGA	<i>Nde</i> I
	OL4054	GCAGATCTTGTACAGCTCGTCCAT	<i>Bgl</i> II
Primers for <i>Leishmania</i> species identification			
Amplification of ITS1 region	OL1853	CTGGATCATTTTCCGATG	
	OL1854	TGATACCACTTATCGCACTT	

Table 2-2 Details of oligonucleotides used in this project (continued)

Description of targeted genes including TriTrypDB gene identifiers for *Leishmania* genes, with nucleotide sequence. Restriction endonuclease sites are indicated in bold and *attB* sequences are underlined with specific *attB* nomenclature included beneath oligo number.

Primers for Multisite Gateway knockout constructs			
<i>L. major</i> ATG8 (LmjF19.1630) 5' UTR with <i>attB</i> sites	OL3639 (<i>attB4</i>)	GGGGACAAC <u>TTTGTATAGAAAAGTTGGCGGCCGCCT</u> GCTCCTTCACAGTCGATGC	Not I
	OL3640 (<i>attB1r</i>)	GGGGACTGCTTTTTTGTACAAACTTGCCTTCGTGG ACAAACGTGCA	
<i>L. major</i> ATG8 (LmjF19.1630) 3' UTR with <i>attB</i> sites	OL3641 (<i>attB2r</i>)	GGGGACAGCTTTCTTGTACAAAGTGGCGATCGTGC GTCGCACACCTC	Bgl II
	OL3642 (<i>attB3</i>)	GGGGACAAC <u>TTTGTATAATAAAGTTGAGATCTGCAC</u> TCCGAGATGCCGCCATC	
<i>L. major</i> DHFR + antibiotic resistance markers with <i>attB</i> sites	OL3816 (<i>attB1</i>)	GGGGACAAGTTTGTACAAAAAAGCAGGCTGTACACA CGTACACACACACG	
	OL3817 (<i>attB2</i>)	GGGGACCACTTTGTACAAGAAAGCTGGGTCATTCGT GGGCTCCAGCTGCG	
Primers to test integration of ATG8 KO constructs in transfected clones	OL3863	GTGGATGCACGCGTGGGC	
	OL3864	CTGGATACCGTGACAAGG	

2.3.3 DNA gel electrophoresis and gel extraction

DNA gel electrophoresis was typically performed in 1 % (w/v) gels made by dissolving agarose (Ultrapure, Invitrogen) in 0.5 x TRIS borate buffer (TBE: 20 mM Tris, 20 mM boric acid, 0.5 mM EDTA, pH 7.2) through heating briefly in a microwave. After cooling, SYBR Safe DNA stain (Invitrogen) was added at 1:5000, and the gel was allowed to set. DNA samples were mixed with 6 x loading dye (0.25 % (w/v) bromophenol blue, 0.25 % (w/v) xylene cyanol FF and 30 % glycerol) before loading. For reference 0.5 µg 1 kb DNA ladder (Invitrogen) was loaded alongside DNA samples. Electrophoresis was carried out at 50 - 100 volts until separation of bands was observed. Gels were viewed and imaged under UV light using a BioRad Gel-Doc Imager and Quantity One software. When the DNA was required for cloning procedures, it was visualised on a DarkReader blue light transilluminator and extracted from the gel using a QIAGEN Gel Extraction kit, or for fragments below 4 kb in size a QIAGEN MinElute gel extraction kit, following the manufacturer's instructions.

2.3.4 Restriction digests

DNA was digested using restriction endonucleases (New England Biolabs). Enzymes were used according to the manufacturer's guidelines using the optimum reaction buffer, and supplemented with bovine serum albumin (BSA) as necessary. Restriction digest reactions were typically performed in 20 - 50 μ l volumes for 1 hour at the recommended temperature. When large amounts of DNA were required, digests were carried out in 100 μ l volumes and incubated overnight. Digested DNA was visualised by agarose gel electrophoresis and, if required, extracted from the gel as described above.

2.3.5 Ligations

PCR products were ligated into the cloning vector pGEM-T Easy (Promega) after addition of A-overhangs and gel extraction (see above). 2 μ l PCR product were introduced into competent *E. coli* by heat shock transformation, before plating bacteria onto LB agar plates containing 100 μ g/ml Ampicillin and supplemented with 0.5 mM IPTG and 80 μ g/ml XGal. Successful transformants were selected by blue/white colony screening: white colonies were picked from plates and mixed in 5 μ l distilled water, then analysed by standard PCR with the colony/water mix as the template and using vector-specific primers T7 and SP6 to verify the presence of an expected sized fragment in the vector's cloning site.

Ligations of DNA fragments into the final vector were performed using T4 DNA ligase and T4 DNA ligase buffer (New England Biolabs). Digested plasmid backbone and insert were mixed together in a 10 μ l reaction in different insert:vector ratios, typically 1:1, 3:1 and 6:1, and incubated overnight at 16°C. For blunt-ended ligations, digested plasmid vectors were treated with CIP (calf intestinal alkaline phosphatase; New England Biolabs) to prevent re-ligation. 2 μ l of ligation reactions were transformed into competent *E. coli* and selected using appropriate antibiotics. Successful ligations were confirmed by colony PCR using vector-specific primers, or by purification of plasmid and subsequent restriction digest analysis. Verification of ligations, both into pGEM-T Easy or into final vectors, was performed by sequencing of the plasmid using vector-specific primers covering the cloning site.

2.3.6 DNA sequencing

DNA sequencing was performed by the DNA sequencing service at the University of Dundee (www.dnaseq.co.uk). Sequence data were analysed using CLC Genomics Workbench 4 (CLC Bio).

2.3.7 Vectors used in this project

Table 2-3 Details of plasmids used or generated in this project.

Plasmid	Backbone	Description
Vectors for labelling ATG8, ATG8-like proteins and ATG5		
pGL1078	pGL1136 (pNUS-GFPnH)	Episomal expression of GFP-ATG8. Hygromycin resistance. Produced by S Besteiro.
pGL1686	pGL1078	Episomal expression of GFP-ATG8. Neomycin resistance. Produced by K Woods.
pGL1662	pGL1043 (pNUS-mRFPnD)	Episomal expression of RFP-ATG8. Blasticidin resistance. Produced by R Williams.
pGL1410	pGL1135 (pNUS-GFPnN)	Episomal expression of GFP-ATG8A. Neomycin resistance. Produced by K Woods.
pGL1412	pGL1135 (pNUS-GFPnH)	Episomal expression of GFP-ATG8B. Neomycin resistance. Produced by K Woods.
pGL1414	pGL1135 (pNUS-GFPnH)	Episomal expression of GFP-ATG8C. Neomycin resistance. Produced by K Woods.
mCherry-ATG5	pNUS-mCherrynH	Episomal expression of mCherry-ATG5. Hygromycin resistance. Produced by R Williams.
pGL2153	pGL1135 (pNUS-GFPnH)	Episomal expression of GFP-ATG12-like (LmjF28.2720). Neomycin resistance.
Cloning vectors		
pGEM-T Easy	-	Produced by Promega.

Table 2-4 Details of plasmids used or generated in this project (continued).

Vectors for labelling organelles		
pGL1601	pGL1043 (pNUS-mRFPnD)	Episomal expression of RFP-SQL (glycosomes). Blasticidin resistance. Produced by R Williams.
pGL1589	pGL1132 (pNUS-GFPcN)	Episomal expression of ROM-GFP (mitochondrion). Neomycin resistance. Produced by D Tonn.
MUP-GFP	pGL1132 (pNUS-GFPcN)	Episomal expression of MUP-GFP (mitochondrion). Neomycin resistance. Produced by R Williams.
pGL1681	pGL1132 (pNUS-GFPcN)	Episomal expression of V-H ⁺ -PPase-GFP (acidocalcisomes). Neomycin resistance. Produced by D Tonn.
pGL1763	pGL1132 (pNUS-GFPcN)	Episomal expression of calpain-GFP (flagellum). Neomycin resistance. Produced by D Tonn.
pGL1077	pGL1042 (pNUS-mRFPcD)	Episomal expression of proCPB-RFP (lysosome). Blasticidin resistance. Produced by S Besteiro.
Vectors used in construction of Multisite Gateway knockout plasmids		
pGL2206	pDONR 221	Entry vector for Multisite Gateway containing SAT resistance cassette flanked by DHFR sequences.
pGL2207	pDONR 221	Entry vector for Multisite Gateway containing hygromycin resistance cassette flanked by DHFR sequences.
pGL2208	pDONR 221	Entry vector for Multisite Gateway containing blasticidin resistance cassette flanked by DHFR sequences.
pGL2209	pDONR 221	Entry vector for Multisite Gateway containing puromycin resistance cassette flanked by DHFR sequences.
pGL2210	pDONR P4-P1r	Entry vector for Multisite Gateway containing 500 bp of <i>L. major</i> ATG8 5' UTR.
pGL2211	pDONR P2r-P3	Entry vector for Multisite Gateway containing 500 bp of <i>L. major</i> ATG8 3' UTR.
pGL2155	pDEST R4-R3 II	Final plasmid containing ATG8 KO construct. SAT resistance.
pGL2156	pDEST R4-R3 II	Final plasmid containing ATG8 KO construct. Blasticidin resistance.
pGL2175	pDEST R4-R3 II	Final plasmid containing ATG8 KO construct. Puromycin resistance.

2.3.7.1 Expression vectors for *Leishmania*

Vectors for the episomal expression of fluorescently tagged fusion proteins were generated using the pNUS vectors (Tetaud et al., 2002). These vectors contain 5'

and 3' untranslated regions (UTRs) of the *Crithidia fasciculata* phosphoglycerate kinase (PGK) gene array to mediate trans-splicing and poly-adenylation of the target gene. In addition, expression of a selective marker is governed by a PGK B 5' UTR and the 3' UTR of *C. fasciculata* glutathionylspermidine synthetase (GSPS) for trans-splicing and poly-adenylation, respectively. The gene of interest was cloned into the multiple cloning site of pNUS vectors containing C- or N-terminal modifications; in this study, green or red fluorescent proteins. Further information on the pNUS vectors and their various modifications can be found on the pNUS site (<http://www.ibgc.u-bordeaux2.fr/pNUS/>).

2.3.7.2 Construction of Multisite Gateway knockout constructs

Knockout vectors were generated using the Multisite Gateway three fragment vector construction kit (Invitrogen), following the manufacturer's guidelines. The aim was to create a variety of plasmids containing selective markers that could be used in combination with plasmids containing the 5' and 3' UTRs of the gene of interest to generate the final knockout constructs using Gateway technology (Figure 2-1). These knockout constructs could then be transfected into *Leishmania* to replace the target gene by homologous recombination. To create entry vectors containing selective markers, *attB* primers (OL3816 and OL3817) were designed to amplify antibiotic resistance cassettes flanked by ~300 bp of the 5' and 3' UTRs of *L. major* dihydrofolate reductase (DHFR), required for trans-splicing and poly-adenylation of the selective marker. The templates used for PCR amplification of these regions were the plasmids pGL158 (SAT), pGL345 (hygromycin), pGL434 (blasticidin) and pGL1160 (puromycin). The resulting *attB*-labelled PCR products were inserted into pDONR 221 in BP recombination reactions to produce the entry vectors pGL2206, pGL2207, pGL2208 and pGL2209. Entry vectors containing 500 bp of the 5' and 3' flanking regions of the *L. major* ATG8 gene (LmjF19.1630) were generated by BP recombination of *attB*-labelled PCR products into pDONR P4-P1r and pDONR P2r-P3, respectively; these were named pGL2210 and pGL2211. Amplification of ATG8 5' and 3' flanking regions from *L. major* genomic DNA was performed with the primer pairs OL3639 and OL3640, and OL3941 and OL3942, respectively. OL3639 and OL3642 were designed to add *Not* I and *Bgl* II sites to the 5' and 3' ends of the final knockout construct, respectively, so that the construct could be cut from the final plasmid by restriction digest. The final vector was generated

by combining pGL2210 (ATG8 5'), pGL2211 (ATG8 3') and the entry vector containing the desired resistance marker in an LR recombination reaction. A restriction digest with *Not* I and *Bgl* II, followed by gel extraction, was performed to isolate the final ATG8 knockout construct, which was then prepared for transfection into parasites.

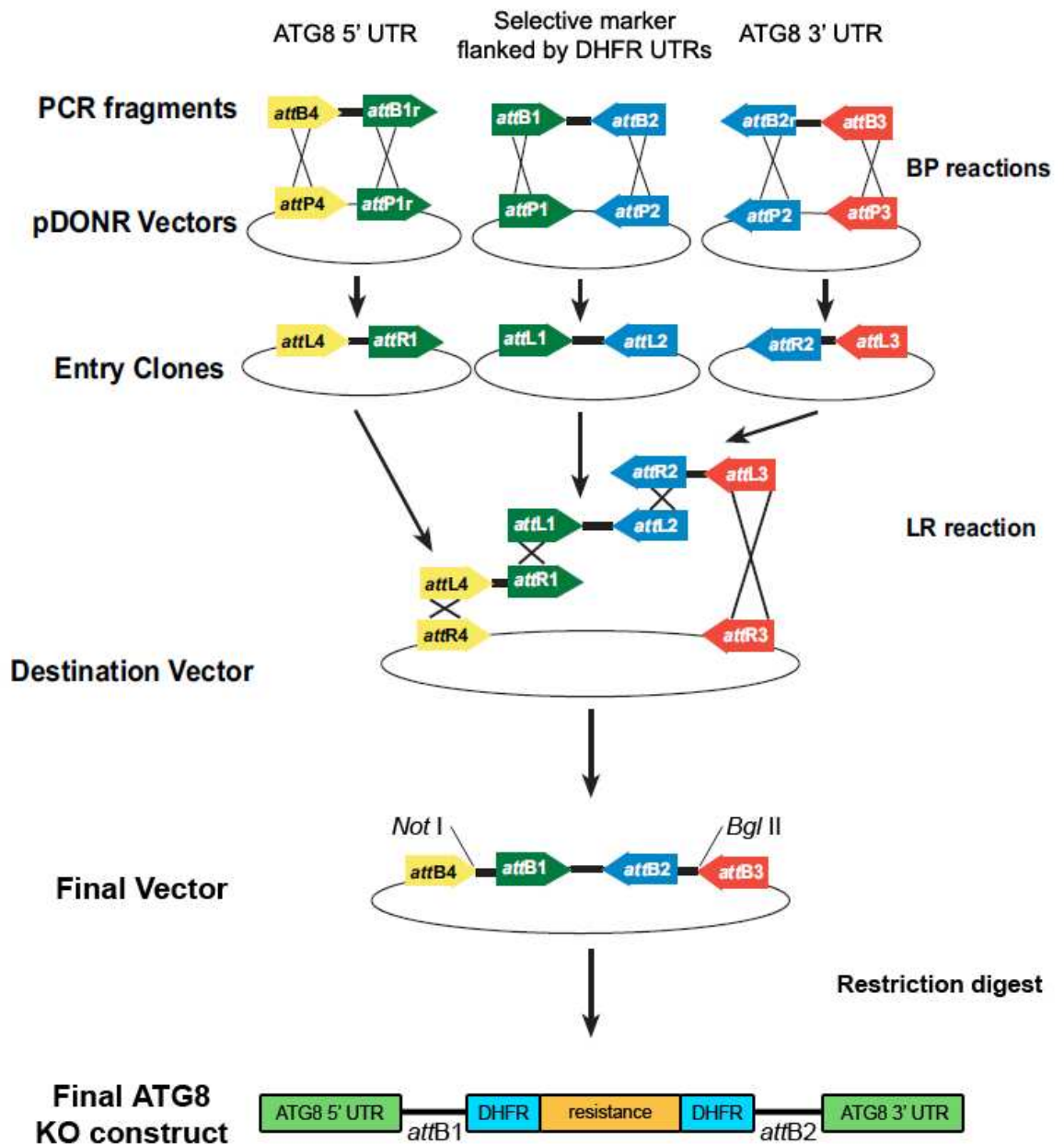


Figure 2-1 Schematic showing Multisite Gateway construction of ATG8 knockout constructs. Modified from Multisite Gateway three fragment vector construction kit manual (Invitrogen).

2.3.8 Bioinformatic analysis

Design of vectors and oligonucleotides, and bioinformatic analyses were performed using CLC Genomics Workbench 4 (CLC Bio). *Leishmania* gene sequences were obtained from genedb (www.genedb.com) or TriTrypDB: the kinetoplastid genome resource (tritrypdb.org), and non-kinetoplastid gene sequences were found on the National Center for Biotechnology Information (NCBI) website (<http://www.ncbi.nlm.nih.gov>).

2.3.9 Purification of plasmids

Plasmids were purified from bacterial cultures using a QIAprep Spin Miniprep kit (QIAGEN) according to the manufacturer's instructions. For large batches, the process was automated using a QIAcube (QIAGEN).

2.3.10 Preparation of DNA for transfection

DNA was quantified using an Eppendorf BioPhotometer to measure the absorption at 260 nm (A_{260}) to estimate DNA concentration and to measure DNA purity through the ratio of A_{260} to A_{280} (DNA to contaminating proteins). To further concentrate DNA, it was ethanol precipitated by addition of two volumes of 100 % ethanol and 10 % volume of 3 M sodium acetate pH 5.2, before incubation at -20°C for at least 1 hour but usually overnight. The DNA sample was then centrifuged at 13,000 g for 30 min at 4°C . The DNA pellet was washed in 70 % ethanol then air-dried in a fume hood and resuspended in sterile water.

2.3.11 Southern blotting

For analysis of *L. major* transfected with ATG8 knockout constructs, 5 μg DNA from resistant clones were digested with *Nde* I and separated overnight on a 0.7 % agarose gel in TBE buffer at 30 volts. The DNA in the gel was depurinated by soaking for 10 min in 0.25 M HCl, denatured for 15 - 30 min in denaturation solution (1.5 M NaCl, 0.5 M NaOH), then neutralised by soaking for 15 - 30 min in neutralisation solution (3 M NaCl, 0.5 M Tris-HCl, pH 7), washing between these steps with distilled water. The DNA was transferred onto a Hybond-N⁺ nylon membrane (Amersham, GE Healthcare) in 20 x SSC (3 M NaCl, 0.3 M sodium citrate, pH 7) by capillary transfer overnight. Transferred DNA fragments were

covalently cross-linked to the membrane by UV cross-linking in a UV Stratalinker 2400 (Stratagene) at 1200 mJoules. The probe (5' UTR sequence of *L. major* ATG8) was prepared at 10 ng/ μ l, labelled with an AlkPhos Direct labelling kit (Amersham, GE Healthcare) following manufacturer's instructions, and incubated with the membrane overnight at 60°C in hybridisation buffer (GE Healthcare). After washing, signal was detected using CDP-Star detection reagent (Amersham, GE Healthcare) and exposed using Kodak photographic film.

2.3.12 Site-directed mutagenesis

Site-directed mutagenesis of plasmids containing GFP fusions of ATG8-like proteins were performed using the QuikChange II Site-Directed Mutagenesis kit (Stratagene) according to manufacturer's instructions. In this study site-directed mutagenesis targeted the C-terminal glycine residue of the ATG8-like proteins required for cleavage by ATG4.1, ATG4.2 or, in the case of ATG12, an unknown peptidase, in order to convert this amino acid to an alanine (Table 2-1).

2.4 Fluorescent microscopy

2.4.1 DeltaVision systems

Fluorescent microscopy was performed on an Applied Precision DeltaVision Core deconvolution microscope equipped with a Photometrics CoolSNAP HQ² camera and DAPI (381 - 399 nm), CFP (426 - 450 nm), GFP (461 - 489 nm), FITC (461 - 489 nm), YFP (505 - 515 nm), mCherry (563 - 588 nm), and Alexa594 (621 - 643 nm) filters. Earlier imaging experiments were carried out using an Applied Precision DeltaVision RT deconvolution microscope with a Photometrics CoolSNAP HQ camera and DAPI (381 - 399 nm), FITC (461 - 489 nm) and RD-TR-PE (529 - 556 nm) filters. Both microscopes are fitted with environmental chambers with temperature and CO₂ concentration regulated by a Weather Station temperature controller (PrecisionControl). DIC images were obtained under polarised light. Typically a 3 μ m Z-stack was imaged through the sample, with 0.2 μ m between Z-stacks. Deconvolution was performed using the conservative ratio method with 10 iterations. Imaging of parasites was performed at 100 x magnification, and infected macrophages at 60 x, using immersion oil with the appropriate refractive index: live parasites in PBS, 1.516; fixed parasites in VectaShield (Vector laboratories), 1.520; infected macrophages at 37°C, 1.518.

2.4.2 Live cell imaging

Live cells were centrifuged for 2 min at 1000 g, and the cell pellet washed twice in PBS by centrifugation at 1000 g for 2 min each time. Parasites were then resuspended in PBS to the appropriate cell density and a small volume was spread thinly on a slide, i.e. 10 μ l cells under a 22 x 40 mm coverslip, sealing the coverslip with nail varnish. Mounted parasites were observed on the microscope immediately, and imaged for up to 1 hour to reduce cellular damage occurring due to prolonged exposure to UV light.

2.4.3 Immobilisation of live parasites for imaging in CyGel

CyGel (Biostat limited) was primed according to the manufacturer's instructions and cooled on ice. Cells were centrifuged at 1000 g for 2 min and resuspended in ~20 μ l PBS before addition of 250 μ l cold CyGel. The cell-CyGel mixture was spread quickly over a microscope slide and allowed to set. A coverslip was applied to the mixture and the slide transferred onto an ice pack to allow the gel to liquefy and spread under the coverslip. The slide was returned to room temperature to allow CyGel to set, and immobilised parasites were viewed by fluorescent microscopy.

2.4.4 DAPI staining

DAPI (4', 6-diamidino-2-phenylindole) was used to stain the DNA of parasites and host macrophages. DAPI was prepared as a stock solution of 10 mg/ml in sterile water and added to cells at a final concentration of 1 μ g/ml, incubated at room temperature for 5 - 10 min then washed in PBS and cells prepared for microscopy as above.

2.4.5 FM4-64 staining

The lipophilic styryl dye FM4-64 (Invitrogen Molecular Probes) is used as an endocytic tracer in *Leishmania* and can be seen to be taken up through the flagellar pocket and then through the endosomes to accumulate in the lysosomal compartment. A stock solution was prepared at 12 mM and the dye was added to cells at a final concentration of 40 μ M, incubated at 4°C for 15 min, washed three times in PBS and then incubated in medium at 25°C for various times to

stain different compartments. Immediately after washing, FM4-64 labels the flagellar pocket and parasite surface, after 15 - 30 min the dye labels the endosomes, and after longer incubations of 45 - 90 min it accumulates in lysosomes.

2.4.6 MitoTracker staining

The mitochondrion was labelled by incubating parasites with MitoTracker Red CMXRos (Invitrogen Molecular Probes), a dye that depends on an intact membrane potential for its accumulation in mitochondria. This dye was prepared at a working solution of 10 μ M and added to cells at 1 - 2 nM. Cells were incubated for 5 - 10 min at 25°C, before washing three times in PBS and preparing for live microscopy as above.

2.4.7 Concanavalin A labelling

Concanavalin A (conA) is a lectin that selectively binds to α -mannopyranosyl and α -glucopyranosol residues of carbohydrates and is taken up by endocytosis to label late endosomes. In this study, conA Alexa Fluor 594 conjugate (Invitrogen Molecular Probes) was used as a label of the flagellar pocket and late endosomes. Parasites were incubated with 50 μ g/ml conA (from a 5 mg/ml stock) for 2 hours at 25°C before washing three times in PBS and preparing for live microscopy.

2.4.8 Immunofluorescence analysis

Parasites were fixed using methanol fixation. Briefly, parasites were spun down at 1000 g for 2 min, washed once in PBS, and then resuspended to the required cell density in PBS. A microscope slide was coated with poly-L-lysine (Sigma) and then wells drawn onto the slide using a hydrophobic barrier pen. The resuspended cells were added to wells and allowed to settle for 2 - 4 min, before removing the excess liquid from wells and placing the slide in 100 % methanol pre-cooled to -20°C. After overnight incubation in methanol at -20°C, the slide was rehydrated in a PBS bath. Primary antibody at the appropriate dilution was added to each well, including a no primary antibody control, and the slide was incubated in a moist chamber for 1 hour at room temperature. After washing wells twice in PBS, the Alexa fluorophore-conjugated secondary

antibody was added at the appropriate concentration and the slide incubated in a moist chamber in the dark for 1 hour at room temperature. Wells were then washed twice in 100 mM HEPES pH 7.5 and a drop of VectaShield (Vector laboratories) was added to a coverslip which was lowered over the wells to stain DNA and prevent photobleaching of fluorophores. Slides were stored at 4°C in the dark until imaged on the DeltaVision fluorescent microscope.

2.5 Analysis of microscopy images

2.5.1 Co-localisation analysis

Co-localisation analyses were performed using the Co-localisation Finder tool of SoftWoRx image analysis software (Applied Precision, Inc). This uses Pearson's correlation coefficient (PCC) to calculate the correlation between two variables; in this case the intensity of the two fluorophores within a selected area, with values close to zero indicating no co-localisation and values close to one indicating that the fluorophores are located within the same area (Bolte and Cordelieres, 2006). When a GFP-/RFP-ATG8-labelled vesicle was suspected to be co-localising with a fluorescent organellar marker, the region of the image containing the autophagosome and cargo was selected and a co-localisation analysis performed on this region. Due to the way autophagosomes and their cargo would be arranged in space during cargo turnover, i.e. with the engulfed cargo *inside* the autophagosome, rather than on the same structure, a PCC value of 0.5 and above was used as the criterion for genuine co-localisation.

2.5.2 Analysis of vesicle size

Image measurements were performed using SoftWoRx Explorer image analysis software (Applied Precision Inc.). Vesicle diameter was measured in both x and y directions at the widest section of the structure and recorded in μm or nm.

2.6 Statistical analyses

Statistical analysis of data was carried out using GraphPad Prism 5 software. For comparison of two datasets an unpaired student's t test was used, and for comparison of 3 or more datasets, a one-way ANOVA (analysis of variance)

followed by a Tukey-Kramer multiple comparison test. Data were considered to be significantly different if the p value was less than 0.05.

2.7 Biochemical methods

2.7.1 SDS-PAGE

Protein extracts from *Leishmania* were loaded into sodium dodecyl sulphate polyacrylamide gels for separation and visualisation of proteins. 12 % (w/v) polyacrylamide gels were cast in plastic casting cassettes (Invitrogen), and then a 5 % stacking gel was cast over this to allow focussing of the proteins before their separation on the 12 % resolving gel. In some cases acrylamide gels containing 6 M urea were prepared, by dissolving urea in the tris and acrylamide with gentle heating before addition of the other ingredients. Electrophoresis was performed in an XCell SureLock Mini Cell chamber (Invitrogen) with 1 x SDS-PAGE running buffer (10 x running buffer: 25 mM Tris, 192 mM glycine and 0.1 % (w/v) SDS) at 180 volts. A broad range protein marker (New England Biolabs) was loaded alongside protein samples at a concentration of 1 - 2 µg per lane to determine sizes of protein bands on the gel.

2.7.2 Coomassie staining

Following electrophoresis, polyacrylamide gels were incubated with Coomassie stain (0.25 % (w/v) Coomassie brilliant blue R250, 45 % (v/v) methanol, 10 % (v/v) glacial acetic acid, in distilled water) for 1 hour at room temperature with agitation. The gels were washed in destain solution (10 % methanol, 10 % acetic acid, in distilled water) for several hours or overnight, at room temperature and with agitation. Destain solution was changed as required until the Coomassie stained protein bands could be seen clearly.

2.7.3 Western blotting

For Western blotting, proteins were transferred from a polyacrylamide gel, following electrophoresis, to a Hybond-C nitrocellulose membrane (Amersham, GE Healthcare). Transfer was carried out by semi-dry blotting using a BioRad Trans-Blot SD Semi-Dry Transfer Cell at 20 volts for 30 min, with the membrane and filter paper soaked in transfer buffer (20 mM Tris-HCl, 15 mM glycine, 20 %

(v/v) methanol, in distilled water). The membrane was subsequently incubated in a blocking solution of 5 % (w/v) milk powder in TBST buffer (25 mM Tris-HCl pH 8, 125 mM NaCl, and 0.1 % Tween) for 1 hour at room temperature or overnight at 4°C, with agitation. This blocking step prevents non-specific binding of antibodies to the membrane. After blocking, the membrane was incubated with primary antibody diluted to an appropriate concentration in fresh TBST with 5 % milk for 1 hour at room temperature. Relevant concentrations of antibody are described in figure legends. The membrane was washed three times in TBST, incubating for 10 min each time, before incubation with horse radish peroxidase (HRP)-conjugated secondary antibodies at 1 in 5000 dilution for 1 hour at room temperature. After washing three times in TBST, the membrane was treated with an ECL (enhanced chemiluminescence) kit (SuperSignal West Pico Chemoluminescent Substrate, Pierce) according to manufacturer's instructions and then exposed on Kodak photographic film.

3 The Role of Autophagy in Organelle Turnover in *L. major*

3.1 Introduction

3.1.1 Autophagic organelle turnover

Autophagy has been considered to be a non-selective degradation system whereby bulk sequestration of cytosol containing macromolecules and organelles, and their breakdown in the lysosome allows recycling of building materials to maintain cellular homeostasis and supply energy. In addition, autophagy acts as a quality control mechanism by selectively targeting organelles, protein aggregates or, in higher eukaryotes, intracellular pathogens to the lysosome for clearance. There is sufficient, and constantly growing, evidence for various organelles being selectively targeted by autophagy: these include pexophagy, mitophagy, reticulophagy, and nucleophagy, the selective degradation of peroxisomes, mitochondria, endoplasmic reticulum and parts of the nucleus, respectively, as well as the Cvt pathway, aggrephagy, ribophagy and xenophagy, in which immature vacuolar hydrolases, protein aggregates, ribosomes, and intracellular pathogens are targeted. These are discussed in more detail below.

3.1.2 Mechanisms of selective autophagy

Specific proteins are required for labelling of cargo for autophagic degradation, subsequent recognition of these “labels”, and recruitment of the core autophagic machinery to the site of cargo engulfment. As a general mechanism, cargo is labelled by either an organelle-specific protein, or a protein on the cargo surface is ubiquitinated; this can be induced when the organelle becomes damaged, or when misfolded proteins aggregate. Proteins known as autophagy adaptors or cargo receptors recognise cargo “labels” and simultaneously bind to the cargo and recruit components of the autophagic apparatus, through direct interactions with Atg8/LC3 (Figure 3-1 A). Most known cargo receptors contain an Atg8-interacting motif (AIM) or LC3-interacting region (LIR) which mediates binding to Atg8/LC3, as well as domains required for interaction with the labelled cargo (Noda et al., 2008), for example a ubiquitin-binding domain (Figure 3-1 B). The AIM/LIR consists of a WXXL motif which binds to two

hydrophobic pockets in the conserved β -strand region of Atg8-family proteins (Noda et al., 2008). Specific autophagy receptors are described below for each cargo.

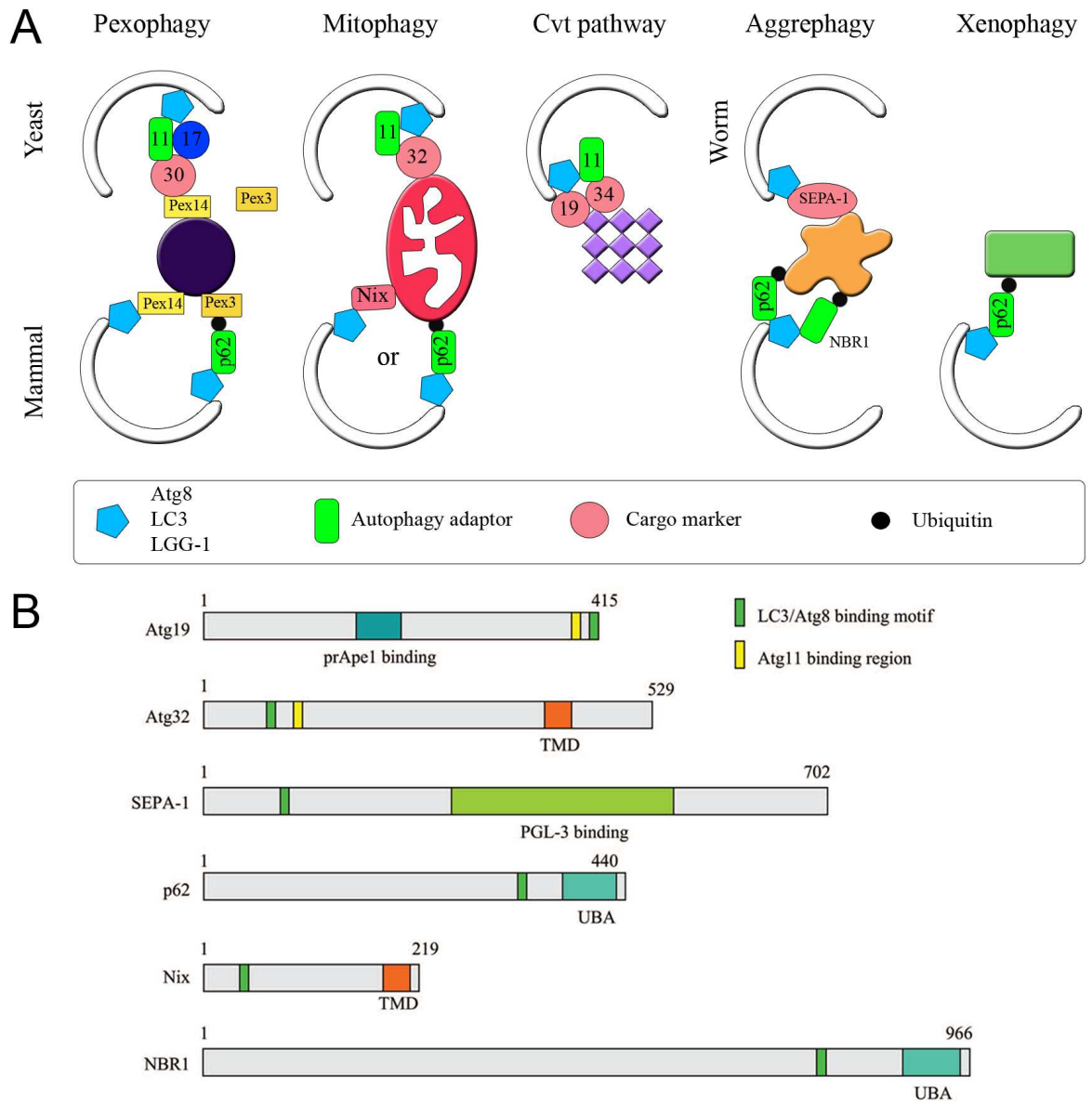


Figure 3-1 Mechanisms of selective autophagy and architecture of proteins involved.

A. Selective autophagy pathways and their mechanisms characterised to date in yeast, mammals and *C. elegans*. See following text for detailed explanations. B. Adapted from Wang & Klionsky 2011. Domain organisation of some of the cargo markers and adaptors involved in selective autophagy, including location of Atg8/LC3 binding motif.

3.1.3 Pexophagy

Peroxisome turnover has been well studied in the methylotrophic yeasts *Pichia pastoris* and *Hansenula polymorpha*, in which pexophagy can be induced by shifting cells from carbon sources for which peroxisomal metabolism is required to carbon sources which do not require peroxisomal enzymes. This triggers the degradation of superfluous peroxisomes by autophagy, which can occur by macropexophagy or micropexophagy. Macropexophagy, which is analogous to macroautophagy, results in sequestration of single peroxisomes in double-membrane autophagosomes and their degradation in the yeast vacuole. Micropexophagy, on the other hand, involves engulfment of clusters of peroxisomes by vacuolar sequestering membranes and the micropexophagy-specific membrane apparatus (MIPA) that extend from the vacuole and phagophore assembly site (PAS), respectively; this process differs from that of classical microautophagy. Interestingly, in *P. pastoris* it has been shown that the type of pexophagy that occurs is dictated by ATP levels in the cell, with high levels of ATP inducing micropexophagy and lower levels macroautophagy (Ano et al., 2005); this is thought to be because the massive membrane rearrangements during micropexophagy require greater energy. Pexophagy can also be induced to remove damaged peroxisomes; removing the peroxisomal membrane protein (PMP) Pex3, through expression of a temperature-sensitive degron-Pex3 fusion, results in peroxisomal degradation by pexophagy (van Zutphen et al., 2011). Pex14, as well as the removal of Pex3, is essential for pexophagy to occur in *H. polymorpha* (Bellu et al., 2001; Bellu et al., 2002). Pex3 is integral to pexophagy signalling as it is required, along with Pex14, for recruitment of the pexophagy receptor Atg30 in *P. pastoris* (Farré et al., 2008). Phosphorylation of Atg30 on the peroxisomal membrane is required for pexophagy induction. Atg30 then interacts with Atg11 and Atg17 at the PAS to recruit the core autophagic machinery. Pex3 has recently been shown to be essential for pexophagy in *Saccharomyces cerevisiae* too; this protein is necessary for interaction with Atg36, an autophagy receptor required for induction of pexophagy in this yeast species (Motley et al., 2012). As with other autophagy receptors in yeast, Atg36 binds to both Atg8 and Atg11 to induce autophagy. However, removal of Pex3 from peroxisomes prior to pexophagy was not required in *S. cerevisiae* (Motley et al., 2012), suggesting mechanistic differences between yeast species.

Pexophagy in mammalian cells is less well understood, but also mediates degradation of excess peroxisomes when their metabolic functions are no longer required (Iwata et al., 2006), as well as basal peroxisome turnover to maintain metabolic homeostasis by degrading old organelles (Huybrechts et al., 2009). The majority (70 - 80 %) of peroxisome turnover in mammalian cells occurs by macropexophagy, although other mechanisms exist, namely the Lon protease system and 15-lipoxygenase-mediated autolysis. It has been shown that Pex14, an essential PMP, interacts directly with LC3-II during starvation conditions, in which peroxisomes are preferentially degraded over cytosolic proteins and other organelles (Hara-Kuge and Fujiki, 2008). LC3-II appears to compete with Pex5 for binding of Pex14, indicating that autophagy may selectively target peroxisomes that are no longer import competent. Intact microtubules were also required for the Pex14-LC3 interaction. There is also evidence that mono-ubiquitination of peroxisomal membrane proteins (PMPs) is sufficient to induce autophagic turnover of peroxisomes (Kim et al., 2008), and that this degradation is dependent on the autophagy adaptor p62.

3.1.4 Mitophagy

Mitochondria accumulate damage as they age, becoming less efficient in the generation of ATP and causing damage to the cell through production of reactive oxygen species (ROS). Therefore, selective removal of non-functional or impaired mitochondria is an important mechanism of cellular homeostasis. Mitophagy has been observed in yeast upon nitrogen starvation (Kissova et al., 2004) as well as in response to mitochondrial damage (Priault et al., 2005; Nowikovsky et al., 2007). This has been described to occur via both macro- and micro-autophagic mechanisms. So far, a number of proteins have been described that are essential for functional mitophagy in yeast. These include Uth1, a SUN family protein that localises to the outer mitochondrial membrane and is required for autophagic elimination of mitochondria during starvation (Kissova et al., 2004), and Aup1, a mitochondrial phosphatase necessary for mitophagy during stationary phase (Tal et al., 2007). Through screens to identify yeast genes required for mitophagy, Atg32 was discovered and found to be a specific marker for this process (Okamoto et al., 2009; Kanki et al., 2009b). Under mitophagy-inducing conditions, Atg32 binds to Atg11, as well as directly to Atg8 via an AIM, to recruit mitochondria to autophagosomes (Okamoto et al., 2009).

Atg33 is required specifically for mitophagy during stationary phase growth, although its role is unknown (Kanki et al., 2009a). Interestingly, deletion of the dynamin-like GTPase (Dnm1), required for mitochondrial fission, inhibited mitophagy in *S. cerevisiae* (Nowikovsky et al., 2007), suggesting that mitochondria need to fragment in order for mitophagy to occur. This is not surprising, as large organelles such as mitochondria would be unable to fit into autophagosomes unless they are first re-shaped to allow their engulfment. Interestingly, directing the *S. cerevisiae* pexophagy adaptor Atg36 to the mitochondrion was also able to induce mitophagy (Motley et al., 2012), suggesting that recruitment of Atg8 and the autophagic machinery to cargo is sufficient for its degradation.

In mammalian cells, the majority of studies indicate that loss of mitochondrial membrane potential and fission are required for mitophagy, with fission usually preceding loss of mitochondrial membrane (Twig et al., 2008; Kim and Lemasters, 2011). The mitochondria continually undergo fission and fusion events in order to achieve homeostasis of the organelle; fission events often generate uneven daughter organelles, one with reduced membrane potential that is unable to re-fuse with the mitochondrial network and is degraded by autophagy (Twig et al., 2008). Under starvation conditions mitochondria elongate to form a tubular network that protects the organelle from autophagic degradation, and this process is mediated through the down-regulation of Drp1 (dynamin-related protein 1) (Rambold et al., 2011; Gomes et al., 2011). Similarly, inhibition of Drp1 or Fis1, another protein involved in fission, or overexpression of Opa1, required for mitochondrial fusion, results in decreased mitophagy (Twig et al., 2008). These data support the idea that autophagy only targets small fragments of the mitochondrion. Although no mammalian homologue of Atg32 has been identified, proteins have been identified that are required for mitophagy. Nix (or BNIP3L) acts as an autophagy receptor for the removal of mitochondria during the differentiation of reticulocytes into erythrocytes (Sandoval et al., 2008), and this is achieved through the recruitment of LC3 and GABARAP via an N-terminal LIR motif (Novak et al., 2010). Another mechanism of mitophagy involves the PINK1-parkin pathway. Parkin is an E3 ubiquitin ligase that is translocated to the surface of damaged mitochondria (Narendra et al., 2008) in a PINK1-dependent manner (Narendra et

al., 2010). PINK1 is imported into all mitochondria where it is degraded by proteolysis; in damaged mitochondria PINK1 proteolysis is inhibited, allowing recruitment of Parkin specifically to damaged organelles (Narendra et al., 2010). Parkin ubiquitinates substrates in the outer mitochondrial membrane, including mitofusin1 and 2 (Gegg et al., 2010), leading to the recognition of damaged mitochondria by the autophagic adaptor p62 (Geisler et al., 2010), which binds to ubiquitin and interacts with LC3 to package ubiquitinated cargo into autophagosomes.

3.1.5 Reticulophagy

The endoplasmic reticulum (ER) is a major site of protein folding and post-translational modifications. Accumulation of misfolded proteins or aggregates in the ER lumen stimulates the unfolded protein response (UPR), a signalling cascade that increases the ER's protein folding activity and leads to elimination of misfolded protein aggregates through inhibition of general translation, and up-regulation of genes encoding ER chaperones and components of the ER-associated degradation (ERAD) pathway. ERAD recognises defective proteins and translocates them to the ER surface where they can be degraded via the ubiquitin-proteasome system. Induction of ER stress with various chemicals stimulates selective autophagy of the ER in yeast (Bernales et al., 2006; Yorimitsu et al., 2006) and mammalian cells (Ogata et al., 2006). It is hypothesised that sections of the ER that contain misfolded proteins are sequestered by autophagosomes and in this way reticulophagy complements the UPR and ERAD in restoring ER homeostasis. Selective uptake of ER fragments has also been observed in yeast during starvation (Hamasaki et al., 2005). Interestingly, reticulophagy induced by ER stress differs from that induced by starvation in that the former involves engulfment of tightly-stacked ER membrane cisternae (Bernales et al., 2006), whereas in the latter autophagosomes contain small ER fragments (Hamasaki et al., 2005). So far no specific cargo receptors have been identified for reticulophagy, although in yeast it is known to require Atg1, Atg8, Atg9, Atg16, Atg19 and Atg20 during ER stress (Bernales et al., 2006); Atg19 and Atg20 are both important for selective autophagy pathways. Starvation-induced reticulophagy requires Atg16 as well as the actin cytoskeleton (Hamasaki et al., 2005). The ER is thought to be the primary site of autophagosomal biogenesis, so reticulophagy may not require a

cargo receptor for recruitment of the core autophagy machinery as it will already be present. ER membranes could be rearranged by the autophagy machinery during reticulophagy to enclose dysfunctional or damaged sections of the organelle. Bernales *et al* observed ER-containing autophagosomes that were continuous with ribosome-studded ER membranes, suggesting that this could indeed be the case.

3.1.6 Nucleophagy

Parts of the nucleus can also be degraded by autophagy. In *S. cerevisiae* this occurs through a process known as piecemeal microautophagy of the nucleus (PMN), whereby nuclear-vacuolar junctions (NVJs) are formed through the interaction of the vacuolar membrane protein Vac8 with Nvj1 on the outer nuclear envelope (Roberts et al., 2003). This leads to parts of the nucleus being pinched off and degraded in the vacuole in a process resembling microautophagy. PMN can be induced during nutrient starvation, which increases Nvj1 expression, but it is thought that rather than providing nutrients, this is likely a mechanism for regulating nuclear processes such as transcription or ribosome biogenesis, or degrading damaged areas of the nucleus. PMN requires all genes encoding the core autophagy machinery, as well as the autophagy adaptor Atg11, suggesting that this is a selective process (Krick et al., 2008). Evidence also exists for nucleophagy in mammalian cells, although in this case it appears to resemble macroautophagy. Large LC3-labelled autophagosomes/autolysosomes were seen surrounding damaged nuclei in cells with mutations in genes encoding nuclear envelope proteins (Park et al., 2009). Inhibition of autophagy led to increased nuclear abnormalities and decreased cell viability, suggesting that nucleophagy is important for maintaining cellular homeostasis through the degradation of damaged nuclear components. Similar perinuclear autophagosomes were observed in WT cells, albeit at much lower levels, which suggests autophagy plays a role in nuclear homeostasis under basal conditions as well as during nuclear stress.

3.1.7 Cytoplasm to vacuole targeting (Cvt) pathway

The Cvt pathway is a selective autophagy pathway that has been identified only in the yeasts *S. cerevisiae* (Kim et al., 1997) and *P. pastoris* (Farré et al., 2007).

It occurs during nutrient rich conditions and mediates the transport of precursor forms of the vacuolar hydrolases aminopeptidase I (ApeI) and α -mannosidase (AmsI) from the cytosol to the vacuole where they are processed into their active forms. Precursor ApeI molecules form large complexes in the cytosol which are bound by the Cvt-specific receptor protein Atg19 (Scott et al., 2001). AmsI is also bound by Atg19, as well as by its paralogue Atg34 (Suzuki et al., 2010). Atg19 and Atg34 interact with the yeast autophagy adaptor protein Atg11 (Yorimitsu and Klionsky, 2005), and with Atg8 (Kim et al., 2002; Suzuki et al., 2010) to recruit the core autophagic machinery and enclose the protein complexes within autophagosomes, which are then trafficked to the yeast vacuole.

3.1.8 Aggrephagy

Aggregation of aberrant proteins interferes with normal cellular functions and build-up of these aggregates is known to be involved in the pathology of neurodegenerative disorders such as Parkinson's, Alzheimer's and Huntington's diseases. Elimination of these toxic protein aggregates by autophagy is known as aggrephagy and is important for maintenance of neurons (Hara et al., 2006; Komatsu et al., 2006). Autophagy is required for the removal of misfolded protein aggregates because proteins need to be unfolded in order to be degraded by the proteasome. Protein aggregates are ubiquitinated and this leads to the recruitment of p62 (SQSTM1) which binds to both mono- and poly-ubiquitin via a UBA domain. Homo-polymerisation of p62 via its PB1 domain allows arrangement of the bound protein aggregates into larger units (Johansen and Lamark, 2011). p62 binds directly to LC3 in order to recruit the autophagy machinery which forms an autophagosome around the protein cargo ready for trafficking to the lysosome (Pankiv et al., 2007). Two other proteins involved in formation of protein aggregates with p62 are the autophagy cargo receptor NBR1 (Kirkin et al., 2009) and the scaffold protein ALFY (Filimonenko et al., 2010). These proteins are recruited to protein inclusions as part of a complex containing p62, LC3, ATG5, ATG12 and ATG16L (Filimonenko et al., 2010), and are thought to collaborate with p62 in order for efficient autophagic clearance of aggregates. HDAC6 is also involved in the process; it is required for formation of protein aggregates and binds to ubiquitin as well as to dynein motors (Iwata et al., 2005). HDAC6 also promotes the formation of an actin network for

transport of protein aggregate-containing autophagosomes to the lysosome (Lee et al., 2010a). Aggrephagy has also been described in *Caenorhabditis elegans*, where it is important for the degradation of P granules during embryogenesis (Zhang et al., 2009). An adaptor protein called SEPA-1 mediates aggregation of P granule proteins, through direct interactions with the P granule component PGL-3. It also binds to LGG-1, the *C. elegans* homologue of Atg8, to initiate the autophagic degradation of P granule aggregates.

3.1.9 Ribophagy

Ribosomes have often been reported within autophagosomes, but only recently has selective autophagy of ribosomes been considered. In starved *S. cerevisiae* ribosomes are degraded more quickly than other cytoplasmic proteins, suggesting a selective degradation. Transport of ribosomes to the vacuole was found to require the core autophagy genes Atg1 and Atg7, as well as the ubiquitin protease Ubp3 and its cofactor Bre5 (Kraft et al., 2008). This suggests a role for ubiquitination in this process, perhaps similar to the selective autophagy mechanisms in mammals. The proposed role of ribophagy during starvation, in addition to provision of amino acids, is the down-regulation of protein translation, a process that consumes energy and amino acids that are needed by the cell for surviving nutrient stress. Ribosomes of mammalian cells are also degraded with different kinetics to other cytoplasmic proteins (Kristensen et al., 2008), perhaps indicating that ribophagy exists in higher eukaryotes.

3.1.10 Xenophagy

Intracellular bacteria and viruses can also be targeted by autophagy which is increasingly recognised as an important immune defence mechanism. Intracytosolic bacteria such as *Listeria monocytogenes* and *Salmonella* spp. are ubiquitinated and subsequently recognised by p62, as well as NDP52 and optineurin (OPTN), which appear to be bacteria-specific autophagy receptors (Thurston et al., 2009; Mostowy et al., 2011; Wild et al., 2011). The targets of ubiquitin modification, presumably bacterial surface proteins, have not been identified to date. Autophagy has been found to control *Mycobacterium tuberculosis* infection through p62-dependent selective targeting of ribosomal and ubiquitinated cytosolic proteins to the lysosome, which are proteolytically

processed into anti-microbial peptides that kill the bacteria (Ponpuak et al., 2010). Some bacterial pathogens have evolved mechanisms to evade autophagic degradation or to utilise the autophagic machinery to aid their intracellular replication (Mostowy and Cossart, 2012).

Research into the selective autophagy of viruses is at an earlier stage, but has been reported to protect against vesicular stomatitis virus infection in *Drosophila* and against CNS infection with Sindbis virus in mice (Sumpter and Levine, 2011). Interestingly, p62 is required for recognition of Sindbis virus capsid and subsequent recruitment of autophagosomes; it is currently unknown whether p62 binds directly to viral capsid protein or if these antigens are ubiquitinated. As with bacteria, some viruses use the autophagy machinery for their own benefit in order to establish infections. In addition, important roles for autophagy are arising in the modulation of the immune system, through presentation of both MHC class I and II antigens as well as in the development of lymphocytes (Crotzer and Blum, 2010).

3.1.11 Evidence of selective autophagy in trypanosomatids

Autophagy has been well-characterised in *Leishmania* and is known to be important for successful life-cycle differentiation of this parasite (Williams et al., 2006; Besteiro et al., 2006a), during which autophagy is hypothesised to remodel cellular architecture and metabolism through the selective autophagy of organelles in order to adapt them to the conditions they will encounter in the next life cycle environment. Likewise, autophagy has been characterised in *T. cruzi* (Alvarez et al., 2008), and more recently in *T. brucei* (Proto, PhD thesis 2010; Li et al., 2012a), and been shown to be involved in the differentiation of the former. Bioinformatic analyses have revealed that trypanosomatids possess the core autophagic machinery, although no evidence of genes encoding known selective autophagy proteins has been found (Brennan et al., 2011). Despite the knowledge that autophagy pathways exist in these organisms, few studies have investigated which cargoes are sequestered by trypanosomatid autophagosomes. Work in *T. brucei* suggests that glycosomes, organelles analogous to peroxisomes, are turned over by an autophagic process during differentiation (Herman et al., 2008). Glycosomes appear to associate with the lysosome upon differentiation of slender bloodstream forms into stumpy forms and in stumpy

forms differentiating into procyclic forms, with a concomitant increase in lysosomal size. Glycosomal enzymes were also detected in the lysosome by immunoelectron microscopy. Additionally, clusters of glycosomes have been identified within double-membrane bound structures (Brennan et al., 2011). A similar autophagic turnover of glycosomes is expected to occur during differentiation of *Leishmania* from the extracellular promastigote stage in the sandfly to the intracellular amastigote residing within mammalian macrophages. Several studies have shown that glycolytic enzymes are upregulated in promastigotes, whereas in amastigotes enzymes required for gluconeogenesis and β -oxidation of fatty acids are more important (Rosenzweig et al., 2008b; Brotherton et al., 2010). In addition, during this transformation glycosome numbers decrease from an estimated 50 - 100 glycosomes per cell in promastigotes (Opperdoes, 1987) to ~10 per cell in amastigotes (Coombs et al., 1986). Other evidence that exists for organelle turnover in trypanosomatids is the appearance of acidocalcisomes in autophagic-like structures in *L. amazonensis* treated with sterol biosynthesis inhibitors (Vannier-Santos et al., 1999). By electron microscopy, electron-dense organelles resembling acidocalcisomes were observed being surrounded by circular ER-like membrane structures, which possibly represent autophagosomes.

3.2 Identification of autophagic cargo in *L. major*

As discussed above, various cargoes have been observed to be degraded by autophagy in yeast and higher eukaryotes. To determine whether different organelles may be autophagy cargo in *Leishmania*, cell lines were generated constitutively expressing GFP- or RFP-ATG8 along with various organelle-specific fluorescent markers. Promastigotes were analysed by live fluorescent microscopy in logarithmic growth phase, stationary phase and after 4 hours starvation in PBS. Autophagy is known to be induced in *Leishmania* during differentiation between life cycle stages as well as during starvation (Williams et al., 2006; Besteiro et al., 2006a). It is expected that organelle turnover increases during *Leishmania* differentiation as the cells remodel themselves in order to adapt their structure and metabolism to the environment encountered by the next life cycle stage. During starvation organelles may also be degraded to supply nutrients in order to ensure cell survival.

There is abundant evidence that autophagy degrades excess peroxisomes in response to changing environmental conditions in yeast and mammalian cells, and some evidence for its involvement in glycosome turnover during differentiation and starvation in *T. brucei* (Herman et al., 2008). To investigate whether autophagy might be involved in a similar degradation of glycosomes in *L. major*, parasites were produced that constitutively expressed GFP-ATG8 and RFP-SQL. The C-terminal SQL motif is a PTS1-type glycosomal targeting sequence sufficient to target proteins to glycosomes (Sommer et al., 1992; Plewes et al., 2003). GFP-ATG8-labelled autophagosomes were observed co-localising with RFP-SQL-labelled glycosomes in promastigotes (Figure 3-2) during log phase, stationary phase and starvation, suggesting that glycosomes indeed constitute autophagic cargo in *Leishmania*. Further analysis of glycosome turnover is presented in Chapter 3.4.

Mitophagy, the selective autophagic degradation of mitochondria, is important for mitochondrial homeostasis in mammalian cells and yeast. However, in *Leishmania* no co-localisation of RFP-ATG8 and ROM-GFP, a rhomboid serine peptidase encoded by LmjF04.0850 and predicted to localise to the inner mitochondrial membrane (Williams et al., 2012b), was detected under normal growth conditions or during starvation (Figure 3-2). Neither was ROM-GFP

observed within tubular structures that are the lysosomal compartment of stationary phase parasites (Mullin et al., 2001). Instead, over half of all autophagosomes were observed in close association with the reticulate structure of the mitochondrion. These data suggest that autophagy is not responsible for turnover of the *Leishmania* mitochondrion during normal growth or starvation. Further analysis of autophagosome interactions with the mitochondrion is presented in Chapter 3.3.

Extending the analysis of autophagic cargo, acidocalcisomes, which are organelles important for cation and pH homeostasis, and osmoregulation (Moreno and Docampo, 2009), were examined. It is conceivable that acidocalcisome numbers could be regulated to adapt the parasites to changing conditions of different life cycle environments and that autophagy could be responsible for their degradation when fewer are needed. V-H⁺-PPase (LmjF31.1220)-GFP was used as a marker of acidocalcisomes (Besteiro et al., 2008). Although V-H⁺-PPase-GFP was seen localised to puncta representing acidocalcisomes, no co-localisation of these structures with RFP-ATG8 autophagosomes was evident during stationary phase or starvation (Figure 3-2; Table 3-1); neither was V-H⁺-PPase-GFP ever observed in lysosomal structures containing RFP-ATG8.

Calpain-GFP was used as a marker of the flagellum (Tonn, PhD thesis 2010) and co-expressed with RFP-ATG8 in *L. major*. Bioinformatic analysis suggests that calpain (encoded by LmjF31.0390) is very likely to be palmitoylated and myristoylated, and therefore membrane-associated rather than an integral membrane protein (Ersfeld et al., 2005). The flagellum is a dynamic organelle which changes its length throughout the parasite life cycle; it is unknown whether autophagy has any role in degradation and recycling of flagellar constituents during flagellar regression. In promastigote stages there appeared to be no co-localisation between RFP-ATG8 puncta and calpain-GFP, with calpain-GFP always remaining localised to the flagellum (Figure 3-2), whether the parasites were in stationary phase or had been starved for 4 h (Table 3-2). Nor was calpain-GFP observed in lysosomal compartments with RFP-ATG8. These data suggest that acidocalcisomes and the flagellum are not cargo of autophagosomes, at least in promastigote stages.

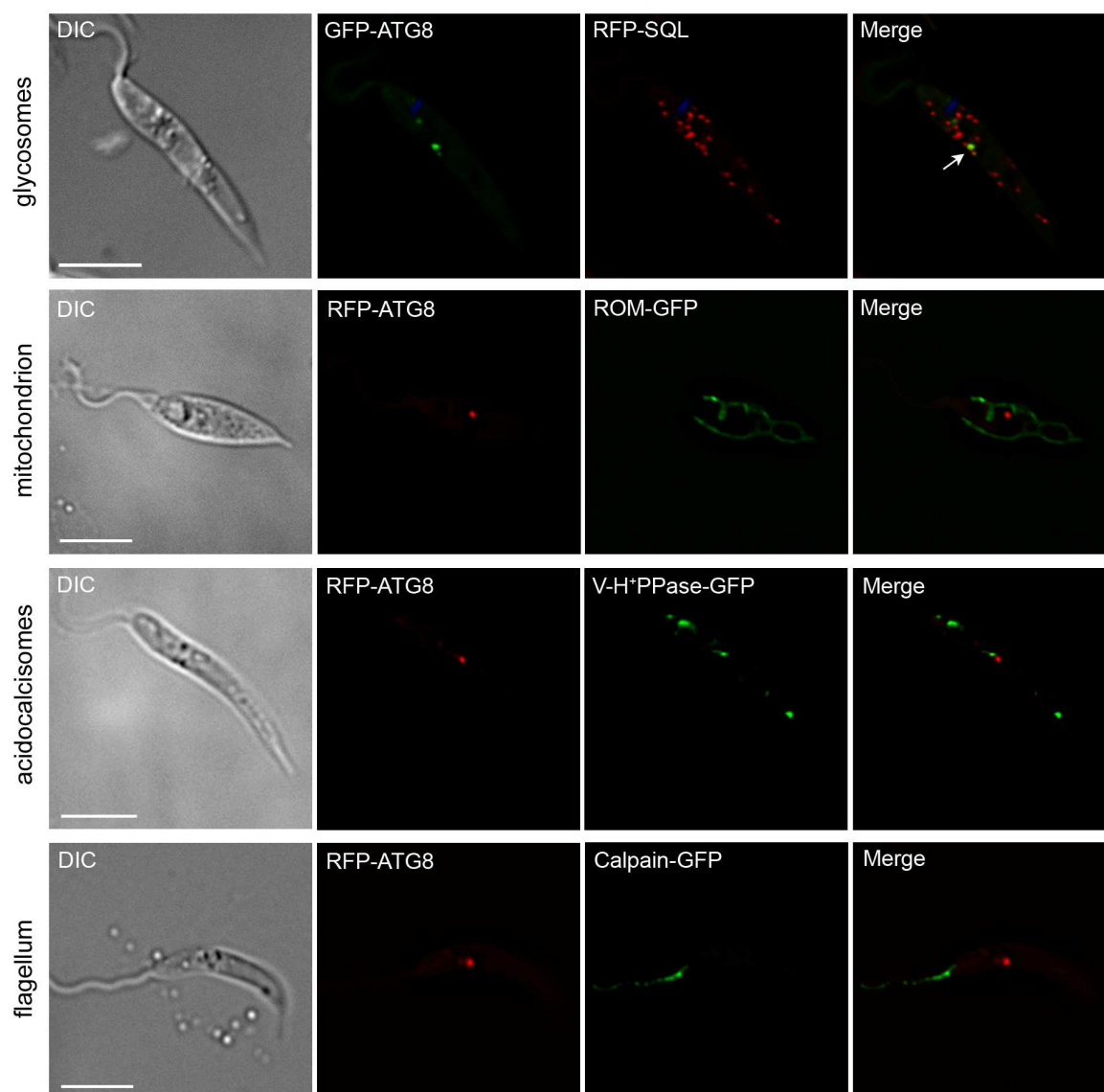


Figure 3-2 Identification of autophagic cargo in *L. major* promastigotes. *L. major* promastigotes co-expressing GFP-/RFP-ATG8 and organelle-specific fluorescent markers in stationary phase were washed and resuspended in PBS and imaged using an Applied Precision DeltaVision Core microscope for maximum 1 h. Arrow marks co-localisation. Images show a single slice from a 3 μm Z stack. Scale bar = 5 μm .

Table 3-1 Summary of autophagosome – acidocalcisome co-localisation experiments. Data are from at least 3 independent experiments. Approximately 200 cells were counted per experiment following preparation for live fluorescent microscopy. % cells with RFP-ATG8 puncta data is expressed as the mean of multiple experiments \pm standard deviation.

RFP-ATG8 + V-H ⁺ -PPase-GFP	No. cells counted	% cells with RFP-ATG8 puncta	No. puncta counted	No. puncta co-localised with acidocalcisomes
Stationary phase	566	32 \pm 10 %	196	0
Logarithmic phase Starved 4 h	773	19 \pm 3 %	178	0

Table 3-2 Summary of autophagosome – flagellum co-localisation experiments. Data are from at least 3 independent experiments. Approximately 200 cells were counted per experiment following preparation for live fluorescent microscopy. % cells with RFP-ATG8 puncta data is expressed as the mean of multiple experiments \pm standard deviation.

RFP-ATG8 + calpain-GFP	No. cells counted	% cells with RFP-ATG8 puncta	No. puncta counted	No. puncta co-localised with flagellum
Stationary phase	376	46 \pm 13 %	184	0
Logarithmic phase Starved 4 h	480	31 \pm 13 %	187	0

3.3 The mitochondrion as a possible source of autophagic membrane

3.3.1 Interactions of autophagosomes with the mitochondrion

RFP-ATG8-labelled autophagosomes in promastigotes were seen to associate closely with the reticulate mitochondrion labelled by ROM-GFP (Figure 3-3 A), rather than to contain ROM-GFP or fragments of the mitochondrion as would be expected if mitophagy were taking place. In addition, ROM-GFP was never seen within the lysosome or MVT-lysosome (Figure 3-3 B), supporting a lack of trafficking of this mitochondrial marker to the lysosome. Quantification of RFP-ATG8 puncta revealed that over 50 % of all autophagosomes during log phase, stationary phase or starvation were associated with the mitochondrion (Table 3-3). Similar results were obtained using a different mitochondrial marker MUP (LmjF26.2070)-GFP, a ubiquitin-like peptidase that localises to the outer mitochondrial membrane (Williams et al., 2012b). This close association led to the hypothesis that the mitochondrion could be a membrane source for autophagosomes in *Leishmania*, as has been shown recently in starved mammalian cells (Hailey et al., 2010).

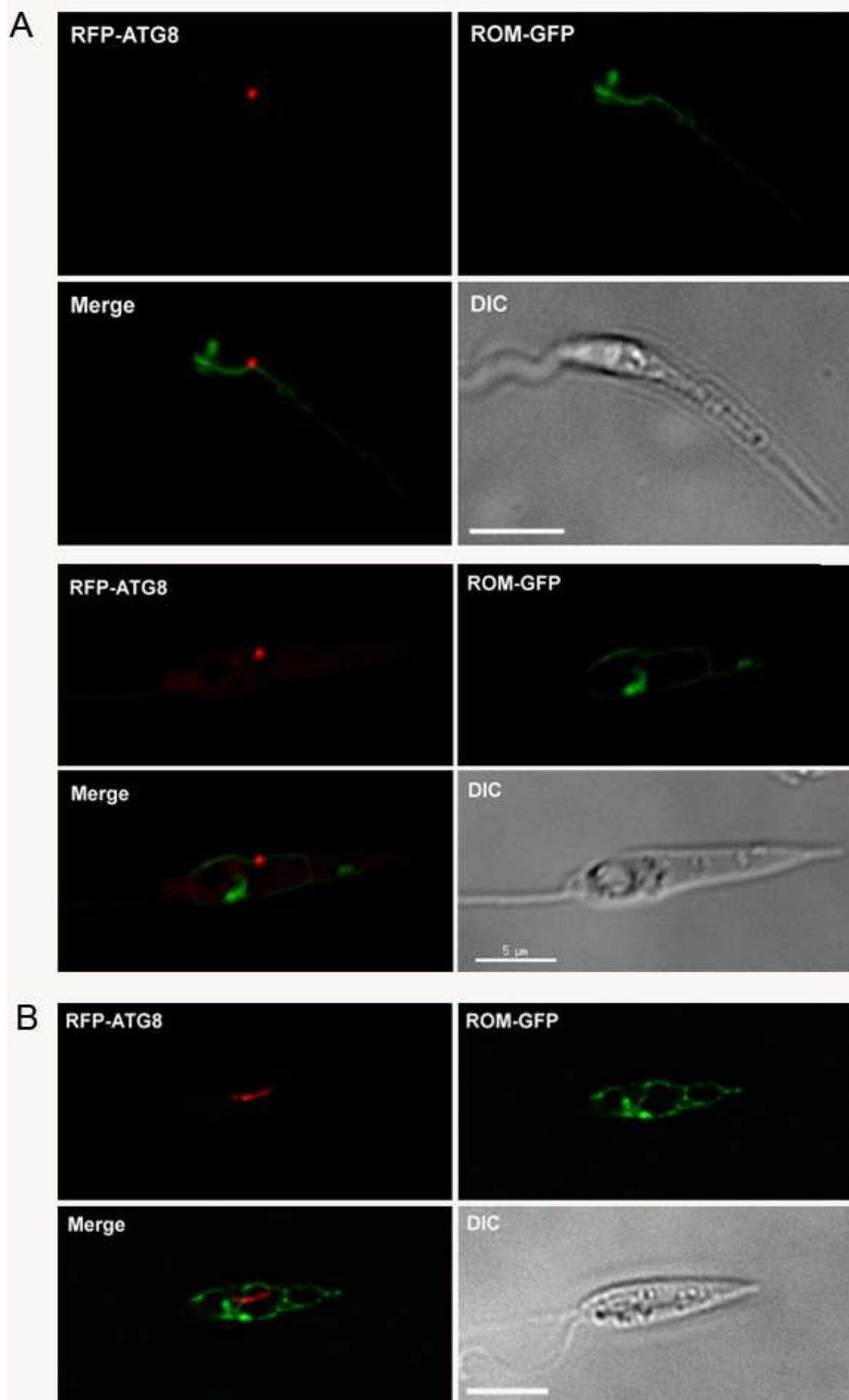


Figure 3-3 Analysis of RFP-ATG8 interactions with the *Leishmania* mitochondrion. Stationary phase *L. major* promastigotes co-expressing RFP-ATG8 and ROM-GFP were washed, resuspended in PBS and imaged on the DeltaVision Core microscope. A. Localisation of RFP-ATG8 to autophagosomes and their association with the mitochondrion. B. RFP-ATG8 labelling MVT-lysosome. Images show a single slice from a 3 µm Z stack. Scale bar = 5 µm.

Table 3-3 Summary of autophagosome - mitochondrion experiments. Data are from at least 6 independent experiments. Approximately 200 cells were counted per experiment following preparation for live fluorescent microscopy % cells and % puncta are expressed as mean \pm standard deviation.

RFP-ATG8 + ROM-GFP	No. cells counted	% cells with RFP-ATG8 puncta	No. puncta counted	% puncta associated with mitochondrion
Stationary phase	525	62 \pm 6 %	281	53 \pm 4 %
Logarithmic phase	4251	8 \pm 3 %	290	68 \pm 7 %
Logarithmic phase Starved 4 h	1673	21 \pm 6 %	310	61 \pm 8 %

3.3.2 Interactions of early autophagosomes with the mitochondrion

To examine whether autophagosomes might be forming from mitochondrial membranes, *L. major* parasites were generated expressing mCherry-ATG5, a marker of early, forming autophagosomes, along with the mitochondrial markers, ROM-GFP or MUP-GFP. These cells were observed in stationary phase as at this stage of promastigote growth the highest occurrence of autophagy is observed. A similar proportion of mCherry-ATG5 puncta were seen to associate with the mitochondrion as with RFP-ATG8 puncta (Figure 3-4; Table 3-4). This supports the hypothesis that autophagosome biogenesis may occur at the mitochondrion using lipids from the mitochondrial membrane.

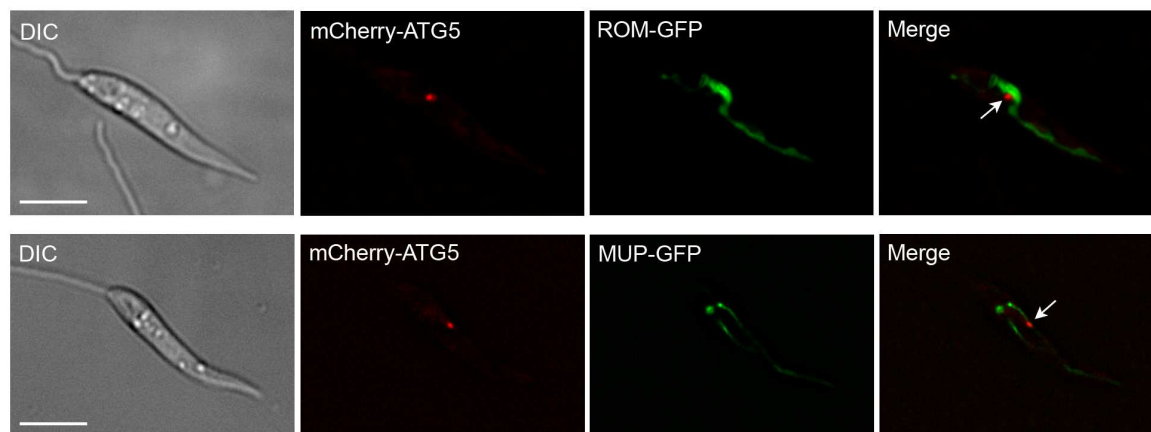


Figure 3-4 Analysis of mCherry-ATG5 interactions with the mitochondrion. Stationary phase cells were washed, resuspended in PBS and imaged on a DeltaVision Core microscope. Arrows mark association of mCherry-ATG5 puncta with the mitochondrion. Images show a single slice of a 3 μ m Z stack. Scale bar = 5 μ m.

Table 3-4 Association of mCherry-ATG5-labelled autophagosomes with the mitochondrion.

Stationary phase	No. cells counted	% cells with mCherry-ATG5 puncta	% puncta associated with mitochondrion
mCherry-ATG5 + ROM-GFP	100	86 %	55 %
mCherry-ATG5 + MUP-GFP	143	62 %	50 %

3.3.3 Autophagy during H₂O₂-induced fragmentation of the mitochondrion

As no mitophagy was detected during normal growth of promastigotes, it was next investigated whether autophagic degradation of the mitochondrion could be induced by fragmentation of this organelle. Treatment with 1 mM H₂O₂ has been used to induce mitochondrial fragmentation in *L. major* (Zalila et al., 2011). It was reasoned that inducing fragmentation of the *Leishmania* mitochondrion would induce autophagy to sequester and degrade mitochondrial fragments. In mammalian cells the mitochondria are constantly undergoing fusion and fission, and it is thought that damaged mitochondria that are unable to fuse to the mitochondrial network are targeted by autophagy (Twig et al., 2008). Indeed, during nutrient starvation, the mammalian mitochondria fuse together to form an elongated network which protects them from autophagic degradation (Rambold et al., 2011; Gomes et al., 2011), suggesting that autophagy can only target small mitochondrial fragments.

Incubation of log phase *L. major* promastigotes in 1 mM H₂O₂ for 1 hour at 25°C caused fragmentation of the mitochondrion in the majority of cells (Figure 3-5 A) but did not significantly increase appearance of RFP-ATG8 puncta compared to an untreated control (Figure 3-5 B). However, RFP-ATG8 puncta were significantly larger in H₂O₂-treated cells (Figure 3-5 A and C). Despite the increased size of RFP-ATG8 puncta, a small proportion (6.5 %) of these structures were seen co-localising with fragments of the mitochondrion labelled with ROM-GFP (Figure 3-5 D), as assessed by Pearson's coefficient of correlation (PCC; see Materials and Methods). These data show that mitophagy appears to be responsible for some degradation of mitochondrial fragments under conditions where the mitochondrion is damaged. Analysis of sizes of RFP-ATG8 puncta demonstrated that there was no difference in vesicle size between those that co-localised with mitochondrial fragments and those that did not, although puncta were significantly bigger than in untreated parasites (Figure 3-5 C).

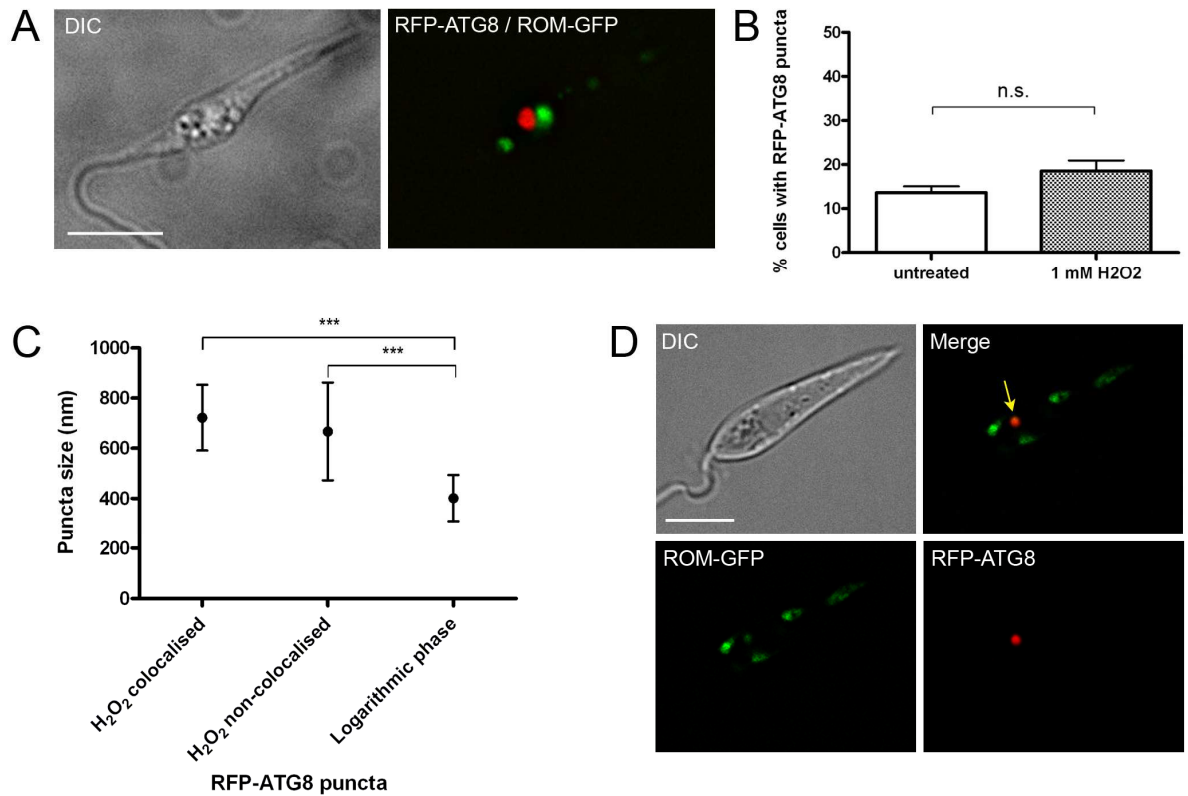


Figure 3-5 Analysis of autophagy in H₂O₂-treated cells. Log phase *L. major* parasites were incubated with 1 mM hydrogen peroxide for 1 h at 25°C before washing and resuspension in PBS. Cells were imaged on DeltaVision Core fluorescent microscope. A. *L. major* co-expressing RFP-ATG8 and ROM-GFP were treated and processed for microscopy as above. B. Percentage of cells exhibiting one or more RFP-ATG8 puncta was determined by counting 200 treated and 200 untreated cells per experiment. Bars show mean and error bars standard deviation of four independent experiments. Data were analysed using a student's t test; n.s. not significant. C. Puncta sizes were measured using SoftWoRx Explorer Image Analysis software. Data were analysed using one-way ANOVA. *** signifies $p < 0.001$. D. Parasites were treated and prepared for microscopy as above. Co-localisation analysis was performed using SoftWoRx Image Analysis software (Applied Precision). Arrow marks co-localisation. Scale bar = 5 μ m.

To determine whether the larger RFP-ATG8 puncta were due to increased trafficking of ATG8 to lysosomes, parasites expressing GFP-ATG8 were incubated with FM4-64 for 1 hour to label the lysosome before incubation in H₂O₂. FM4-64 is a lipophilic dye which is taken into the cell at the flagellar pocket by endocytosis and can be traced through the endocytic system until it accumulates in the lysosome (Mullin et al., 2001; Besteiro et al., 2006a). All large GFP-ATG8 structures were seen to co-localise with FM4-64 (Figure 3-6, top panels), suggesting that this compartment is lysosomal. Interestingly, however, FM4-64 staining following H₂O₂ incubation resulted in visualisation of FM4-64 on the cell membrane and flagellar pocket membrane, implying that H₂O₂ disrupts membrane trafficking, possibly through damage to membrane lipids. Eukaryotic membranes are primarily composed of glycerophospholipids, such as

phosphatidylcholine, phosphatidylethanolamine, phosphatidylserine and phosphatidylinositol. Unsaturated membrane lipids are susceptible to oxidative attack from ROS, and modification of lipids in this manner can alter membrane fluidity (Smolen and Shoet, 1974; Tai et al., 2010), regulation of which is important for intracellular trafficking processes. Therefore, the large ATG8 puncta observed in treated cells may be aberrant autophagosomes whose formation has been disrupted by H_2O_2 and the appearance of FM4-64 in these vesicles could be a result of disruption of endosomal trafficking pathways that are linked to autophagosome formation. To further examine the nature of these structures, parasites co-expressing GFP-ATG8 and the lysosome-specific marker, proCPB-RFP, were examined after H_2O_2 treatment, and in these parasites the large ATG8-labelled vesicles also contained proCPB-RFP (Figure 3-6, lower panels) suggesting that these structures are indeed lysosomal. This raises the possibility that sequestration of mitochondrial fragments may be occurring in a microautophagic manner, as no evidence for co-localisation of ATG8-labelled autophagosomes with mitochondrial markers was obtained.

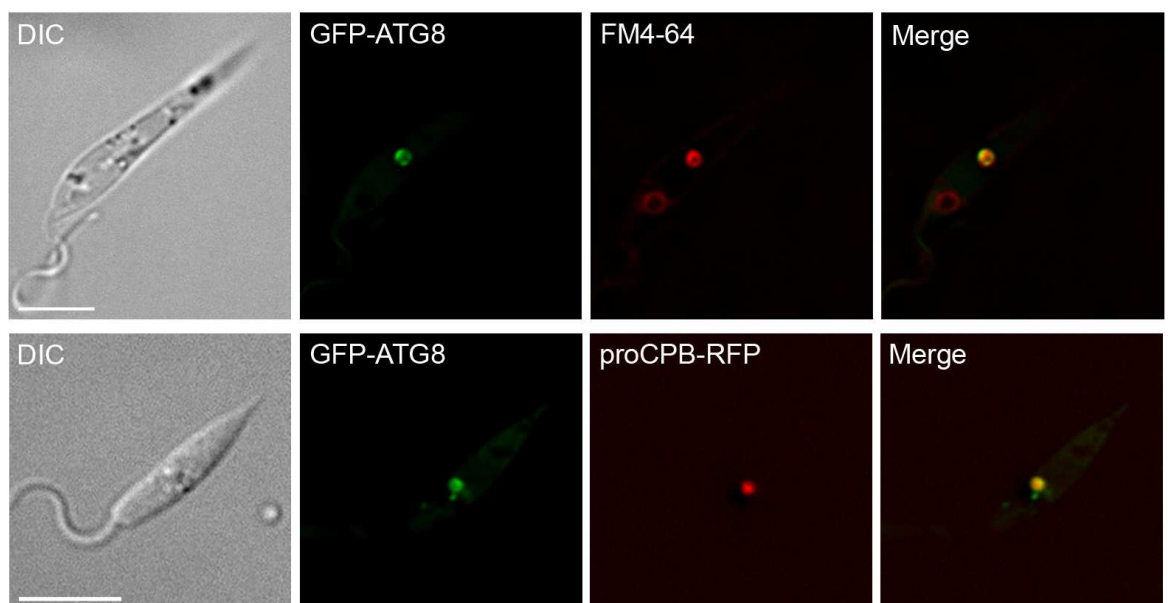


Figure 3-6 Analysis of large ATG8-labelled structures induced by treatment with 1 mM H_2O_2 . Log phase *L. major* promastigotes were treated as described below and imaged on a DeltaVision Core fluorescent microscope. Upper panels: *L. major* expressing GFP-ATG8 were incubated with 40 μ M FM4-64 for 1 h then washed in PBS before treatment with 1 mM H_2O_2 for 1 h at 25°C. Cells were washed in PBS before preparing for microscopy. Lower panels: *L. major* co-expressing GFP-ATG8 and proCPB-RFP were treated with 1 mM H_2O_2 for 1 h at 25°C before preparing for microscopy by washing and resuspension in PBS. Microscopy images show a single slice from a 3 μ m Z-stack. Scale bar = 5 μ m.

Some evidence suggests that mitochondrial depolarisation acts as a signal for the selective autophagy of this organelle (Priault et al., 2005; Narendra et al., 2008), although this is not always the case (Kim and Lemasters, 2011). To determine whether H₂O₂ treatment induces depolarisation of the *Leishmania* mitochondrion, parasites expressing ROM-GFP were labelled with MitoTracker Red, a fluorescent dye that depends on a functional membrane potential for its localisation to mitochondria (Invitrogen Molecular Probes), following H₂O₂ treatment. MitoTracker localised to the reticulate mitochondrion of untreated cells, as expected, and also labelled all mitochondrial fragments in treated cells, labelling even small fragments that would be expected to be degraded by autophagy (Figure 3-7). This shows that the fragmented mitochondrion does not lose membrane potential, and suggests that the fragments may possess some normal function. Furthermore, this could indicate that depolarisation is not required for autophagic degradation of the mitochondrion in *Leishmania*, or alternatively, that 1 hour's treatment with 1 mM H₂O₂ is insufficient to induce depolarisation of mitochondrial fragments which may be required for their targeting by autophagy. This lack of significant mitochondrial depolarisation was observed previously, as assessed by TMRM fluorescence (Zalila et al., 2011); mitochondrial membrane potential only reduced significantly after 3 - 4 hours incubation of *L. major* parasites in 0.5 mM H₂O₂.

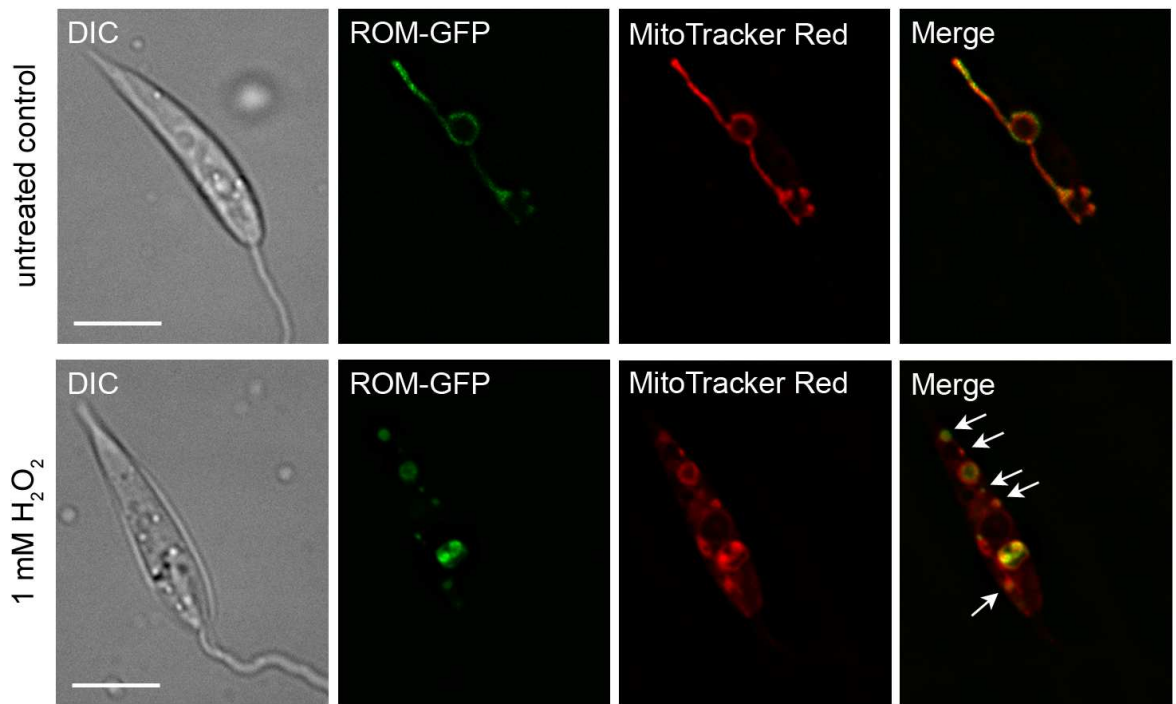


Figure 3-7 Detection of membrane potential in a fragmented mitochondrion. Log phase *L. major* promastigotes were incubated with or without 1 mM H₂O₂ for 1 h at 25°C before incubation with 2 nM MitoTracker Red for 2 min at 25°C. Cells were then washed and resuspended in PBS and imaged on a DeltaVision Core microscope. Images show a single slice from a 2 μm Z-stack. Scale bar = 5 μm. Arrows indicate small mitochondrial fragments labelled with both ROM-GFP and MitoTracker.

3.4 A role for autophagy in glycosome turnover

3.4.1 Analysis of glycosome turnover by autophagy

Co-localisation experiments showed that in *L. major* GFP-ATG8-labelled autophagosomes co-localised with glycosomes (Figure 3-2). To measure the extent to which autophagosome - glycosome co-localisation occurs, and whether it might increase during differentiation, a detailed analysis of these interactions was performed. Co-localisation events between GFP-ATG8 and RFP-SQL were analysed by Pearson's correlation coefficient (PCC; Figure 3-8), with a value of 0.5 and above used as the criterion for autophagosome - glycosome co-localisation (see Materials and Methods). As previously characterised in *L. major* (Besteiro et al., 2006a), the percentage of cells with autophagosomes increased upon starvation to 19 %, and to a greater extent during stationary phase (42 %), compared to 4 % cells in normal log phase growth (Table 3-5; Figure 3-9 A). In procyclic promastigote stages the percentage of autophagosomes co-localising with glycosomes was approximately 16 - 19 % whether in log phase, stationary phase or after 4 hours starvation of log phase cells in PBS (Table 3-5; Figure 3-9 B). As can be seen by the standard deviation in Figure 3-9 B, the percentage of autophagosomes co-localising with glycosomes varied somewhat during log phase and stationary phase experiments. In log phase this can be explained by the small number of autophagosomes observed in each experiment: any co-localisation events greatly affect the percentage in a small sample size. Also, in contrast to starvation and amastigote differentiation which were recorded at discrete time points, log and stationary phases represent a continuum and there is likely to be some variation in these populations over time, although best efforts were made to ensure cells were at the same stage of growth. The increased autophagic induction during stationary phase and starvation leads to a corresponding increase in glycosome turnover proportional to the increase in autophagy (Table 3-5; Figure 3-9 C) due to the fact that at any time 16 - 19 % of autophagosomes contain glycosomes as their cargo. Autophagosomes were similarly observed co-localising with glycosomes during differentiation of metacyclic promastigotes to amastigotes within murine macrophages (Figure 3-10); this analysis was performed 18 hours following infection, as this is known to be the time period at which autophagosome numbers are greatest during promastigote - amastigote transformation in macrophages (Williams et al.,

2006). At this stage of the life cycle 90 % of parasites contained autophagosomes (Table 3-5; Figure 3-9 A), 11 % of which co-localised with glycosomes (Table 3-5; Figure 3-9 B), and the greatest number of cells containing co-localised glycosomes occurred (Table 3-5; Figure 3-9 C). These data suggest that a population of autophagosomes target glycosomes throughout the parasite's life cycle and that autophagy may be a mechanism by which *Leishmania* control the size and composition of their glycosome population. The percentage of autophagosomes containing glycosomes appears to remain constant, but autophagy itself is up-regulated in different life-cycle stages, which results in an increase in glycosome turnover. During stationary phase and promastigote - amastigote differentiation approximately 3 % of glycosomes were found to be co-localised with autophagosomes, compared to 1 % in log phase promastigotes (Appendix, Table A-2), supporting the hypothesis that increased glycosome turnover by autophagy occurs during differentiation.

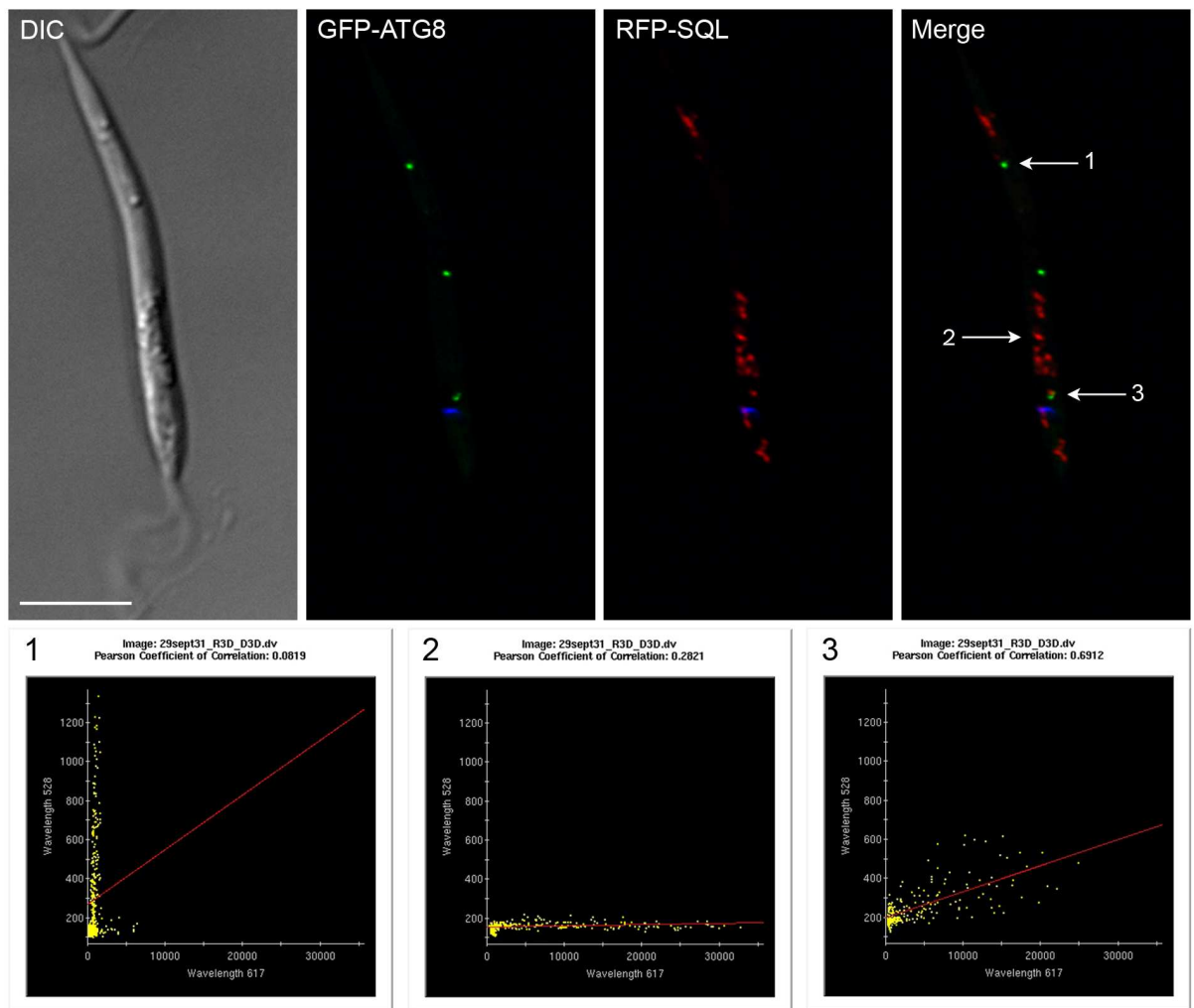


Figure 3-8 Example of co-localisation analysis in glycosome turnover experiments. *L. major* promastigotes co-expressing GFP-ATG8 and RFP-SQL were washed and resuspended in PBS and imaged on a DeltaVision RT fluorescent microscope. Co-localisation analysis was performed using Co-localisation Finder in SoftWoRx Image Analysis software. (1) Autophagosome not co-localising with glycosome. Pixels appear along y axis (wavelength 528 nm), PCC = 0.08; (2) Glycosome not co-localising with autophagosome. Pixels appear along x axis (wavelength 617 nm), PCC = 0.28; (3) Autophagosome – glycosome co-localisation. Pixels appear along a line between x and y axes, PCC = 0.69. Images show a single slice from a 3 μ m Z-stack. Scale bar = 5 μ m.

Table 3-5 Summary of autophagosome – glycosome co-localisation experiments. Data are from six or seven independent experiments for promastigotes and from two independent experiments for amastigotes. Logarithmic phase corresponds to promastigotes at a density of $\sim 5 \times 10^6$ /ml and stationary phase $\sim 2 \times 10^7$ /ml. Amastigote data were obtained from purified metacyclic promastigotes 18 h after infection of macrophages. Log phase promastigotes were starved for 4 h in PBS. Percentages are expressed as the mean \pm standard deviation of multiple experiments. Raw data is included in Appendix, Table A-1.

GFP-ATG8 + RFP-SQL	No. Cells Counted	% with Autophagosomes	Total No. Autos Counted	% Autos Co-localised PCC > 0.5	% Cells with Glycosomes Co-localised
Logarithmic phase	5384	3.9 \pm 2 %	294	19.4 \pm 15 %	0.9 \pm 0.4 %
Stationary phase	593	41.7 \pm 6 %	422	16.0 \pm 9 %	11.2 \pm 6 %
18h Amastigotes	376	90.1 \pm 3 %	758	11.4 \pm 2 %	23.1 \pm 6 %
Logarithmic starved	853	18.8 \pm 5 %	295	16.8 \pm 4 %	6.0 \pm 2 %

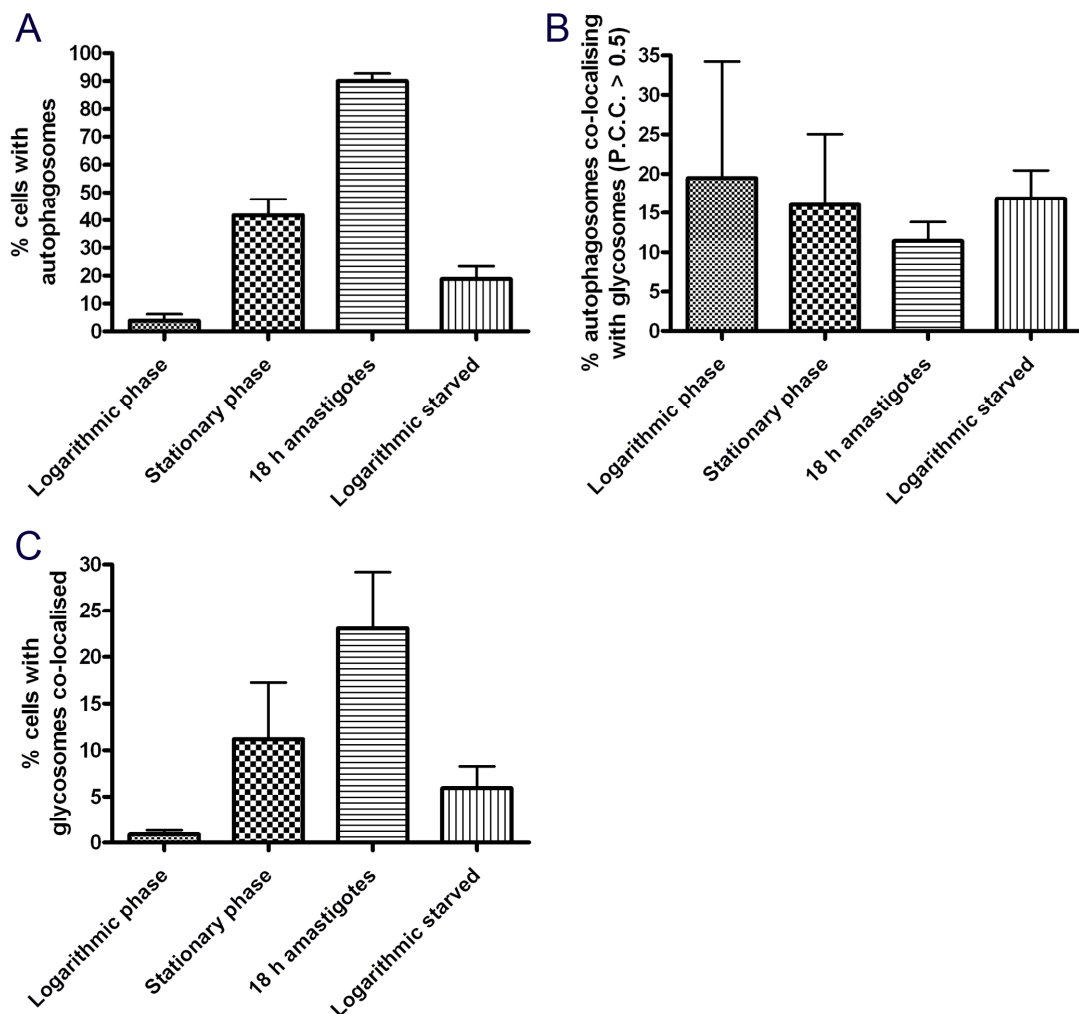


Figure 3-9 Graphical representation of data in Table 3-5.

Bars represent the mean and error bars represent the standard deviation of data.

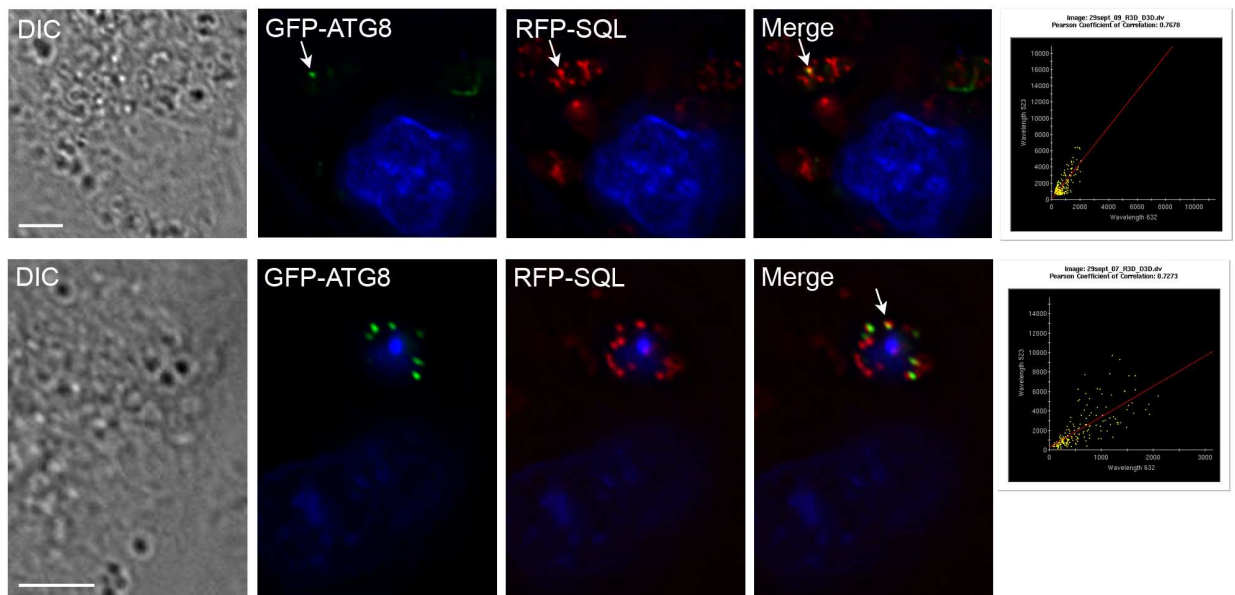


Figure 3-10 Autophagosome – glycosome co-localisation in differentiating amastigotes. Purified *L. major* metacyclic promastigotes co-expressing GFP-ATG8 and RFP-SQL were used to infect murine peritoneal macrophages. 18 h after infection, cells were DAPI-stained before imaging on DeltaVision Core fluorescent microscope in an environmental chamber set to 37°C and 5 % CO₂. Co-localisation analyses were performed using Co-localisation Finder in SoftWoRx Image Analysis software: PCC plots are shown at right hand side of images and correspond to autophagosome – glycosome co-localisation marked by arrow. Upper panel PCC = 0.77, lower panel PCC = 0.73. Images show a single slice from a 3 µm Z-stack. Scale bar = 5 µm.

3.4.2 Trafficking of autophagosomes and glycosomes to the lysosomal compartment

The autophagy pathway includes multiple steps following its induction; from autophagosome formation and cargo selection, to closure of the autophagosome and, finally, fusion of autophagosomes with the lysosome before the degradation of autophagosomal components and contents. Therefore, in order to confirm that glycosomes are degraded by autophagy, rather than co-localisation signifying some other autophagosome - glycosome interaction, autophagosomes need to be observed with their cargo at various stages of the overall process. Indeed, as well as co-localising with glycosomes, GFP-ATG8 was sometimes seen to label cup-shaped structures (Figure 3-11) resembling forming autophagosomes; in some cases these appeared to be developing around single glycosomes. Furthermore, both GFP-ATG8 and RFP-SQL were seen to label large tubular structures in stationary phase promastigotes that resemble the MVT-lysosome, the lysosomal compartment of metacyclic promastigotes (Figure 3-12 A) (Mullin et al., 2001). In log phase parasites, as well as in some stationary phase parasites, GFP-ATG8 and RFP-SQL appeared to accumulate in large

structures that we hypothesised might be lysosomes (Figure 3-12 A). These large structures were also present labelled with either GFP-ATG8 or RFP-SQL alone (Figure 3-12 A), and were visible during metacyclic promastigote - amastigote differentiation (Figure 3-12 B) corresponding to the megasomes of *Leishmania* amastigotes. To determine whether this compartment was the lysosome, we employed two different lysosomal markers in *L. major* promastigotes expressing GFP-ATG8: FM4-64, an endocytic tracer that accumulates in the lysosome (Mullin et al., 2001; Besteiro et al., 2006a); and proCPB-RFP, the propeptide region of the lysosomal cysteine peptidase B (Huete-Pérez et al., 1999). Both of these markers co-localised with GFP-ATG8 in large structures similar to those co-labelled by GFP-ATG8 and RFP-SQL (Figure 3-12 C), showing that this compartment is indeed the lysosome. Additionally, in cells expressing GFP-ATG8 and proCPB-RFP, smaller GFP-ATG8-labelled puncta could be seen associated with large structures containing both GFP-ATG8 and proCPB-RFP, suggesting that the smaller puncta were autophagosomes in the process of fusing with lysosomes (Figure 3-13). Together these data show that GFP-ATG8 and RFP-SQL interact at all stages of the autophagy pathway and support the hypothesis that glycosomes are sequestered by autophagosomes for their subsequent trafficking to and degradation in the lysosome.

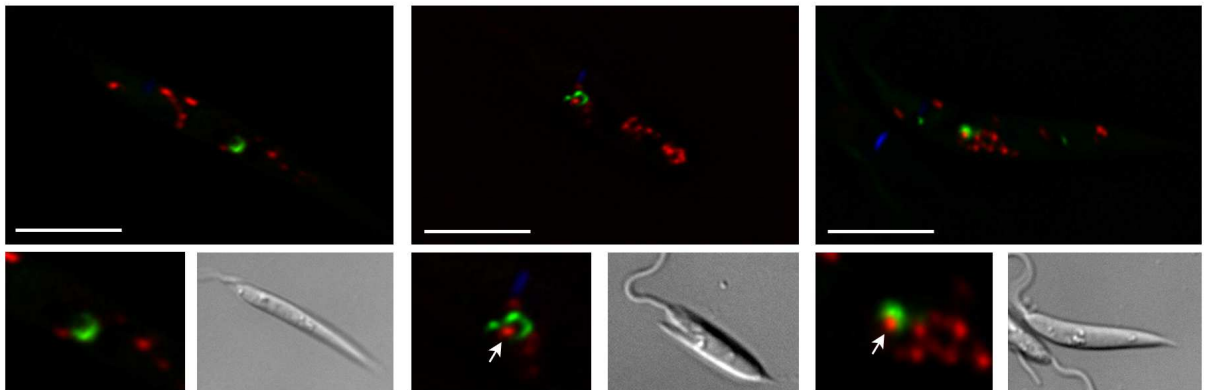


Figure 3-11 Visualisation of GFP-ATG8 labelling nascent autophagosomal structures. *L. major* promastigotes co-expressing GFP-ATG8 and RFP-SQL were washed and resuspended in PBS and imaged on a DeltaVision RT fluorescent microscope. Panels at lower left show enlarged images of cup shaped structures labelled with GFP-ATG8; arrows mark glycosomes that are being surrounded by these GFP-ATG8 structures. Images show a single slice from a 3 µm Z-stack. Scale bar = 5 µm.

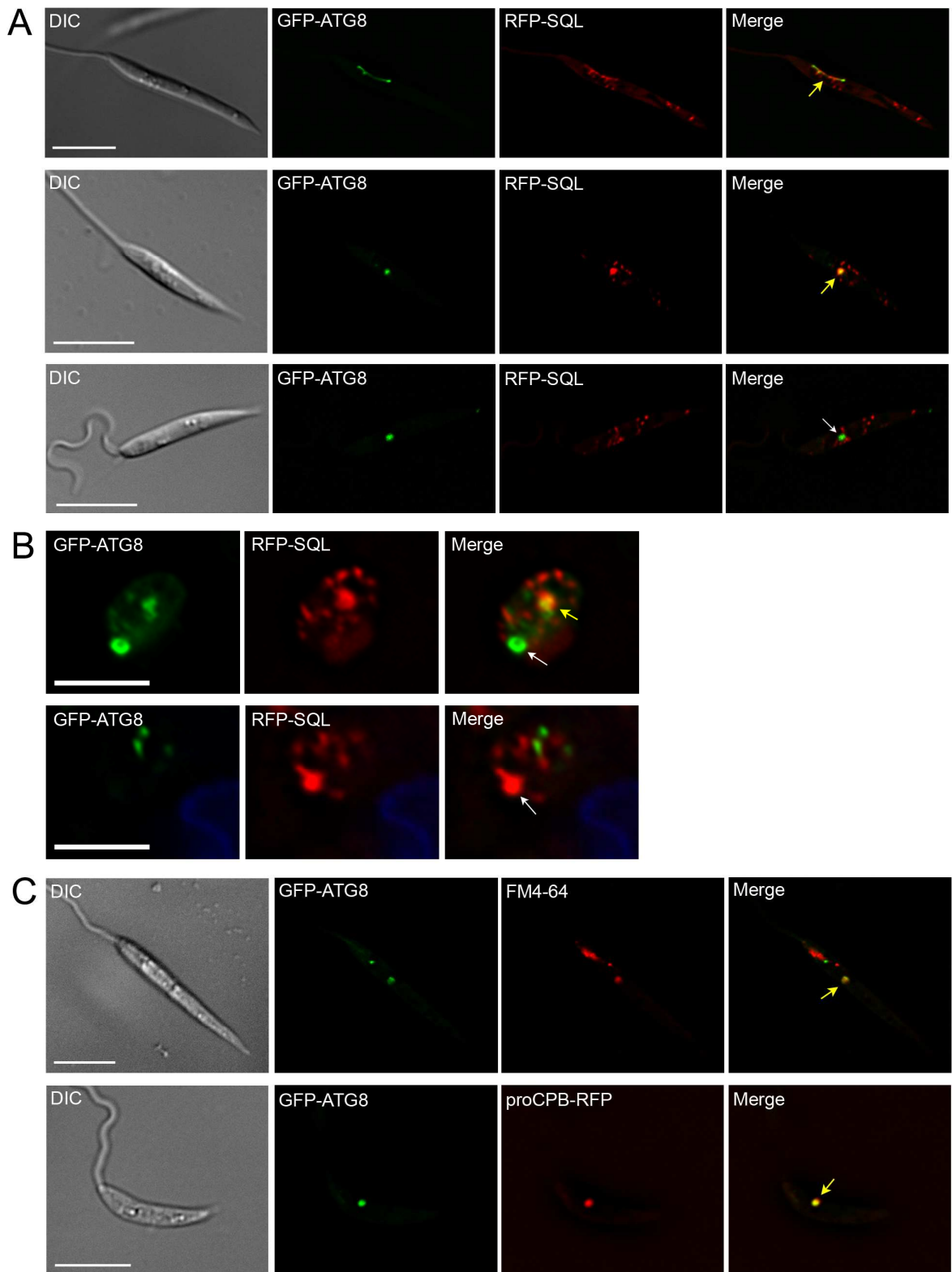


Figure 3-12 Trafficking of GFP-ATG8 to the lysosomal compartment. A, B. Visualisation of GFP-ATG8 and RFP-SQL in the lysosomal compartment. *L. major* co-expressing GFP-ATG8 and RFP-SQL were imaged on a DeltaVision Core fluorescent microscope as promastigotes in PBS (A) or differentiating amastigotes in murine macrophages (B). C. Confirmation of GFP-ATG8 localisation to lysosomes using lysosomal markers. Stationary phase *L. major* promastigotes expressing GFP-ATG8 were incubated with 40 μ M FM4-64 for 1 h to label lysosome before washing and resuspension in PBS for imaging. Stationary phase *L. major* co-expressing GFP-ATG8 and proCPB-RFP were prepared in PBS for imaging. Yellow arrows show co-localisation of signals in lysosomes, white arrows show localisation of only GFP-ATG8 or RFP-SQL to lysosomes. Images show a single slice from a 3 μ m Z-stack. Scale bar = 5 μ m.

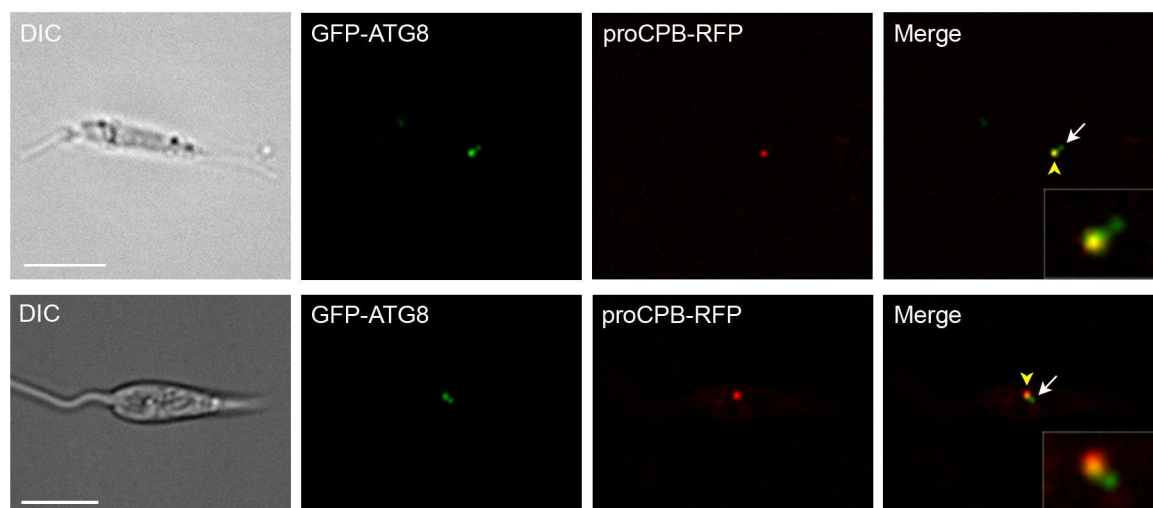


Figure 3-13 Visualisation of autophagosome fusion with the lysosome. Stationary phase *L. major* co-expressing GFP-ATG8 and proCPB-RFP were imaged on the DeltaVision Core after washing and resuspension in PBS. Enlarged images of the putative autophagosome – lysosome fusion are displayed in insets. White arrow indicates autophagosome; yellow arrowhead marks lysosome containing GFP-ATG8 and proCPB-RFP. Images show a single slice from a 3 μm Z-stack. Scale bar = 5 μm .

3.4.3 Characterisation of autophagosomes and lysosomes based on size of vesicles

To extend analysis of the lysosomal compartment and to further differentiate lysosomes from autophagosomes, a size comparison of labelled vesicles was carried out in stationary phase parasites expressing GFP-ATG8 and incubated with FM4-64 for 1 hour to allow it to accumulate in lysosomes. Measurements of vesicle diameter show that GFP-ATG8⁺ FM4-64⁻ vesicles (autophagosomes) are on average significantly smaller (0.34 μm) than GFP-ATG8⁺ FM4-64⁺ vesicles (autolysosomes/lysosomes, 0.62 μm ; Figure 3-14 A). Frequency distribution of the data show that the majority of GFP-ATG8-only labelled vesicles were approximately 0.3 μm in diameter, whereas most GFP-ATG8⁺ FM4-64⁺ vesicles were greater than 0.4 μm (Figure 3-14 A). Some overlap of GFP-ATG8⁺ FM4-64⁻ vesicles with GFP-ATG8⁺ FM4-64⁺ vesicles of size 0.4 - 0.6 μm suggests that this population may represent autolysosomes or a possible endosomal - autophagosomal intermediate, as autophagosomes are known to interact with the endosomal system (Köchler et al., 2006). As FM4-64 is not a specific lysosomal marker and may also be labelling endosomal compartments, it cannot be discounted that the large GFP-ATG8⁺ FM4-64⁺ vesicles are large endosomal - autophagosomal intermediates rather than lysosomes. Therefore a similar

analysis of vesicle size was performed in stationary phase *L. major* expressing GFP-ATG8 and proCPB-RFP, which is known to label the *Leishmania* lysosome (Huete-Pérez et al., 1999). This more thorough analysis produced similar results, with GFP-ATG8-labelled vesicles exhibiting a mean diameter of 0.36 μm , whereas vesicles labelled with both GFP-ATG8 and proCPB-RFP, or proCPB-RFP alone, had mean diameters of 0.59 μm and 0.53 μm , respectively (Figure 3-14 B). The majority of structures labelled by GFP-ATG8 and proCPB-RFP together or proCPB-RFP alone were tubular compartments corresponding to the MVT-lysosome (Figure 3-14 B), which were not included in the analysis in Figure 3-14 A. Frequency distribution of vesicle size data corresponded to that seen with GFP-ATG8 and FM4-64, with a population of smaller vesicles labelled with GFP-ATG8, that can be characterised as autophagosomes, a population of large vesicles that either displayed labelling with only proCPB-RFP or with both proCPB-RFP and GFP-ATG8, which are probably lysosomal structures, and a third population that occurred in the overlap between the other two populations, that are possibly autolysosomes (Figure 3-14 B). This analysis has led to the characterisation of autophagosomes and lysosomes in *L. major* based on their size and labelling, and confirms that the large structures containing GFP-ATG8 and RFP-SQL are lysosomal.

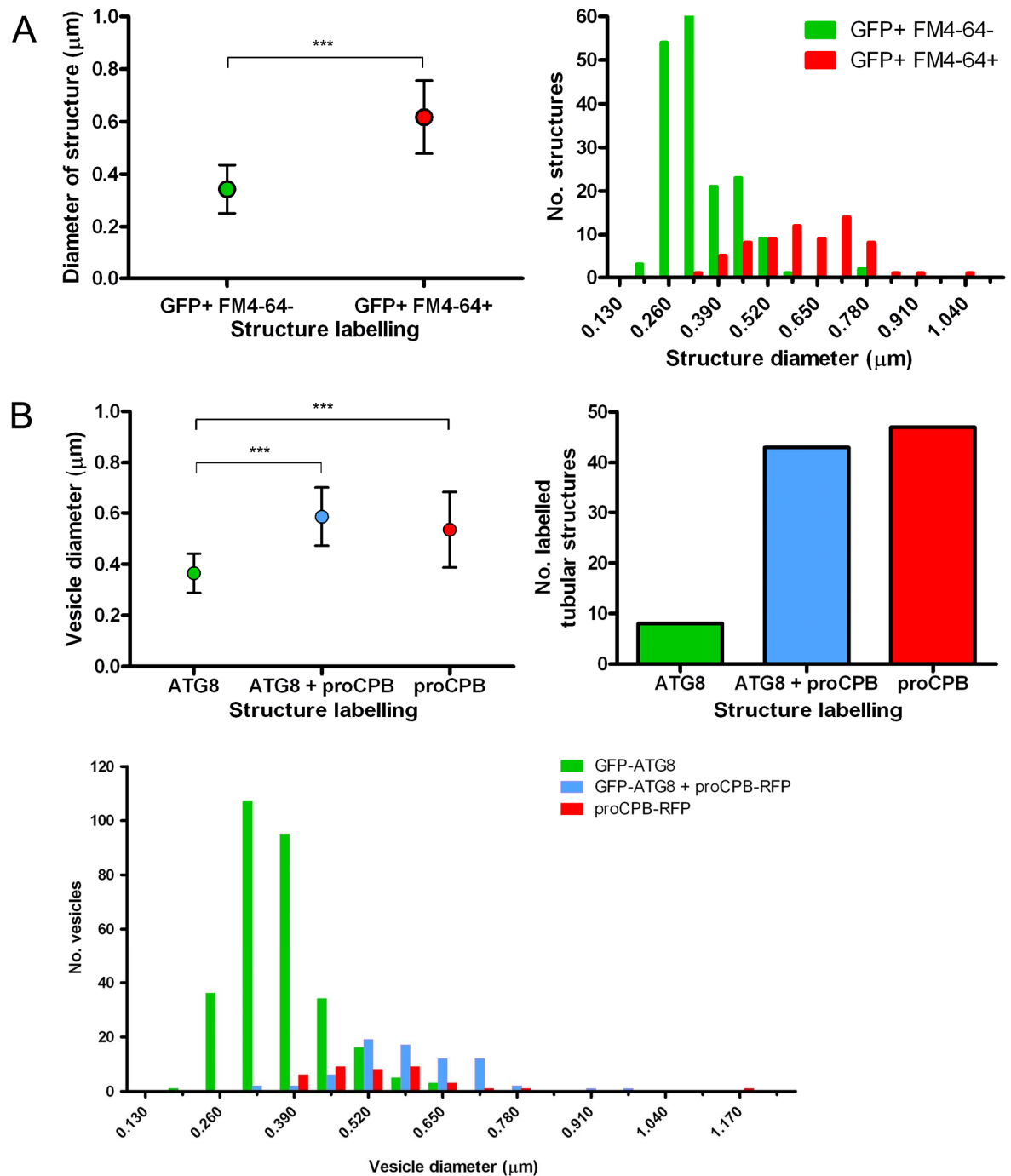


Figure 3-14 Characterisation of vesicle size in stationary phase *L. major* parasites.

A. *L. major* expressing GFP-ATG8 were incubated with 40 μM FM4-64 for 1 h to stain the lysosomal compartment, before washing and resuspension in PBS, and imaging on a DeltaVision Core microscope. B. *L. major* co-expressing GFP-ATG8 and proCPB-RFP were washed and resuspended in PBS before imaging on DeltaVision Core. Vesicle sizes were measured using SoftWoRx Explorer Image analysis software. Graphs show the mean data with error bars signifying standard deviation. Data were analysed using a student t test (A; for two datasets) or one-way ANOVA with a Tukey-Kramer multiple comparison test (B; for three datasets). *** denotes $p < 0.001$. Frequency distribution data were binned by 0.065 μm intervals, which correspond to the limit of measurement accuracy based on the microscopy image pixels.

3.4.4 Comparison of autophagosome size based on cargo

As autophagosomes engulf a variety of cargoes, some of them large organelles, it is expected that the size of autophagic vesicles will be determined by the size of the cargo that it engulfs. To determine whether this is true, GFP-ATG8 vesicles that co-localised with glycosomes (according to criterion $PCC > 0.5$) were compared with those that did not co-localise (Figure 3-15). Autophagosomes that co-localised with glycosomes were significantly bigger on average ($0.43 \mu\text{m}$) than those that did not co-localise with glycosomes ($0.34 \mu\text{m}$). This suggests that autophagosomes that contain glycosomes as cargo are larger than those that do not, although it cannot be discounted that some of the larger vesicles containing both GFP-ATG8 and RFP-SQL included in this analysis were autolysosomes.

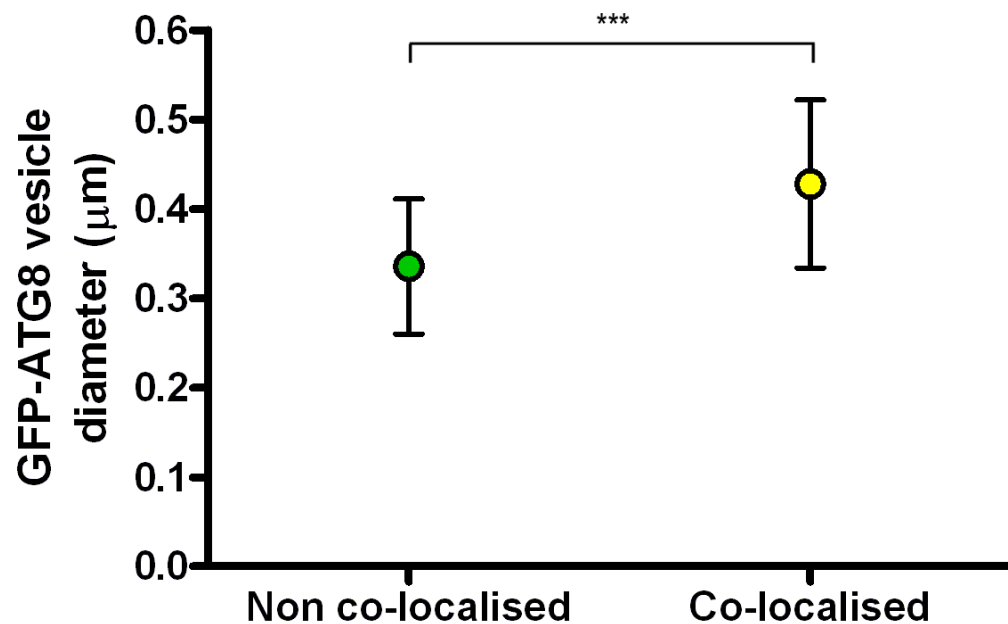


Figure 3-15 Comparison of sizes of GFP-ATG8 puncta during glycosome turnover. GFP-ATG8 puncta in images from the glycosome turnover experiments using GFP-ATG8 and RFP-SQL expressing promastigotes were measured using SoftWoRx Explorer Image Analysis software. Data were compared by student's t test; *** signifies $p < 0.001$.

3.4.5 Glycosome numbers throughout *Leishmania major* life cycle

Changes in the size of the glycosome population throughout the life cycle of *L. major* were determined by counting RFP-SQL-labelled glycosomes per cell in images from the glycosome turnover experiments. The number of glycosomes per cell decreased from an average of 17 glycosomes/cell in stationary phase promastigotes to 13 glycosomes/cell in differentiating amastigotes 18 h following macrophage infection (Figure 3-16), similar to previously published data (Coombs et al., 1986). Differences in glycosome numbers at this stage are likely due to differences in cell volume between the promastigote and amastigote, although it is probable that the reduction in glycosome numbers here are due to the massively increased autophagy during metacyclic - amastigote differentiation (Figure 3-9 A). No difference in glycosome numbers between the log and stationary phase promastigotes were observed, indicating that glycosome numbers in procyclic and metacyclic promastigotes are similar, although there may be differences in glycosomal content between these life-cycle stages. Unexpectedly, many parasites contained very low numbers of labelled glycosomes (Figure 3-16). This may be due to brightly fluorescing glycosomes masking others in the same cell or reduced numbers of glycosomes in dead or dying cells. However, these low numbers of glycosomes were not recorded in WT parasites in later experiments (Figures 3-17, 3-18), suggesting that counting technique has improved over time.

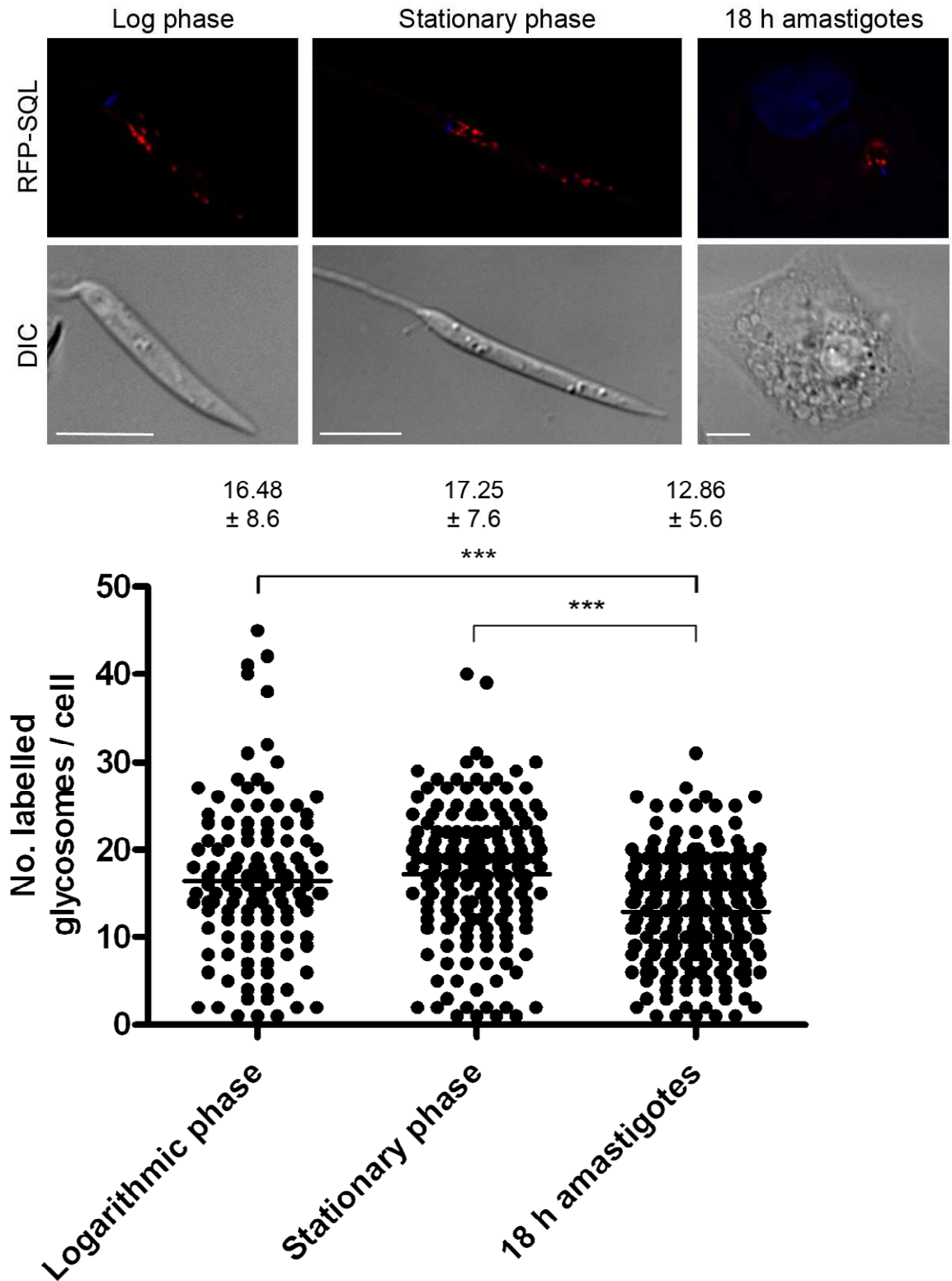


Figure 3-16 Analysis of glycosome numbers per parasite in different stages of the life cycle. The number of RFP-SQL-labelled puncta per cell were counted in images of GFP-ATG8 and RFP-SQL expressing parasites from the glycosome turnover experiments. Each spot represents a single measurement with the horizontal line representing the mean. The mean \pm standard deviation is included above each dataset. Data were analysed with a one-way ANOVA with a Tukey-Kramer multiple comparison test; *** denotes $p < 0.001$. Log phase, $n = 131$; stationary phase, $n = 167$; 18 h amastigotes, $n = 262$. Representative images from each life cycle stage are included at the top of the figure (GFP-ATG8 fluorescence not shown). Images show a single slice from a 3 μm Z-stack. Scale bar = 5 μm .

3.4.6 Comparison of glycosome turnover in autophagy-deficient mutants

As glycosomes appear to be turned over by autophagy, it was next investigated whether glycosome turnover would be impaired in $\Delta atg5$ mutants which are unable to form autophagosomes and therefore deficient in macroautophagy (Williams et al., 2012b). A comparison of RFP-SQL-labelled glycosome numbers in stationary phase *L. major* wild-type (WT), the $\Delta atg5$ mutant and a $\Delta atg5$ cell line re-expressing ATG5 ($\Delta atg5::ATG5$) revealed that the $\Delta atg5$ parasites contained higher numbers (average of 22 glycosomes/cell) compared to both the WT (average of 18 glycosomes/cell) and $\Delta atg5::ATG5$ (average of 19 glycosomes/cell) (Figure 3-17, left). This small, but significant, difference suggests that a lack of autophagy results in a decreased turnover of glycosomes in the $\Delta atg5$ cells. Interestingly, $\Delta atg5$ parasites also displayed significantly less RFP-SQL-containing lysosome-like structures, as described in 3.4.2 above, when compared to WT and $\Delta atg5::ATG5$ parasites (Figure 3-17, right). These observations support the hypothesis that glycosomes are degraded by autophagy.

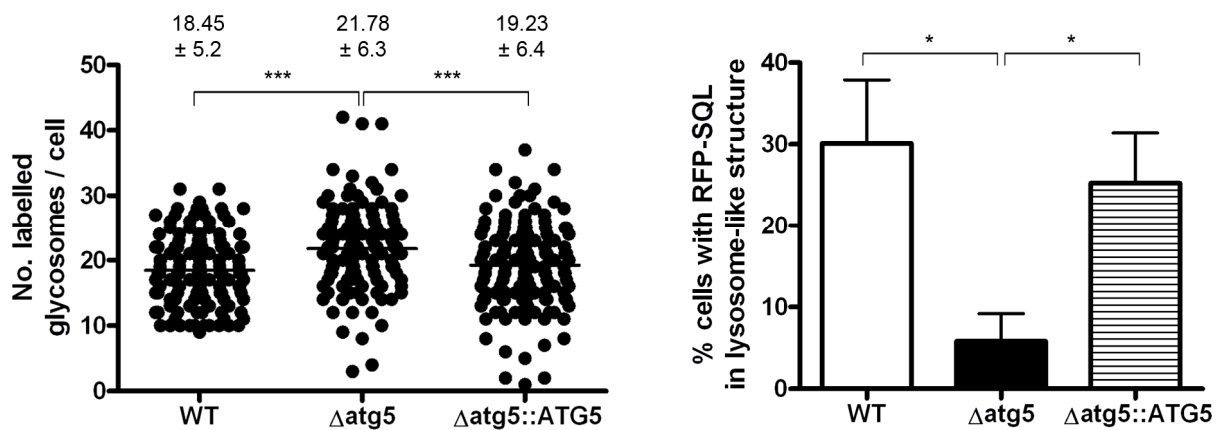


Figure 3-17 Comparison of glycosome turnover in WT, $\Delta atg5$ and $\Delta atg5::ATG5$ parasites. *L. major* promastigotes expressing RFP-SQL in stationary phase of growth were washed and resuspended in PBS, and imaged on the DeltaVision Core fluorescent microscope system. Left: Number of glycosomes per cell were counted for approximately 150 cells for each cell line. Each spot represents a single measurement with the horizontal line representing the mean. The mean \pm standard deviation are included above each dataset. Right: The percentage of cells with structures resembling lysosomes that contained RFP-SQL was determined for each cell line. Bars show mean and error bars standard deviation. Data were analysed using a one-way ANOVA with a Tukey-Kramer multiple comparison test; *** denotes $p < 0.001$ and * denotes $p < 0.05$.

As the greatest reduction in glycosome numbers occurs during metacyclic promastigote - amastigote differentiation, the numbers of RFP-SQL-labelled glycosomes were next determined for WT and $\Delta atg5$ parasites before, during and after parasite differentiation within macrophages. Glycosome numbers in purified metacyclic promastigotes were slightly, but significantly, higher in $\Delta atg5$ parasites (average 19 glycosomes/cell) compared to those in WT (average 17 glycosomes/cell; Figure 3-18). 18 hours following infection of murine macrophages, the glycosome numbers in $\Delta atg5$ remained at levels similar to those in promastigotes (average 18 glycosomes/cell), whereas in WT parasites numbers had decreased to an average 12 glycosomes/cell by this time (Figure 3-18). 48 hours following macrophage infection, by which time intracellular parasites should have fully differentiated into the amastigote form, glycosome numbers in $\Delta atg5$ had dropped slightly to 16 glycosomes/cell, but still remained significantly higher than those of WT parasites (average 11 glycosomes/cell) at this time point (Figure 3-18). These observations provide strong evidence to support the hypothesis that glycosomes are degraded by autophagy, and that this is important for the regulation of glycosome numbers during differentiation. Interestingly, however, glycosome numbers in $\Delta atg5$ mutants decreased significantly over the 48 hours differentiation, implying that macroautophagy is not the only mechanism for glycosome turnover. In addition, although glycosome numbers decreased significantly over the 48 hours in $\Delta atg5$, the glycosome numbers in 48 hour amastigotes were still similar to the numbers in WT promastigotes indicating that glycosome turnover was severely affected by the loss of macroautophagy.

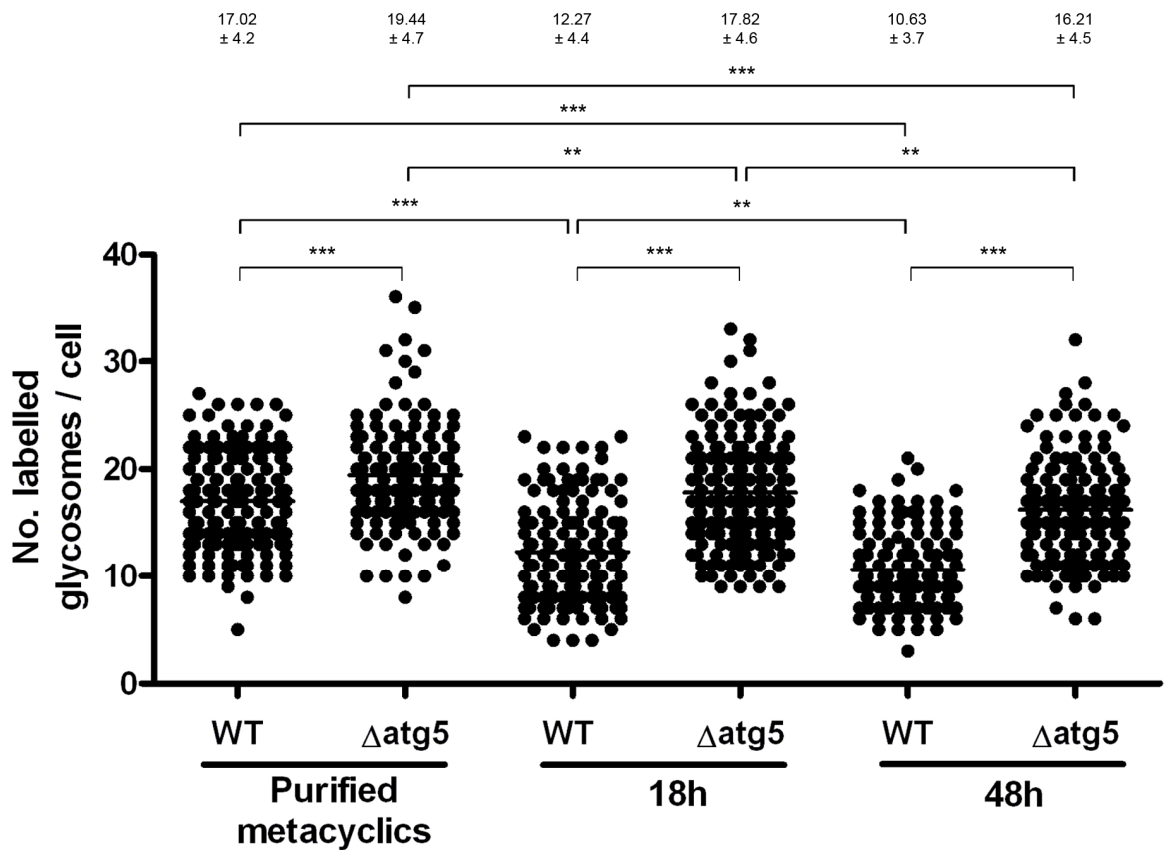


Figure 3-18 Comparison of glycosome turnover in WT and $\Delta atg5$ parasites during promastigote – amastigote differentiation. Purified metacyclic promastigotes expressing RFP-SQL were used to infect murine peritoneal macrophages. Glycosomes per cell were counted in metacyclic promastigotes, and in parasites within macrophages either 18 or 48 h after infection. The number of glycosomes per cell was counted for at least 150 cells for each cell line at each time point. Each spot represents a single measurement with the horizontal line representing the mean. The mean \pm standard deviation are included above each dataset. Data were analysed using a one-way ANOVA with a Tukey-Kramer multiple comparison test. *** denotes $p < 0.001$ and ** $p < 0.01$.

3.5 Discussion

Autophagy in *Leishmania* is induced under starvation conditions as well as during life cycle differentiation, when it is believed to be responsible for protein and organelle turnover during the cellular remodelling that occurs during this period. In this study, autophagy and its possible cargoes have been investigated through fluorescent microscopy, primarily in promastigote stages.

Analysis of acidocalcisomes suggests that autophagosomes do not target these organelles during starvation of promastigotes or during metacyclogenesis in stationary phase parasites (Figure 3-2; Table 3-1). In *L. major*, acidocalcisome numbers are low in replicating procyclic promastigotes then greatly increase in stationary phase parasites to numbers similar to those in amastigotes (Zhang et al., 2005). This suggests that acidocalcisomes are important in infective stages of the parasite, probably due to their osmoregulatory role which aids parasite survival in the face of extreme changes in the osmotic environment as they transit from the insect vector to mammalian host (Moreno and Docampo, 2009). Therefore, if autophagy of acidocalcisomes occurs, it would likely happen during amastigote - procyclic promastigote differentiation in the sandfly when there is a dramatic decrease in acidocalcisome numbers. It is unlikely that acidocalcisomes are targeted by autophagy during stationary phase, when they are being synthesised and their numbers increase. Upon treatment of *L. amazonensis* with the sterol binding inhibitors ketoconazole and terbinafine, an increase of “circular ER cisternae” were visualised in cells, some of which contained acidocalcisomes (Vannier-Santos et al., 1999). This suggests that these drugs induce autophagy in *Leishmania*, and that acidocalcisomes are targeted by autophagy, but whether this treatment is relevant to physiological conditions experienced by the parasites is questionable. Ketoconazole was found to increase formation of GFP-ATG8-labelled puncta in *L. major* (R. Williams, unpublished data), although treatment also caused cells to round up, implying that autophagy was being induced as a cell survival mechanism rather than specifically induced by this drug. Thus acidocalcisomes may be autophagic cargo under extreme stress conditions.

No evidence was obtained for autophagic degradation of the flagellum (Figure 3-2; Table 3-2), although only a single flagellar component, the membrane-

associated peptidase calpain-GFP was examined; it would be informative to repeat the experiments with a structural flagellar protein such as a paraflagellar rod protein. In addition, parasites were only observed as promastigotes during starvation and stationary phase. The most dramatic changes to the flagellum occur during promastigote - amastigote differentiation when this structure is considerably shortened; it is possible that autophagy is involved in recycling of flagellar proteins during this process. However, the involvement of autophagy in degradation of flagella has not been reported in any organism to date, although to my knowledge neither has this been investigated. An increase in ubiquitination of flagellar proteins has been reported during flagellar resorption in the biflagellate alga *Chlamydomonas reinhardtii* (Huang et al., 2009). Ubiquitinated proteins were trafficked back to the cell body by intraflagellar transport (IFT). Whether ubiquitination could act as a signal for recruitment of the autophagic machinery, through an autophagy adaptor similar to p62, to degrade the flagellar proteins as they reach the cell body is a possibility, although so far no homologues of any autophagy adaptor proteins have been identified in this organism, or indeed in *Leishmania*.

In promastigotes no co-localisation of autophagosomes with the mitochondrion was observed during normal growth conditions or in response to starvation (Figure 3-2), although a low number of autophagosomes were observed to co-localise with mitochondrial fragments in parasites treated with 1 mM H₂O₂ (Figure 3-5). This suggests that mitophagy can occur during conditions in which the mitochondrion becomes damaged or fragmented; however, this still occurred in a surprisingly low number of cells. These observations raise the question of how *Leishmania* and other organisms with a single mitochondrion maintain homeostasis of this organelle. It is possible that basal mitophagy occurs at a low level that is undetectable in the experiments performed here, or that mitophagy takes place upon cell division when the mitochondrion is divided between two cells; during this process, damaged sections of the organelle could be separated and degraded. It would also be interesting to examine whether autophagosome - mitochondrion co-localisation occurs during promastigote - amastigote differentiation, when the mitochondrial mass is significantly reduced. Analysis of starvation-induced autophagy in mammalian cells suggests that it is an ordered process, with cytosolic proteins being preferentially degraded at early starvation

and proteins from large organelles such as mitochondria being targeted only at later stages of starvation, i.e. > 24 hours (Kristensen et al., 2008). This suggests that accessible energy sources are targeted first before degradation of organelles that are energetically costly to synthesise and important for survival. Therefore, it is possible that prolonged starvation of *Leishmania* would induce autophagic turnover of the mitochondrion. Treatment with 1 mM H₂O₂ for 1 hour was unable to cause depolarisation of the *Leishmania* mitochondrion (Figure 3-7) but was however able to induce a low level of mitophagy, implying that mitophagy in *Leishmania* can be triggered by mitochondrial fragmentation independently of membrane potential. In the event of mitochondrial depolarisation, a greater up-regulation of mitophagy may be seen as a response to mitochondrial damage. This has been traditionally induced in mammalian mitochondria using uncoupling agents such as CCCP (Narendra et al., 2008), but this has not been effective in yeast (Wang and Klionsky, 2011).

Recently an autophagy-independent vesicular pathway for delivery of mitochondrial proteins to the lysosome was reported (Soubannier et al., 2012). Mitochondrial-derived vesicles (MDVs) selectively transport mitochondrial cargo to lysosomes as an early response to oxidative stress, before depolarisation occurs, and this is independent of Drp1, Atg5 and LC3, suggesting that neither mitochondrial fission or autophagy are required for this pathway. This vesicular mitochondrial quality control mechanism appears to be an early response to mitochondrial damage, whereas mitophagy acts to eliminate mitochondria at later stages of damage. Another mechanism of mitochondrial quality control is the mitochondria-associated degradation (MAD) pathway. Similar to the ER-associated degradation (ERAD) pathway, MAD results in translocation of damaged inner mitochondrial membrane or matrix proteins to the outer mitochondrial membrane where they are ubiquitinated by E3 ligases (including Parkin), and targeted by the proteasome for degradation (Taylor and Rutter 2011). A protein called Vms1 is required for recruitment of Cdc48/p97 and Npl4 to the mitochondria; the Vms1-Cdc48/p97-Npl4 complex presents ubiquitinated proteins to the proteasome (Heo et al., 2010). Mutation of Vms1 results in accumulation of ubiquitinated proteins on the mitochondrial surface and mitochondrial dysfunction. Vms1 appears to be conserved throughout eukaryotes, suggesting that MAD is an important eukaryotic mechanism for

mitochondrial quality control (Heo et al., 2010). It is thought that autophagy and the ubiquitin-proteasome system (UPS) work synergistically to maintain mitochondrial homeostasis in yeast (Takeda et al., 2010); this group found that mitophagy increased following inhibition of the proteasome, suggesting that autophagy up-regulation compensates for lack of protein degradation by the UPS, which may be the primary mechanism for mitochondrial quality control. However, studies in mammalian cells imply that Parkin-mediated mitophagy depends on activity of the UPS, which is thought to be important for degradation of ubiquitinated proteins on the outer mitochondrial membrane prior to mitophagy and facilitating fission via degradation of mitofusins (Tanaka et al., 2010; Chan et al., 2011). On the other hand, inhibition of autophagy by RNAi knockdown of Atg7 or Atg12 leads to decreased activity of the UPS, due to build-up of p62 bound to ubiquitinated proteins that prevents access of these proteins to the proteasome (Korolchuk et al., 2009). Thus, autophagy and the UPS are clearly linked, and it is possible that in *Leishmania* MAD and the UPS are the primary means of maintaining homeostasis of the single mitochondrion, whereas mitophagy is only employed during extreme mitochondrial stress. *Leishmania* may also utilise MDVs as a method of mitochondrial quality control, but as yet this pathway has only been observed in mammals (Soubannier et al., 2012).

An interesting finding from this study is that a large proportion of RFP-ATG8-labelled autophagosomes appear to associate with the mitochondrion (Figure 3-3; Table 3-3). In addition, a similar proportion of early autophagosomes labelled with mCherry-ATG5 display a similar association (Figure 3-4). The ATG12-ATG5 machinery is thought to be absent from completed autophagosomes, so puncta labelled with ATG12 and ATG5 suggest that these are immature autophagosomes still undergoing formation. A role for the mitochondrion in supplying membranes for autophagosome biogenesis has been put forward by scientists working on mammalian cells (Hailey et al., 2010), and it is possible that this is also the case in *Leishmania*. This hypothesis would also explain why little evidence of mitophagy was found in *Leishmania* promastigotes; if the mitochondrion is important for autophagosome formation, it is possibly less likely to be targeted for degradation by the same process. Interestingly, *L. major* mutants that lack the *ATG5* gene ($\Delta atg5$) displayed mitochondrial defects, exhibiting swollen or fragmented mitochondria with reduced membrane potential and increased

mitochondrial levels of phospholipids, notably PE, compared to WT parasites (Williams et al., 2012b). Therefore, as little evidence exists for mitophagy under normal growth conditions, it is possible that autophagosome formation from the mitochondrion is one mechanism for maintenance of mitochondrial phospholipid levels, and that in $\Delta atg5$ mutants disturbance of the autophagy pathway results in the mitochondrial defects observed due to phospholipid accumulation. The ER is also a source of membrane for autophagosome biogenesis in mammals (Axe et al., 2008; Hayashi-Nishino et al., 2009; Yla-Anttila et al., 2009), whereas in yeast the Golgi (Geng et al., 2010; van der Vaart et al., 2010; Yamamoto et al., 2012) or an Atg9-labelled compartment adjacent to mitochondria (Mari et al., 2010) are implicated. As in these organisms, it is possible that *Leishmania* are able to use multiple membrane sources for autophagosome biogenesis, which may be utilised in response to different stimuli. This could be investigated with co-localisation studies using fluorescently tagged ATG8 and specific markers for the ER/Golgi.

Glycosome turnover is hypothesised to be important for metabolic changes during the differentiation of trypanosomatid parasites in order to adapt these pathogens to the distinct environments encountered in their insect vector and mammalian host. Autophagy has been championed as the primary mechanism for this turnover (Besteiro et al., 2007; Brennand et al., 2011). There is some evidence for this in *T. brucei*, in which glycosomal proteins were observed in the lysosome during life-cycle differentiation, interpreted as suggesting that this occurred via a microautophagic process (Herman et al., 2008). In the present study, glycosomes have been observed co-localising with GFP-ATG8-labelled autophagosomes at all observed stages of the *L. major* life cycle (Figures 3-2, 3-8, 3-10), providing evidence that glycosome turnover in *Leishmania* is mediated by macroautophagy. Cup-shaped structures labelled with GFP-ATG8 were observed, sometimes forming around single glycosomes (Figure 3-11), indicating the selective sequestration of glycosomes within autophagosomes. In addition, both GFP-ATG8 and the glycosomal marker RFP-SQL were observed to accumulate within large punctate or tubular structures; similar structures were labelled with both FM4-64 and proCPB-RFP (Figure 3-12), suggesting that these are the lysosomal compartments of *Leishmania*. GFP-ATG8 puncta were also seen adjacent to large structures labelled with both proCPB-RFP and GFP-ATG8,

suggestive of autophagosome fusion with the lysosome (Figure 3-13). These data all support a glycosome turnover mechanism whereby single glycosomes are targeted by autophagosomes and trafficked to the lysosome for degradation, similar to macropexophagy in yeast and mammals. 16 - 19 % of autophagosomes co-localise with glycosomes at any time during promastigote stages (Figure 3-9), implying that there may be a set population of autophagosomes that are involved in glycosome turnover. Interestingly, this proportion of co-localising autophagosomes remains the same when autophagy is induced, but due to the increased numbers of autophagosomes there is an increase in glycosome turnover. Thus the level of glycosome turnover by autophagy appears to be dependent on, and proportional to, the overall level of autophagy in the parasites. During promastigote - amastigote differentiation almost all parasites contain multiple GFP-ATG8 puncta and the proportion of these that co-localise with glycosomes is lower than that in promastigotes (11 %); this is likely due to the fact that there is extensive remodelling of the cell during this period and so autophagy is involved in turnover of multiple organellar and protein substrates, and therefore the percentage of autophagosomes involved in glycosome turnover is reduced. However, autophagy's role in glycosome turnover is important during this stage as numbers of glycosomes, as previously described in the literature (Coombs et al., 1986), decrease significantly upon differentiation of promastigotes into amastigotes. This decrease was ablated in $\Delta atg5$ parasites differentiating into amastigotes (Figure 3-18), highlighting the role of autophagy in degradation of glycosomes. Numbers of glycosomes did not differ significantly between log and stationary phase promastigotes (Figure 3-16), although there are possibly changes in glycosome content as degraded glycosomes are replaced with newly synthesised organelles that contain different configurations of metabolic enzymes to adapt parasites to host invasion. The existence of autophagosome - glycosome co-localisation and appearance of both GFP-ATG8 and RFP-SQL in lysosomes during log phase suggest that autophagy is involved in basal turnover of glycosomes, which is presumably important for degradation of old and damaged members of the glycosome population. Glycosome numbers in stationary phase $\Delta atg5$ parasites were significantly higher than in WT and $\Delta atg5::ATG5$ parasites in the same stage of growth, and decreased delivery of RFP-SQL to lysosomal structures was observed (Figure 3-17), suggesting that glycosome turnover does occur during procyclic - metacyclic promastigote

differentiation; whether this is for adaptation of the glycosomal metabolic contents or basal homeostasis cannot be determined by these data. Autophagic glycosome turnover also occurs during starvation which suggests that glycosomes can be degraded in order to provide essential amino acids to facilitate cell survival; as a small, easily accessible organelle, glycosomes represent a ready source of energy that can be utilised following depletion of cytosolic proteins. Alternatively, glycosomes and their contents may be degraded during starvation, preceding production of a new set with enzyme content tailored to maximisation of energy generation during starvation.

These results suggest that glycosome turnover in *Leishmania* is mediated by macroautophagy, but cannot exclude the possibility that microautophagy may also be involved. In stationary phase $\Delta atg5$ mutants RFP-SQL could still be seen in lysosomal compartments (Figure 3-17); however, the core autophagy machinery is required for selective forms of microautophagy in yeast (Sakai et al., 2006; Krick et al., 2008), suggesting that a small amount of RFP-SQL is trafficked to the lysosome independently of autophagy. In some cells, glycosomes appeared to be adjacent to lysosomal structures (e.g. Figure 3-12 A, first panel) but this was not a frequent observation. Live cell imaging experiments have been planned that aim to track glycosomes and their delivery to the lysosomal compartment: these include triple-labelling with ATG8, SQL and lysosomal markers, and tracking single glycosomes using a photo-activatable Kaede-SQL construct, which allows irreversible photoconversion of labelled organelles from green to red fluorescence upon UV irradiation (Ando et al., 2002). These experiments will hopefully clarify the mechanisms by which glycosomes are trafficked by autophagy.

An interesting question related to glycosome turnover is that of the mechanism by which these organelles, and others, are recognised by the autophagy machinery for degradation. Are damaged glycosomes labelled in some way which is recognised by and recruits the core autophagy proteins, possibly via an adaptor protein as in yeast? How do signals on damaged glycosomes differ from those on glycosomes that are degraded to adapt to changing metabolic conditions, or is there a universal degradation signal? Perhaps a subset of autophagosomes exists whose function it is to target glycosomes, as suggested by the co-localisation data above, and this population is increased in response to

conditions necessitating glycosome turnover. So far no homologues of the autophagy cargo receptors involved in yeast pexophagy, Atg30 in *P. pastoris* and Atg36 in *S. cerevisiae*, have been identified in any other organism. It is possible that *Leishmania* and other trypanosomatids encode divergent proteins with similar functions for this role. The precise mechanism for mammalian pexophagy is also yet to be discovered. It is thought that p62, which links ubiquitinated substrates to the autophagy pathway, acts as a universal adaptor for recognition of autophagic cargoes. Ubiquitination of cytosolic proteins and peroxisomes was sufficient for their p62-dependent autophagic degradation (Kim et al., 2008), suggesting that in mammals ubiquitination is a common signal for autophagic degradation. However, although proteins with similar domain combinations to p62 (Lamark et al., 2009) have been identified in the free-living protists *Dictyostelium discoideum*, *Monosegia brevis*, *Naegleria gruberi* and *Phytophthora* spp. (Duszenko et al., 2011), none have been found in the trypanosomatids. The presence of ubiquitin and ubiquitin-like modifiers, and their deconjugating enzymes, in *Leishmania* and other protozoan parasites (Ponder and Bogyo, 2007) suggest that ubiquitination is also important in these organisms, and could have roles in the selection of autophagic cargo. In addition, many uncharacterised ubiquitin-like proteins are encoded in the *Leishmania* genome, some of which may be proteins with roles related to selective autophagy.

Analysis of the sizes of compartments differentially labelled by GFP-ATG8 and markers of the lysosome (Figure 3-14) has provided new characterisation of the vesicles involved in the autophagy pathway in *Leishmania*. Firstly, autophagosomes were found to be approximately 0.30 - 0.36 μm in diameter, making them smaller in size than those of yeast, which were measured by electron microscopy to have an average diameter of 0.3 - 0.9 μm (Takeshige et al., 1992; Xie et al., 2009), and mammalian cells, which measure 0.5 - 1.5 μm . Interestingly, autophagosomes that co-localised with glycosomes were found to be significantly larger than those that did not (average 0.43 μm versus 0.34 μm ; Figure 3-15), suggesting that autophagosome size can be altered by the size of their cargo. A population of larger structures containing GFP-ATG8 and proCPB-RFP, or only proCPB-RFP, of approximately 0.6 μm correspond to lysosomes; this is supported by the occurrence of most GFP-ATG8 and proCPB-RFP co-

localisation (and proCPB-RFP only) in tubular structures, corresponding to MVT-lysosomes. Overlap of vesicles labelled only by GFP-ATG8 with vesicles labelled by both GFP-ATG8 and proCPB-RFP suggests that this represents a population of autolysosomes, autophagosomes in the process of lysosomal fusion. Additional data using FM4-64 complemented data obtained using proCPB-RFP as the lysosomal marker. These data may also provide a useful reference for recognition of *Leishmania* compartments based on their size and shape.

Recently, the accumulation of protein aggregates and autophagosomes was observed in yeast mutants lacking the metacaspase Yca1 (Lee et al., 2010b), suggesting that autophagy can clear protein aggregates to compensate for the absence of the aggregate-clearing activity of Yca1. Similarly, *Leishmania* possess a single metacaspase, MCA, which localises to cytosolic punctate structures (Castanys-Muñoz et al., 2012) perhaps marking aggregation of proteins. Early studies, however, show no link between MCA and autophagy, as GFP-ATG8 puncta formation remained similar in both MCA KO and WT parasites (E. Castanys-Muñoz, unpublished data). It will be interesting to see whether autophagosomes might co-localise with MCA-labelled puncta and whether autophagy might exist in trypanosomatids.

Here I have shown that 16 - 19 % of autophagosomes appear to contain glycosomes in various life-cycle stages of *L. major* (Figure 3-9). However, none of the other cargoes examined here in promastigotes were observed to be degraded by autophagy (Figure 3-2), with the exception of mitochondrial fragments during oxidative stress (Figure 3-5). Therefore, which cargoes are sequestered within the remaining 81 - 84 % of autophagic vesicles? The organelles that have not been investigated here, i.e. ER and Golgi, may make up part of autophagosome cargo, and these can be investigated using organelle-specific fluorescent markers in co-localisation experiments with ATG8-labelled autophagosomes. Nucleophagy has not been investigated in trypanosomatid parasites to date, but by treating *L. major* expressing GFP-ATG8 with DNA-damaging drugs, such as hydroxyurea or phleomycin, we may be able to determine whether interactions of autophagosomes with the nucleus or kinetoplast occur in response to DNA damage. It is possible that the majority of autophagosomes sequester bulk cytoplasm containing cytosolic proteins and amino acids, in order to recycle these constituents. Biochemical assays have

been useful in characterising autophagic cargoes in other eukaryotes (Klionsky et al., 2007), and these could also prove useful in *Leishmania*. Immunodetection of known cytosolic proteins and monitoring of their levels during differentiation and starvation of WT and $\Delta atg5$ parasites could be informative in determination of autophagy's role in their degradation. Biochemical analyses would also be useful in following the degradation of various organelles by autophagy, and following the levels of various glycosomal enzymes could be informative in tracking the metabolic changes that occur during differentiation. For example, during promastigote - amastigote differentiation, we would expect levels of glycosomal glycolytic enzymes to decrease and enzymes for β -oxidation of fatty acids to increase, and that these content changes might be prevented by the loss of macroautophagy in $\Delta atg5$ mutants. However, I have been unable to perform these experiments due to a lack of glycosomal antibodies. Degradation of organelle-specific proteins has also been followed in yeast by the detection of free GFP by immunoblotting after trafficking of a GFP-labelled organellar marker (for example Pex14-GFP to monitor pexophagy) to the vacuole where the GFP is cleaved from the chimera (Klionsky et al., 2007). This would be relatively easy to perform in *Leishmania*, because of the GFP fusion proteins that are already in use as organelle markers. Another approach that has been used to measure protein degradation is to label proteins with a radioactive amino acid, such as ^{14}C -valine, and track the radioactivity release over a period of a few hours in order to determine the reduction in levels of long-lived proteins (Klionsky et al., 2007). The contribution of autophagy to the degradation of radio-labelled cytosolic or organellar proteins could be investigated by comparing radioactivity release in WT and $\Delta atg5$ parasites. SILAC (stable isotope labelling of amino acids in cell culture) in combination with mass spectrometry-based quantitative proteomics has previously been used to determine the relative abundance of proteins over time in starved mammalian cells in order to determine autophagy substrates (Kristensen et al., 2008). As SILAC has recently been developed for use in *Leishmania* (Chawla et al., 2011), a similar approach could be used to perform quantitative proteomic analyses in log phase versus stationary phase cultures, or WT versus $\Delta atg5$ parasites, in order to determine which organellar and cytosolic proteins are substrates for autophagy.

4 Further Characterisation of *Leishmania major* ATG8-like proteins

4.1 Introduction

4.1.1 Multiple ATG8 homologues in eukaryotes

Atg8 is an essential component of the autophagic machinery, being central to autophagosome expansion and maturation through its roles in membrane elongation. Whereas yeasts encode a single Atg8, some other eukaryotic organisms possess multiple Atg8 homologues. For example, humans contain 9 homologues of Atg8, whereas the plants *Arabidopsis thaliana* and *Oryza sativa* (rice) have 9 and 5 copies of Atg8, respectively. Among the trypanosomatids, *T. brucei* and *T. cruzi* possess three and two Atg8 homologues, respectively, whereas *L. major* uniquely possess 26, which can be divided into four classes, although the number of Atg8 homologues within each class varies between different *Leishmania* species. It is currently unknown exactly why these organisms require multiple Atg8 isoforms, but evidence from mammalian studies is beginning to uncover possible roles of these proteins in autophagy and other processes.

4.1.1.1 Atg8 homologues in mammals

The human Atg8s are divided into two subfamilies based on their protein sequence homology; the LC3 subfamily, comprising LC3A (of which 2 transcriptional variant isoforms v1 and v2 exist), LC3B, LC3B2 and LC3C, and the GABARAP/GATE16 group, which contains GABARAP (γ -aminobutyric acid type A receptor-associated protein), GABARAPL1 (also known as Atg8L), GATE-16 (Golgi-associated ATPase enhancer of 16 kDa; also known as GABARAPL2), and GABARAPL3 (Xin et al., 2001; He et al., 2003; Hemelaar et al., 2003; Bai et al., 2012). These Atg8 homologues appear to be conserved amongst mammals, although LC3Av2, LC3B2 and LC3C are yet to be identified in non-human species (Bai et al., 2012). The mammalian Atg8 homologues require the conserved autophagic machinery for their activation and conjugation to membranes, namely Atg4, Atg7 and Atg3. A recent study on the human LC3 family has shown that whereas the localisation of LC3Av1 and LC3B to puncta is greatly increased in response to starvation, LC3Av2 or LC3B2 puncta increase only slightly (Bai et

al., 2012), implying that the different members of this family act differently during autophagy. LC3C constantly labels small puncta whose distribution is not affected by starvation or treatment with the autophagy inhibitors wortmannin and 3-MA (Bai et al., 2012), suggesting that this protein has autophagy-independent functions. Mammalian cells possess four homologues of the yeast cysteine peptidase Atg4, which mediates processing of Atg8 at its conserved C-terminal glycine, and these are named Atg4A, B, C and D. Of these, Atg4B appears to have broad substrate specificity and is able to cleave LC3, GABARAP, GATE-16 and Atg8L (Hemelaar et al., 2003; Li et al., 2011), whereas Atg4A hydrolyses GABARAP, GATE-16 and Atg8L, but not LC3 (Li et al., 2011). Atg8C and Atg8D show only minimal activity against LC3 and GATE-16, but are not active against GABARAP or Atg8L (Li et al., 2011). In line with this, other roles have been uncovered for Atg4C and Atg4D. Although Atg4C was not essential for autophagy during normal conditions, Atg4C-deficient mice displayed a reduced autophagy response during starvation conditions and were more susceptible to cancer development, suggesting that this isoform may be important during stress-induced autophagy (Mariño et al., 2007). Atg4D, on the other hand, has been found to be cleaved by caspase-3 (Betin and Lane, 2009); this processing event increases the activity of Atg4D against GABARAPL1. Interestingly, over-expression of caspase-cleaved Atg4D induced apoptotic cell death and this was preceded by localisation of the Atg4D product to the mitochondria (Betin and Lane, 2009), perhaps linking Atg4D to regulation of apoptosis.

LC3 is processed by Atg4B into LC3-I, which lacks the C-terminal 22 residues, and is conjugated to PE to produce LC3-II, which localises to autophagosomal membranes; the amount of LC3-II detected correlates with the extent of autophagosomal formation (Kabeya et al., 2000). GABARAP and GATE-16 can be processed by either Atg4A or Atg4B, and are also converted to form II which localises to membrane fractions. In addition, they were shown to localise to LC3-positive puncta (Kabeya et al., 2004), suggesting that these Atg8 homologues also have roles in autophagosomal formation. More recently it has been discovered that both LC3 and GABARAP/GATE-16 subfamilies are essential for autophagosomal biogenesis, but that they act at different stages of this process. By selectively down-regulating each subfamily through targeted siRNA, the authors showed that knockdown of either of the Atg8 subfamilies led to an

inhibition of autophagic flux and a decrease in overall protein degradation (Weidberg et al., 2010). Knockdown of either subfamily resulted in increased numbers of puncta labelled by Atg5 and Atg16, and silencing of the GABARAPs led to these puncta being larger than normal, whereas knockdown of LC3s produced small puncta. Likewise, over-expression of an inactive Atg4A^{C77A}, a GABARAP/GATE-16-specific peptidase, resulted in the appearance of large autophagosomes, many of which were not fully closed when visualised by electron microscopy (Weidberg et al., 2010). These results suggest that the LC3 subfamily's function is the elongation of the phagophore, whilst members of the GABARAP/GATE-16 subfamily act at a later stage of the process, perhaps in the sealing of autophagosomes. Similar observations of unclosed autophagic membranes were recorded in two studies which disrupted the entire mammalian Atg8 conjugation system (Sou et al., 2008; Fujita et al., 2008), either by knockout of Atg3 (the E2-like enzyme for Atg8 conjugation) or by over-expression of an inactive Atg4B^{C74A} (a peptidase able to process all mammalian Atg8 homologues), highlighting the essential roles of the Atg8s in autophagosome maturation. Further *in vitro* work has shown that, upon conjugation of their C-termini to PE, LC3 and GATE-16 facilitate liposome tethering and membrane fusion, and that this action is required for autophagosome formation (Weidberg et al., 2011). This activity is dependent on the proteins' N-terminal α -helices, and specific residues within this region. The mammalian Atg8s also play roles in cargo recruitment during selective autophagy through binding to the cargo receptor p62 and organelle-specific proteins such as Nix (discussed in detail in Chapter 3). It appears that although both LC3 and GATE-16 can bind to p62 in their soluble forms, only LC3-II interacts with p62 (Shvets et al., 2011), suggesting that LC3 specifically has roles in recruitment of p62-labelled cargo into autophagosomes. NBR1, a cargo receptor that binds to ubiquitin-labelled aggregates and interacts with p62, also associates with LC3 and GATE-16 (Kirkin et al., 2009) which may mean that NBR1 links the GABARAP family to autophagosomes containing p62-labelled cargo. GABARAP is also known to interact with Nix (Schwarten et al., 2009), and GABARAPL1 binds to Stbd1 (Jiang et al., 2011), suggesting that these proteins may be involved in mitophagy and apoptosis, or autophagic degradation of glycogen, respectively.

The multiple Atg8 homologues are differentially expressed in human tissues (Xin et al., 2001; He et al., 2003), suggesting that they might have tissue-specific functions or that they may be important for autophagy in different tissue types. Notably, various Atg8 homologues are highly expressed in the heart, brain, liver, skeletal muscle and testis (Xin et al., 2001; He et al., 2003), suggesting that autophagy is especially important in these tissues. As well as its involvement in autophagy, GABARAP has been studied previously for its roles in clustering of GABA_A receptors in synapses, which is thought to modulate synaptic transmission (Wang et al., 1999; Chen et al., 2000). This activity is achieved through interactions of GABARAP with the $\gamma 2$ subunit of GABA_A receptors, and with tubulin and microtubules in the cytoskeleton (Wang and Olsen, 2000). In addition, both GABARAP and GATE-16 are known to interact with *N*-ethylmaleimide-sensitive factor (NSF), a protein that is critical for intracellular membrane trafficking events (Sagiv et al., 2000; Kittler et al., 2001). GATE-16 also interacts with the Golgi-specific SNARE GOS-28 (Sagiv et al., 2000), suggesting that it may have other roles in intra-Golgi protein trafficking. The fact that GABARAP and GATE-16 interact with components of the SNARE machinery fits in well with their proposed role in autophagosome maturation (Weidberg et al., 2010), as SNAREs are required during autophagosome formation for the fusion of autophagosomes to endosomal compartments and to the lysosome (Fader et al., 2009; Furuta et al., 2010).

4.1.1.2 Atg8 homologues in plants

The model plant *A. thaliana* encodes 9 homologues of yeast Atg8, named *AtAtg8a - i*, which can be grouped into clades based on their similarity to the yeast protein (Doelling et al., 2002; Hanaoka et al., 2002). *AtAtg8a - g* cluster in one clade, showing 84 - 96 % amino acid sequence similarity to yeast ATG8 and the other *AtAtg8s* in this group. The second clade contains *AtAtg8h* and *i* which are 69 - 75 % similar to *AtAtg8s* of the first clade and lack the extra amino acids downstream of the conserved C-terminal glycine residue (Doelling et al., 2002; Hanaoka et al., 2002). The *AtAtg8s* also show similarity to the mammalian Atg8 homologues LC3 (33 - 41 %), GABARAP (42 - 59 %) and GATE-16 (48 - 60 %). It was later confirmed that *AtAtg8a - g* are cleaved at the C-terminal glycine by *AtAtg4a* and *b*, and that the *AtAtg4s* are required for deconjugation of *AtAtg8a - i* in order for completion of autophagy (Yoshimoto et al., 2004). In addition,

representative *AtAtg8s* and *AtAtg4b* were able to complement *S. cerevisiae* $\Delta atg8$ and $\Delta atg4$ mutants, respectively (Ketelaar et al., 2004). These authors also showed that *AtAtg8s* could interact with microtubules, suggesting that in plants autophagosomes are linked to the cytoskeleton by Atg8, similar to the situation in mammalian cells (Köchler et al., 2006; Jahreiss et al., 2008). Disrupting plant autophagy genes results in reduced seed production, accelerated leaf senescence, and reduced root growth (Doelling et al., 2002; Hanaoka et al., 2002; Yoshimoto et al., 2004), as well as making plants less able to survive starvation (Doelling et al., 2002; Hanaoka et al., 2002; Yoshimoto et al., 2004; Sláviková et al., 2005). Thus, in plants autophagy appears to be important for survival during nutritional stress and nutrient cycling during cellular homeostasis, as in other organisms. *AtAtg8s* localise preferentially to the roots, and each appears to localise to different regions of this organ (Sláviková et al., 2005), perhaps suggesting non-redundant region-specific roles for these proteins. More recently, both *AtAtg8f* and *AtAtg8h* have been shown to bind to two plant-specific Atg8-interacting proteins, ATI1 and ATI2 (Honig et al., 2012). During carbon starvation these proteins localise to novel ER-associated vesicles that move dynamically along the ER network and appear to be transported to the vacuole; however, these vesicles do not appear to be canonical autophagosomes. This might suggest that *AtAtg8* is involved in packaging cargo into ATI vesicles before their trafficking along the ER. In addition, a heme-binding protein called TSPO, which contains an Atg8-interacting motif, requires the autophagic pathway for its degradation (Vanhee et al., 2011), implying roles for autophagy in the regulation of heme uptake. Multiple Atg8 homologues have also been detected in numerous other plants, many of which are important crop plants (Doelling et al., 2002), suggesting that similar autophagy pathways exist in many plants, although these have only been characterised in rice (Su et al., 2006) and soybean (Xia et al., 2012) to date.

4.1.1.3 Atg8 homologues in trypanosomes

The genome of the African trypanosome *T. brucei* encodes 3 proteins with a high level of sequence identity to yeast Atg8, designated TbATG8.1, TbATG8.2 and TbATG8.3 (Duszenko et al., 2011). The third of these is most similar to the ATG12 of *L. major* (Williams et al., 2009) suggesting that it may be an ATG12 rather than an ATG8. Both ATG8.1 and ATG8.2 are known to label puncta in

procyclic trypanosomes, whose formation can be greatly increased by starvation and inhibited by wortmannin (Proto, PhD thesis 2010; Li et al., 2012a). This suggests that these puncta are autophagosomes, as they display characteristics of those from other organisms in which autophagy has been characterised. ATG8.1 shares ~ 82 % sequence identity with ATG8.2, but ends in a C-terminal glycine, suggesting that processing is not required for its conjugation to lipid. ATG8.1 and ATG8.2 co-localise on all autophagosomes, suggesting that they function synergistically in autophagosome formation; however, the localisation of ATG8.1 to puncta is ATG8.2-dependent, whereas ATG8.2 localisation to autophagosomes does not require ATG8.1 (Li et al., 2012a). Thus it is possible that ATG8.2 acts at an earlier stage of autophagosome formation than ATG8.1, similarly to LC3 and GABARAP/GATE-16 in mammals (Weidberg et al., 2010).

The two Atg8 homologues of *T. cruzi*, TcATG8.1 and TcATG8.2, share 43 % sequence identity and are both cleaved at a conserved C-terminal glycine by the *T. cruzi* Atg4 homologues, TcATG4.1 and TcATG4.2 (Alvarez et al., 2008). However only ATG8.1 localised to punctate structures upon starvation or during parasite differentiation, and could partially replace Atg8 function in a yeast $\Delta atg8$ strain (Alvarez et al., 2008), suggesting that ATG8.1 is the functional homologue of yeast Atg8. ATG8.2 only localised to puncta after prolonged starvation implying that it has different functions to ATG8.1, although its similarity to *L. major* ATG12 suggests that ATG8.2 possibly functions as the *T. cruzi* ATG12.

4.1.2 The multiple ATG8 families of *Leishmania*

The identification of candidate autophagy genes in *L. major* showed that in addition to a single copy ATG8, which shows 46 % identity to *S. cerevisiae* Atg8, the *L. major* genome encodes an estimated 25 ATG8-like proteins (Williams et al., 2006). These can be grouped into four subfamilies: ATG8 (1 gene), ATG8A (3 genes), ATG8B (9 genes) and ATG8C (13 genes). Although they show low similarity to the ATG8s of other organisms, they were identified as ATG8-like proteins because of their conserved glycine residue at the putative Atg4-processing site (Figure 4-1). These elaborate expanded ATG8-like families appear to be unique to *Leishmania*, and show some conservation across *Leishmania* species: *L. infantum* possesses 1 ATG8A, 3 ATG8Bs and 4 ATG8Cs; *L. mexicana* has 1 ATG8A, 6 ATG8Bs and 1 ATG8C; *L. braziliensis* contains 1 ATG8A, 2 ATG8Bs and 2 ATG8Cs (TriTrypDB). In all species ATG8A and ATG8B are interspersed on a gene array located on chromosome 19, and the ATG8C genes are located on chromosome 9. The inter-species variations in copy number of ATG8-like genes may be explained by the fact that different *Leishmania* species have increased gene expression through the expansion of single genes or replication of whole chromosomes. For example, chromosome 9 is trisomic in *L. infantum*, *L. mexicana* and *L. braziliensis* (Rogers et al., 2011), which could explain why these species possess fewer genes encoding ATG8Cs than *L. major* does.

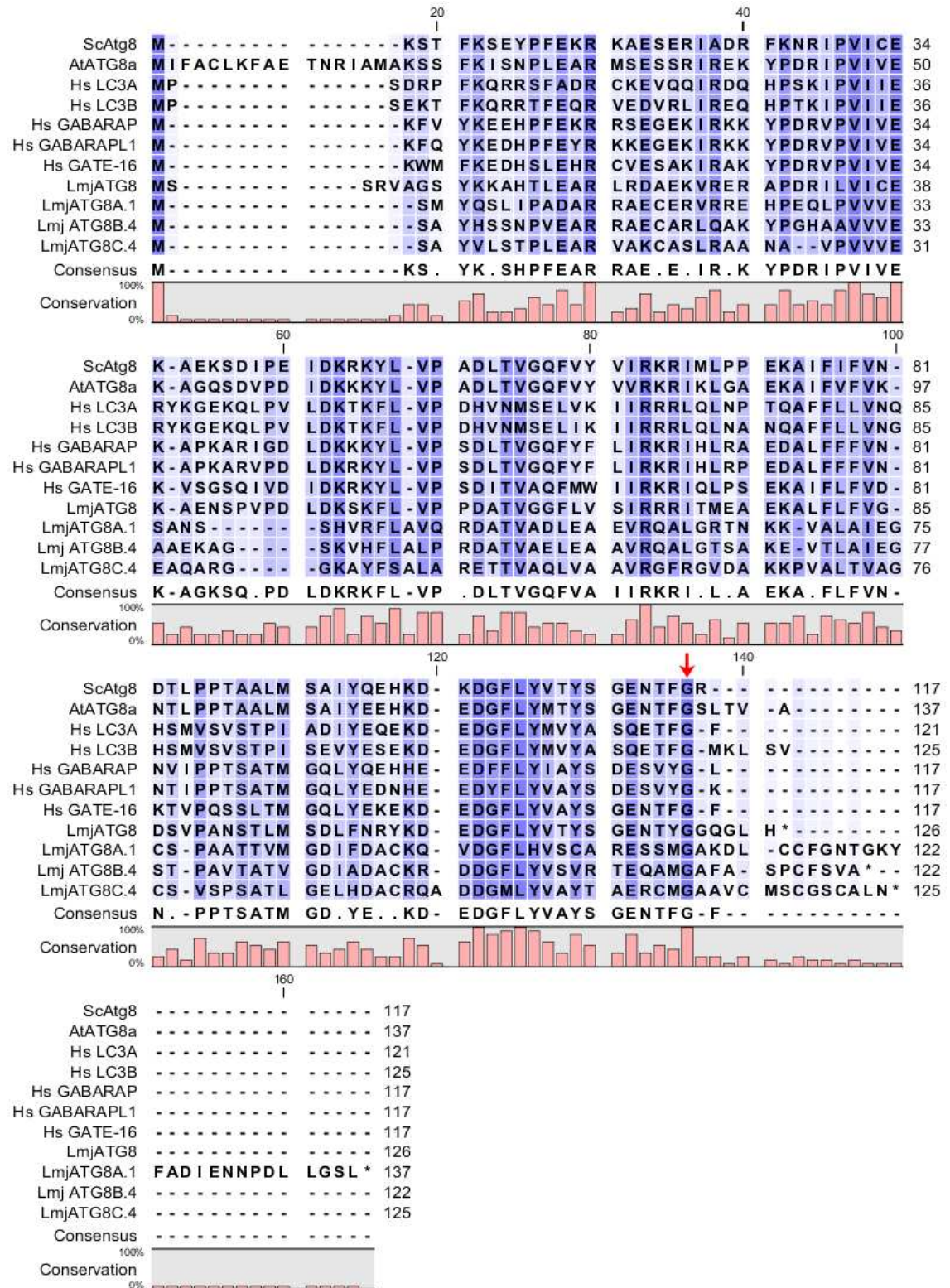


Figure 4-1 Alignment of *L. major* ATG8-like proteins with those of other eukaryotes. Protein sequence alignment of representative Atg8 homologues from *S. cerevisiae* (Sc), *A. thaliana* (At), *Homo sapiens* (Hs) and *L. major* (Lmj). Sequence alignment was performed using Genomics Workbench 4 (CLC Bio). Conservation of amino acids is indicated by blue shading, light – dark corresponding to low – high similarity. The amino acid sequence consensus and conservation are displayed below the alignment. The conserved glycine residue at the Atg4 processing site is indicated by a red arrow. Accession numbers and TriTrypDB designations are as follows: ScAtg8 (NP_009475), AtATG8a (AEE84538), HsLC3A (NP_115903), HsLC3B (NP_073729), HsGABARAP (CAG33324), HsGABARAPL1 (CAG38511), HsGATE-16 (CAG47013), LmjATG8 (LmjF19.1630), LmjATG8A.1 (LmjF19.0840), LmjATG8B.4 (LmjF19.0850) and LmjATG8C.4 (LmjF09.0156).

In *Leishmania* autophagy has been relatively well studied amongst trypanosomatid parasites and ATG8 is known to be important for autophagy during life cycle differentiation and survival during nutritional stress in both *L. major* (Besteiro et al., 2006a) and *L. mexicana* (Williams et al., 2006). GFP-ATG8 puncta formation is inhibited by wortmannin and their trafficking to the lysosome is prevented by treatment with microtubule-disrupting agents (Williams et al., 2006), as in other eukaryotes. The *L. major* ATG8s are selectively cleaved at their C-terminal glycine by the parasite's two Atg4 cysteine peptidases; ATG4.1 shows activity against ATG8, ATG8B and ATG8C, and ATG4.2 preferentially cleaves ATG8A, but also shows activity against ATG8 (Williams et al., 2009). Additionally, representative genes from each *Leishmania* ATG8 family are able to complement autophagy defects in yeast $\Delta atg8$ strains and form puncta when expressed as GFP fusion proteins in *L. major* (Williams et al., 2009). Whereas GFP-ATG8 forms puncta during starvation and differentiation, corresponding to a role in autophagosome formation, GFP-ATG8A puncta form in the majority of cells in response to starvation, and both GFP-ATG8B and GFP-ATG8C label single puncta at the anterior of the cell close to the flagellar pocket irrespective of growth conditions (Williams et al., 2009). The localisation of GFP-ATG8A to puncta is time-dependent: after 2 hours of starvation ~ 20 % cells contain 2 or 3 puncta localised close to the flagellar pocket, and after 4 hours ~ 90 % cells contain puncta with GFP-ATG8A labelling multiple puncta throughout the cell body in addition to those at the flagellar pocket (Woods, PhD thesis 2009). Furthermore, the formation of ATG8A puncta is inhibited by addition of amino acids or glucose, suggesting that ATG8A may play a role in surviving nutritional stress. In parasites co-expressing GFP-ATG8A and RFP-ATG8, puncta were sometimes observed labelled with both proteins, although the formation of GFP-ATG8A puncta cannot be inhibited by the autophagy inhibitor wortmannin (Woods, PhD thesis 2009), suggesting that ATG8A puncta are autophagy-independent. ATG8A puncta can also be induced by metabolic stress caused by culturing parasites anaerobically or in the presence of 1 mM cyanide, suggesting that ATG8A responds to stress conditions, not specifically to starvation (K. Woods, unpublished data). Analysis of ATG8A and ATG8B expression in different life-cycle stages reveal that these proteins are highly expressed in metacyclic promastigotes but are not detected in amastigotes (Woods, PhD thesis 2009), perhaps suggesting that they have

functions related to the infection process or development in the sandfly mouthparts. ATG8A and ATG8B, in addition to ATG8, were found to localise to the membrane bound fraction during subcellular fractionation experiments, although there is no evidence that ATG8A or ATG8B are lipidated by PE, as the migration of these proteins on SDS-PAGE gels was unaffected by phospholipase D treatment, known to remove PE from conjugated ATG8 (Woods, PhD thesis 2009). Although ATG8 is known to function in autophagy, and ATG8A is implicated in a stress survival role, the functions of ATG8B and ATG8C remain a mystery. They are unlikely to be involved in autophagy, as they only form single puncta in < 10 % of the population, these puncta having a defined localisation at the anterior pole of the parasite, and this phenotype is not altered by any stimuli known to induce autophagy. GFP-ATG8C and RFP-ATG8B have been shown to co-localise to the same structures (Woods, PhD thesis 2009), suggesting that ATG8B and ATG8C may carry out similar functions within a novel vesicle.

The structure of ATG8 proteins from various organisms have been solved to date, including GABARAP (Coyle et al., 2002), GATE-16 (Paz et al., 2000), and LC3B (Sugawara et al., 2004) from mammals, yeast Atg8 (Schwarten et al., 2010) and *T. brucei* ATG8.2 (Koopmann et al., 2009). Structurally, the ATG8 proteins display strong similarity to ubiquitin, with a four-stranded β -sheet in which the two central strands ($\beta 2$ and $\beta 3$) are parallel to each other, and the outer two strands ($\beta 1$ and $\beta 4$) are anti-parallel to the central strands. Two α -helices are located between $\beta 2$ and $\beta 3$, and between $\beta 3$ and $\beta 4$, respectively. This ubiquitin core structure is shared by a number of ubiquitin-like proteins that carry out diverse functional roles in the cell through the post-translational modification of various protein targets. In addition to the ubiquitin core, ATG8 proteins possess two characteristic N-terminal α -helices. The $\alpha 1$ and $\alpha 2$ N-terminal helices are attached to the ubiquitin core by various interactions including salt bridges and hydrogen bonds; these occur between residues that are largely conserved between mammalian Atg8-like proteins (Sugawara et al., 2004). Many of these residues are also conserved in the sequence of *L. major* ATG8, and partially conserved in ATG8A, ATG8B and ATG8C (Woods, PhD thesis 2009), suggesting that ATG8, and possibly the ATG8-like proteins, of *L. major* are able to maintain a characteristic ATG8 structure.

Despite early analyses suggesting that the ATG12-ATG5 conjugation system was absent from trypanosomatids (Herman et al., 2006), proteins with some similarity to ATG5, ATG10, ATG12 and ATG16 have since been identified in *Leishmania* (Williams et al., 2006). The ATG12 of *Leishmania* (LmjF22.1300) appears more related to ATG8s than to ATG12s (Figure 4-2) and, unlike the ATG12s described in other eukaryotes, possesses an extended tail following the C-terminal glycine residue, suggesting that cleavage is required before ATG12 can interact with ATG5. Indeed, the full length *L. major* ATG12 was unable to complement the autophagy defect in $\Delta atg12$ *S. cerevisiae*, but a mutant ATG12 truncated to expose the C-terminal glycine could (Williams et al., 2009). *L. major* ATG5 and ATG10 could also reverse the autophagy defect in *S. cerevisiae* $\Delta atg5$ and $\Delta atg10$ strains, respectively (Williams et al., 2009) and the ATG12-ATG5 conjugation has recently been reconstituted *in vitro* (Williams et al., 2012b), confirming that *Leishmania* possess a functional ATG12 pathway. The identity of the enzyme that is presumably required for the C-terminal cleavage of ATG12 remains to be identified. In addition, GFP-ATG12 localises to punctate structures upon autophagy induction, with some of these structures also labelled with RFP-ATG8 (Williams et al., 2009) and all of them dually labelled with GFP-ATG12 and mCherry-ATG5 (Williams et al., 2012b), showing that ATG12 is the functional homologue of yeast and mammalian Atg12 and is involved in autophagosome formation.

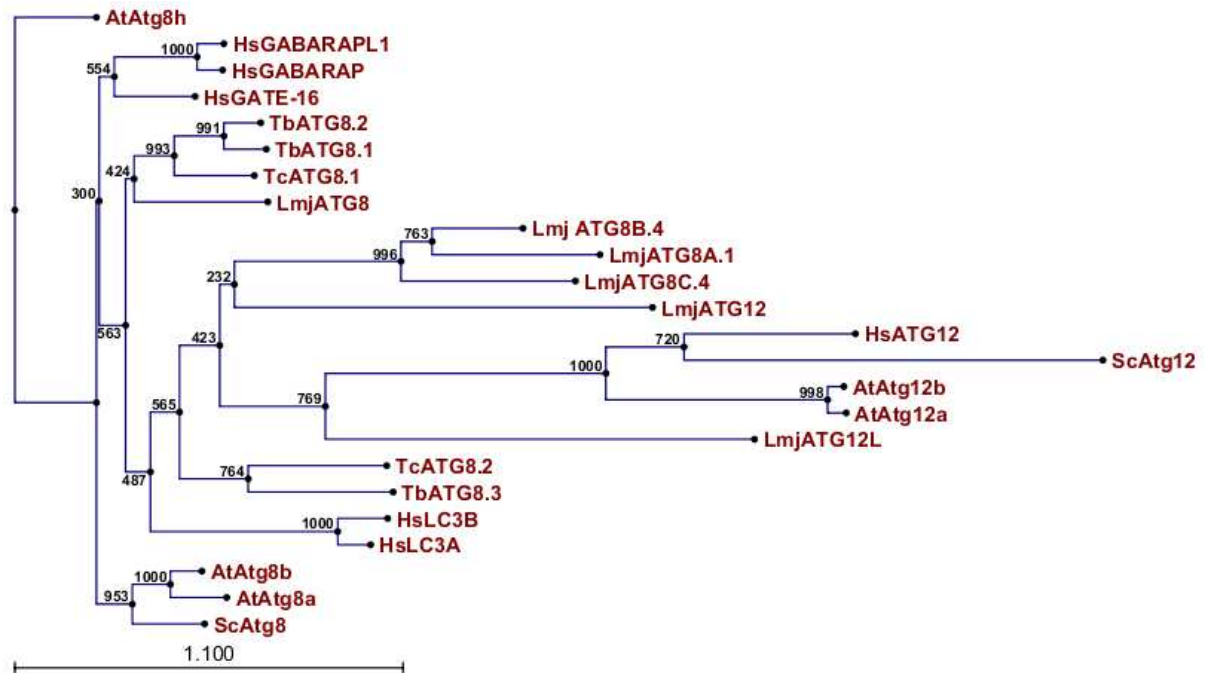


Figure 4-2 Phylogenetic analysis of ATG8 and ATG12 proteins in trypanosomatids, yeast and higher eukaryotes. This unrooted phylogenetic tree was constructed using CLC Genomics Workbench 4 (CLC Bio) using the neighbour joining method, with bootstrap values from 1000 replicates indicated on tree nodes. Scale bar represents a distance of 1.1 amino acid substitutions per site. Accession numbers and TriTrypDB designations are as follows: ScAtg8 (NP_009475), ScAtg12 (NP_009776), AtAtg8a (AEE84538), AtAtg8b (AEE82404), AtAtg8h (Q8S925), AtAtg12a (Q8S924), AtAtg12b (Q9LVK3), HsLC3A (NP_115903), HsLC3B (NP_073729), HsGABARAP (CAG33324), HsGABARAPL1 (CAG38511), HsGATE-16 (CAG47013), HsATG12 (ACD74941), LmjATG8 (LmjF19.1630), LmjATG8A.1 (LmjF19.0840), LmjATG8B.4 (LmjF19.0850), LmjATG8C.4 (LmjF09.0156), LmjATG12 (LmjF22.1300), LmjATG12L (Lmj28.2720), TbATG8.1 (Tb927.7.5900), TbATG8.2 (Tb927.7.5910), TbATG8.3 (Tb927.7.3320), TcATG8.1 (TcCLB.508173.47), TcATG8.2 (TcCLB.510533.180).

4.1.3 Additional functions of ubiquitin-like proteins

In addition to the roles of the ATG8s in autophagosome formation, ubiquitin-like proteins carry out a diverse range of functions through the modification of various substrates. These post-translational modifications can be mediated by ubiquitin itself or by a number of different ubiquitin-like proteins (Ubls). Homologues of many Ubl family members have been identified in trypanosomatid parasites, including ubiquitin, Nedd8 (Neuronal precursor cell-Expressed Developmentally Down-regulated protein 8), SUMO (small ubiquitin-related modifier), and Urm1 (ubiquitin-related modifier 1), as well as Atg8 and Atg12 (Ponder and Bogoy, 2007). These proteins carry out diverse roles including protein degradation, histone regulation, internalisation, transcriptional regulation, protein localisation and autophagy. In addition to ATG8 in trypanosomes and *Leishmania*, and ATG12 in *Leishmania*, which are known to

have roles in autophagy, few UbIs have been well characterised in trypanosomatids. Ubiquitination in *T. brucei* and *T. cruzi* is involved in degradation of proteins by the ubiquitin - proteasome system (de Diego et al., 2001) as well as internalisation of transmembrane surface proteins for degradation through an endosomal pathway (Chung et al., 2008). Interestingly, ubiquitin-encoding genes are up-regulated during *T. cruzi* differentiation (Manning-Cela et al., 2006) and increased degradation of ubiquitinated flagellar cytoskeletal proteins is observed during trypomastigote - amastigote differentiation (de Diego et al., 2001), implying that the ubiquitin - proteasome system is important for protein turnover during remodelling throughout transformation between life-cycle stages. Nedd8 also appears to be involved in the internalisation of transmembrane domain-containing surface proteins in *T. brucei*, and degradation of internalised proteins occurs in a ubiquitin-independent manner involving trafficking to an acidic compartment (Chung et al., 2008). SUMO has also been characterised in trypanosomes. In *T. brucei* it localises to the nucleus following processing at a C-terminal diglycine motif and plays essential roles in cell cycle regulation, being especially important for chromosome segregation during mitosis (Liao et al., 2010). The SUMO pathway has been characterised in *T. cruzi* and, similarly to in *T. brucei*, SUMO localises predominantly to the nucleus and C-terminal processing at the conserved diglycine motif is essential for its maturation (Bayona et al., 2011). Identification of potential SUMO targets found many proteins that are involved in nuclear processes such as DNA replication and repair, mRNA metabolism, chromatin remodelling, ribosome biogenesis and nuclear transport, as well as proteins related to biological processes in the cytoplasm or mitochondrion, such as carbohydrate and lipid metabolism, RNA editing and intracellular protein transport (Bayona et al., 2011), functions that have been associated with SUMOylation in other organisms. Another study in *T. cruzi* recorded localisation of SUMO to the nucleus as well as to the paraflagellar rod protein, PFR1, during amastigote - trypomastigote transformation (Annoura et al., 2012). This suggests that SUMOylation, as well as ubiquitination, is important for flagellar homeostasis, and may play roles in flagellar elongation, as SUMO is known to be able to act antagonistically to ubiquitin. A SUMO pathway is also predicted to exist in *Leishmania*, but as yet this has not been characterised. Recent identification and characterisation of the Ubl ubiquitin-fold modifier 1 (Ufm1) in

Leishmania donovani showed that components of this pathway are associated with the mitochondrion (Gannavaram et al., 2011), suggesting that Ufm1 substrates are mitochondrial proteins, although their identity and the function of Ufm1 modification are yet to be discovered. As evidenced here, Ubl modifications regulate a broad range of biological functions and it is possible that members of the ATG8-like families of *Leishmania* may be involved in other processes unrelated to autophagy. Interestingly, *Leishmania* encodes many Ubls, highlighting the importance of post-translational modifications for regulating protein function in an organism that employs constitutive polycistronic transcription for gene expression (Kramer, 2012).

4.2 Analysis of ATG8, ATG8A, ATG8B and ATG8C

4.2.1 Generation and analysis of ATG8 and ATG8A C-terminal glycine mutants

The *L. major* ATG8-like proteins are processed at a conserved glycine residue by the cysteine peptidases ATG4.1 and ATG4.2 (Figure 4-1), and this cleavage is thought to be key to their activation, as it is for other eukaryotic ATG8s. To determine whether this is the case in *Leishmania*, I produced ATG8-like proteins with the putative ATG4 processing site glycine mutated to an alanine. This was carried out using mutagenic primers (see Table 2-1) and plasmids encoding GFP fusions of ATG8 and ATG8A. It was hoped that by expressing mutant ATG8 proteins in *Leishmania*, these might compete with endogenous ATG8s for ATG4 binding and therefore exert a dominant negative effect. Using this approach, plasmids encoding GFP-ATG8^{G120A} and GFP-ATG8A^{G109A} were generated.

4.2.1.1 Comparison of GFP-ATG8 and GFP-ATG8^{G120A}

L. major promastigotes expressing GFP-ATG8^{G120A} were compared with promastigotes expressing GFP-ATG8 to examine any differences caused by the mutation of the ATG4 processing site. Autophagosome formation was analysed over 11 days of parasite growth; autophagy is known to increase during early stationary phase (day 6 - 7) as parasites begin to differentiate into metacyclic promastigotes (Besteiro et al., 2006a). In parasites expressing the WT protein, an increase in the percentage of cells containing GFP-labelled autophagosomes was observed during early stationary phase, peaking at approximately 30 % with

a corresponding increase in the average number of puncta per positive cell (Figure 4-3 A). In contrast, the mutant ATG8 was greatly impaired in its ability to localise to autophagosomes, with consistently 0 - 2 % cells containing GFP-labelled puncta over the 11 day period (Figure 4-3 A). Whereas GFP-ATG8 expressing parasites often contained 1 - 3 puncta per cell, *Leishmania* expressing GFP-ATG8^{G120A} very rarely contained GFP-labelled puncta and primarily showed GFP fluorescence distributed in the cytoplasm (Figure 4-3 B). Similarly, after starvation of both cell lines for 4 hours in PBS, appearance of GFP-ATG8-labelled puncta increased to 14 % in GFP-ATG8 expressing cells, but remained low at < 1 % in those expressing GFP-ATG8^{G120A} (Figure 4-3 C). GFP-LC3 over-expression in mammalian cells results in some autophagy-independent aggregation of GFP-LC3 into punctate structures (Kuma et al., 2007); this may explain why a small number of *Leishmania* expressing GFP-ATG8^{G120A} contain GFP-labelled puncta. These data together confirm that the glycine 120 residue of *L. major* ATG8 is required for its association to autophagosomes, presumably because it is the site at which cleavage by ATG4 occurs, allowing ATG8 to be conjugated to PE. Similarly, a GFP-LC3^{G120A} mutant expressed in mammalian cells was not processed into the conjugation-competent LC3-I form (Kabeya et al., 2000) and an HA-Atg8.1^{G121A} in *T. cruzi* could not localise to autophagosomes (Alvarez et al., 2008).

As autophagy is known to be important for the successful differentiation of *Leishmania* (Williams et al., 2006; Besteiro et al., 2006a) I next determined whether parasites expressing the mutant GFP-ATG8^{G120A} were able to efficiently differentiate from procyclic promastigotes to metacyclic promastigotes; this would determine whether the mutant protein was having a dominant negative effect. Cells in stationary phase of growth (day 6 - 7), at which time metacyclogenesis occurs, were prepared for Western blot and probed with an antibody against HASPB, a protein expressed only in metacyclic promastigotes and amastigotes (McKean et al., 2001). HASPB was expressed both in parasites expressing GFP-ATG8 and those expressing GFP-ATG8^{G120A}, although perhaps at a lower level in the mutant (Figure 4-3 D), suggesting that both cell lines had successfully undergone metacyclogenesis, although further analyses using other differentiation markers such as SHERP expression and cell morphology are required to confirm this. Therefore, although GFP-ATG8^{G120A} is unable to localise

to autophagosomes, it appears unable to produce a dominant negative effect and so parasites expressing this mutant are able to perform functional autophagy using endogenous ATG8.

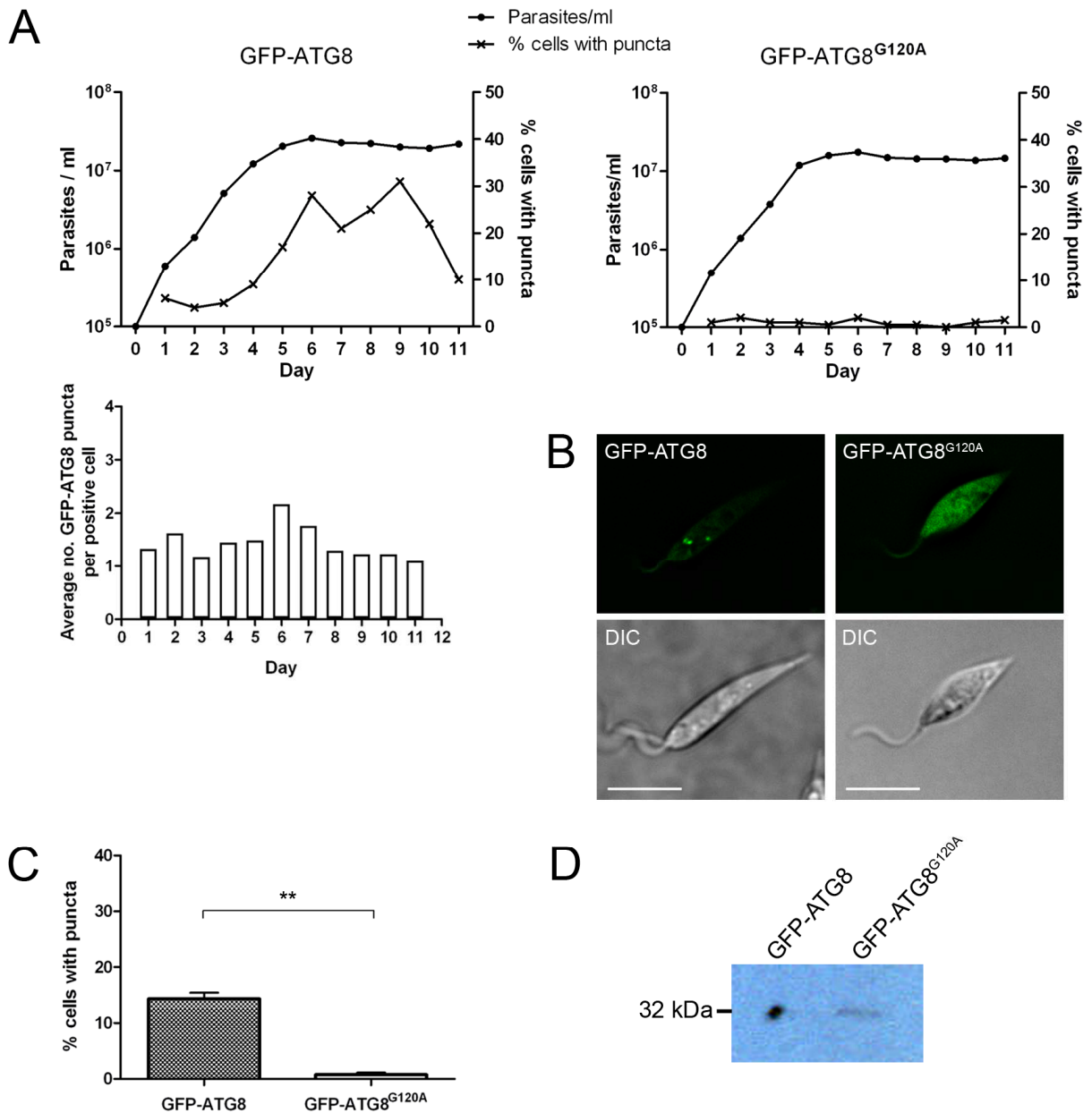


Figure 4-3 Comparison of *L. major* promastigotes expressing GFP-ATG8 or GFP-ATG8^{G120A}. A. Parasite cell density and the percentage of cells containing 1 or more GFP-labelled puncta were determined each day over an 11 day period. Average GFP-ATG8 puncta per cell containing puncta were determined each day for cells expressing GFP-ATG8. B. Live cells were washed and resuspended in PBS before mounting on slides. Parasites were viewed and imaged on a DeltaVision RT microscope. Images show a single slice from a 2 μm Z-stack. Scale bar = 5 μm. C. Parasites were washed then incubated in PBS for 4 h before preparing for live microscopy as above. Bars represent the mean and the error bars standard deviation of 2 independent experiments, each counting at least 200 cells. Data were compared by student's t test; ** signifies $p < 0.01$. D. Cell lysates of stationary phase parasites were prepared by boiling in 1 x SDS-PAGE buffer with peptidase inhibitor cocktail. Western blot was probed with rabbit α-HASPB primary antibody at 1:3000 for 1 h at room temperature followed by α-rabbit HRP-conjugated secondary antibody at 1:5000 for 1 h at room temperature. 32 kDa corresponds to the size of HASPB protein.

4.2.1.2 Comparison of GFP-ATG8A and GFP-ATG8A^{G109A}

L. major ATG8A is known to form multiple punctate structures in response to starvation (Williams et al., 2009). Localisation of GFP-ATG8A^{G109A} was compared with that of GFP-ATG8A after parasites had been incubated in nutrient-free medium for 4 hours. No differences were observed in the percentage of cells containing GFP-labelled puncta or the average number of puncta per cell, with the majority of cells displaying multiple puncta with the characteristic distribution of ATG8A (Figure 4-4). The only difference observed in parasites expressing GFP-ATG8A^{G109A} was that some cells displayed GFP fluorescence in large central puncta (Figure 4-4 C, bottom panel), suggesting that the mutant protein had been trafficked to the lysosome.

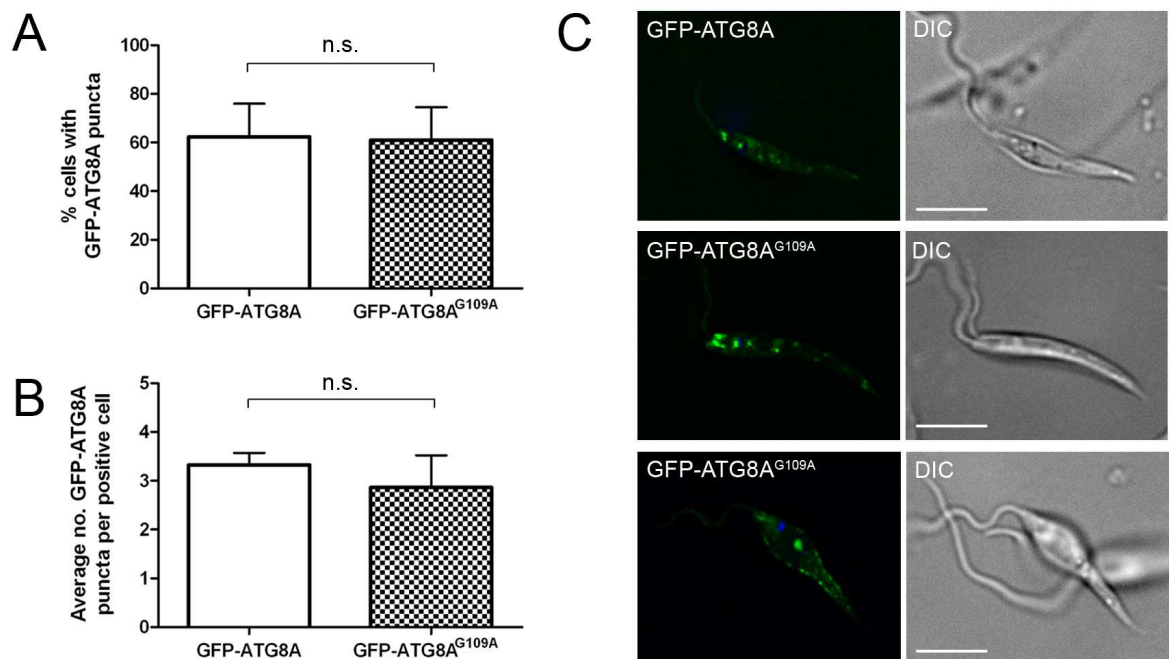


Figure 4-4 Comparison of GFP-ATG8A and GFP-ATG8A^{G109A} localisation during starvation. Log phase *L. major* expressing GFP-ATG8A or GFP-ATG8A^{G109A} were washed, incubated in PBS for 4 h at 25°C and then prepared for live fluorescent microscopy. A, B. The percentage of cells containing at least one GFP-labelled punctate structure and the average number of puncta per puncta-containing cell were determined from 2 independent experiments, counting 100 cells each time. Bars show mean and error bars the standard deviation of the data. Data were compared with a student's t test; n.s. not significant. C. Live cells were imaged on the DeltaVision RT fluorescent microscope. Images show a single slice from a 3 µm Z-stack. Scale bar = 5 µm.

To determine whether any changes occur during the post-translational processing of GFP-ATG8A^{G109A} due to the C-terminal mutation, Western blots were performed on lysates of untransfected cells and cells expressing GFP-

ATG8A or GFP-ATG8A^{G109A}, and probed with antibodies against GFP or ATG8A (Figure 4-5 A). Immunodetection with α -GFP showed two bands in the lane containing lysates of GFP-ATG8A-expressing parasites, which correspond to the sizes of GFP-ATG8A and its cleaved form, at 42 and 39 kDa, respectively. In contrast, the 39 kDa species was not present in GFP-ATG8A^{G109A}-expressing parasites, suggesting that the mutant protein is not processed correctly. However, if the mutant is unable to be cleaved, one might expect to observe an increased intensity of the band at 42 kDa due to accumulation of the uncleaved form, although it is possible that the protein is degraded if not processed correctly. When probing lysates of GFP-ATG8A-expressing cells with α -ATG8A, large amounts of two products were detected at 39 and 32 kDa; the protein at 39 kDa was particularly intense and may be masking the uncleaved GFP-ATG8A species at 42 kDa. The 42 kDa band of GFP-ATG8A^{G109A} was not detected by α -ATG8A, only bands at 58, 55, 45, 29 and 25 kDa, which were detected in all samples and may represent cross-reacting proteins. As expected, no GFP-ATG8A products were detected in lanes containing lysates of WT *L. major*. The expected 15 kDa band representing endogenous ATG8A was not detected by α -ATG8A in any sample, although this antibody has previously been reported to show poor detection of the native protein, which is expressed at low levels in log phase promastigotes (Woods, PhD thesis 2009). To determine whether the G109A mutation of ATG8A prevents its cleavage, *in vitro* experiments were carried out using recombinant ATG8A and an ATG8A^{G109A} mutant with N-terminal histidine (His) and C-terminal haemagglutinin (HA) fusions (R. Williams, unpublished data). Neither protein was cleaved by ATG4.1, an enzyme specific to ATG8, ATG8B and ATG8C, but both His-ATG8A-HA and His-ATG8A^{G109A}-HA were processed in the presence of ATG4.2, the peptidase with activity against ATG8A, resulting in detection of lower mass bands corresponding to proteins lacking the C-terminal region (Figure 4-5 B). This implies that ATG8A^{G109A} can be cleaved by ATG4.2, and this could occur at a different residue within the protein's C-terminus. However, although *in vitro* work suggests that cleavage of the G109A mutant is possible, GFP-ATG8A^{G109A} still displayed significant differences in its processing when compared to GFP-ATG8A (Figure 4-5 A). It appears that the abnormal cleavage of GFP-ATG8A^{G109A} caused by the mutation of its C-terminal glycine results in degradation of this protein; this is supported by the appearance of GFP-ATG8A^{G109A} in the lysosome in live parasites (Figure 4-4 C).

Despite the apparent defects in processing of GFP-ATG8A^{G109A} the protein was able to localise to puncta normally (Figure 4-4 C), suggesting that its ability to form these structures does not require its C-terminal processing. This function may be mediated by the N-terminal region of the protein, which has been shown to be important for the membrane fusion activity of LC3 and GATE-16, required for these proteins' roles in autophagosome formation (Weidberg et al., 2011). However, the C-terminal conjugation of LC3 and GATE-16 to PE is hypothesised to lead to a conformational change in their N-termini that promotes the membrane tethering activity of this region (Weidberg et al., 2011). GFP-ATG8A^{G109A} expression does not appear to show a dominant negative effect as GFP-labelled puncta appeared similarly to GFP-ATG8A. It is possible that GFP-ATG8A^{G109A} can mediate vesicle formation by a mechanism independent of C-terminal processing or be incorporated into vesicles formed by endogenous ATG8As, perhaps through direct interactions with functional ATG8As in the vesicle membrane or with the vesicular cargo. As suggested by Figure 4-5 B, some GFP-ATG8A^{G109A} could be processed, and this small amount of the cleaved form, although undetectable by Western blot, could be sufficient for formation of GFP-labelled puncta.

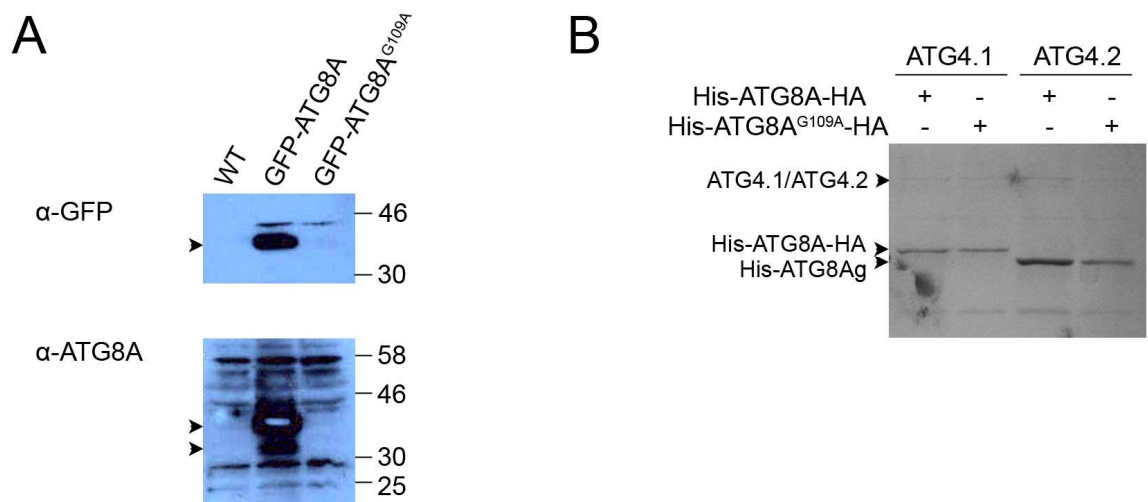


Figure 4-5 Comparison of GFP-ATG8A and GFP-ATG8A^{G109A} processing by Western blot. A. Cell lysates of *L. major* that had been starved, by incubation in PBS for 4 h at 25°C, were prepared by boiling in 1 x SDS-PAGE buffer supplemented with peptidase inhibitor cocktail. Western blots were probed with mouse α -GFP at 1:1000 or sheep α -ATG8A at 1:200 and incubated for 1 h at room temperature. HRP-conjugated secondary antibodies were goat α -mouse (1:5000) and donkey α -sheep (1:5000). Arrowheads highlight bands that are present in cells expressing GFP-ATG8A but not those expressing GFP-ATG8A^{G109A}. B. Immunodetection of recombinant His-ATG8A-HA and His-ATG8A^{G109A}-HA with α -His. Soluble fractions of *E. coli* co-expressing modified ATG8A proteins and ATG4.1 or ATG4.2 were incubated for 30 min at 30°C in 50 mM Tris-HCl, pH 8.0, 125 mM NaCl and 40 mM β -mercaptoethanol before separation by SDS-PAGE and probing with α -His. Experiment performed by R. Williams.

4.2.2 Expression of ATG8-like proteins in $\Delta atg5$ mutants

The Atg8 of yeast and the mammalian LC3 are processed by Atg4 before conjugation to PE through the actions of Atg7 and Atg3, and the involvement of the Atg12-Atg5 conjugate. Components of the Atg12-Atg5 pathway are essential for autophagosome formation (Mizushima et al., 1998; Mizushima et al., 2001). Similarly, a $\Delta atg5$ *L. major* cell line is defective in autophagosome formation (Williams et al., 2012b). To determine whether the ATG8-like proteins of *L. major* require the ATG12-ATG5 conjugation machinery in order to form vesicles, GFP fusions of a representative from each ATG8 family were expressed in *L. major* $\Delta atg5$ and these cells compared with WT *L. major* expressing the same GFP-ATG8s. As previously published (Williams et al., 2012b), the $\Delta atg5$ mutant was unable to form GFP-ATG8 autophagosomes, whereas 16 % of WT parasites in mid-log phase of growth contained 1 - 3 autophagosomes (Figure 4-6 A). Both WT and $\Delta atg5$ showed the characteristic formation of GFP-ATG8A structures; after 2 hours starvation, 2 or 3 puncta appeared at the anterior of the cell close to the flagellar pocket, and after 4 hours starvation multiple GFP-ATG8A structures appeared throughout the cell, in addition to the puncta at the flagellar pocket (Figure 4-6 B). Appearance of GFP-ATG8A occurred to a comparable extent in both WT and $\Delta atg5$ mutants (Figure 4-6 B). Similarly, the localisation of GFP-ATG8B and GFP-ATG8C to punctate structures close to the flagellar pocket was unaffected by the loss of ATG5, occurring at a similar level in WT and $\Delta atg5$ parasites (Figure 4-6 C).

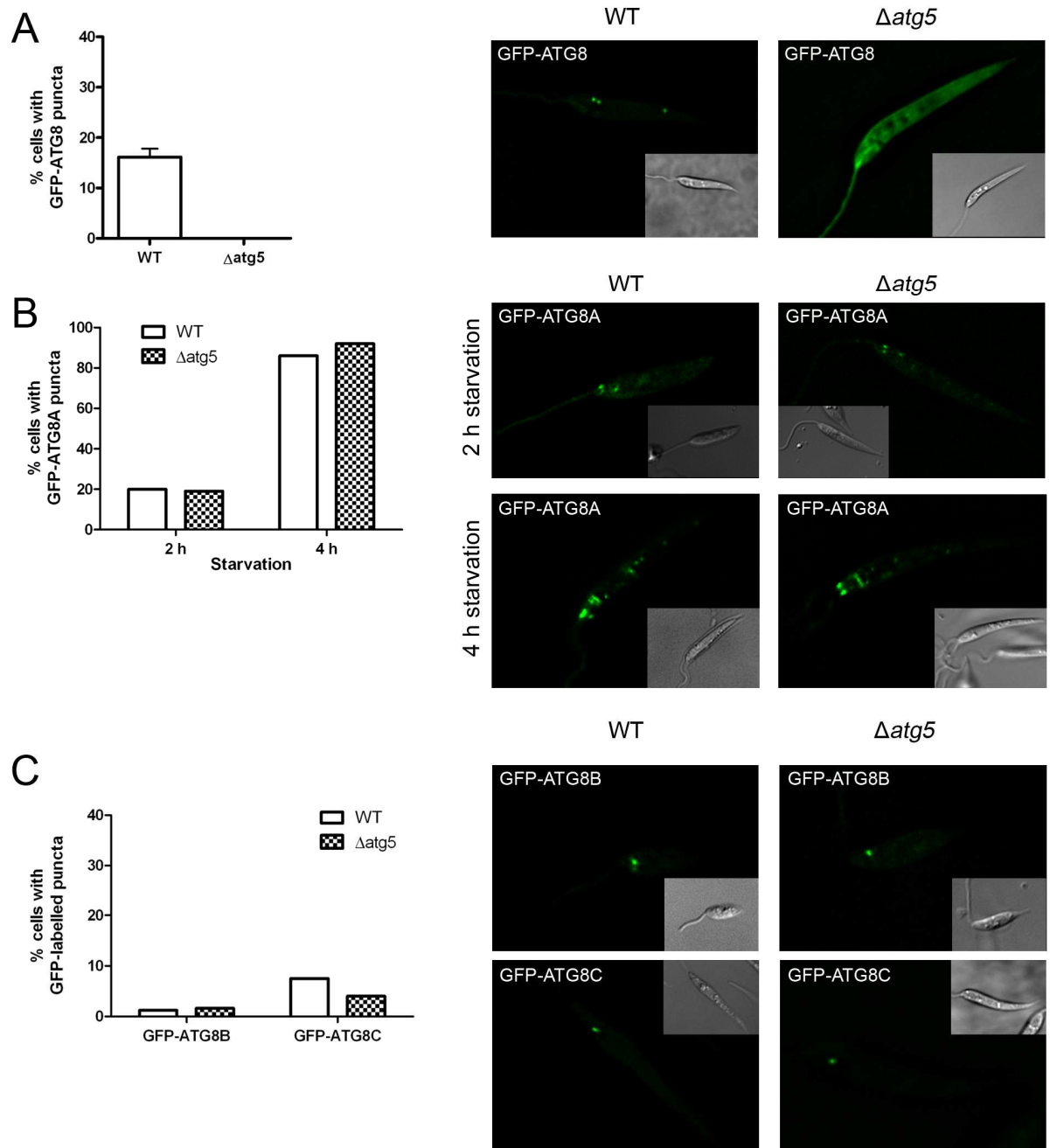


Figure 4-6 Localisation of *L. major* ATG8-like proteins in WT and $\Delta atg5$ parasites. Parasites were washed and resuspended in PBS before viewing by fluorescent microscopy on a DeltaVision Core microscope. Percentage of cells with puncta was determined by counting the number of cells in a sample with at least 1 GFP-labelled punctate structure. Images show a single image from a 2 μ m Z-stack with the corresponding DIC image inset. A. Graph shows the mean data from 3 independent experiments, each time counting 200 cells. Error bar represents standard deviation. B. Log phase parasites expressing GFP-ATG8A were incubated in nutrient-free medium (PBS) for 2 or 4 h before visualisation by fluorescent microscopy. Graph shows data from a single experiment where 100 cells were counted from each sample. C. Stationary phase parasites expressing GFP-ATG8B or GFP-ATG8C were visualised by fluorescent microscopy. Graph shows data from a single set of experiments in which at least 200 cells were counted from each sample.

These data show that although ATG5 is required for the integration of ATG8 into autophagosomes in order to direct their biogenesis, it is dispensable for the localisation of ATG8A, ATG8B and ATG8C to their respective punctate structures. This suggests that formation of these structures is not mediated by the core autophagic machinery and that independent systems are in place for their initiation. Furthermore, formation of GFP-ATG8A puncta in response to starvation was not inhibited by wortmannin, a classical autophagy inhibitor (Blommaert et al., 1997), when added to parasites at a concentration sufficient to inhibit formation of GFP-ATG8 autophagosomes (Woods, PhD thesis 2009), suggesting that ATG8A has roles independent of autophagy. It must be noted, however, that an Atg5/Atg7-independent autophagy pathway has been described in mice, in which autophagosomes form and traffic to the lysosome in response to certain stresses (Nishida et al., 2009), and that ATG8A could also be involved in a similar ATG5-independent pathway in *Leishmania*, although it is unknown whether such a mechanism exists in this parasite. Due to the localisation of GFP-ATG8B and GFP-ATG8C puncta close to the flagellar pocket in a very low proportion of the parasite population under various conditions, they are not expected to be involved in the canonical autophagy pathway, so it is not surprising that their formation is unaffected by loss of ATG5.

4.2.3 Further analysis of ATG8A and ATG8B localisation

The puncta labelled with *L. major* ATG8-like proteins ATG8A, ATG8B and ATG8C localise to the anterior region of the cell, close to the flagellar pocket (Williams et al., 2009), the site of endo- and exocytosis in trypanosomatids. Thus it was reasoned that these vesicles might be involved in processes of the endo-/exocytic system, which may or may not be independent of autophagy; interactions with the endosomal system are essential for the maturation of autophagosomes in mammals (Köchler et al., 2006) and *Leishmania* (Besteiro et al., 2006a). *L. major* expressing GFP-ATG8A or GFP-ATG8B were labelled with markers of the endosomal compartments. Concanavalin A (conA) is a lectin that is known to localise to Rab7-labelled late endosomes in *Leishmania* (Denny et al., 2002). FM4-64 is an endocytic tracer that can be followed from its uptake into the flagellar pocket, through the endosomal compartments to its accumulation in the lysosome (Besteiro et al., 2006a). As the localisation of ATG8C puncta resembles that of ATG8B puncta, and they have been shown to co-localise (Woods, PhD thesis 2009), GFP-ATG8C was not included in this analysis as it is thought to label the same compartment as GFP-ATG8B.

Parasites expressing GFP-ATG8A were starved for 2 hours in order to study the localisation of the 2 - 3 puncta that appear during the early starvation response. Incubation of these cells with conA conjugated to AlexaFluor 594 resulted in labelling of the flagellar pocket (Figure 4-7 A, upper panel) before internalisation of the lectin to label vesicles anterior to the kinetoplast, resembling late endosomes (Figure 4-7 A, lower panel). GFP-ATG8A puncta did not co-localise with conA-labelled compartments, instead appearing either side of the flagellar pocket (Figure 4-7 A). Incubation with FM4-64 for 15 min at 4°C resulted in labelling of the flagellar pocket and endosomal system (during live cell microscopy at room temperature). As seen with conA labelling, GFP-ATG8A puncta did not co-localise with the flagellar pocket, neither did they overlap with FM4-64-labelled structures of the endosomal system (Figure 4-7 B). These images show that ATG8A structures display a distinct localisation at the anterior pole of the *Leishmania* promastigote, appearing either side of the flagellar pocket.

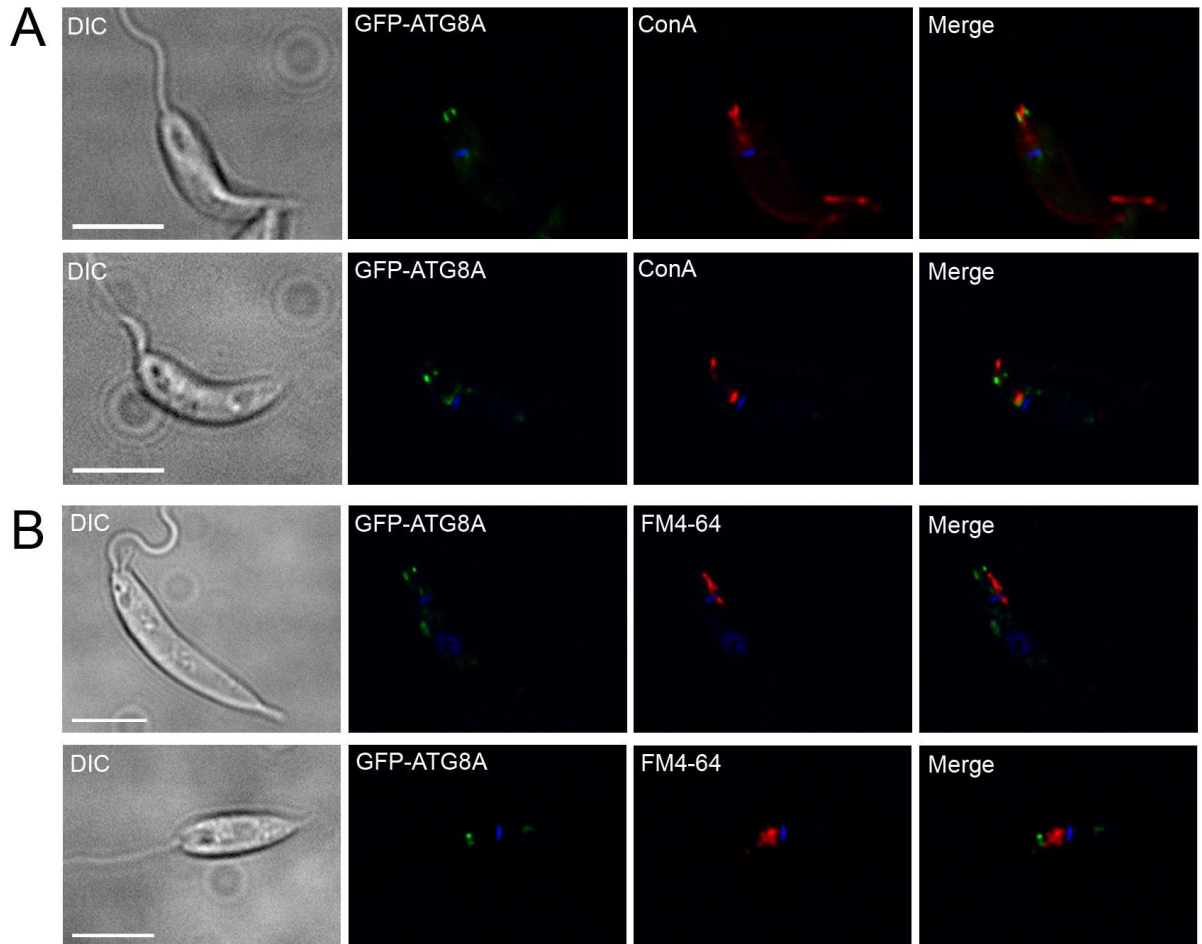


Figure 4-7 Localisation of GFP-ATG8A in relation to markers of the endosomal system. Log phase *L. major* promastigotes expressing GFP-ATG8A were washed and starved for 2 h by incubating in PBS at 25°C. Cells were then labelled with endosomal markers, washed in PBS, DAPI-stained and washed again prior to preparing for live microscopy and visualisation on a DeltaVision Core fluorescent microscope. Images show a single slice from a 2 µm Z-stack. Scale bar = 5 µm. A. Following 2 h starvation, cells were incubated in PBS with 50 µg/ml ConA AlexaFluor 594 conjugate for a further 2 h at 25°C. B. After 2 h starvation, cells were incubated in PBS with 40 µM FM4-64 for 15 min at 4°C.

Labelling of GFP-ATG8B-expressing promastigotes with conA showed that GFP-ATG8B puncta also show a distinct localisation, always appearing just anterior to conA-labelled late endosomes but never overlapping or co-localising with this marker (Figure 4-8 A). Nor did GFP-ATG8B co-localise with the flagellar pocket or early endosomal compartments that were stained by FM4-64 (Figure 4-8 B). These data suggest that *L. major* ATG8-like proteins, whilst seemingly not important for autophagy, associate with compartments that appear distinct from endosomal compartments (although further labelling experiments are required to confirm this) and that these structures may be related to novel functions of ATG8-like proteins.

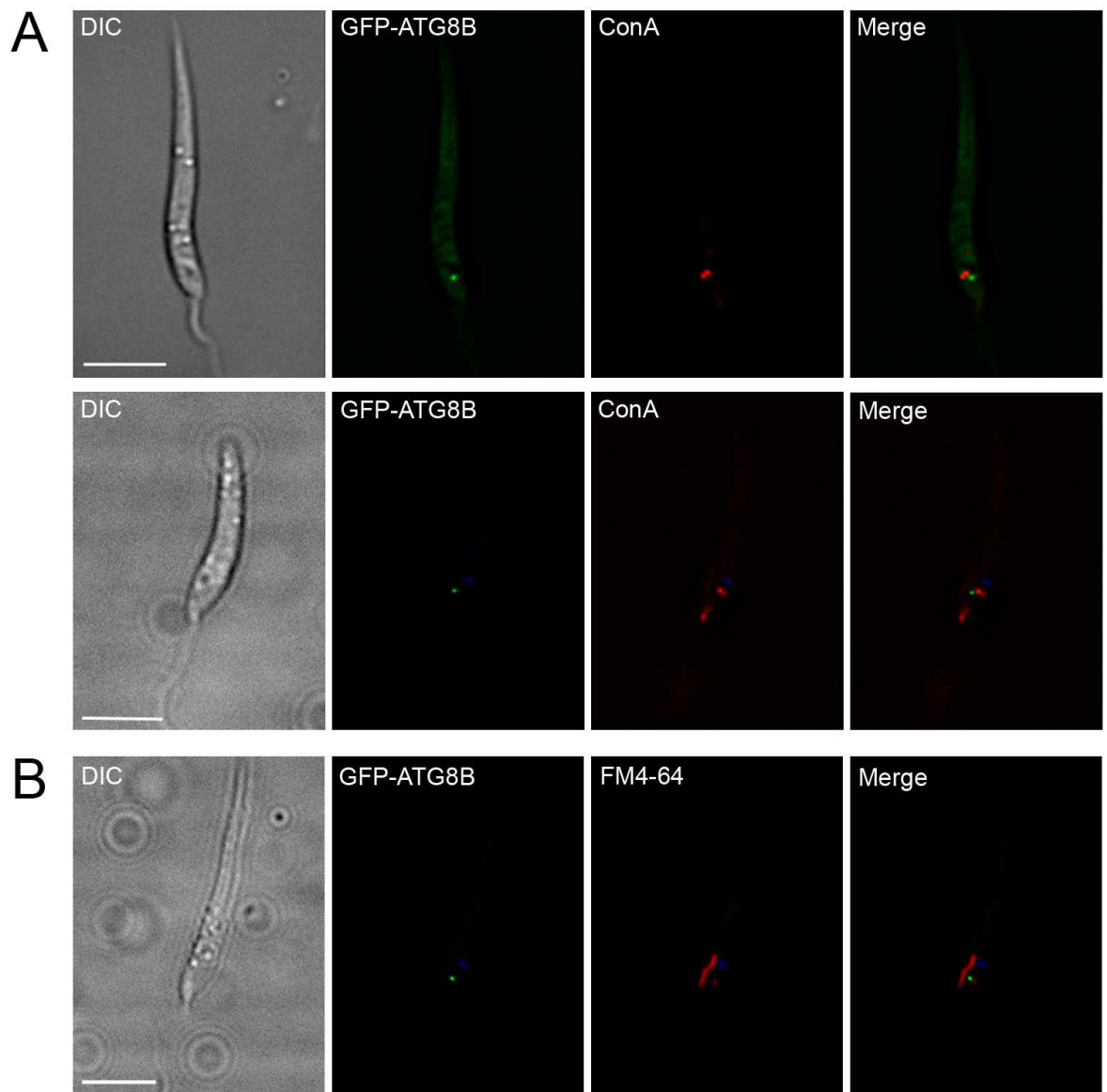


Figure 4-8 Localisation of GFP-ATG8B puncta in relation to endosomal markers. Late log phase *L. major* promastigotes expressing GFP-ATG8B were labelled with endosomal markers, washed in PBS, DAPI-stained, washed again and then prepared for live microscopy on the DeltaVision Core fluorescent microscope. Images show a single slice from a 2 μm Z-stack. Scale bar = 5 μm . A. Cells were incubated in medium with 50 $\mu\text{g}/\text{ml}$ ConA AlexaFluor 594 conjugate for 2 h at 25°C. B. Parasites were incubated in medium with 40 μM FM4-64 for 15 min at 4°C.

4.2.4 Analysis of ATG8-like proteins in secretion mutants

Recently a role has been discovered for autophagy in unconventional secretory pathways. In starved yeast cells, the unconventionally secreted protein Acb1 is packaged into autophagosomes that bypass lysosomal fusion and instead fuse with the plasma membrane in order to release their contents (Duran et al., 2010). This process was found to require the core autophagy machinery as well as the Golgi-associated GRASP protein and a plasma membrane SNARE, Sso1

(Duran et al., 2010). A similar autophagy-based unconventional secretion pathway has also been described in mammalian cells for the secretion of the pro-inflammatory cytokine IL-1 β (Dupont et al., 2011). The unconventionally secreted HASPB protein of *Leishmania* was found to be trafficked to the cell surface and this appears to involve exosomes, although evidence suggests that autophagy is not involved in this process (MacLean et al., 2012). Exosome secretion has been reported in *Leishmania* as a means of protein delivery into host cells (Silverman et al., 2010a) and this pathway is involved in the modulation of immune responses during parasite infection (Silverman et al., 2010b). It is possible that autophagosomes or autophagosome-like vesicles are involved in the exosome-based secretory pathway in *Leishmania* and that regulation of these structures could be mediated by ATG8 or the ATG8-like proteins. The localisation of ATG8A, ATG8B and ATG8C to structures close to the flagellar pocket suggests that they could be involved in endocytic or secretory pathways. To examine the possible role of *L. major* ATG8s in exosome secretion, GFP-fusions of ATG8, ATG8A and ATG8B were expressed in *L. major* Δ *isp1/2/3* mutants, which display disrupted membrane dynamics at the flagellar pocket (Morrison et al., 2012). These mutants excessively secrete small vesicles of ~100 nm in size, which might be exosomes, so it was reasoned that if ATG8 family members were involved in the exosome secretory pathway, then perhaps we would see differences in their localisation in these secretion mutants when compared to WT parasites.

The formation of GFP-ATG8-labelled autophagosomes was unaffected in the Δ *isp1/2/3* cell line, with comparable visualisation of puncta apparent in the mutant and WT parasite populations (Figure 4-9). There was a slight difference in the average number of autophagosomes per cell, although the p value was 0.495, only just below the significance cut-off of $p < 0.05$.

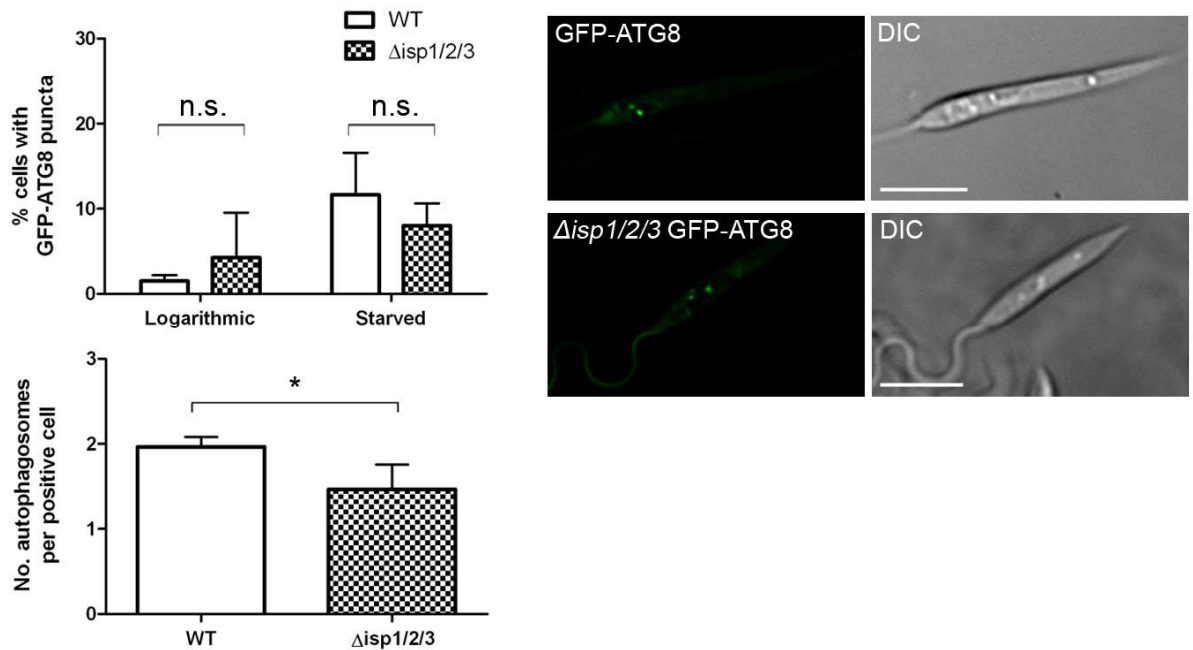


Figure 4-9 Comparison of GFP-ATG8 localisation in WT and $\Delta isp1/2/3$ parasites. *L. major* promastigotes expressing GFP-ATG8 were washed and resuspended in PBS before preparing for live cell microscopy on the DeltaVision RT fluorescent microscope. Starved cells were incubated in PBS for 4 h at 25°C before processing for microscopy. The percentage of cells containing at least 1 GFP-ATG8 punctate structure was determined both in log phase and log phase starved cells in 2 or 3 independent experiments, respectively, counting at least 200 cells each time. The lower graph shows the number of GFP-ATG8 puncta per cell containing puncta in starved cells; data are the mean of 3 independent experiments. Bars represent the mean and error bars standard deviation. Data were analysed using a student's t test: n.s. not significant; * $p < 0.05$. Images show a single slice from a 3 μ m Z-stack. Scale bar = 5 μ m.

Localisation of GFP-ATG8A to multiple puncta upon starvation was apparent in both WT and $\Delta isp1/2/3$ parasites, and occurred at similar levels in both cell lines (Figure 4-10 A), although levels were lower than previously observed. In stationary phase parasites growing in nutrient rich medium, no GFP-ATG8A puncta were observed in either the WT or $\Delta isp1/2/3$ parasites, in line with previous work where very few (0 - 6 %) cells contained GFP-ATG8A puncta (Woods, PhD thesis 2009). Occurrence of GFP-ATG8B puncta in $\Delta isp1/2/3$ parasites matched that in WT parasites (Figure 4-10 B). Together these data do not support a role for ATG8, ATG8A or ATG8B in exosome secretion. Of course, using these mutants in which secretion is affected is not a specific enough way in which to test this, and further studies, such as determining whether proteins known to be secreted in exosomes co-localise with the ATG8-like proteins, should be attempted in order to address this question.

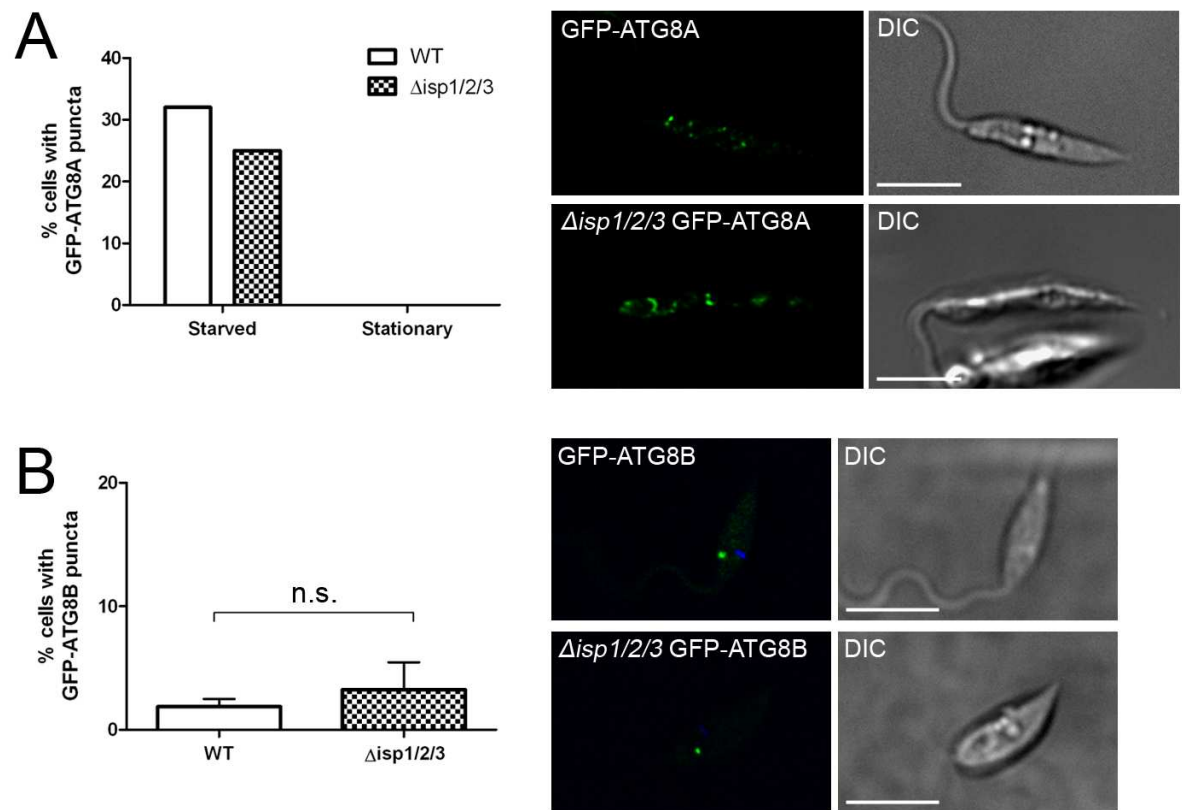


Figure 4-10 Localisation of GFP-ATG8A and GFP-ATG8B in WT and $\Delta isp1/2/3$ parasites. *L. major* promastigotes expressing GFP-ATG8A or GFP-ATG8B were washed and resuspended in PBS before preparing for microscopy on a DeltaVision RT fluorescent microscope. Images show a single slice from a 3 μ m Z-stack. Scale bar = 5 μ m. A. Log phase *L. major* expressing GFP-ATG8A were starved in PBS for 4 h at 25°C, or grown to stationary phase, before visualisation. Graph shows data from a single experiment in which 200 cells were counted. B. Stationary phase *L. major* expressing GFP-ATG8B were visualised. Graph shows mean and standard deviation of data from 3 independent experiments in which at least 200 cells were counted. Data were analysed using a student's t test: n.s. not significant.

4.3 Analysis of an ATG12-like protein

The recent identification of a gene encoding a possible Atg8/Atg12-like protein in the trypanosomatids (D. Rigden, personal communication) prompted us to study this gene in *Leishmania*. It encodes an uncharacterised hypothetical protein that contains a ubiquitin core characteristic of Atg8 and Atg12 proteins, and ends in a C-terminal glycine, but does not possess the large insertion observed in the Atg12 of yeast and humans, and in the previously identified *L. major* ATG12, although this region is also absent from plant Atg12s (Figure 4-11). Correspondingly, this ATG12-like protein (ATG12L) appears more closely related to the Atg12 proteins of plants than *L. major* ATG12 does, but shares less identity with yeast and human Atg12s (Table 4-1). In addition, *L. major* ATG12

Table 4-1 Comparison of sequence identity between *L. major* ATG12s and those of other organisms. Comparison of sequences was performed using CLC Genomics Workbench 4 (CLC Bio). Accession numbers and TriTrypDB designations are as detailed in Figure 4-11.

	ScAtg12	AtAtg12a	AtAtg12b	HsATG12	LmjATG12
LmjATG12	12 %	13 %	14 %	15 %	-
LmjATG12L	9 %	16 %	15 %	10 %	8 %

To further study ATG12L, an episomal construct was generated containing the gene sequence of *L. major* ATG12L (LmjF28.2720) with an N-terminal GFP fusion. GFP-ATG12L was expressed in both WT and $\Delta atg5$ *L. major* parasites in order to determine the protein's localisation and whether this was affected by lack of ATG5. Over an eleven day growth curve GFP-ATG12L labelled punctate structures in a small percentage (0 - 10 %) of the WT population, and the percentage of cells with these puncta increased gradually during stationary phase, peaking at ~ 10 % in late stationary phase (Figure 4-12 A). GFP-ATG12L puncta were also observed in $\Delta atg5$ parasites although occurred at a lower level than in WT, but also peaked towards late stationary phase (Figure 4-12 A). As previously published, the $\Delta atg5$ mutants displayed a growth defect (Williams et al., 2012b), hence the differences in parasite numbers throughout the experiment. Analysis of GFP-ATG12L puncta formation in WT parasites showed that puncta were present in 12 % cells in stationary phase and 5 % starved parasites (Figure 4-12 B). Occurrence of GFP-ATG12L puncta appeared to be lower in $\Delta atg5$ parasites, although this was not statistically significant. The average number of puncta per puncta-containing cell was comparable in WT and $\Delta atg5$ cells, both in stationary phase and after starvation (Figure 4-12 B). GFP-ATG12L usually labelled single puncta that were close to the anterior pole of the cell, but single puncta were also observed throughout the cell body and appeared not to show a distinct localisation. It was also common to see cells with 2 or 3 GFP-ATG12L and occasionally cells containing up to 10 GFP-ATG12L puncta were observed (Figure 4-12 C); these patterns of localisation occurred similarly in both WT and $\Delta atg5$ *Leishmania*. These data suggest that, similarly to ATG8-like proteins, GFP-ATG12L localises to punctate structures suggesting that it may carry out similar or related functions to these proteins.

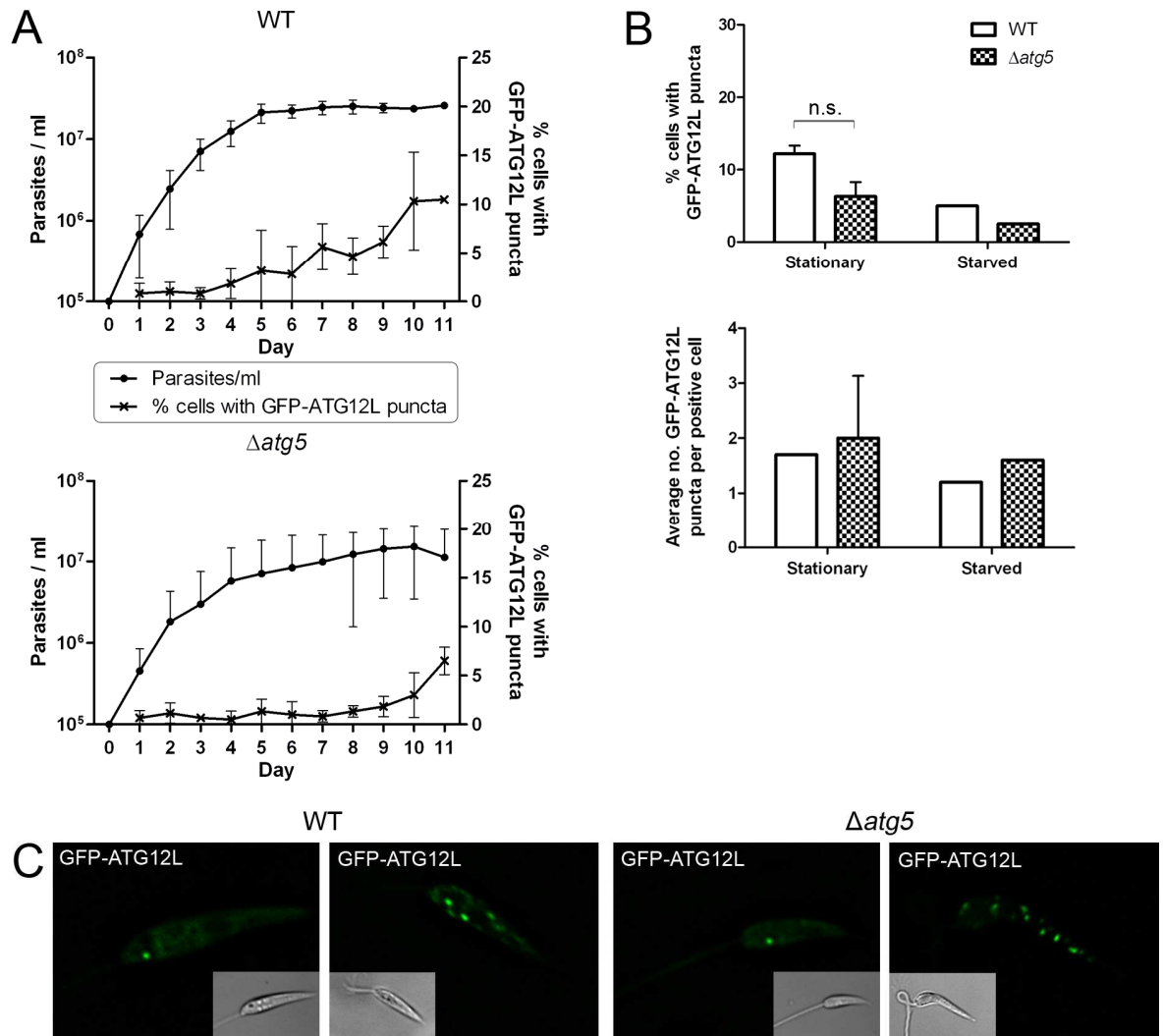


Figure 4-12 Occurrence of GFP-ATG12L puncta formation in WT and $\Delta atg5$ parasites. *L. major* WT and $\Delta atg5$ parasites expressing GFP-ATG12L were washed and resuspended in PBS for live cell microscopy on DeltaVision Core fluorescent microscope. A. Parasite density and the percentage of cells containing puncta were counted each day for 11 days. Growth curves and puncta counts were replicated three times. B. The percentage of cells with GFP-ATG12L puncta and the average number of puncta per positive cell were determined from at least 200 cells in each experiment. Stationary phase data are the mean of 2 independent experiments, whereas starved data are from a single experiment counting cells that were starved in PBS for 4 h at 25°C. Data were compared by a student's t test; n.s. not significant. C. Localisation of GFP-ATG12L to single (1st and 3rd panels) or multiple (2nd and 4th panels) puncta in WT and $\Delta atg5$ cells. Images show a single slice from a 2 μ m Z-stack. DIC images are inset.

As ATG12L shows sequence similarity to Atg12s, and the localisation of GFP-ATG12L appeared to be affected slightly by lack of ATG5, I looked at whether GFP-ATG12L showed any co-localisation with mCherry-ATG5, which labels early autophagosomes. In stationary phase *L. major* a small percentage of GFP-ATG12L co-localised with mCherry-ATG5 puncta (~ 3 %) and a similar proportion of mCherry-ATG5 co-localised with GFP-ATG12L puncta (Figure 4-13; Table 4-2). This shows that ATG5 and ATG12L localise to some of the same puncta, although

the majority of GFP-ATG12L puncta are not labelled with ATG5, and as ATG5 is not required for the formation of GFP-ATG12L puncta (Figure 4-12), this suggests that ATG12L is not a canonical ATG12. In contrast, the ATG12 homologue of *L. major*, encoded by the LmjF22.1300 gene, has been shown to co-localise with all ATG5 puncta during starvation (Williams et al., 2012b), showing that these proteins form the ATG12-ATG5 complex that localises to early autophagosomes. In addition, both ATG12 and ATG5 are observed on ATG8-labelled puncta and processed ATG12 can complement a yeast $\Delta atg12$ mutant (Williams et al., 2009; Williams et al., 2012b), although ATG12L's ability to complement *Atg12*-deficient yeast has not been evaluated. Therefore ATG12L does seem to have some involvement in autophagy although only localises rarely to ATG5-labelled puncta. This might suggest that ATG12L's function is more akin to the ATG8-like proteins' than to ATG12's. It would be interesting to determine whether ATG12L also localises to structures labelled by ATG8, ATG8A, ATG8B and ATG8C, although their different distributions suggest that their puncta would not co-localise completely.

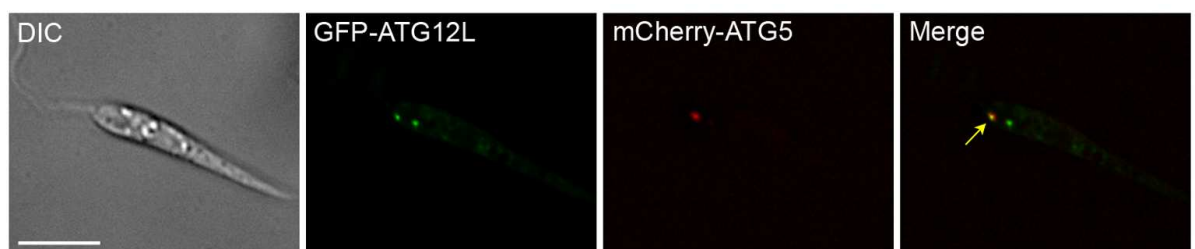


Figure 4-13 Co-localisation of GFP-ATG12L with mCherry-ATG5 on punctate structures. Stationary phase *L. major* promastigotes co-expressing GFP-ATG12L and mCherry-ATG5 were washed and resuspended in PBS then prepared for live cell microscopy on a DeltaVision Core fluorescent microscope. Images show a single slice from a 2 μ m Z-stack. Scale bar = 5 μ m. Arrow shows co-localisation.

Table 4-2 Analysis of GFP-ATG12L and mCherry-ATG5 co-localisation on puncta.

No. cells with puncta counted	No. GFP-ATG12L puncta counted	% co-localised with mCherry-ATG5	No. mCherry-ATG5 puncta counted	% co-localised with GFP-ATG12L
72	104	2.9 %	83	3.6 %

4.4 Discussion

Leishmania appear unique in that they possess additional families of ATG8-like proteins. The ATG8 families belong to four classes, but the gene number within each class is dependent on the *Leishmania* species; this could be related to differences in expression levels between species. These ATG8-like proteins have been characterised to some extent in *L. major* (Williams et al., 2009), but their exact roles and whether they are involved in the autophagic pathway have not been clarified. Although displaying similarity and some apparent functional conservation to yeast Atg8, the ATG8-like proteins of *Leishmania* do not appear to function in canonical autophagy. In this study, the localisation and mechanisms of ATG8-like puncta formation have been further investigated. It is unknown whether the ATG8-like genes of *L. major* are essential: my early attempts to knock out the ATG8A/B gene array by homologous gene replacement were unsuccessful, although the difficulties encountered may be due to the repetitive nature of the gene array rather than the essentiality of these gene copies. The next approach was to produce dominant negative mutant ATG8-like proteins with their putative ATG4 cleavage site glycine mutated to an alanine to prevent correct processing, thought to be required for their function. Although unable to exert dominant negative effects, these mutants have provided some useful information about ATG8 and ATG8A. The GFP-ATG8^{G120A} mutant has confirmed that this glycine residue is the site of C-terminus processing by Atg4 and that this processing is required for the localisation of ATG8 to autophagosomes, as in yeast (Kirisako et al., 2000), mammals (Kabeya et al., 2000) and *T. cruzi* (Alvarez et al., 2008). The GFP-ATG8^{G120A} can also be used as a useful negative control for future experiments in order to discount GFP puncta that are formed by aggregation of GFP-labelled protein, rather than by localisation of GFP-ATG8 to autophagosomes (Kuma et al., 2007).

The G109A mutation of GFP-ATG8A did not appear to affect the localisation of this protein to punctate structures induced by starvation, although differences were observed in its processing by Western blotting. This suggests that C-terminal processing by ATG4.2 is not required for localisation to ATG8A-containing vesicles but may affect the protein's function, as the defectively processed GFP-ATG8^{G109A} appeared to be degraded in the lysosome. However, an *in vitro* cleavage assay showed that His-ATG8A^{G109A}-HA was cleaved by ATG4.2,

suggesting that ATG8A may be cleaved at a different residue; notably, there are multiple glycine residues in its C-terminal tail that could be targeted by ATG4.2. In addition, the concentrations of ATG4.2 used *in vitro* probably do not represent those present within the cell. The processing of ATG8A may be important for conjugation to a target protein, rather than for attachment to membrane lipids. In support of this, ATG8A does not appear to be lipidated by PE as occurs with ATG8. GFP-ATG8 can be observed on a urea gel as two bands, corresponding to unlipidated and lipidated forms; treatment with phospholipase D (PLD) results in deconjugation of ATG8 from PE and disappearance of the lower band. However, PLD treatment is unable to remove the multiple bands containing GFP-ATG8A (Woods, PhD thesis 2009). As a ubiquitin-like protein (Ubl) with similarity to GABARAP and GATE-16, it is entirely possible that ATG8A is involved in similar intracellular trafficking processes and that it may be important for the packaging of certain cargoes into vesicles in response to specific stimuli. The localisation of GFP-ATG8A to puncta in response to starvation has been well-documented (Williams et al. 2009; Woods, PhD thesis 2009), first occurring at puncta in proximity to the flagellar pocket and then at multiple puncta throughout the cell body after prolonged starvation. GFP-ATG8A puncta have also been observed to form in response to other metabolic stresses, i.e. anaerobic culture and treatment with cyanide, suggesting that ATG8A is important for stress responses. However, the ATG8A response must occur independently from stress-induced autophagy, as formation of GFP-ATG8A puncta is not inhibited by wortmannin (Woods, PhD thesis 2009), nor does it require the ATG12-ATG5 conjugation system, as shown by formation of GFP-ATG8A puncta in $\Delta atg5$ mutants. In contrast, both wortmannin treatment and loss of ATG5 prevent the formation of starvation-induced GFP-ATG8-labelled autophagosomes (Besteiro et al., 2006a; Williams et al., 2012b). Further study of the localisation of GFP-ATG8A puncta revealed that these structures initially form at either side of the flagellar pocket at the extreme anterior end of the promastigote cell (Figure 4-14). What then, is the function of ATG8A? Perhaps, in response to stress, ATG8A is responsible for the concentration of certain cargoes within vesicular structures at the flagellar pocket; these might be stress-response proteins or cargoes that can be recycled in order to produce energy for the cell. These cargoes may have been obtained from the environment through endocytosis, or may be proteins that are usually secreted into the environment

under favourable conditions, hence their proximity to the flagellar pocket. Cargo-loaded ATG8A vesicles, in response to prolonged stress, are distributed throughout the cell body so that cargo is delivered to all parts of the promastigote. This hypothesis explains the time-dependent occurrence of ATG8A puncta, but as yet there is no experimental evidence to support these ideas. It would be useful to identify ATG8A-interacting proteins by co-immunoprecipitation assays; these may represent cargoes or additional components of ATG8A structures. Determining whether ATG8A puncta are routed to the lysosome is another important question, and will reveal whether ATG8A is involved in labelling or packaging cargo for degradation or some other purpose within the lysosome. From my observations to date, GFP-ATG8A does not appear to label the lysosome; however, no experiments have been performed specifically to examine this. The physiological role of ATG8A has been suggested to be exerted during development of *Leishmania* promastigotes in the sandfly vector (Woods, PhD thesis 2009). Following their differentiation to infective metacyclic promastigotes, *Leishmania* await transmission to the host in the sandfly mouthparts, a nutrient-poor area of the insect vector. Thus, ATG8A may be important for surviving nutrient deprivation prior to the sandfly taking a bloodmeal and ejecting promastigotes into the mammalian bloodstream, therefore implicating an important function for ATG8A in transmission. This hypothesis is supported by the observation that ATG8A is highly expressed in metacyclic promastigotes (Woods, PhD thesis 2009).

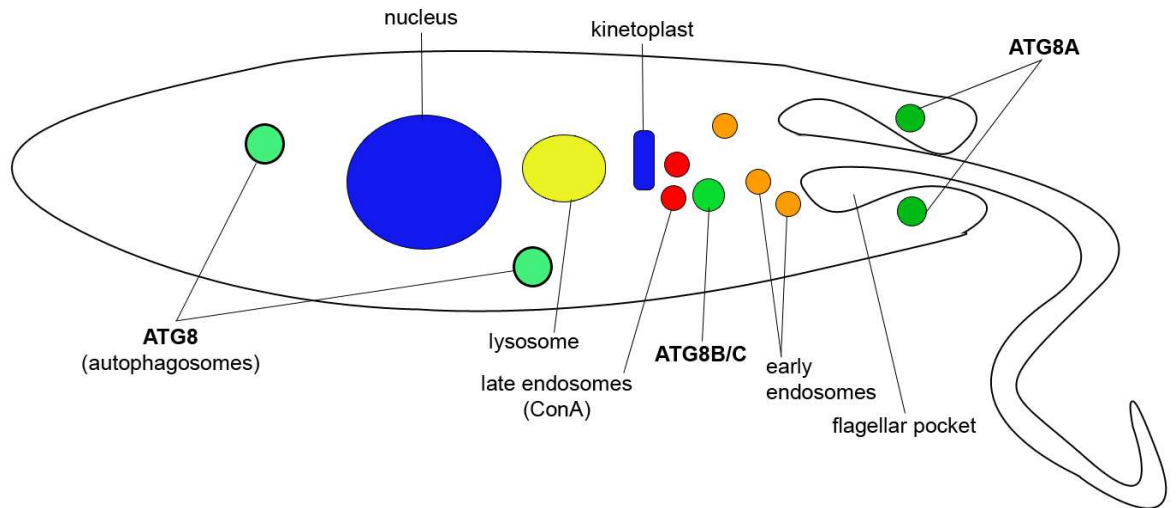


Figure 4-14 Localisation of ATG8-like punctate structures in *L. major* promastigotes. Schematic showing the localisation of punctate structures labelled by *L. major* ATG8-like proteins in relation to components of the endosomal system in promastigotes.

Similarly to ATG8A, formation of GFP-ATG8B and GFP-ATG8C puncta was not affected by the loss of ATG5, suggesting that these puncta are not formed through the action of the canonical autophagic machinery. So far there is little evidence for ATG8B or ATG8C being involved in autophagy, even though they are able to complement the autophagy defect in $\Delta atg8$ yeast (Williams et al., 2009); their ubiquitin-like structure may be sufficient for this complementation. Their localisation to puncta appears to be independent of stimuli that usually induce formation of ATG8-labelled autophagosomes (Williams et al., 2009), and in this regard they are similar to human LC3C which labels puncta that appear unrelated to canonical autophagosomes (Bai et al., 2012). The appearance of GFP-ATG8B or GFP-ATG8C on a single punctum in the same location, and the occurrence of these puncta in a similar proportion of cells under identical conditions, strongly suggests that ATG8B and ATG8C are present on the same structure. Indeed, RFP-ATG8B and GFP-ATG8C were observed labelling the same structure (Woods, PhD thesis 2009). Therefore, here I have assumed that ATG8B and ATG8C label the same compartment. The positioning of ATG8B/C puncta at a defined location close to the anterior end of the cell (Figure 4-14) is very interesting, and this single punctum (when labelled with GFP-ATG8B) was always close to, but never overlapped with, conA-labelled late endosomes or components of the endosomal system labelled with FM4-64. This suggests that ATG8B/C may localise to a novel vesicular compartment, although further

labelling experiments (e.g. with Rab11) are required to confirm that ATG8B/C do not associate with any endosomal compartments. It is possible that the Ubls ATG8B and ATG8C play roles in modification of cargo, which aids internalisation or intracellular trafficking. The defined localisation of ATG8B/C puncta suggests that these structures could be sorting stations for the organisation or modification of protein cargo prior to their trafficking to other compartments or packaging into vesicles for secretion. The localisation of ATG8B/C puncta close to the flagellar pocket supports a hypothesis for these proteins playing roles in secretion or endocytosis. Interestingly, the ATG8-like proteins are highly expressed in the infective metacyclic promastigote stages (Woods, PhD thesis 2009), giving rise to the idea that they may be involved in secretion of virulence factors, or other processes during infection. However, no evidence of altered ATG8B/C localisation was obtained in $\Delta isp1/2/3$ mutants, which display abnormally increased secretion of exosome-like vesicles, although this does not rule out the involvement of ATG8B/C in exosome secretion. Again, it would be informative to carry out co-immunoprecipitation experiments in order to identify proteins that interact with ATG8B and ATG8C, which would help to elucidate their functions. Previous pull-down experiments with *L. major* ATG8B, although inconsistent, identified a number of SNAREs and ubiquitin-like proteins as interacting partners (Woods, PhD thesis 2009). Interestingly, the mammalian Atg8 homologues GABARAP and GATE-16 are also known to interact with SNARE proteins (Sagiv et al., 2000; Kittler et al., 2001). As SNAREs are required for membrane fusion events, this may suggest a role for ATG8B and ATG8C in formation of vesicular structures that may have functions in endocytic or secretory pathways. FM4-64, a marker known to be endocytosed by *Leishmania*, is not observed associating with ATG8B/C puncta, implying that ATG8B/C structures are not involved in regular endocytic processes. It would be interesting to examine fluorescently labelled proteins that are known to be secreted in *Leishmania* vesicles and determine whether these localise to ATG8B/C-labelled puncta. Many proteins have been reported to be contained within *Leishmania* exosomes (Silverman et al., 2010a), and these might transit through ATG8B/C structures *en route* to packaging in exosomes. However, none of the proteins identified in the proteome of exosomes have yet been described as a definitive marker for these vesicles.

Both yeast and mammalian autophagy proteins have been reported to have roles in unconventional secretion pathways (Duran et al., 2010; Manjithaya et al., 2010; Dupont et al., 2011). In this situation, autophagosomes, instead of fusing with the lysosome, are directed to the plasma membrane where the contents of the autophagosome are released. This process relies on Golgi reassembly stacking protein (GRASP). *Leishmania* possess genes encoding putative GRASP homologues, so it would be possible to investigate whether ATG8-labelled vesicles show any interactions with fluorescently labelled GRASP, which may reveal whether this unconventional secretion pathway is conserved in *Leishmania*. A study on HASPB, an unconventionally secreted protein of *Leishmania*, did not find any evidence that autophagy was involved in its trafficking to the plasma membrane; rather, RFP-ATG8 puncta co-localised with a mutant HASPB that is not trafficked correctly, suggesting that autophagy was clearing accumulated defective protein (MacLean et al., 2012). Further studies will be required in order to elucidate whether autophagy or the ATG8-like families are involved in the unconventional secretion of HASPB or other proteins. It is unlikely that ATG8B or ATG8C are involved in a GRASP-dependent unconventional secretory pathway, as previous localisation studies have shown no association of ATG8B with the Golgi apparatus (Woods, PhD thesis 2009).

Although members of each *L. major* ATG8-like family functionally replace yeast Atg8 in $\Delta atg8$ autophagy-deficient mutants, it is unknown whether members of the ATG8A, ATG8B and ATG8C subfamilies show any functional redundancy with *L. major* ATG8. To address this question, I have attempted to generate ATG8 KO parasites, which could be transfected with GFP-labelled ATG8A, ATG8B or ATG8C to determine whether these proteins might be able to mediate autophagosome formation if the primary ATG8 is absent. *L. major* ATG8^{+/-} heterozygotes were generated, but as yet I have been unable to produce parasites lacking both alleles. This might suggest that the ATG8 gene is essential, signifying that the function of the ATG8-like families differs significantly from ATG8 such that they are unable to perform similar roles in autophagosome formation. Experimental data so far certainly suggest that their roles differ from those of ATG8 in autophagy.

The ATG12L protein of *L. major* forms punctate structures, suggesting that it localises to vesicles. GFP-ATG12L puncta formation appeared to be reduced

slightly in $\Delta atg5$ parasites compared to WT, and, in addition, GFP-ATG12L and mCherry-ATG5 co-localised on a small percentage of puncta. These results suggest that ATG12L is somehow connected to early autophagosomes, although ATG5 is not required for formation of ATG12L puncta. ATG12L may be a component involved in general vesicle formation, or in packaging cargo into vesicles, as it appears in multiple puncta throughout the cell that appear to have no distinct localisation. Therefore, it would be interesting to determine whether ATG12L co-localises with the different ATG8-like proteins, and whether it co-localises with ATG8 on autophagosomes. In most cells GFP-ATG12L formed 1 or 2 puncta, resembling the distribution of ATG8 autophagosomes, although occasionally GFP-ATG12L could be seen labelling up to 10 puncta per cell, something that was not seen with GFP-ATG8 in promastigotes. GFP-ATG12L puncta formed in a very low proportion of parasites, and were only slightly increased upon starvation or in late stationary phase cells. Therefore it would seem that ATG12L might localise to a small proportion of autophagosomes under these conditions, in addition to labelling an autophagy-independent population of vesicles with unknown function. Further experiments are required to identify the structures labelled by ATG12L. It is possible that some ATG12L interacts with other ATG proteins, as there is evidence that ATG12 interacts with ATG3 in mammalian cells and that this interaction plays autophagy-independent roles in mitochondrial homeostasis (Radoshevich et al., 2010). Interestingly, the gene encoding ATG12L is conserved in trypanosomatids, suggesting that this protein may have novel functions amongst this group of organisms. In contrast to ATG12L, *L. major* ATG12 localises exclusively to puncta labelled with ATG5 and to some puncta labelled with ATG8 (Williams et al., 2012b), supportive of this protein mediating autophagosome formation and being the functional homologue of yeast Atg12. One fascinating aspect of *L. major* ATG12 is the amino acid extension following its C-terminal glycine, and the finding that cleavage at this site is required for ATG12 function (Williams et al., 2009). The peptidase involved is unknown, although it is apparently neither of *L. major*'s ATG4s (Williams et al., 2009). Hopefully, future studies will identify the peptidase required for this processing event and bring to light the reason for the existence of this mechanism of ATG12 regulation in *Leishmania*, which is absent from other eukaryotic ATG12s.

Table 4-3 Summary of current knowledge on *Leishmania major* ATG8-like proteins.

Protein	Localisation	Processing	Conjugation	Function
ATG8	Autophagosomes throughout cell. Induced by starvation & differentiation. Formation requires ATG5. Inhibited by wortmannin. Trafficked to lysosome.	ATG4.1; ATG4.2 involved in deconjugation from PE	PE	Autophagy (important for cellular homeostasis, surviving nutrient starvation & cellular remodelling during differentiation)
ATG8A	Localised to 2 – 3 puncta at either side of the flagellar pocket upon 2 h starvation. Prolonged starvation results in formation of multiple puncta throughout cell. Formation does not require ATG5. Not inhibited by wortmannin. ATG8A puncta do not appear to be targeted to lysosome, but may be possible.	ATG4.2	Unknown Not PE	Roles in stress response?
ATG8B	Single punctum at anterior end of cell close to late endosomes in 0 – 10 % promastigotes. Formation does not require ATG5. Puncta appear static.	ATG4.1	Unknown Not PE	Unknown. Possibly involved in vesicular sorting pathways?
ATG8C	Similar localisation to ATG8B. Co-localisation with ATG8B suggests that they localise to same structure.	ATG4.1	Unknown	Unknown. Possibly involved in vesicular sorting pathways?
ATG12	Localises to puncta labelled with ATG8 and ATG5. Thought to dissociate from autophagosomes prior to their fusion with the lysosome.	Unknown	ATG5	Autophagy
ATG12L	Localises to puncta in a low number of cells. Puncta formation increased slightly by starvation or in late stationary phase. 3% puncta co-localise with ATG5 puncta. Usually labels 1 – 3 puncta but can label up to 10 per cell. No evidence of trafficking to lysosome.	Not thought to require processing as ends with C-terminal glycine.	Unknown, but may interact with ATG5 during autophagy	Some activity in autophagosome formation? Other unknown roles

5 General Discussion

The core molecular machinery required for autophagosome formation in yeast is conserved in *Leishmania*, and autophagy has been experimentally observed in both *L. major* and *L. mexicana* (Williams et al., 2006; Besteiro et al., 2006a). An outstanding feature of the *ATG* genes in *Leishmania* is the expansion of the ATG8 family into four classes; ATG8, ATG8A, ATG8B and ATG8C. ATG8 appears to be the functional homologue of *S. cerevisiae* Atg8, which functions in autophagosome expansion, and has been shown to label autophagosomes in *Leishmania*, whereas the functions of the other ATG8-like proteins are unknown. Despite their designation as ATG8-like, it is unclear whether they play roles in autophagy.

A functioning autophagy pathway is essential for the successful transformation of *Leishmania* parasites between their various developmental forms, during which increased protein turnover occurs as the cell is remodelled to adjust its structure and metabolism for survival within the next life cycle environment. Utilising fluorescently-tagged ATG8 to follow autophagosomes, this project has begun to identify organelles that are targeted by autophagy during both metacyclogenesis and promastigote - amastigote differentiation within macrophages. Glycosomes were suspected to be degraded by autophagy during differentiation, as the composition of glycosomal metabolic enzymes is known to differ between insect and mammalian stages of both *Leishmania* (Rosenzweig et al., 2008b; Brotherton et al., 2010) and trypanosomes (Herman et al., 2008), and this pathway represents a mechanism by which glycosomes can be quickly turned over whilst a population of new organelles containing enzymes required for survival in the next environment is synthesised. Indeed, there is some evidence of this occurring in trypanosomes (Herman et al., 2008), and pexophagy is a well-described phenomenon in methylophilic yeasts, which occurs in response to changing environmental carbon sources (Dunn et al., 2005). In *L. major* autophagosomes were observed to co-localise with glycosomes, as defined by a Pearson's correlation coefficient value of ≥ 0.5 . During log phase growth ~ 19 % of autophagosomes co-localised with glycosomes, but during differentiation, when autophagy is up-regulated, the greater numbers of autophagosomes resulted in increased glycosome turnover although the

percentage of autophagosome - glycosome co-localisation remained at a similar level. This indicates that increased glycosome turnover results from an overall increase in autophagy, rather than increased selection of glycosomes as cargo. Autophagosomes co-localising with glycosomes were significantly larger on average than non-co-localised autophagosomes, suggesting that sequestration of glycosomes requires expansion of the autophagic vesicle around its cargo. Occasionally, GFP-ATG8 labelled cup-shaped structures reminiscent of developing autophagosomes, which appeared to form around single glycosomes in a process resembling macropexophagy seen in methylotrophic yeasts (Dunn et al., 2005). In addition, both GFP-ATG8 and RFP-SQL accumulated in structures that are likely to be lysosomes due to their labelling with the lysosomal markers proCPB-RFP and FM4-64, supporting the idea that glycosomes are trafficked to the lysosome by macroautophagy (Figure 5-1). The importance of autophagy for the regulation of the glycosome population was corroborated by the finding that following differentiation glycosome numbers were significantly higher in macroautophagy-deficient $\Delta atg5$ mutants compared to WT parasites, and fewer $\Delta atg5$ cells contained RFP-SQL within putative lysosomal structures. These data are consistent with the hypothesis that autophagy is involved in the turnover of glycosomes during parasite differentiation, and that this process is important for adapting the metabolism of *Leishmania* to nutritional conditions encountered in its next life cycle environment. It would be beneficial to apply biochemical or proteomic methods, such as SILAC (stable isotope labelling by amino acids in cell culture) followed by high resolution mass spectrometry (Chawla et al., 2011), to compare changes in glycosomal content during promastigote - amastigote differentiation in WT and $\Delta atg5$ parasites. If macroautophagy is important for glycosome turnover, one might expect differences in glycosomal enzymes between the two cell lines following differentiation. Autophagy is also induced by starvation, during which it facilitates survival through the degradation of non-essential cellular components, which provide a ready source of nutrients. During starvation autophagosome - glycosome co-localisation was also increased, with an increased appearance of both GFP-ATG8 and RFP-SQL within lysosomal structures, which suggests that glycosomes are targeted by autophagy and recycled as an easily accessible nutrient source. Presumably, degradation of glycosomes in this manner does not negatively affect cell survival, as in the

absence of nutrients their metabolic functions are not required and so cells can afford to reduce glycosome numbers.

This project has led to the first comparison of glycosome numbers within the different life cycle stages of *L. major*. A previous study using electron microscopy on *L. mexicana* determined there to be ~ 10 glycosomes per amastigote (Coombs et al., 1986), and other work estimates that *L. amazonensis* promastigotes contain 50 - 100 glycosomes, although there were no experimental data presented to confirm this (Oppendoes, 1987). In line with the first of these studies, determination of glycosome numbers in *L. major* showed that amastigotes contain an average of 11 glycosomes per cell. However, in *L. major* promastigotes there were approximately 20 glycosomes per cell, fewer than previous estimates. This could mean that the PTS1-type targeting signal used in this study is unable to label all glycosomes and that another population of glycosomes exist that import proteins with alternative recognition motifs. There may also be differences in glycosome numbers between *Leishmania* species, but as no experimental data are available on glycosome numbers in promastigotes of other *Leishmania* species, it is difficult to compare. However, data from *L. mexicana* expressing RFP-SQL also suggest that the majority of promastigotes contain ~ 20 labelled glycosomes per cell (R. Williams, unpublished data).

Glycosome turnover by autophagy appears to be a selective process, as autophagosomes were not observed to co-localise with the other organelles studied in this project during log phase growth, metacyclogenesis or under starvation conditions. Markers of the acidocalcisomes or flagellum did not appear within RFP-ATG8-labelled autophagosomes, suggesting that under the conditions tested these organelles are not cargo for autophagy, although other markers could be used to confirm these observations. It would be interesting to determine whether autophagy is involved in the turnover of acidocalcisomes or the flagellum during the other differentiation events of the *Leishmania* life cycle, as these were not studied in this project, and acidocalcisome numbers decrease during amastigote - promastigote differentiation whereas the flagellum shortens dramatically during promastigote - amastigote differentiation. The mitochondrion does not appear to be degraded by autophagy under normal growth conditions, but fragmentation of this organelle by H₂O₂ treatment

resulted in a small number of mitochondrial fragments co-localising with RFP-ATG8-labelled structures. Interestingly, these compartments appeared to be lysosomal, suggesting that mitophagy may occur by a microautophagic mechanism in response to extreme stress conditions. However, H₂O₂ treatment appeared to disrupt normal endocytic function, suggesting that vesicle-trafficking pathways, including autophagy, are affected by H₂O₂, making it difficult to study whether autophagy is actually involved in mitochondrial turnover. It is also questionable whether H₂O₂ treatment represents a natural situation in which the mitochondrion would fragment. As mitochondrial fragmentation appears to be important for mitophagy to function in yeast and mammals (Nowikovsky et al., 2007; Twig et al., 2008), it will be important to identify situations in which fragmentation of the *Leishmania* mitochondrion occurs in order to examine whether mitophagy functions in this parasite. As with the other organelles studied here, it would be informative to test whether autophagy mediates mitochondrial turnover during promastigote - amastigote differentiation, which results in a reduction in mitochondrial size.

The ER has been observed within autophagosomes in other organisms (Hamasaki et al., 2005; Bernales et al., 2006; Ogata et al., 2006) and also appears to be an important source of autophagic membranes in mammalian cells (Hayashi-Nishino et al., 2009; Yla-Anttila et al., 2009). As the ER was not investigated in this project, future studies should examine whether the ER of *Leishmania* is targeted by autophagy and/or acts as a site of autophagosome formation (Figure 5-1). The Golgi appears to contribute membrane to autophagosomes in yeast (Yamamoto et al., 2012), so this organelle could also be involved in this process in *Leishmania*. Whereas in yeast membrane is delivered to the PAS for autophagosome biogenesis, in mammalian cells autophagosomes appear to form directly from (or close to) membrane sources, including the ER (Axe et al., 2008), mitochondria (Hailey et al., 2010) and the plasma membrane (Ravikumar et al., 2010). An interesting finding from this project is that over half of all ATG8-labelled autophagosomes appeared in close association with the reticulate mitochondrion, suggesting that autophagic vesicles may be formed from mitochondrial membrane (Figure 5-1). This is supported by recent data showing that *Leishmania* mutants unable to form autophagosomes show mitochondrial swelling and fragmentation, coupled with abnormal mitochondrial lipid profiles

exhibiting high levels of PE (Williams et al., 2012b). As PE is an important component of autophagosomal membranes, this may suggest that in the absence of autophagosome formation PE is not transferred from the mitochondrion to autophagosomes, resulting in a lipid imbalance that disrupts mitochondrial function. The *Leishmania* mitochondrion is a large organelle that extends the length of the cell and this makes it a suitable membrane source, both because of the quantity of lipids contained within its membranes, and because it allows autophagosomes to form at many locations throughout the cell. These are also true of the ER, which suggests that this organelle could also be an important membrane source for autophagosome formation in *Leishmania*.

In organisms in which selective autophagy has been well studied, specific proteins have been identified that are required for the recruitment of the autophagic machinery to specific organelles. For example, in *S. cerevisiae* these include Atg36 for pexophagy and Atg32 for mitophagy, and in mammals, p62 for the selective degradation of ubiquitinated protein aggregates (and possibly organelles). Interestingly, proteins with domain organisation similar to that of p62 were identified in five protists; *Dictyostelium discoideum*, *Monosiga brevicollis*, *Thalassiosira pseudonana*, *Phytophthora* spp. and *Naegleria gruberi* (Duszenko et al., 2011), suggesting that selective autophagy pathways may be present in these organisms. However, many of the *ATG* genes characterised in *S. cerevisiae* for selective types of autophagy appear to be fungi-specific, which suggests that other organisms may encode divergent proteins that perform similar functions. Therefore, although few homologues of yeast selective autophagy genes have been identified in trypanosomatids, it is possible that these parasites possess different mechanisms to mediate this process. The observations that glycosomes are trafficked to the lysosome in *T. brucei* (Herman et al., 2008), and are found to co-localise with autophagosomes and traffic to the lysosome in *L. major* imply that selective autophagy of glycosomes occurs in these parasites. Future studies will be needed in order to identify any specific cargo adaptor proteins that may be involved in this process. The presence of multiple ubiquitin-like proteins encoded in trypanosomatid genomes (Ponder and Bogyo, 2007) may indicate that these are possible candidates for selective autophagy mechanisms, and ubiquitin is known to be involved in the sorting of proteins into vesicles (Hicke and Dunn, 2003). Proteomic studies

comparing WT and $\Delta atg5$ *L. major* may be able to identify novel proteins that are up-regulated in the absence of autophagic degradation; these may represent proteins involved in selective autophagy which would be expected to be degraded along with their cargo during functional autophagy.

The ATG8-like families ATG8A, ATG8B and ATG8C are encoded by multi-gene arrays, with the number of copies varying between different *Leishmania* species. To date ATG8-like proteins have only been studied in *L. major*, but it is probable that they perform the same roles in the various species. Although they label punctate structures, can complement a yeast $\Delta atg8$ strain, and are cleaved by *Leishmania* ATG4s (Williams et al., 2009), these proteins do not appear to function in canonical autophagy as their localisation is unaffected in $\Delta atg5$ parasites and they do not traffic to the lysosome. In addition, formation of puncta labelled by ATG8A, ATG8B or ATG8C is not induced by differentiation, which is known to cause the most dramatic increases in autophagy in *Leishmania*. As ATG8A responds to starvation and other metabolic stresses (Woods, PhD thesis 2009) it appears to function in stress responses that may be important for parasite survival. However, the roles that ATG8A structures might play in this process are unknown; perhaps they distribute nutrients or stress-response proteins throughout the cell, which may facilitate survival in the face of extreme conditions. The localisation of ATG8A puncta either side of the flagellar pocket (Figure 5-1) and the finding that they do not co-localise with markers known to label endosomal compartments indicates that these structures are probably not involved in endocytosis. ATG8A function could be important for parasite development in the sand fly vector, allowing promastigotes suspended in promastigote secretory gel (Rogers et al., 2002) to tolerate the nutrient-poor environment within the thoracic midgut (Bates, 2007). The increased expression of ATG8A by metacyclic promastigotes supports a role in transmission, which may indeed be related to survival in the vector.

ATG8B and ATG8C are expected to localise to the same structure (Figure 5-1), which appears in only a small proportion of promastigotes at any time, and in even fewer amastigotes (Woods, PhD thesis 2009). This suggests that ATG8B/C do not play essential roles in promastigotes or amastigotes, although they may be important for processes that occur within the sand fly vector, a stage that we are unable to study in our lab. Their localisation to a defined structure suggests

that ATG8B/C could belong to a sorting station and be involved in the packaging of various cargoes into vesicles that go on to enter the endosomal system for secretion or distribution. ATG8B has been found to co-immunoprecipitate with various SNAREs (Woods, PhD thesis 2009), supporting a role for this protein in membrane fusion events and cargo packaging.

Clearly, further investigations are required in order to elucidate the functions of the novel ATG8-like proteins of *Leishmania*. However, attempts to knock out the genes encoding ATG8A and ATG8B have been hampered by the fact that they are present on multi-gene arrays, although knockout of such arrays has been achieved in the past (Mottram et al., 1996). Considering the repetitive nature of these gene arrays (Rogers et al., 2011), the ATG8-like families represent feasible targets for RNAi knockdown if an inducible system is successfully developed in *L. braziliensis*, a species that appears to possess components of a functional RNAi system (Peacock et al., 2007). As the ATG8-like proteins are expected to function similarly in all *Leishmania* species, RNAi would be hugely beneficial for the study of these proteins. Co-immunoprecipitation experiments would also be useful in the clarification of ATG8-like protein functions; identification of interaction partners with known functions could provide information on processes that ATG8A, ATG8B or ATG8C are involved in.

The ATG8-like proteins are processed by ATG4.1 or ATG4.2, but whereas the cleavage of ATG8 allows it to be lipidated by PE in autophagosomal membranes, the significance of the cleavage of ATG8A, ATG8B and ATG8C is unknown. Western blot analysis of ATG8A and ATG8B showed that these proteins run as two differently sized bands, but these were not affected by phospholipase D (PLD) treatment, which is known to cleave ATG8 from PE resulting in the appearance of a single protein species rather than the usual two. The multiple bands of ATG8A and ATG8B suggest that they are conjugated to another target, which may be a protein or a lipid that is not cleaved by PLD. The targets of ATG8A or ATG8B modification might be membrane lipids that allow these proteins to become associated with vesicular membranes, or proteins that may be modified for their sorting into ATG8A- or ATG8B-labelled structures.

Unconventional secretion processes mediated by autophagy have recently been reported in yeast and mammalian cells (Duran et al., 2010; Manjithaya et al.,

2010; Dupont et al., 2011), and it is also possible that such a pathway also exists in other eukaryotes, including *Leishmania* (Denny et al., 2000; MacLean et al., 2012). Autophagy-mediated unconventional protein secretion is dependent on autophagosome formation and GRASP. As *Leishmania* possess a GRASP homologue, it will be interesting to examine whether this protein localises to compartments labelled by any of the ATG8 family proteins, which may have roles in this type of unconventional secretion pathway. However, studies of the unconventionally secreted HASPB protein found no involvement of autophagy in its trafficking to the membrane (MacLean et al., 2012), although presumably there are other proteins that could utilise this pathway in *Leishmania*.

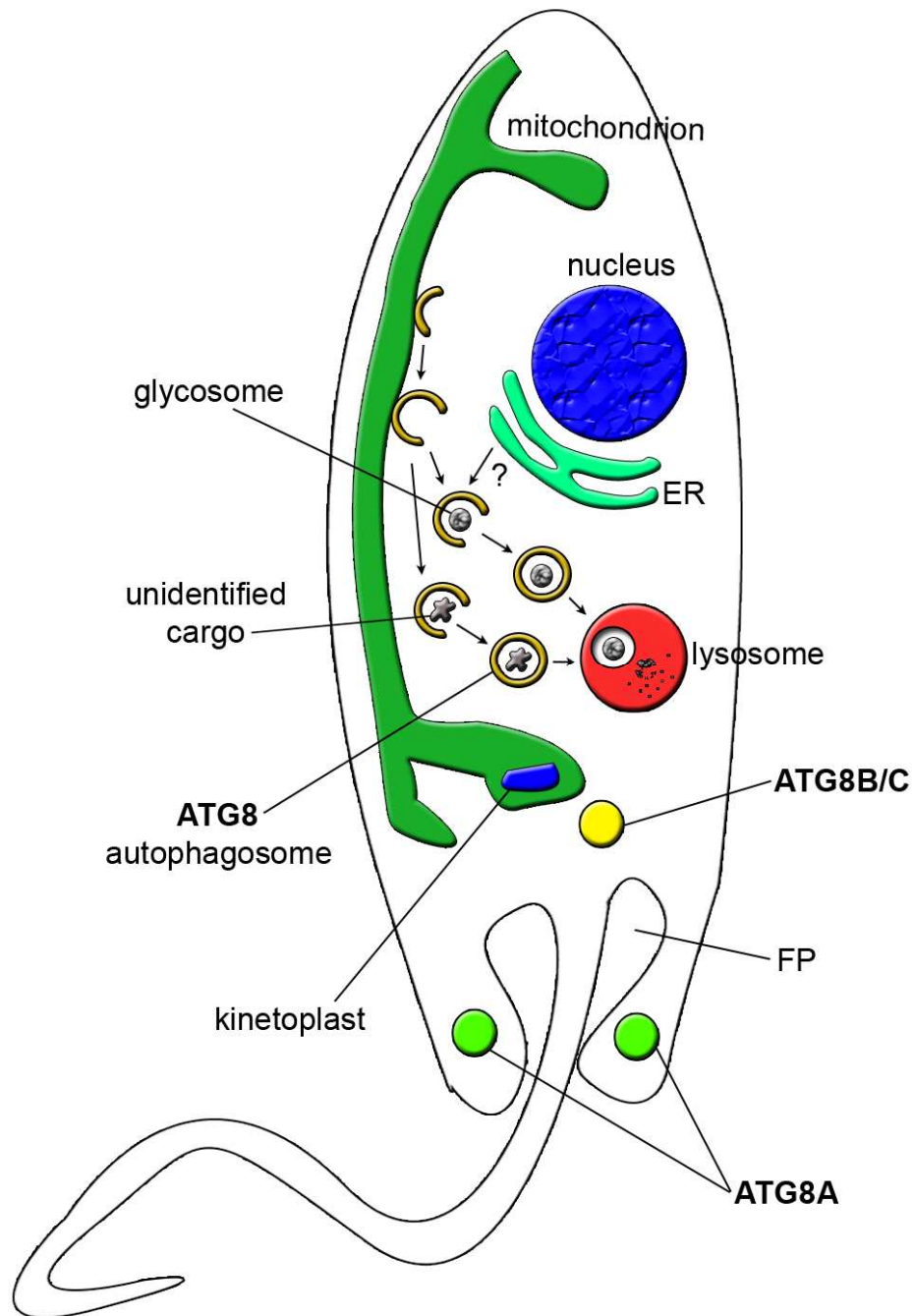


Figure 5-1 Schematic showing the structures labelled by the ATG8 families of *L. major*. ATG8 labels autophagosomes that are involved in the trafficking of glycosomes and other as yet unidentified cargoes to the lysosome. Autophagosomes appear to be generated from the mitochondrion, although the ER could also be an important membrane source. ATG8A initially localises to structures either side of the flagellar pocket, then labels multiple puncta throughout the cell upon prolonged starvation (not shown). ATG8B and ATG8C appear to localise to a distinct structure between the kinetoplast and flagellar pocket. ER: endoplasmic reticulum. FP: flagellar pocket.

Appendix

Table A-1 Raw data from glycosome turnover experiments. These data are summarised in Table 3-5. Columns headed in blue are represented in Figure 3-9.

Life cycle stage	n	% with autos	autos counted	No. coloc with glycs	% autos colocalised with glycs	% cells with glycs coloc
Log	503	2 %	15	7	46.7 %	1.4 %
	1204	2 %	41	13	31.7 %	1.1 %
	505	6 %	56	7	12.5 %	1.4 %
	577	6 %	51	2	3.9 %	0.3 %
	1215	2 %	48	8	16.7 %	0.7 %
	775	2 %	20	3	15.0 %	0.4 %
	605	7 %	63	6	9.5 %	1.0 %
total	5384		294	46		
mean		3.9 %	42	7	19.4 %	0.9 %
std dev		2.3 %			14.8 %	0.4 %
Stationary	97	35 %	60	6	10.0 %	6.2 %
	102	41 %	59	5	8.5 %	4.9 %
	75	43 %	50	13	26.0 %	17.3 %
	100	51 %	107	16	15.0 %	16.0 %
	101	44 %	60	17	28.3 %	16.8 %
	118	36 %	86	7	8.1 %	5.9 %
total	593		422	64		
mean		41.7 %	70	11	16.0 %	11.2 %
std dev		5.9 %			9.0 %	6.1 %
18h amastigotes	197	92.0 %	383	37	9.7 %	18.8 %
	179	88.1 %	375	49	13.1 %	27.4 %
total	376		758	86		
mean		90.1 %	379	43	11.4 %	23.1 %
std dev		2.8 %			2.4 %	6.1 %
Log starved	134	22.4 %	49	9	18.4 %	6.7 %
	71	22.6 %	31	7	22.6 %	9.9 %
	195	16.9 %	66	10	15.2 %	5.1 %
	203	13.3 %	47	8	17.0 %	3.9 %
	136	23.6 %	77	9	11.7 %	6.6 %
	114	14.0 %	25	4	16.0 %	3.5 %
total	853		295	47		
mean		18.8 %	49	8	16.8 %	6.0 %
std dev		4.6 %			3.6 %	2.3 %

Table A-2 Percentage of glycosomes co-localised with autophagosomes in different life cycle stages.

lifecycle stage	no. cells	glycs coloc	total glycs	% glycs colocalised with autos
log	25	5	365	1.4%
	33	2	571	0.4%
	22	7	399	1.8%
	13	3	238	1.3%
	37	6	556	1.1%
total	130	23	2129	
mean	26	4.6	425.8	1.2%
SD	9.43	2.07	139.39	0.01
stationary	38	6	638	0.9%
	23	17	263	6.5%
	19	5	359	1.4%
	26	13	468	2.8%
	55	16	1051	1.5%
total	161	57	2779	
mean	32.2	11.4	555.8	2.6%
SD	14.58	5.59	309.90	0.02
amastigotes	104	37	1200	3.1%
	113	49	1717	2.9%
total	217	86	2917	
mean	108.5	43	1458.5	3.0%
SD	6.36	8.49	365.57	0.00

References

- Aga,E., Katschinski,D.M., van Zandbergen,G., Laufs,H., Hansen,B., Müller,K., Solbach,W., and Laskay,T. (2002). Inhibition of the spontaneous apoptosis of neutrophil granulocytes by the intracellular parasite *Leishmania major*. *J Immunol* **169**, 898-905.
- Alexander,J. and Brombacher,F. (2012). T helper1/T helper2 cells and resistance/susceptibility to *Leishmania* infection: is this paradigm still relevant? *Front Immunol* **3**.
- Alvar,J., Yactayo,S., and Bern,C. (2006). Leishmaniasis and poverty. *Trends Parasitol* **22**, 552-557.
- Alvarez,V.E., Kosec,G., Anna,C.S., Turk,V., Cazzulo,J.J., and Turk,B. (2008). Autophagy is involved in nutritional stress response and differentiation in *Trypanosoma cruzi*. *J Biol Chem* **283**, 3454-3464.
- Ambit,A., Woods,K.L., Cull,B., Coombs,G.H., and Mottram,J.C. (2011). Morphological events during the cell cycle of *Leishmania major*. *Eukaryot Cell* **10**, 1429-1438.
- Ando,R., Hama,H., Yamamoto-Hino,M., Mizuno,H., and Miyawaki,A. (2002). An optical marker based on the UV-induced green-to-red photoconversion of a fluorescent protein. *Proc Natl Acad Sci USA* **99**, 12651-12656.
- Annoura,T., Makiuchi,T., Sariago,I., Aoki,T., and Nara,T. (2012). SUMOylation of paraflagellar rod protein, PFR1, and its stage-specific localization in *Trypanosoma cruzi*. *PLoS One* **7**, e37183.
- Ano,Y., Hattori,T., Kato,N., and Sakai,Y. (2005). Intracellular ATP correlates with mode of pexophagy in *Pichia pastoris*. *Biosci Biotech Biochem* **69**, 1527-1533.
- Antoine,J.C., Lang,T., Prina,E., Courret,N., and Hellio,R. (1999). H-2M molecules, like MHC class II molecules, are targeted to parasitophorous vacuoles of *Leishmania*-infected macrophages and internalized by amastigotes of *L. amazonensis* and *L. mexicana*. *J Cell Sci* **112**, 2559-2570.
- Arias,E. and Cuervo,A.M. (2011). Chaperone-mediated autophagy in protein quality control. *Curr Opin Cell Biol* **23**, 184-189.

- Axe, E.L., Walker, S.A., Manifava, M., Chandra, P., Roderick, H.L., Habermann, A., Griffiths, G., and Ktistakis, N.T. (2008). Autophagosome formation from membrane compartments enriched in phosphatidylinositol 3-phosphate and dynamically connected to the endoplasmic reticulum. *J Cell Biol* **182**, 685-701.
- Bañuls, A.L., Hide, M., and Prugnolle, F. (2007). Leishmania and the leishmaniasis: A parasite genetic update and advances in taxonomy, epidemiology and pathogenicity in humans. *Adv Parasitol* **64**, 1-109.
- Bai, H., Inoue, J., Kawano, T., and Inazawa, J. (2012). A transcriptional variant of the LC3A gene is involved in autophagy and frequently inactivated in human cancers. *Oncogene*, advance online publication 16 Jan 2012.
- Barquilla, A. and Navarro, M. (2009a). Trypanosome TOR as a major regulator of cell growth and autophagy. *Autophagy* **5**, 256-258.
- Barquilla, A. and Navarro, M. (2009b). Trypanosome TOR complex 2 functions in cytokinesis. *Cell Cycle* **8**, 697-699.
- Barquilla, A., Saldivia, M., Diaz, R., Bart, J.M., Vidal, I., Calvo, E., Hall, M.N., and Navarro, M. (2012). Third target of rapamycin complex negatively regulates development of quiescence in *Trypanosoma brucei*. *Proc Natl Acad Sci USA* **109**, 14399-14404.
- Barr, S.C., Warner, K.L., Kornreic, B.G., Piscitelli, J., Wolfe, A., Benet, L., and McKerrow, J.H. (2005). A cysteine protease inhibitor protects dogs from cardiac damage during infection by *Trypanosoma cruzi*. *Antimicrob Agents Chemother* **49**, 5160-5161.
- Bates, P.A. (2007). Transmission of *Leishmania* metacyclic promastigotes by phlebotomine sand flies. *Int J Parasitol* **37**, 1097-1106.
- Bayona, J.C., Nakayasu, E.S., Laverrière, M., Aguilar, C., Sobreira, T.J.P., Choi, H., Nesvizhskii, A.I., Almeida, I.C., Cazzulo, J.J., and Alvarez, V.E. (2011). SUMOylation pathway in *Trypanosoma cruzi*: Functional characterization and proteomic analysis of target proteins. *Mol Cell Proteomics* **10**, M110.007369.
- Bellu, A.R., Komori, M., van der Klei, I.J., Kiel, J.A.K.W., and Veenhuis, M. (2001). Peroxisome biogenesis and selective degradation converge at Pex14p. *J Biol Chem* **276**, 44570-44574.

- Bellu,A.R., Salomons,F.A., Kiel,J.A.K.W., Veenhuis,M., and van der Klei,I.J. (2002). Removal of Pex3p is an important initial stage in selective peroxisome degradation in *Hansenula polymorpha*. *J Biol Chem* **277**, 42875-42880.
- Bernales,S., McDonald,K.L., and Walter,P. (2006). Autophagy counterbalances endoplasmic reticulum expansion during the unfolded protein response. *PLoS Biol* **4**, e423.
- Besteiro,S., Tonn,D., Tetley,L., Coombs,G.H., and Mottram,J.C. (2008). The AP3 adaptor is involved in the transport of membrane proteins to acidocalcisomes of *Leishmania*. *J Cell Sci* **121**, 561-570.
- Besteiro,S., Williams,R.A.M., Coombs,G.H., and Mottram,J.C. (2007). Protein turnover and differentiation in *Leishmania*. *Int J Parasitol* **37**, 1063-1075.
- Besteiro,S., Williams,R.A.M., Morrison,L.S., Coombs,G.H., and Mottram,J.C. (2006a). Endosome sorting and autophagy are essential for differentiation and virulence of *Leishmania major*. *J Biol Chem* **281**, 11384-11396.
- Besteiro,S., Coombs,G., and Mottram,J. (2006b). The SNARE protein family of *Leishmania major*. *BMC Genomics* **7**, 250.
- Betin,V.M.S. and Lane,J.D. (2009). Caspase cleavage of Atg4D stimulates GABARAP-L1 processing and triggers mitochondrial targeting and apoptosis. *J Cell Sci* **122**, 2554-2566.
- Blommaart,E.F.C., Krause,U., Schellens,J.P.M., Vreeling-Sindelárová,H., and Meijer,A.J. (1997). The phosphatidylinositol 3-kinase inhibitors wortmannin and LY294002 inhibit autophagy in isolated rat hepatocytes. *Eur J Biochem* **243**, 240-246.
- Bolte,S. and Cordelières,F.P. (2006). A guided tour into subcellular colocalization analysis in light microscopy. *J Microsc* **224**, 213-232.
- Brennan,A., Gualdrón-López,M., Coppens,I., Rigden,D.J., Ginger,M.L., and Michels,P.A.M. (2011). Autophagy in parasitic protists: Unique features and drug targets. *Mol Biochem Parasitol* **177**, 83-99.
- Brooks,D.R., Denise,H., Westrop,G.D., Coombs,G.H., and Mottram,J.C. (2001). The stage-regulated expression of *Leishmania mexicana* CPB cysteine proteases is mediated by an intercistronic sequence element. *J Biol Chem* **276**, 47061-47069.

- Brotherton, M.C., Racine, G., Foucher, A.L., Drummelsmith, J., Papadopoulou, B., and Ouellette, M. (2010). Analysis of stage-specific expression of basic proteins in *Leishmania infantum*. *J Proteome Res* **9**, 3842-3853.
- Brun, R. and Krassner, S.M. (Brun and Krassner, 1976). Quantitative ultrastructural investigations of mitochondrial development in *Leishmania donovani* during transformation. *J Protozool* **3**, 493-497.
- Bruns, C., McCaffery, J.M., Curwin, A.J., Duran, J.M., and Malhotra, V. (2011). Biogenesis of a novel compartment for autophagosome-mediated unconventional protein secretion. *J Cell Biol* **195**, 979-992.
- Castanys-Muñoz, E., Brown, E., Coombs, G.H., and Mottram, J.C. (2012). *Leishmania mexicana* metacaspase is a negative regulator of amastigote proliferation in mammalian cells. *Cell Death Dis* **3**, e385.
- Chakraborty, B., Biswas, S., Mondal, S., and Bera, T. (2010). Stage specific developmental changes in the mitochondrial and surface membrane associated redox systems of *Leishmania donovani* promastigote and amastigote. *Biochemistry (Mosc)* **75**, 494-504.
- Chan, N.C., Salazar, A.M., Pham, A.H., Sweredoski, M.J., Kolawa, N.J., Graham, R.L.J., Hess, S., and Chan, D.C. (2011). Broad activation of the ubiquitin-proteasome system by Parkin is critical for mitophagy. *Hum Mol Genet* **20**, 1726-1737.
- Chawla, B., Jhingran, A., Panigrahi, A., Stuart, K.D., and Madhubala, R. (2011). Paromomycin affects translation and vesicle-mediated trafficking as revealed by proteomics of paromomycin -susceptible -resistant *Leishmania donovani*. *PLoS One* **6**, e26660.
- Chen, L., Wang, H., Vicini, S., and Olsen, R.W. (2000). The γ -aminobutyric acid type A (GABA_A) receptor-associated protein (GABARAP) promotes GABA_A receptor clustering and modulates the channel kinetics. *Proc Natl Acad Sci USA* **97**, 11557-11562.
- Cherra, S.J., Kulich, S.M., Uechi, G., Balasubramani, M., Mountzouris, J., Day, B.W., and Chu, C.T. (2010). Regulation of the autophagy protein LC3 by phosphorylation. *J Cell Biol* **190**, 533-539.
- Chung, W.L., Leung, K.F., Carrington, M., and Field, M.C. (2008). Ubiquitylation is required for degradation of transmembrane surface proteins in trypanosomes. *Traffic* **9**, 1681-1697.

- Coombs,G.H., Tetley,L., Moss,V.A., and Vickerman,K. (Coombs et al., 1986). Three dimensional structure of the *Leishmania* amastigote as revealed by computer-aided reconstruction from serial sections. *Parasitology* **92**, 13-23.
- Coyle,J.E., Qamar,S., Rajashankar,K.R., and Nikolov,D.B. (2002). Structure of GABARAP in two conformations: Implications for GABA_A receptor localization and tubulin binding. *Neuron* **33**, 63-74.
- Croft,S.L. and Olliaro,P. (2011). Leishmaniasis chemotherapy - challenges and opportunities. *Clin Microbiol Infect* **17**, 1478-1483.
- Crotzer,V.L. and Blum,J.S. (2010). Autophagy and adaptive immunity. *Immunology* **131**, 9-17.
- Dargemont,C. and Ossareh-Nazari,B. (2012). Cdc48/p97, a key actor in the interplay between autophagy and ubiquitin/proteasome catabolic pathways. *Biochim Biophys Acta* **1823**, 138-144.
- de Diego,J.L., Katz,J.M., Marshall,P., Gutiérrez,B., Manning,J.E., Nussenzweig,V., and González,J. (2001). The ubiquitin-proteasome pathway plays an essential role in proteolysis during *Trypanosoma cruzi* remodeling. *Biochemistry* **40**, 1053-1062.
- de Jesus,T.C.L., Tonelli,R.R., Nardelli,S.C., Silva Augusto,L., Motta,M.C., Girard-Dias,W., Miranda,K., Ulrich,P., Jimenez,V., Barquilla,A., Navarro,M., Docampo,R., and Schenkman,S. (2010). Target of rapamycin (TOR)-like 1 kinase is involved in the control of polyphosphate levels and acidocalcisome maintenance in *Trypanosoma brucei*. *J Biol Chem* **285**, 24131-24140.
- de Souza,W., Attias,M., and Rodrigues,J.C.F. (2009). Particularities of mitochondrial structure in parasitic protists (de Souza et al., 2009). *Int J Biochem Cell Biol* **41**, 2069-2080.
- Delgado,M., Anderson,P., Garcia-Salcedo,J.A., Caro,M., and Gonzalez-Rey,E. (2008). Neuropeptides kill African trypanosomes by targeting intracellular compartments and inducing autophagic-like cell death. *Cell Death Differ* **16**, 406-416.
- Denny,P.W., Gokool,S., Russell,D.G., Field,M.C., and Smith,D.F. (2000). Acylation-dependent protein export in *Leishmania*. *J Biol Chem* **275**, 11017-11025.

- Denny,P.W., Lewis,S., Tempero,J.E., Goulding,D., Ivens,A.C., Field,M.C., and Smith,D.F. (2002). Leishmania RAB7: characterisation of terminal endocytic stages in an intracellular parasite. *Mol Biochem Parasitol* **123**, 105-113.
- Denton,D., Nicolson,S., and Kumar,S. (2012). Cell death by autophagy: facts and apparent artefacts. *Cell Death Differ* **19**, 87-95.
- Docampo,R., Ulrich,P., and Moreno,S.N.J. (2010). Evolution of acidocalcisomes and their role in polyphosphate storage and osmoregulation in eukaryotic microbes. *Philos Trans R Soc Lond B Biol Sci* **365**, 775-784.
- Doelling,J.H., Walker,J.M., Friedman,E.M., Thompson,A.R., and Vierstra,R.D. (2002). The APG8/12-activating enzyme APG7 is required for proper nutrient recycling and senescence in *Arabidopsis thaliana*. *J Biol Chem* **277**, 33105-33114.
- Downing,T., Imamura,H., Decuypere,S., Clark,T.G., Coombs,G.H., Cotton,J.A., Hilley,J.D., de Doncker,S., Maes,I., Mottram,J.C., Quail,M.A., Rijal,S., Sanders,M., Schönian,G., Stark,O., Sundar,S., Vanaerschot,M., Hertz-Fowler,C., Dujardin,J.C., and Berriman,M. (2011). Whole genome sequencing of multiple *Leishmania donovani* clinical isolates provides insights into population structure and mechanisms of drug resistance. *Genome Res* **21**, 2143-2156.
- Doyle,P.S., Zhou,Y.M., Engel,J.C., and McKerrow,J.H. (2007). A cysteine protease inhibitor cures Chagas' disease in an immunodeficient-mouse model of infection. *Antimicrob Agents Chemother* **51**, 3932-3939.
- Dunn,W.A., Cregg,J.M., Kiel,J.A.K.W., van der Klei,I.J., Oku,M., Sakai,Y., Sibirny,A.A., Stasyk,O.V., and Veenhuis,M. (2005). Pexophagy - The selective autophagy of peroxisomes. *Autophagy* **1**, 75-83.
- Dupont,N., Jiang,S., Pilli,M., Ornatowski,W., Bhattacharya,D., and Deretic,V. (2011). Autophagy-based unconventional secretory pathway for extracellular delivery of IL-1 β . *EMBO J* **30**, 4701-4711.
- Duran,J.M., Anjard,C., Stefan,C., Loomis,W.F., and Malhotra,V. (2010). Unconventional secretion of Acb1 is mediated by autophagosomes. *J Cell Biol* **188**, 527-536.
- Duszenko,M., Ginger,M.L., Brennand,A., Gualdrón-López,M., Colombo,M.I., Coombs,G.H., Coppens,I., Jayabalasingham,B., Langsley,G., Lisboa de Castro,S., Menna-Barreto,R., Mottram,J.C., Navarro,M., Rigden,D.J., Romano,P.S., Stoka,V., Turk,B., and Michels,P.A.M. (2011). Autophagy in protists. *Autophagy* **7**, 127-158.

- Ersfeld, K., Barraclough, H., and Gull, K. (2005). Evolutionary relationships and protein domain architecture in an expanded calpain superfamily in kinetoplastid parasites. *J Mol Evol* **61**, 742-757.
- Fader, C.M., Sánchez, D.G., Mestre, M.B., and Colombo, M.I. (2009). TI-VAMP/VAMP7 and VAMP3/cellubrevin: two v-SNARE proteins involved in specific steps of the autophagy/multivesicular body pathways. *Biochim Biophys Acta* **1793**, 1901-1916.
- Farré, J.C., Manjithaya, R., Mathewson, R.D., and Subramani, S. (2008). PpAtg30 tags peroxisomes for turnover by selective autophagy. *Dev Cell* **14**, 365-376.
- Farré, J.C., Vidal, J., and Subramani, S. (2007). A cytoplasm to vacuole targeting pathway in *P. pastoris*. *Autophagy* **3**, 230-234.
- Figarella, K., Uzcategui, N.L., Zhou, Y., LeFurgey, A., Ouellette, M., Bhattacharjee, H., and Mukhopadhyay, R. (2007). Biochemical characterization of *Leishmania major* aquaglyceroporin LmAQP1: possible role in volume regulation and osmotaxis. *Mol Microbiol* **65**, 1006-1017.
- Filimonenko, M., Isakson, P., Finley, K.D., Anderson, M., Jeong, H., Melia, T.J., Bartlett, B.J., Myers, K.M., Birkeland, H.C.G., Lamark, T., Krainc, D., Brech, A., Stenmark, H., Simonsen, A., and Yamamoto, A. (2010). The selective macroautophagic degradation of aggregated proteins requires the PI3P-binding protein Alfy. *Mol Cell* **38**, 265-279.
- Filimonenko, M., Stuffers, S., Raiborg, C., Yamamoto, A., Malerød, L., Fisher, E.M.C., Isaacs, A., Brech, A., Stenmark, H., and Simonsen, A. (2007). Functional multivesicular bodies are required for autophagic clearance of protein aggregates associated with neurodegenerative disease. *J Cell Biol* **179**, 485-500.
- Forestier, C.L., Machu, C., Loussert, C., Pescher, P., and Späth, G.F. (2011). Imaging host cell-*Leishmania* interaction dynamics implicates parasite motility, lysosome recruitment, and host cell wounding in the infection process. *Cell Host Microbe* **9**, 319-330.
- Fujita, N., Hayashi-Nishino, M., Fukumoto, H., Omori, H., Yamamoto, A., Noda, T., and Yoshimori, T. (2008). An Atg4B mutant hampers the lipidation of LC3 paralogues and causes defects in autophagosome closure. *Mol Biol Cell* **19**, 4651-4659.

- Furuta,N., Fujita,N., Noda,T., Yoshimori,T., and Amano,A. (2010). Combinational soluble N-ethylmaleimide-sensitive factor attachment protein receptor proteins VAMP8 and Vti1b mediate fusion of antimicrobial and canonical autophagosomes with lysosomes. *Mol Biol Cell* **21**, 1001-1010.
- Gannavaram,S., Sharma,P., Duncan,R.C., Salotra,P., and Nakhasi,H.L. (2011). Mitochondrial associated ubiquitin fold modifier-1 mediated protein conjugation in *Leishmania donovani*. *PLoS One* **6**, e16156.
- Gegg,M.E., Cooper,J.M., Chau,K.Y., Rojo,M., Schapira,A.H.V., and Taanman,J.W. (2010). Mitofusin 1 and mitofusin 2 are ubiquitinated in a PINK1/parkin-dependent manner upon induction of mitophagy. *Hum Mol Genet* **19**, 4861-4870.
- Geisler,S., Holmstrom,K.M., Skujat,D., Fiesel,F.C., Rothfuss,O.C., Kahle,P.J., and Springer,W. (2010). PINK1/Parkin-mediated mitophagy is dependent on VDAC1 and p62/SQSTM1. *Nat Cell Biol* **12**, 119-131.
- Geng,J., Nair,U., Yasumura-Yorimitsu,K., and Klionsky,D.J. (2010). Post-Golgi Sec proteins are required for autophagy in *Saccharomyces cerevisiae*. *Mol Biol Cell* **21**, 2257-2269.
- Ghedini,E., Debrabant,A., Engel,J.C., and Dwyer,D.M. (2001). Secretory and endocytic pathways converge in a dynamic endosomal system in a primitive protozoan. *Traffic* **2**, 175-188.
- Gluezn,E., Ginger,M.L., and McKean,P.G. (2010a). Flagellum assembly and function during the *Leishmania* life cycle. *Curr Opin Microbiol* **13**, 473-479.
- Gluezn,E., Höög,J.L., Smith,A.E., Dawe,H.R., Shaw,M.K., and Gull,K. (2010b). Beyond 9+0: noncanonical axoneme structures characterize sensory cilia from protists to humans. *FASEB J* **24**, 3117-3121.
- Gomes,L.C., Benedetto,G.D., and Scorrano,L. (2011). During autophagy mitochondria elongate, are spared from degradation and sustain cell viability. *Nat Cell Biol* **13**, 589-598.
- Gualdrón-López,M., Brennand,A., Hannaert,V., Quiñones,W., Cáceres,A.J., Bringaud,F., Concepción,J.L., and Michels,P.A.M. (2012). When, how and why glycolysis became compartmentalised in the Kinetoplastea. A new look at an ancient organelle. *Int J Parasitol* **42**, 1-20.

- Hailey,D.W., Rambold,A.S., Satpute-Krishnan,P., Mitra,K., Sougrat,R., Kim,P.K., and Lippincott-Schwartz,J. (2010). Mitochondria supply membranes for autophagosome biogenesis during starvation. *Cell* **141**, 656-667.
- Hamasaki,M., Noda,T., Baba,M., and Ohsumi,Y. (2005). Starvation triggers the delivery of the endoplasmic reticulum to the vacuole via autophagy in yeast. *Traffic* **6**, 56-65.
- Hanada,T., Noda,N.N., Satomi,Y., Ichimura,Y., Fujioka,Y., Takao,T., Inagaki,F., and Ohsumi,Y. (2007). The Atg12-Atg5 conjugate has a novel E3-like activity for protein lipidation in autophagy. *J Biol Chem* **282**, 37298-37302.
- Hanaoka,H., Noda,T., Shirano,Y., Kato,T., Hayashi,H., Shibata,D., Tabata,S., and Ohsumi,Y. (2002). Leaf senescence and starvation-induced chlorosis are accelerated by the disruption of an *Arabidopsis* autophagy gene. *Plant Physiol* **129**, 1181-1193.
- Hara,T., Nakamura,K., Matsui,M., Yamamoto,A., Nakahara,Y., Suzuki-Migishima,R., Yokoyama,M., Mishima,K., Saito,I., Okano,H., and Mizushima,N. (2006). Suppression of basal autophagy in neural cells causes neurodegenerative disease in mice. *Nature* **441**, 885-889.
- Hara,T., Takamura,A., Kishi,C., Iemura,S.i., Natsume,T., Guan,J.L., and Mizushima,N. (2008). FIP200, a ULK-interacting protein, is required for autophagosome formation in mammalian cells. *J Cell Biol* **181**, 497-510.
- Hara-Kuge,S. and Fujiki,Y. (2008). The peroxin Pex14p is involved in LC3-dependent degradation of mammalian peroxisomes. *Exp Cell Res* **314**, 3531-3541.
- Hayashi-Nishino,M., Fujita,N., Noda,T., Yamaguchi,A., Yoshimori,T., and Yamamoto,A. (2009). A subdomain of the endoplasmic reticulum forms a cradle for autophagosome formation. *Nat Cell Biol* **11**, 1433-1437.
- He,C., Baba,M., Cao,Y., and Klionsky,D.J. (2008). Self-interaction is critical for Atg9 transport and function at the phagophore assembly site during autophagy. *Mol Biol Cell* **19**, 5506-5516.
- He,C. and Klionsky,D.J. (2009). Regulation mechanisms and signaling pathways of autophagy. *Annu Rev Genet* **43**, 67-93.
- He,H., Dang,Y., Dai,F., Guo,Z., Wu,J., She,X., Pei,Y., Chen,Y., Ling,W., Wu,C., Zhao,S., Liu,J.O., and Yu,L. (2003). Post-translational modifications of three members of the human MAP1LC3 family and detection of a novel type of modification for MAP1LC3B. *J Biol Chem* **278**, 29278-29287.

- Hemelaar, J., Lelyveld, V.S., Kessler, B.M., and Ploegh, H.L. (2003). A single protease, Apg4B, is specific for the autophagy-related ubiquitin-like proteins GATE-16, MAP1-LC3, GABARAP, and Apg8L. *J Biol Chem* **278**, 51841-51850.
- Heo, J.M., Livnat-Levanon, N., Taylor, E.B., Jones, K.T., Dephore, N., Ring, J., Xie, J., Brodsky, J.L., Madeo, F., Gygi, S.P., Ashrafi, K., Glickman, M.H., and Rutter, J. (2010). A stress-responsive system for mitochondrial protein degradation. *Mol Cell* **40**, 465-480.
- Herman, M., Gillies, S., Michels, P.A., and Rigden, D.L. (2006). Autophagy and related processes in trypanosomatids - Insights from genomic and bioinformatic analyses. *Autophagy* **2**, 107-118.
- Herman, M., Perez-Mora, D., Schtickzelle, N., and Michels, P.A.M. (2008). Turnover of glycosomes during life-cycle differentiation of *Trypanosoma brucei*. *Autophagy* **4**, 294-308.
- Hicke, L. and Dunn, R. (2003). Regulation of membrane protein transport by ubiquitin and ubiquitin-binding proteins. *Annu Rev Cell Dev Biol* **19**, 141-172.
- Honig, A., Avin-Wittenberg, T., Ufaz, S., and Galili, G. (2012). A new type of compartment, defined by plant-specific Atg8-interacting proteins, is induced upon exposure of *Arabidopsis* plants to carbon starvation. *Plant Cell* **24**, 288-303.
- Huang, K., Diener, D.R., and Rosenbaum, J.L. (2009). The ubiquitin conjugation system is involved in the disassembly of cilia and flagella. *J Cell Biol* **186**, 601-613.
- Huete-Pérez, J.A., Engel, J.C., Brinen, L.S., Mottram, J.C., and McKerrow, J.H. (1999). Protease trafficking in two primitive eukaryotes is mediated by a prodomain protein motif. *J Biol Chem* **274**, 16249-16256.
- Huybrechts, S.J., Van Veldhoven, P.P., Brees, C., Mannaerts, G.P., Los, G.V., and Franssen, M. (2009). Peroxisome dynamics in cultured mammalian cells. *Traffic* **10**, 1722-1733.
- Ichimura, Y., Kirisako, T., Takao, T., Satomi, Y., Shimonishi, Y., Ishihara, N., Mizushima, N., Tanida, I., Kominami, E., Ohsumi, M., Noda, T., and Ohsumi, Y. (2000). A ubiquitin-like system mediates protein lipidation. *Nature* **408**, 488-492.

- Ishihara,N., Hamasaki,M., Yokota,S., Suzuki,K., Kamada,Y., Kihara,A., Yoshimori,T., Noda,T., and Ohsumi,Y. (2001). Autophagosome requires specific early Sec proteins for its formation and NSF/SNARE for vacuolar fusion. *Mol Biol Cell* **12**, 3690-3702.
- Ivens,A.C., Peacock,C.S., Worthey,E.A., Murphy,L., Aggarwal,G., Berriman,M., Sisk,E., Rajandream,M.A., Adlem,E., Aert,R., Anupama,A., Apostolou,Z., Attipoe,P., Bason,N., Bauser,C., Beck,A., Beverley,S.M., Bianchetti,G., Borzym,K., Bothe,G., Bruschi,C.V., Collins,M., Cadag,E., Ciarloni,L., Clayton,C., Coulson,R.M.R., Cronin,A., Cruz,A.K., Davies,R.M., De Gaudenzi,J., Dobson,D.E., Duesterhoeft,A., Fazelina,G., Fosker,N., Frasch,A.C., Fraser,A., Fuchs,M., Gabel,C., Goble,A., Goffeau,A., Harris,D., Hertz-Fowler,C., Hilbert,H., Horn,D., Huang,Y., Klages,S., Knights,A., Kube,M., Larke,N., Litvin,L., Lord,A., Louie,T., Marra,M., Masuy,D., Matthews,K., Michaeli,S., Mottram,J.C., Müller-Auer,S., Munden,H., Nelson,S., Norbertczak,H., Oliver,K., O'Neil,S., Pentony,M., Pohl,T.M., Price,C., Purnelle,B., Quail,M.A., Rabbinowitsch,E., Reinhardt,R., Rieger,M., Rinta,J., Robben,J., Robertson,L., Ruiz,J.C., Rutter,S., Saunders,D., Schäfer,M., Schein,J., Schwartz,D.C., Seeger,K., Seyler,A., Sharp,S., Shin,H., Sivam,D., Squares,R., Squares,S., Tosato,V., Vogt,C., Volckaert,G., Wambutt,R., Warren,T., Wedler,H., Woodward,J., Zhou,S., Zimmermann,W., Smith,D.F., Blackwell,J.M., Stuart,K.D., Barrell,B., and Myler,P.J. (2005). The genome of the kinetoplastid parasite, *Leishmania major*. *Science* **309**, 436-442.
- Iwata,A., Riley,B.E., Johnston,J.A., and Kopito,R.R. (2005). HDAC6 and microtubules are required for autophagic degradation of aggregated huntingtin. *J Biol Chem* **280**, 40282-40292.
- Iwata,J., Ezaki,J., Komatsu,M., Yokota,S., Ueno,T., Tanida,I., Chiba,T., Tanaka,K., and Kominami,E. (2006). Excess peroxisomes are degraded by autophagic machinery in mammals. *J Biol Chem* **281**, 4035-4041.
- Jahreiss,L., Menzies,F.M., and Rubinsztein,D.C. (2008). The itinerary of autophagosomes: From peripheral formation to kiss-and-run fusion with lysosomes. *Traffic* **9**, 574-587.
- Jiang,S., Wells,C.D., and Roach,P.J. (2011). Starch-binding domain-containing protein 1 (Jiang et al., 2011) and glycogen metabolism: Identification of the Atg8 family interacting motif (AIM) in Stbd1 required for interaction with GABARAPL1. *Biochem Biophys Res Commun* **413**, 420-425.
- Johansen,T. and Lamark,T. (2011). Selective autophagy mediated by autophagic adapter proteins. *Autophagy* **7**, 279-296.

- Kabeya,Y., Mizushima,N., Uero,T., Yamamoto,A., Kirisako,T., Noda,T., Kominami,E., Ohsumi,Y., and Yoshimori,T. (2000). LC3, a mammalian homologue of yeast Apg8p, is localized in autophagosome membranes after processing. *EMBO J* **19**, 5720-5728.
- Kabeya,Y., Kamada,Y., Baba,M., Takikawa,H., Sasaki,M., and Ohsumi,Y. (2005). Atg17 functions in cooperation with Atg1 and Atg13 in yeast autophagy. *Mol Biol Cell* **16**, 2544-2553.
- Kabeya,Y., Mizushima,N., Yamamoto,A., Oshitani-Okamoto,S., Ohsumi,Y., and Yoshimori,T. (2004). LC3, GABARAP and GATE16 localize to autophagosomal membrane depending on form-II formation. *J Cell Sci* **117**, 2805-2812.
- Kamada,Y., Yoshino,K.i., Kondo,C., Kawamata,T., Oshiro,N., Yonezawa,K., and Ohsumi,Y. (2010). Tor directly controls the Atg1 kinase complex to regulate autophagy. *Mol Cell Biol* **30**, 1049-1058.
- Kamhawi,S. (2000). The biological and immunomodulatory properties of sand fly saliva and its role in the establishment of *Leishmania* infections. *Microbes Infect* **2**, 1765-1773.
- Kamhawi,S. (2006). Phlebotomine sand flies and *Leishmania* parasites: friends or foes? *Trends Parasitol* **22**, 439-445.
- Kanki,T., Wang,K., Baba,M., Bartholomew,C.R., Lynch-Day,M.A., Du,Z., Geng,J., Mao,K., Yang,Z., Yen,W.L., and Klionsky,D.J. (2009a). A genomic screen for yeast mutants defective in selective mitochondria autophagy. *Mol Biol Cell* **20**, 4730-4738.
- Kanki,T., Wang,K., Cao,Y., Baba,M., and Klionsky,D.J. (2009b). Atg32 is a mitochondrial protein that confers selectivity during mitophagy. *Dev Cell* **17**, 98-109.
- Katta,S.S., Sahasrabudde,A.A., and Gupta,C.M. (2009). Flagellar localization of a novel isoform of myosin, myosin XXI, in *Leishmania*. *Mol Biochem Parasitol* **164**, 105-110.
- Kawamata,T., Kamada,Y., Kabeya,Y., Sekito,T., and Ohsumi,Y. (2008). Organization of the pre-autophagosomal structure responsible for autophagosome formation. *Mol Biol Cell* **19**, 2039-2050.
- Kaye,P. and Scott,P. (2011). Leishmaniasis: complexity at the host-pathogen interface. *Nat Rev Microbiol* **9**, 604-615.

- Ketelaar,T., Voss,C., Dimmock,S.A., Thumm,M., and Hussey,P.J. (2004). *Arabidopsis* homologues of the autophagy protein Atg8 are a novel family of microtubule binding proteins. *FEBS Lett* **567**, 302-306.
- Kim,I. and Lemasters,J.J. (2011). Mitochondrial degradation by autophagy (mitophagy) in GFP-LC3 transgenic hepatocytes during nutrient deprivation. *Am J Physiol Cell Physiol* **300**, C308-C317.
- Kim,J., Huang,W.P., Stromhaug,P.E., and Klionsky,D.J. (2002). Convergence of multiple autophagy and cytoplasm to vacuole targeting components to a perivacuolar membrane compartment prior to *de novo* vesicle formation. *J Biol Chem* **277**, 763-773.
- Kim,J., Scott,S.V., Oda,M.N., and Klionsky,D.J. (1997). Transport of a large oligomeric protein by the cytoplasm to vacuole protein targeting pathway. *J Cell Biol* **137**, 609-618.
- Kim,P.K., Hailey,D.W., Mullen,R.T., and Lippincott-Schwartz,J. (2008). Ubiquitin signals autophagic degradation of cytosolic proteins and peroxisomes. *Proc Natl Acad Sci USA* **105**, 20567-20574.
- Kirisako,T., Ichimura,Y., Okada,H., Kabeya,Y., Mizushima,N., Yoshimori,T., Ohsumi,M., Takao,T., Noda,T., and Ohsumi,Y. (2000). The reversible modification regulates the membrane-binding state of Apg8/Aut7 essential for autophagy and the cytoplasm to vacuole targeting pathway. *J Cell Biol* **151**, 263-276.
- Kirkin,V., Lamark,T., Sou,Y.S., Bjørkøy,G., Nunn,J.L., Bruun,J.A., Shvets,E., McEwan,D.G., Clausen,T.H., Wild,P., Bilusic,I., Theurillat,J.P., Øyvervatn,A., Ishii,T., Elazar,Z., Komatsu,M., Dikic,I., and Johansen,T. (2009). A role for NBR1 in autophagosomal degradation of ubiquitinated substrates. *Mol Cell* **33**, 505-516.
- Kissová,I., Deffieu,M., Manon,S., and Camougrand,N. (2004). Uth1p is involved in the autophagic degradation of mitochondria. *J Biol Chem* **279**, 39068-39074.
- Kittler,J.T., Rostaing,P., Schiavo,G., Fritschy,J.M., Olsen,R., Triller,A., and Moss,S.J. (2001). The subcellular distribution of GABARAP and its ability to interact with NSF suggest a role for this protein in the intracellular transport of GABA_A receptors. *Mol Cell Neurosci* **18**, 13-25.
- Klionsky,D.J., Cuervo,A.M., and Seglen,P.O. (2007). Methods for monitoring autophagy from yeast to human. *Autophagy* **3**, 181-206.

- Köchl,R., Hu,X.W., Chan,E.Y.W., and Tooze,S.A. (2006). Microtubules facilitate autophagosome formation and fusion of autophagosomes with endosomes. *Traffic* **7**, 129-145.
- Komatsu,M., Waguri,S., Chiba,T., Murata,S., Iwata,J.i., Tanida,I., Ueno,T., Koike,M., Uchiyama,Y., Kominami,E., and Tanaka,K. (2006). Loss of autophagy in the central nervous system causes neurodegeneration in mice. *Nature* **441**, 880-884.
- Koopmann,R., Muhammad,K., Perbandt,M., Betzel,C., and Duszenko,M. (2009). *Trypanosoma brucei* ATG8: Structural insights into autophagic-like mechanisms in protozoa. *Autophagy* **5**, 1085-1091.
- Korolchuk,V.I., Mansilla,A., Menzies,F.M., and Rubinsztein,D.C. (2009). Autophagy inhibition compromises degradation of ubiquitin-proteasome pathway substrates. *Mol Cell* **33**, 517-527.
- Kraft,C., Deplazes,A., Sohrmann,M., and Peter,M. (2008). Mature ribosomes are selectively degraded upon starvation by an autophagy pathway requiring the Ubp3p/Bre5p ubiquitin protease. *Nat Cell Biol* **10**, 602-610.
- Kramer,S. (2012). Developmental regulation of gene expression in the absence of transcriptional control: The case of kinetoplastids. *Mol Biochem Parasitol* **181**, 61-72.
- Krick,R., Muehe,Y., Prick,T., Bremer,S., Schlotterhose,P., Eskelinen,E.L., Millen,J., Goldfarb,D.S., and Thumm,M. (2008). Piecemeal microautophagy of the nucleus requires the core macroautophagy genes. *Mol Biol Cell* **19**, 4492-4505.
- Kristensen,A.R., Schandorff,S., Hoyer-Hansen,M., Nielsen,M.O., Jaattela,M., Dengjel,J., and Andersen,J.S. (2008). Ordered organelle degradation during starvation-induced autophagy. *Mol Cell Proteomics* **7**, 2419-2428.
- Kuma,A., Matsui,M., and Mizushima,N. (2007). LC3, an autophagosome marker, can be incorporated into protein aggregates independent of autophagy. *Autophagy* **3**, 323-328.
- Kuma,A., Mizushima,N., Ishihara,N., and Ohsumi,Y. (2002). Formation of the ~350-kDa Apg12-Apg5-Apg16 multimeric complex, mediated by Apg16 oligomerization, is essential for autophagy in yeast. *J Biol Chem* **277**, 18619-18625.

- Kwon,S.I., Cho,H.J., Jung,J.H., Yoshimoto,K., Shirasu,K., and Park,O.K. (2010). The Rab GTPase RabG3b functions in autophagy and contributes to tracheary element differentiation in *Arabidopsis*. *Plant J* **64**, 151-164.
- Lahav,T., Sivam,D., Volpin,H., Ronen,M., Tsigankov,P., Green,A., Holland,N., Kuzyk,M., Borchers,C., Zilberstein,D., and Myler,P.J. (2011). Multiple levels of gene regulation mediate differentiation of the intracellular pathogen *Leishmania*. *FASEB J* **25**, 515-525.
- Lamark,T., Kirkin,V., Dikic,I., and Johansen,T. (2009). NBR1 and p62 as cargo receptors for selective autophagy of ubiquitinated targets. *Cell Cycle* **8**, 1986-1990.
- Lambertz,U., Silverman,J.M., Nandan,D., McMaster,W.R., Clos,J., Foster,L.J., and Reiner,N.E. (2012). Secreted virulence factors and immune evasion in visceral leishmaniasis. *J Leukoc Biol* **91**, 887-899.
- Landfear,S.M. and Ignatushchenko,M. (2001). The flagellum and flagellar pocket of trypanosomatids. *Mol Biochem Parasitol* **115**, 1-17.
- Laskay,T., van Zandbergen,G., and Solbach,W. (2003). Neutrophil granulocytes - Trojan horses for *Leishmania major* and other intracellular microbes? *Trends Microbiol* **11**, 210-214.
- Lee,I.H. and Finkel,T. (2009). Regulation of autophagy by the p300 acetyltransferase. *J Biol Chem* **284**, 6322-6328.
- Lee,J.Y., Koga,H., Kawaguchi,Y., Tang,W., Wong,E., Gao,Y.S., Pandey,U.B., Kaushik,S., Tresse,E., Lu,J., Taylor,J.P., Cuervo,A.M., and Yao,T.P. (2010a). HDAC6 controls autophagosome maturation essential for ubiquitin-selective quality-control autophagy. *EMBO J* **29**, 969-980.
- Lee,R.E.C., Brunette,S., Puente,L.G., and Megeney,L.A. (2010b). Metacaspase Yca1 is required for clearance of insoluble protein aggregates. *Proc National Acad Sci USA* **107**, 13348-13353.
- Legakis,J.E., Yen,W.L., and Klionsky,D.J. (2007). A cycling protein complex required for selective autophagy. *Autophagy* **3**, 422-432.
- Li,F.J., Shen,Q., Wang,C., Sun,Y., Yuan,A.Y., and He,C.Y. (2012a). A role of autophagy in *Trypanosoma brucei* cell death. *Cell Microbiol* **14**, 1242-1256
- Li,M., Hou,Y., Wang,J., Chen,X., Shao,Z.M., and Yin,X.M. (2011). Kinetics comparisons of mammalian Atg4 homologues indicate selective preferences toward diverse Atg8 substrates. *J Biol Chem* **286**, 7327-7338.

- Li,W.W., Li,J., and Bao,J.K. (2012b). Microautophagy: lesser-known self-eating. *Cell Mol Life Sci* **69**, 1125-1136.
- Liao,S., Wang,T., Fan,K., and Tu,X. (2010). The small ubiquitin-like modifier (SUMO) is essential in cell cycle regulation in *Trypanosoma brucei*. *Exp Cell Res* **316**, 704-715.
- Luciani,M.F., Giusti,C., Harms,B., Oshima,Y., Kikuchi,H., Kubohara,Y., and Golstein,P. (2011). Atg1 allows second-signaled autophagic cell death in *Dictyostelium*. *Autophagy* **7**, 501-508.
- MacLean,L.M., O'Toole,P.J., Stark,M., Marrison,J., Seelenmeyer,C., Nickel,W., and Smith,D.F. (2012). Trafficking and release of *Leishmania* metacyclic HASPB on macrophage invasion. *Cell Microbiol* **14**, 740-761.
- Madeira da Silva,L. and Beverley,S.M. (2010). Expansion of the target of rapamycin (TOR) kinase family and function in *Leishmania* shows that TOR3 is required for acidocalcisome biogenesis and animal infectivity. *Proc National Acad Sci USA* **107**, 11965-11970.
- Manjithaya,R., Anjard,C., Loomis,W.F., and Subramani,S. (2010). Unconventional secretion of *Pichia pastoris* Acb1 is dependent on GRASP protein, peroxisomal functions, and autophagosome formation. *J Cell Biol* **188**, 537-546.
- Mannaert,A., Downing,T., Imamura,H., and Dujardin,J.C. (2012). Adaptive mechanisms in pathogens: universal aneuploidy in *Leishmania*. *Trends Parasitol* **28**, 370-376.
- Manning-Cela,R., Jaishankar,S., and Swindle,J. (2006). Life-cycle and growth-phase-dependent regulation of the ubiquitin genes of *Trypanosoma cruzi*. *Arch Med Res* **37**, 593-601.
- Mari,M., Griffith,J., Rieter,E., Krishnappa,L., Klionsky,D.J., and Reggiori,F. (2010). An Atg9-containing compartment that functions in the early steps of autophagosome biogenesis. *J Cell Biol* **190**, 1005-1022.
- Mariño,G., Salvador-Montoliu,N., Fueyo,A., Knecht,E., Mizushima,N., and López-Otín,C. (2007). Tissue-specific autophagy alterations and increased tumorigenesis in mice deficient in Atg4C/autophagin-3. *J Biol Chem* **282**, 18573-18583.
- McKean,P.G., Denny,P.W., Knuepfer,E., Keen,J.K., and Smith,D.F. (2001). Phenotypic changes associated with deletion and overexpression of a stage-regulated gene family in *Leishmania*. *Cell Microbiol* **3**, 511-523.

- Meijer, W.H., van der Klei, I.J., Veenhuis, M., and Kiel, J.A.K.W. (2007). ATG genes involved in non-selective autophagy are conserved from yeast to man, but the selective Cvt and pexophagy pathways also require organism-specific genes. *Autophagy* **3**, 106-116.
- Michels, P.A.M., Bringaud, F., Herman, M., and Hannaert, V. (2006). Metabolic functions of glycosomes in trypanosomatids. *Biochim Biophys* **1763**, 1463-1477.
- Mizushima, N., Levine, B., Cuervo, A.M., and Klionsky, D.J. (2008). Autophagy fights disease through cellular self-digestion. *Nature* **451**, 1069-1075.
- Mizushima, N., Noda, T., Yoshimori, T., Tanaka, Y., Ishii, T., George, M.D., Klionsky, D.J., Ohsumi, M., and Ohsumi, Y. (1998). A protein conjugation system essential for autophagy. *Nature* **395**, 395-398.
- Mizushima, N., Yamamoto, A., Hatano, M., Kobayashi, Y., Kabeya, Y., Suzuki, K., Tokuhi, T., Ohsumi, Y., and Yoshimori, T. (2001). Dissection of autophagosome formation using Apg5-deficient mouse embryonic stem cells. *J Cell Biol* **152**, 657-668.
- Mizushima, N., Yoshimori, T., and Ohsumi, Y. (2011). The role of Atg proteins in autophagosome formation. *Annu Rev Cell Dev Biol* **27**, 107-132.
- Morales, M.A., Watanabe, R., Dacher, M., Chafey, P., Fortéa, J., Scott, D.A., Beverley, S.M., Ommen, G., Clos, J., Hem, S., Lenormand, P., Rousselle, J.C., Namane, A., and Späth, G.F. (2010). Phosphoproteome dynamics reveal heat-shock protein complexes specific to the *Leishmania donovani* infectious stage. *Proc Natl Acad Sci USA* **107**, 8381-8386.
- Moreno, S.N.J. and Docampo, R. (2009). The role of acidocalcisomes in parasitic protists. *J Eukaryot Microbiol* **56**, 208-213.
- Morrison, L.S., Goundry, A., Faria, M.S., Tetley, L., Eschenlauer, S.C., Westrop, G.D., Dostalova, A., Volf, P., Coombs, G.H., Lima, A.P., and Mottram, J.C. (2012). Ecotin-like serine peptidase inhibitor ISP1 of *Leishmania major* plays a role in flagellar pocket dynamics and promastigote differentiation. *Cell Microbiol* **14**, 1271-1286.
- Mostowy, S. and Cossart, P. (2012). Bacterial autophagy: restriction or promotion of bacterial replication? *Trends Cell Biol* **22**, 283-291.

- Mostowy,S., Sancho-Shimizu,V., Hamon,M.A., Simeone,R., Brosch,R., Johansen,T., and Cossart,P. (2011). p62 and NDP52 proteins target intracytosolic *Shigella* and *Listeria* to different autophagy pathways. *J Biol Chem* **286**, 26987-26995.
- Motley,A.M., Nuttall,J.M., and Hettema,E.H. (2012). Pex3-anchored Atg36 tags peroxisomes for degradation in *Saccharomyces cerevisiae*. *EMBO J* **31**, 2852-68.
- Mottram,J.C., Souza,A.E., Hutchison,J.E., Carter,R., Frame,M.J., and Coombs,G.H. (1996). Evidence from disruption of the *lmcpb* gene array of *Leishmania mexicana* that cysteine proteinases are virulence factors. *Proc Natl Acad Sci USA* **93**, 6008-6013.
- Mullin,K.A., Foth,B.J., Ilgoutz,S.C., Callaghan,J.M., Zawadzki,J.L., McFadden,G.I., and McConville,M.J. (2001). Regulated degradation of an endoplasmic reticulum membrane protein in a tubular lysosome in *Leishmania mexicana*. *Mol Biol Cell* **12**, 2364-2377.
- Naderer,T. and McConville,M.J. (2008). The *Leishmania*-macrophage interaction: a metabolic perspective. *Cell Microbiol* **10**, 301-308.
- Nair,U., Cao,Y., Xie,Z., and Klionsky,D.J. (2010). Roles of the lipid-binding motifs of Atg18 and Atg21 in the cytoplasm to vacuole targeting pathway and autophagy. *J Biol Chem* **285**, 11476-11488.
- Nair,U., Jotwani,A., Geng,J., Gammoh,N., Richerson,D., Yen,W.L., Griffith,J., Nag,S., Wang,K., Moss,T., Baba,M., McNew,J.A., Jiang,X., Reggiori,F., Melia,T.J., and Klionsky,D.J. (2011). SNARE proteins are required for macroautophagy. *Cell* **146**, 290-302.
- Nair,U., Yen,W.L., Mari,M., Cao,Y., Xie,Z., Baba,M., Reggiori,F., and Klionsky,D.J. (2012). A role for Atg8-PE deconjugation in autophagosome biogenesis. *Autophagy* **8**, 780-793.
- Nakatogawa,H., Ichimura,Y., and Ohsumi,Y. (2007). Atg8, a ubiquitin-like protein required for autophagosome formation, mediates membrane tethering and hemifusion. *Cell* **130**, 165-178.
- Nakatogawa,H., Ishii,J., Asai,E., and Ohsumi,Y. (2012). Atg4 recycles inappropriately lipidated Atg8 to promote autophagosome biogenesis. *Autophagy* **8**, 177-186.

- Narendra,D., Tanaka,A., Suen,D.F., and Youle,R.J. (2008). Parkin is recruited selectively to impaired mitochondria and promotes their autophagy. *J Cell Biol* **183**, 795-803.
- Narendra,D.P., Jin,S.M., Tanaka,A., Suen,D.F., Gautier,C.A., Shen,J., Cookson,M.R., and Youle,R.J. (2010). PINK1 is selectively stabilized on impaired mitochondria to activate Parkin. *PLoS Biol* **8**, e1000298.
- Nazarko,T.Y., Huang,J., Nicaud,J.M., Klionsky,D.J., and Sibirny,A.A. (2005). Trs85 is required for macroautophagy, pexophagy and cytoplasm to vacuole targeting in *Yarrowia lipolytica* and *Saccharomyces cerevisiae*. *Autophagy* **1**, 37-45.
- Ng,L.G., Hsu,A., Mandell,M.A., Roediger,B., Hoeller,C., Mrass,P., Iparraguirre,A., Cavanagh,L.L., Triccas,J.A., Beverley,S.M., Scott,P., and Weninger,W. (2008). Migratory dermal dendritic cells act as rapid sensors of protozoan parasites. *PLoS Pathog* **4**, e1000222.
- Nishida,Y., Arakawa,S., Fujitani,K., Yamaguchi,H., Mizuta,T., Kanaseki,T., Komatsu,M., Otsu,K., Tsujimoto,Y., and Shimizu,S. (2009). Discovery of Atg5/Atg7-independent alternative macroautophagy. *Nature* **461**, 654-U99.
- Noda,N.N., Kumeta,H., Nakatogawa,H., Satoo,K., Adachi,W., Ishii,J., Fujioka,Y., Ohsumi,Y., and Inagaki,F. (2008). Structural basis of target recognition by Atg8/LC3 during selective autophagy. *Genes Cells* **13**, 1211-1218.
- Noda,T., Kim,J., Huang,W.P., Baba,M., Tokunaga,C., Ohsumi,Y., and Klionsky,D.J. (2000). Apg9p/Cvt7p is an integral membrane protein required for transport vesicle formation in the Cvt and autophagy pathways. *J Cell Biol* **148**, 465-480.
- Noda,T. and Ohsumi,Y. (1998). Tor, a phosphatidylinositol kinase homologue, controls autophagy in yeast. *J Biol Chem* **273**, 3963-3966.
- Novak,I., Kirkin,V., McEwan,D.G., Zhang,J., Wild,P., Rozenknop,A., Rogov,V., Lohr,F., Popovic,D., Occhipinti,A., Reichert,A.S., Terzic,J., Dotsch,V., Ney,P.A., and Dikic,I. (2010). Nix is a selective autophagy receptor for mitochondrial clearance. *EMBO Rep* **11**, 45-51.
- Nowikovsky,K., Reipert,S., Devenish,R.J., and Schweyen,R.J. (2007). Mdm38 protein depletion causes loss of mitochondrial K⁺/H⁺ exchange activity, osmotic swelling and mitophagy. *Cell Death Differ* **14**, 1647-1656.

- Obara,K., Noda,T., Niimi,K., and Ohsumi,Y. (2008a). Transport of phosphatidylinositol 3-phosphate into the vacuole via autophagic membranes in *Saccharomyces cerevisiae*. *Genes Cells* **13**, 537-547.
- Obara,K., Sekito,T., Niimi,K., and Ohsumi,Y. (2008b). The Atg18-Atg2 complex is recruited to autophagic membranes via phosphatidylinositol 3-phosphate and exerts an essential function. *J Biol Chem* **283**, 23972-23980.
- Ogata,M., Hino,S.i., Saito,A., Morikawa,K., Kondo,S., Kanemoto,S., Murakami,T., Taniguchi,M., Tanii,I., Yoshinaga,K., Shiosaka,S., Hammarback,J.A., Urano,F., and Imaizumi,K. (2006). Autophagy is activated for cell survival after endoplasmic reticulum stress. *Mol Cell Biol* **26**, 9220-9231.
- Okamoto,K., Kondo-Okamoto,N., and Ohsumi,Y. (2009). Mitochondria-anchored receptor Atg32 mediates degradation of mitochondria via selective autophagy. *Dev Cell* **17**, 87-97.
- Opperdoes,F.R. (1987). Compartmentation of carbohydrate metabolism in trypanosomes. *Annu Rev Microbiol* **41**, 127-151.
- Orsi,A., Razi,M., Dooley,H.C., Robinson,D., Weston,A.E., Collinson,L.M., and Tooze,S.A. (2012). Dynamic and transient interactions of Atg9 with autophagosomes, but not membrane integration, are required for autophagy. *Mol Biol Cell* **23**, 1860-1873.
- Pankiv,S., Clausen,T.H., Lamark,T., Brech,A., Bruun,J.A., Outzen,H., Øyvervatn,A., Bjørkøy,G., and Johansen,T. (2007). p62/SQSTM1 binds directly to Atg8/LC3 to facilitate degradation of ubiquitinated protein aggregates by autophagy. *J Biol Chem* **282**, 24131-24145.
- Park,Y.E., Hayashi,Y.K., Bonne,G., Arimura,T., Noguchi,S., Nonaka,I., and Nishino,I. (2009). Autophagic degradation of nuclear components in mammalian cells. *Autophagy* **5**, 795-804.
- Paz,Y., Elazar,Z., and Fass,D. (2000). Structure of GATE-16, membrane transport modulator and mammalian ortholog of autophagocytosis factor Aut7p. *J Biol Chem* **275**, 25445-25450.

- Peacock,C.S., Seeger,K., Harris,D., Murphy,L., Ruiz,J.C., Quail,M.A., Peters,N., Adlem,E., Tivey,A., Aslett,M., Kerhornou,A., Ivens,A., Fraser,A., Rajandream,M.A., Carver,T., Norbertczak,H., Chillingworth,T., Hance,Z., Jagels,K., Moule,S., Ormond,D., Rutter,S., Squares,R., Whitehead,S., Rabbinowitsch,E., Arrowsmith,C., White,B., Thurston,S., Bringaud,F., Baldauf,S.L., Faulconbridge,A., Jeffares,D., Depledge,D.P., Oyola,S.O., Hilley,J.D., Brito,L.O., Tosi,L.R.O., Barrell,B., Cruz,A.K., Mottram,J.C., Smith,D.F., and Berriman,M. (2007). Comparative genomic analysis of three *Leishmania* species that cause diverse human disease. *Nat Genet* **39**, 839-847.
- Peters,N.C., Egen,J.G., Secundino,N., Debrabant,A., Kimblin,N., Kamhawi,S., Lawyer,P., Fay,M.P., Germain,R.N., and Sacks,D. (2008). *In vivo* imaging reveals an essential role for neutrophils in leishmaniasis transmitted by sand flies. *Science* **321**, 970-974.
- Plewes,K.A., Barr,S.D., and Gedamu,L. (2003). Iron superoxide dismutases targeted to the glycosomes of *Leishmania chagasi* are important for survival. *Infect Immun* **71**, 5910-5920.
- Ponder,E.L. and Bogyo,M. (2007). Ubiquitin-like modifiers and their deconjugating enzymes in medically important parasitic protozoa. *Eukaryot Cell* **6**, 1943-1952.
- Ponpuak,M., Davis,A.S., Roberts,E.A., Delgado,M.A., Dinkins,C., Zhao,Z., Virgin IV,H.W., Kyei,G.B., Johansen,T., Vergne,I., and Deretic,V. (2010). Delivery of cytosolic components by autophagic adaptor protein p62 endows autophagosomes with unique antimicrobial properties. *Immunity* **32**, 329-341.
- Priault,M., Salin,B., Schaeffer,J., Vallette,F.M., di Rago,J.P., and Martinou,J.C. (2005). Impairing the bioenergetic status and the biogenesis of mitochondria triggers mitophagy in yeast. *Cell Death Differ* **12**, 1613-1621.
- Proto,W.R. (2010). Characterisation of autophagy and a metacaspase in *Trypanosoma brucei*. *PhD thesis, University of Glasgow*.
- Radoshevich,L., Murrow,L., Chen,N., Fernandez,E., Roy,S., Fung,C., and Debnath,J. (2010). ATG12 conjugation to ATG3 regulates mitochondrial homeostasis and cell death. *Cell* **142**, 590-600.
- Rambold,A.S., Kostelecky,B., Elia,N., and Lippincott-Schwartz,J. (2011). Tubular network formation protects mitochondria from autophagosomal degradation during nutrient starvation. *Proc Natl Acad Sci USA* **108**, 10190-10195.

- Ravikumar,B., Moreau,K., Jahreiss,L., Puri,C., and Rubinsztein,D.C. (2010). Plasma membrane contributes to the formation of pre-autophagosomal structures. *Nat Cell Biol* **12**, 747-757.
- Reggiori,F., Monastyrska,I., Shintani,T., and Klionsky,D.J. (2005). The actin cytoskeleton is required for selective types of autophagy, but not nonspecific autophagy, in the yeast *Saccharomyces cerevisiae*. *Mol Biol Cell* **16**, 5843-5856.
- Ribeiro-Gomes,F.L., Peters,N.C., Debrabant,A., and Sacks,D.L. (2012). Efficient capture of infected neutrophils by dendritic cells in the skin inhibits the early anti-*Leishmania* response. *PLoS Pathog* **8**, e1002536.
- Rigden,D.J., Michels,P., and Ginger,M.L. (2009). Autophagy in protists: examples of secondary loss, lineage-specific innovations, and the conundrum of remodeling a single mitochondrion. *Autophagy* **5**, 784-794.
- Ritter,U., Frischknecht,F., and van Zandbergen,G. (2009). Are neutrophils important host cells for *Leishmania* parasites? *Trends Parasitol* **25**, 505-510.
- Roberts,P., Moshitch-Moshkovitz,S., Kvam,E., O'Toole,E., Winey,M., and Goldfarb,D.S. (2003). Piecemeal microautophagy of nucleus in *Saccharomyces cerevisiae*. *Mol Biol Cell* **14**, 129-141.
- Rogers,M.B., Hilley,J.D., Dickens,N.J., Wilkes,J., Bates,P.A., Depledge,D.P., Harris,D., Her,Y., Herzyk,P., Imamura,H., Otto,T.D., Sanders,M., Seeger,K., Dujardin,J.C., Berriman,M., Smith,D.F., Hertz-Fowler,C., and Mottram,J.C. (2011). Chromosome and gene copy number variation allow major structural change between species and strains of *Leishmania*. *Genome Res* **21**, 2129-2142.
- Rogers,M.E. and Bates,P.A. (2007). *Leishmania* manipulation of sand fly feeding behavior results in enhanced transmission. *PLoS Pathog* **3**, e91.
- Rogers,M.E., CHANCE,M., and Bates,P.A. (2002). The role of promastigote secretory gel in the origin and transmission of the infective stage of *Leishmania mexicana* by the sandfly *Lutzomyia longipalpis*. *Parasitology* **124**, 495-507.
- Rogers,M.E., Ilg,T., Nikolaev,A.V., Ferguson,M.A.J., and Bates,P.A. (2004). Transmission of cutaneous leishmaniasis by sand flies is enhanced by regurgitation of fPPG. *Nature* **430**, 463-467.

- Rosenzweig,D., Smith,D., Myler,P.J., Olafson,R.W., and Zilberstein,D. (2008a). Post-translational modification of cellular proteins during *Leishmania donovani* differentiation. *Proteomics* **8**, 1843-1850.
- Rosenzweig,D., Smith,D., Opperdoes,F., Stern,S., Olafson,R.W., and Zilberstein,D. (2008b). Retooling *Leishmania* metabolism: from sand fly gut to human macrophage. *FASEB J* **22**, 590-602.
- Sacks,D.L., Hieny,S., and Sher,A. (Sacks et al., 1985). Identification of cell surface carbohydrate and antigenic changes between noninfective and infective developmental stages of *Leishmania major* promastigotes. *J Immunol* **135**, 564-569.
- Sádlová,J., Price,H.P., Smith,B.A., Votýpka,J., Volf,P., and Smith,D.F. (2010). The stage-regulated HASPB and SHERP proteins are essential for differentiation of the protozoan parasite *Leishmania major* in its sand fly vector, *Phlebotomus papatasi*. *Cell Microbiol* **12**, 1765-1779.
- Sagiv,Y., Legesse-Miller,A., Porat,A., and Elazar,Z. (2000). GATE-16, a membrane transport modulator, interacts with NSF and the Golgi v-SNARE GOS-28. *EMBO J* **19**, 1494-1504.
- Sakai,Y., Oku,M., van der Klei,I.J., and Kiel,J.A.K.W. (2006). Pexophagy: Autophagic degradation of peroxisomes. *Biochim Biophysica Acta* **1763**, 1767-1775.
- Sandoval,H., Thiagarajan,P., Dasgupta,S.K., Schumacher,A., Prchal,J.T., Chen,M., and Wang,J. (2008). Essential role for Nix in autophagic maturation of erythroid cells. *Nature* **454**, 232-235.
- Sant'Anna,C., Parussini,F., Lourenço,D., de Souza,W., Cazzulo,J., and Cunha-e-Silva,N. (2008). All *Trypanosoma cruzi* developmental forms present lysosome-related organelles. *Histochem Cell Biol* **130**, 1187-1198.
- Schönian,G., Nasereddin,A., Dinse,N., Schweynoch,C., Schallig,H.D.F.H., Presber,W., and Jaffe,C.L. (2003). PCR diagnosis and characterization of *Leishmania* in local and imported clinical samples. *Diagn Microbiol Infect Dis* **47**, 349-358.
- Schwarten,M., Mohrlüder,J., Ma,P., Stoldt,M., Thielmann,Y., Stangler,T., Hersch,N., Hoffmann,B., Merkel,R., and Willbold,D. (2009). Nix directly binds to GABARAP: A possible crosstalk between apoptosis and autophagy. *Autophagy* **5**, 690-698.

- Schwarten,M., Stoldt,M., Mohrlüder,J., and Willbold,D. (2010). Solution structure of Atg8 reveals conformational polymorphism of the N-terminal domain. *Biochem Biophys Res Commun* **395**, 426-431.
- Scott,S.V., Guan,J., Hutchins,M.U., Kim,J., and Klionsky,D.J. (2001). Cvt19 is a receptor for the cytoplasm-to-vacuole targeting pathway. *Mol Cell* **7**, 1131-1141.
- Sekito,T., Kawamata,T., Ichikawa,R., Suzuki,K., and Ohsumi,Y. (2009). Atg17 recruits Atg9 to organize the pre-autophagosomal structure. *Genes Cells* **14**, 525-538.
- Shen,H.M. and Codogno,P. (2011). Autophagic cell death: Loch Ness monster or endangered species? *Autophagy* **7**, 457-465.
- Shvets,E., Abada,A., Weidberg,H., and Elazar,Z. (2011). Dissecting the involvement of LC3B and GATE-16 in p62 recruitment into autophagosomes. *Autophagy* **7**, 683-688.
- Silverman,J.M., Clos,J., De'Oliveira,C.C., Shirvani,O., Fang,Y., Wang,C., Foster,L.J., and Reiner,N.E. (2010a). An exosome-based secretion pathway is responsible for protein export from *Leishmania* and communication with macrophages. *J Cell Sci* **123**, 842-852.
- Silverman,J.M., Clos,J., Horakova,E., Wang,A.Y., Wiesgigl,M., Kelly,I., Lynn,M.A., McMaster,W.R., Foster,L.J., Levings,M.K., and Reiner,N.E. (2010b). *Leishmania* exosomes modulate innate and adaptive immune responses through effects on monocytes and dendritic cells. *J Immunol* **185**, 5011-5022.
- Singh,S.B., Tandon,R., Krishnamurthy,G., Vikram,R., Sharma,N., Basu,S.K., and Mukhopadhyay,A. (2003). Rab5-mediated endosome-endosome fusion regulates hemoglobin endocytosis in *Leishmania donovani*. *EMBO J* **22**, 5712-5722.
- Sláviková,S., Shy,G., Yao,Y., Glzman,R., Levanony,H., Pietrokovski,S., Elazar,Z., and Galili,G. (2005). The autophagy-associated Atg8 gene family operates both under favourable growth conditions and under starvation stresses in *Arabidopsis* plants. *J Exp Bot* **56**, 2839-2849.
- Smolen,J.E. and Shohet,S.B. (Smolen and Shohet, 1974). Permeability changes induced by peroxidation in liposomes prepared from human erythrocyte lipids. *J Lipid Res* **15**, 273-280.

- Sommer, J.M., Cheng, Q.L., Keller, G.A., and Wang, C.C. (1992). *In vivo* import of firefly luciferase into the glycosomes of *Trypanosoma brucei* and mutational analysis of the C-terminal targeting signal. *Mol Biol Cell* **3**, 749-759.
- Sou, Y.S., Waguri, S., Iwata, J.i., Ueno, T., Fujimura, T., Hara, T., Sawada, N., Yamada, A., Mizushima, N., Uchiyama, Y., Kominami, E., Tanaka, K., and Komatsu, M. (2008). The Atg8 conjugation system is indispensable for proper development of autophagic isolation membranes in mice. *Mol Biol Cell* **19**, 4762-4775.
- Soubannier, V., McLelland, G.L., Zunino, R., Braschi, E., Rippstein, P., Fon, E.A., and McBride, H.M. (2012). A vesicular transport pathway shuttles cargo from mitochondria to lysosomes. *Curr Biol* **22**, 135-141.
- Späth, G.F., Garraway, L.A., Turco, S.J., and Beverley, S.M. (2003). The role(s) of lipophosphoglycan (Späth et al., 2003) in the establishment of *Leishmania major* infections in mammalian hosts. *Proc Natl Acad Sci USA* **100**, 9536-9541.
- Stephan, J.S., Yeh, Y.Y., Ramachandran, V., Deminoff, S.J., and Herman, P.K. (2009). The Tor and PKA signaling pathways independently target the Atg1/Atg13 protein kinase complex to control autophagy. *Proc Natl Acad Sci USA* **106**, 17049-17054.
- Su, W., Ma, H., Liu, C., Wu, J., and Yang, J. (2006). Identification and characterization of two rice autophagy associated genes, OsAtg8 and OsAtg4. *Mol Biol Rep* **33**, 273-278.
- Sugawara, K., Suzuki, N.N., Fujioka, Y., Mizushima, N., Ohsumi, Y., and Inagaki, F. (2004). The crystal structure of microtubule-associated protein light chain 3, a mammalian homologue of *Saccharomyces cerevisiae* Atg8. *Genes Cells* **9**, 611-618.
- Sumpter, R. and Levine, B. (2011). Selective autophagy and viruses. *Autophagy* **7**, 260-265.
- Sundar, S., Sinha, P.K., Rai, M., Verma, D.K., Nawin, K., Alam, S., Chakravarty, J., Vaillant, M., Verma, N., Pandey, K., Kumari, P., Lal, C.S., Arora, R., Sharma, B., Ellis, S., Strub-Wourgaft, N., Balasegaram, M., Olliaro, P., Das, P., and Modabber, F. (2005). Comparison of short-course multidrug treatment with standard therapy for visceral leishmaniasis in India: an open-label, non-inferiority, randomised controlled trial. *Lancet* **377**, 477-486.

- Suzuki,K., Kondo,C., Morimoto,M., and Ohsumi,Y. (2010). Selective transport of α -mannosidase by autophagic pathways: Identification of a novel receptor, Atg34p. *J Biol Chem* **285**, 30019-30025.
- Suzuki,K., Kubota,Y., Sekito,T., and Ohsumi,Y. (2007). Hierarchy of Atg proteins in pre-autophagosomal structure organization. *Genes Cells* **12**, 209-218.
- Tai,W.Y., Yang,Y.C., Lin,H.J., Huang,C.P., Cheng,Y.L., Chen,M.F., Yen,H.L., and Liau,I. (2010). Interplay between structure and fluidity of model lipid membranes under oxidative attack. *J Phys Chem B* **114**, 15642-15649.
- Takeda,K., Yoshida,T., Kikuchi,S., Nagao,K., Kokubu,A., Pluskal,T., Villar-Briones,A., Nakamura,T., and Yanagida,M. (2010). Synergistic roles of the proteasome and autophagy for mitochondrial maintenance and chronological lifespan in fission yeast. *Proc Natl Acad Sci USA* **107**, 3540-3545.
- Takehige,K., Baba,M., Tsuboi,S., Noda,T., and Ohsumi,Y. (1992). Autophagy in yeast demonstrated with proteinase-deficient mutants and conditions for its induction. *J Cell Biol* **119**, 301-311.
- Tal,R., Winter,G., Ecker,N., Klionsky,D.J., and Abeliovich,H. (2007). Aup1p, a yeast mitochondrial protein phosphatase homolog, is required for efficient stationary phase mitophagy and cell survival. *J Biol Chem* **282**, 5617-5624.
- Tanaka,A., Cleland,M.M., Xu,S., Narendra,D.P., Suen,D.F., Karbowski,M., and Youle,R.J. (2010). Proteasome and p97 mediate mitophagy and degradation of mitofusins induced by Parkin. *J Cell Biol* **191**, 1367-1380.
- Taylor,E.B. and Rutter,J. (2011). Mitochondrial quality control by the ubiquitin-proteasome system. *Biochem Soc Trans* **39**, 1509-1513.
- Tetaud,E., Lecuix,I., Sheldrake,T., Baltz,T.o., and Fairlamb,A.H. (2002). A new expression vector for *Crithidia fasciculata* and *Leishmania*. *Mol Biochem Parasitol* **120**, 195-204.
- Thurston,T.L.M., Ryzhakov,G., Bloor,S., von Muhlinen,N., and Randow,F. (2009). The TBK1 adaptor and autophagy receptor NDP52 restricts the proliferation of ubiquitin-coated bacteria. *Nat Immunol* **10**, 1215-1221.
- Tian,Y., Li,Z., Hu,W., Ren,H., Tian,E., Zhao,Y., Lu,Q., Huang,X., Yang,P., Li,X., Wang,X., Kovács,A.L., Yu,L., and Zhang,H. (2010). *C. elegans* screen identifies autophagy genes specific to multicellular organisms. *Cell* **141**, 1042-1055.

- Tonn,D. (2009). Intracellular trafficking of *Leishmania major* peptidases. *PhD thesis, University of Glasgow*.
- Twig,G., Elorza,A., Molina,A.J.A., Mohamed,H., Wikstrom,J.D., Walzer,G., Stiles,L., Haigh,S.E., Katz,S., Las,G., Alroy,J., Wu,M., Py,B.F., Yuan,J., Deeney,J.T., Corkey,B.E., and Shirihai,O.S. (2008). Fission and selective fusion govern mitochondrial segregation and elimination by autophagy. *EMBO J* **27**, 433-446.
- Ueda-Nakamura,T., Attias,M., and de Souza,W. (2001). Megasome biogenesis in *Leishmania amazonensis*: a morphometric and cytochemical study. *Parasitol Res* **87**, 89-97.
- Ueda-Nakamura,T., da Conceição Rocha Sampaio,M., Cunha-e-Silva,N.L., Traub-Cseko,Y., and de Souza,W. (2002). Expression and processing of megasome cysteine proteinases during *Leishmania amazonensis* differentiation. *Parasitol Res* **88**, 332-337.
- van der Vaart,A., Griffith,J., and Reggiori,F. (2010). Exit from the Golgi is required for the expansion of the autophagosomal phagophore in yeast *Saccharomyces cerevisiae*. *Mol Biol Cell* **21**, 2270-2284.
- van Meer,G., Voelker,D.R., and Feigenson,G.W. (2008). Membrane lipids: where they are and how they behave. *Nat Rev Mol Cell Biol* **9**, 112-124.
- van Zutphen,T., Veenhuis,M., and van der Klei,I.J. (2011). Damaged peroxisomes are subject to rapid autophagic degradation in the yeast *Hansenula polymorpha*. *Autophagy* **7**, 863-872.
- Vanhee,C., Zapotoczny,G., Masquelier,D., Ghislain,M., and Batoko,H. (2011). The *Arabidopsis* multistress regulator TSPO is a heme binding membrane protein and a potential scavenger of porphyrins via an autophagy-dependent degradation mechanism. *Plant Cell* **23**, 785-805.
- Vannier-Santos,M.A., Martiny,A., Lins,U., Urbina,J.A., Borges,V.M., and de Souza,W. (1999). Impairment of sterol biosynthesis leads to phosphorus and calcium accumulation in *Leishmania* acidocalcisomes. *Microbiology* **145**, 3213-3220.
- Volf,P., Hajmova,M., Sadlova,J., and Votypka,J. (2004). Blocked stomodeal valve of the insect vector: similar mechanism of transmission in two trypanosomatid models. *Int J Parasitol* **34**, 1221-1227.

- Wanderley, J.L.M., Moreira, M.E.C., Benjamin, A., Bonomo, A.C., and Barcinski, M.A. (2006). Mimicry of apoptotic cells by exposing phosphatidylserine participates in the establishment of amastigotes of *Leishmania (L) amazonensis* in mammalian hosts. *J Immunol* **176**, 1834-1839.
- Wang, H., Bedford, F.K., Brandon, N.J., Moss, S.J., and Olsen, R.W. (1999). GABA_A-receptor-associated protein links GABA_A receptors and the cytoskeleton. *Nature* **397**, 69-72.
- Wang, H. and Olsen, R.W. (2000). Binding of the GABA_A receptor-associated protein (GABARAP) to microtubules and microfilaments suggests involvement of the cytoskeleton in GABARAP-GABA_A receptor interaction. *J Neurochem* **75**, 644-655.
- Wang, K. and Klionsky, D.J. (2011). Mitochondria removal by autophagy. *Autophagy* **7**, 297-300.
- Weidberg, H., Shpilka, T., Shvets, E., Abada, A., Shimron, F., and Elazar, Z. (2011). LC3 and GATE-16 N termini mediate membrane fusion processes required for autophagosome biogenesis. *Dev Cell* **20**, 444-454.
- Weidberg, H., Shvets, E., Shpilka, T., Shimron, F., Shinder, V., and Elazar, Z. (2010). LC3 and GATE-16/GABARAP subfamilies are both essential yet act differently in autophagosome biogenesis. *EMBO J* **29**, 1792-1802.
- Wenzel, U.A., Bank, E., Florian, C., Förster, S., Zimara, N., Steinacker, J., Klinger, M., Reiling, N., Ritter, U., and van Zandbergen, G. (2012). *Leishmania major* parasite stage-dependent host cell invasion and immune evasion. *FASEB J* **26**, 29-39.
- Wheeler, R.J., Gluenz, E., and Gull, K. (2011). The cell cycle of *Leishmania*: morphogenetic events and their implications for parasite biology. *Mol Microbiol* **79**, 647-662.
- Wild, P., Farhan, H., McEwan, D.G., Wagner, S., Rogov, V.V., Brady, N.R., Richter, B., Korac, J., Waidmann, O., Choudhary, C., Dötsch, V., Bumann, D., and Dikic, I. (2011). Phosphorylation of the autophagy receptor Optineurin restricts *Salmonella* growth. *Science* **333**, 228-233.
- Williams, R.A., Tetley, L., Mottram, J.C., and Coombs, G.H. (2006). Cysteine peptidases CPA and CPB are vital for autophagy and differentiation in *Leishmania mexicana*. *Mol Microbiol* **61**, 655-674.

- Williams,R.A.M., Woods,K.L., Juliano,L., Mottram,J.C., and Coombs,G.H. (2009). Characterization of unusual families of ATG8-like proteins and ATG12 in the protozoan parasite *Leishmania major*. *Autophagy* **5**, 159-172.
- Williams,R.A.M., Mottram,J.C., and Coombs,G.H. (2012a). Distinct roles in autophagy and importance in infectivity of the two ATG4 cysteine peptidases of *Leishmania major*. *J Biol Chem*, jbc.M112.415372.
- Williams,R.A.M., Smith,T.K., Cull,B., Mottram,J.C., and Coombs,G.H. (2012b). ATG5 is essential for ATG8-dependent autophagy and mitochondrial homeostasis in *Leishmania major*. *PLoS Pathog* **8**, e1002695.
- Wong,A.S.L., Cheung,Z.H., and Ip,N.Y. (2011). Molecular machinery of macroautophagy and its deregulation in diseases. *Biochim Biophys Acta* **1812**, 1490-1497.
- Woods,K.L. (2009). Regulators of autophagy in *Leishmania major*. *PhD thesis, University of Glasgow*.
- Xia,T., Xiao,D., Liu,D., Chai,W., Gong,Q., and Wang,N.N. (2012). Heterologous expression of *ATG8c* from soybean confers tolerance to nitrogen deficiency and increases yield in *Arabidopsis*. *PLoS One* **7**, e37217.
- Xie,Z.P., Nair,U., and Klionsky,D.J. (2008). Atg8 controls phagophore expansion during autophagosome formation. *Mol Biol Cell* **19**, 3290-3298.
- Xie,Z., Nair,U., Geng,J., Szeffler,M.B., Rothman,E.D., and Klionsky,D.J. (2009). Indirect estimation of the area density of Atg8 on the phagophore. *Autophagy* **5**, 217-220.
- Xin,Y., Yu,L., Chen,Z., Zheng,L., Fu,Q., Jiang,J., Zhang,P., Gong,R., and Zhao,S. (2001). Cloning, expression patterns, and chromosome localization of three human and two mouse homologues of GABA_A receptor-associated protein. *Genomics* **74**, 408-413.
- Yamamoto,H., Kakuta,S., Watanabe,T.M., Kitamura,A., Sekito,T., Kondo-Kakuta,C., Ichikawa,R., Kinjo,M., and Ohsumi,Y. (2012). Atg9 vesicles are an important membrane source during early steps of autophagosome formation. *J Cell Biol* **198**, 219-233.
- Yen,W.L., Shintani,T., Nair,U., Cao,Y., Richardson,B.C., Li,Z., Hughson,F.M., Baba,M., and Klionsky,D.J. (2010). The conserved oligomeric Golgi complex is involved in double-membrane vesicle formation during autophagy. *J Cell Biol* **188**, 101-114.

- Yla-Anttila,P., Vihinen,H., Jokitalo,E., and Eskelinen,E.L. (2009). 3D tomography reveals connections between the phagophore and endoplasmic reticulum. *Autophagy* **5**, 1180-1185.
- Yorimitsu,T. and Klionsky,D.J. (2005). Atg11 links cargo to the vesicle-forming machinery in the cytoplasm to vacuole targeting pathway. *Mol Biol Cell* **16**, 1593-1605.
- Yorimitsu,T., Nair,U., Yang,Z., and Klionsky,D.J. (2006). Endoplasmic reticulum stress triggers autophagy. *J Biol Chem* **281**, 30299-30304.
- Yoshimoto,K., Hanaoka,H., Sato,S., Kato,T., Tabata,S., Noda,T., and Ohsumi,Y. (2004). Processing of ATG8s, ubiquitin-like proteins, and their deconjugation by ATG4s are essential for plant autophagy. *Plant Cell* **16**, 2967-2983.
- Young,A.R.J., Chan,E.Y.W., Hu,X.W., Köchl,R., Crawshaw,S.G., High,S., Hailey,D.W., Lippincott-Schwartz,J., and Tooze,S.A. (2006). Starvation and ULK1-dependent cycling of mammalian Atg9 between the TGN and endosomes. *J Cell Sci* **119**, 3888-3900.
- Yu,Z.Q., Ni,T., Hong,B., Wang,H.Y., Jiang,F.J., Zou,S., Chen,Y., Zheng,X.L., Klionsky,D.J., Liang,Y., and Xie,Z. (2012). Dual roles of Atg8-PE deconjugation by Atg4 in autophagy. *Autophagy* **8**, 877-876.
- Zalila,H., González,I.J., El Fadili,A.K., Delgado,M.B., Desponds,C., Schaff,C., and Fasel,N. (2011). Processing of metacaspase into a cytoplasmic catalytic domain mediating cell death in *Leishmania major*. *Mol Microbiol* **79**, 222-239.
- Zhang,K., Hsu,F.F., Scott,D.A., Docampo,R., Turk,J., and Beverley,S.M. (2005). *Leishmania* salvage and remodelling of host sphingolipids in amastigote survival and acidocalcisome biogenesis. *Mol Microbiol* **55**, 1566-1578.
- Zhang,Y., Yan,L., Zhou,Z., Yang,P., Tian,E., Zhang,K., Zhao,Y., Li,Z., Song,B., Han,J., Miao,L., and Zhang,H. (2009). SEPA-1 mediates the specific recognition and degradation of P granule components by autophagy in *C. elegans*. *Cell* **136**, 308-321.